

INFORMATION TO USERS

This manuscript has been reproduced from the microfilm master. UMI films the text directly from the original or copy submitted. Thus, some thesis and dissertation copies are in typewriter face, while others may be from any type of computer printer.

The quality of this reproduction is dependent upon the quality of the copy submitted. Broken or indistinct print, colored or poor quality illustrations and photographs, print bleedthrough, substandard margins, and improper alignment can adversely affect reproduction.

In the unlikely event that the author did not send UMI a complete manuscript and there are missing pages, these will be noted. Also, if unauthorized copyright material had to be removed, a note will indicate the deletion.

Oversize materials (e.g., maps, drawings, charts) are reproduced by sectioning the original, beginning at the upper left-hand corner and continuing from left to right in equal sections with small overlaps. Each original is also photographed in one exposure and is included in reduced form at the back of the book.

Photographs included in the original manuscript have been reproduced xerographically in this copy. Higher quality 6" x 9" black and white photographic prints are available for any photographs or illustrations appearing in this copy for an additional charge. Contact UMI directly to order.

UMI

A Bell & Howell Information Company
300 North Zeeb Road, Ann Arbor MI 48106-1346 USA
313/761-4700 800/521-0600

RICE UNIVERSITY

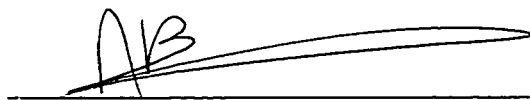
INTRAMOLECULAR COORDINATION IN COMPOUNDS OF ALUMINUM

by

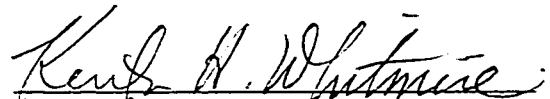
JULIE A. FRANCIS

A THESIS SUBMITTED
IN PARTIAL FULFILLMENT OF THE
REQUIREMENTS FOR THE DEGREE OF
DOCTOR OF PHILOSOPHY

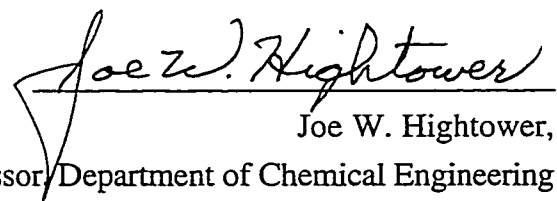
APPROVED, THESIS COMMITTEE



Andrew R. Barron, Advisor,
Professor of Chemistry and Material Science



Kenton H. Whitmire,
Professor of Chemistry



Joe W. Hightower,
Professor, Department of Chemical Engineering

Houston, Texas

March 1999

UMI Number: 9928533

**Copyright 1999 by
Francis, Julie Ann**

All rights reserved.

**UMI Microform 9928533
Copyright 1999, by UMI Company. All rights reserved.**

**This microform edition is protected against unauthorized
copying under Title 17, United States Code.**

UMI
300 North Zeeb Road
Ann Arbor, MI 48103

Copyright

Julie A. Francis

1999

Abstract

Intramolecular Coordination in Compounds of aluminum

by

Julie A. Francis

To develop an understanding of the steric and electronic factors that control the strength of the Lewis acid-base interaction of neutral donor atoms with aluminum in organoaluminum compounds, $[R_2Al\{\mu-O(CH_2)_nER'_x\}]_2$ ($n = 2, 3$; $ER'_x = OR', SR', NR'_2$) have been prepared from AlR_3 and the appropriate substituted alcohol, thiol, or amine ($R = ^tBu, ^iBu, Et$, and Me). The equilibrium that exists between the four-coordinate isomer, $[R_2Al\{\mu-O(CH_2)_nER'_x\}]_2$, and the five-coordinate isomer, $[R_2Al\{\mu-O(CH_2)_nER'_x\}]_2$, where $K_{eq} = [4\text{-coord.}]/[5\text{-coord.}]$, has been probed by ^{13}C and ^{27}Al NMR spectroscopy using the alkoxide derivatives, $[R_2Al(\mu-O^nBu)]_2$ $R = ^tBu, ^iBu$, and Et as comparisons. The solution equilibria have been determined using the ^{13}C NMR shift of the OCH_2 carbon as a measure of the $Al-O-Al$ angle and hence coordination environment at aluminum. The measured bond dissociation energies for the intramolecular coordination were found to be surprisingly weak. Factors that control the extent of this equilibrium and hence the strength of intramolecular coordination include: the steric bulk of the substituents at aluminum and the Lewis base donor, the basicity of the neutral donor group and the chelate ring size. In addition, the sterically demanding aryloxide, 2,6-di-*tert*-butyl-4-methylphenol, was used as the substituent on the aluminum to investigate the effect of increased steric bulk on the degree of oligomerization. To develop an understanding of the geometric factors influencing the extent of oligomerization and coordination number at the aluminum center $[(^tBu)_2Al(\mu-O-2-C_5H_4N)]_2$, $(^tBu)_2Al(OCH_2-2-C_5H_4N)$, $(^tBu)_2Al(O-8-C_9H_6N)$, and $(^tBu)_2Al(OCH_2-8-C_9H_6N)$ were synthesized. It was found that the formation of monomeric structures for compounds is associated with the rigid

conformation of the pyridine and quinoline ligands and not upon the basicity of the chelating ligand. Consequently, the stability of monomeric versus dimeric structures in this system depends not only on basicity and steric factors, but also on the ligand conformation.

" In three words I can sum up everything I've learned about life. It goes on."

Robert Frost

For Dad.

For Mom.

For Lou.

Acknowledgments

There are many people whose assistance has been invaluable over the course of my graduate studies and I will always be grateful. I would like to thank my advisor, Professor Andrew Barron, for his guidance, his generosity and his enthusiasm. In addition, I thank him for willingly providing opportunities for me to grow professionally. I would also like to thank Dr. C. Niamh McMahon, for her friendship, for her assistance in the lab and for lending a kind ear when necessary. Thanks to Dr. Simon Bott, who determined most of the crystal structures presented in the thesis.

I would be in big trouble if I forgot to say thank you to the other members of the Barron group who provided me with endless encouragement, a raucous cheering section and lots of laughter. For the insightful crosswords, Maelstrom, educational smoking breaks, and long chats, I thank you.

There are people who deserve to share this accomplishment with me not for help with chemistry and research, but for helping me to keep life in perspective. I would especially like to acknowledge my husband, Andrew, my Mom and my family whose support never faltered and whose belief in my abilities never wavered. Thank you. Lastly, I want to thank my Dad, who instilled the importance of education in all his children at a very early age. May he rest in peace.

Table of Contents

Introduction	1
Chapter 1. Steric Effects in Aluminum Compounds Containing Monoanionic Potentially Bidentate Ligands: Towards a Quantitative Measure of Steric Bulk	
Introduction	12
Results and Discussion	14
Ether-alkoxide ligands	14
Thioether-alkoxide ligands	33
Determination of intramolecular bond dissociation energies	40
Towards a quantitative measure of steric bulk	43
Conclusions	52
Experimental	53
References	67
Chapter 2. Aluminum Compounds Containing Bidentate Ligands: Chelate Ring Size and Rigid Conformation Effects.	
Introduction	73
Results and Discussion	75
Monomer versus dimer: rigid conformation effects	87
Conclusion	88
Experimental	89
References	94

Chapter 3. Are Intramolecularly Stabilized Compounds of Aluminum**Suitable Structural Models of the S_N2 Transition State?**

Introduction	97
Results and Discussion	100
Synthesis and Characterization of [(^t Bu) ₂ Al(μ-OC ₆ H ₄ -2-OMe)] ₂	100
Effect on molecular geometry of the alkyl substituent (R) in [R ₂ Al(μ-OC ₆ H ₄ -2-OMe)] ₂	103
Ab Initio calculations on the model compound [H ₂ Al(μ-OCH ₂ CH ₂ OH)] ₂	105
Are intramolecularly stabilized compounds of aluminum suitable structural models of the S _N 2 Transition State?	108
Conclusion	112
Experimental	112
References	115

Chapter 4. Sterically Crowded Aryloxides of Aluminum: Intramolecular Coordination of Bidentate Ligands

Introduction	118
Results and Discussion	119
Lithium Aluminates	125
Conclusions	130
Experimental	131
References	138

**Chapter 5. Hydroalumination of H₂C=CHCH₂SMe: Synthesis
and Molecular Structure of (^tBu)₂Al(CH₂CH₂CH₂SMe)**

Introduction	139
Results and Discussion	140
Conclusion	142
Experimental	143
References	146

Chapter 6. Molecular Structure of [(^tBu)₂Al(μ-Cl)]₂

Introduction	149
Results and Discussion	149
Conclusion	154
Experimental	155
References	157
Conclusions	159

List of Figures

Chapter 1

Figure 1.1. Molecular structures of (a) $[(^t\text{Bu})_2\text{Al}(\mu\text{-OCH}_2\text{CH}_2\text{OMe})]_2$ (1.1) and (b) $[(^i\text{Bu})_2\text{Al}(\mu\text{-OCH}_2\text{CH}_2\text{OMe})]_2$ (2). Hydrogen atoms are omitted, and only one of the disordered positions of the methyl groups attached to C(11) and C(21) in compound 1.1 are shown, for clarity. 16

Figure 1.2. Plot of (a) the Al…O_(ether) bond distance (\AA) in $[\text{R}_2\text{Al}(\mu\text{-OCH}_2\text{CH}_2\text{OMe})]_2$ and (b) the Al…N bond distance (\AA) in $[\text{R}_2\text{Al}(\mu\text{-OCH}_2\text{CH}_2\text{NMe}_2)]_2$ as a function of the aluminum alkyl (R) cone angle ($^\circ$). The value for $[\text{R}_2\text{Al}(\mu\text{-OC}_6\text{H}_4\text{-2-OMe})]_2$ and $[\text{Me}_2\text{Al}\{\mu\text{-OC(OMe)=C(H)NMe}_2\}]_2$, are shown for comparison in 1.2 (a) and 1.2(b) respectively. 19

Figure 1.3. Molecular structures of (a) $[(^t\text{Bu})_2\text{Al}(\mu\text{-OCH}_2\text{CH}_2\text{CH}_2\text{OMe})]_2$ (1.6) and (b) $[\text{Me}_2\text{Al}(\mu\text{-OCH}_2\text{CH}_2\text{CH}_2\text{OMe})]_2$ (1.7). Hydrogen atoms are omitted, and only one of the disordered positions of the methyl groups attached to C(11) and C(21) in compound 1.6 are shown, for clarity. 21

Figure 1.4. Plot of the ^{13}C NMR shift of the OCH_2 carbon as a function of the Tolman cone angle ($\theta, {}^\circ$) for the aluminum substituents (R) in $[\text{R}_2\text{Al}(\mu\text{-O}^n\text{Bu})]_2$ ($R = 0.992$). 29

Figure 1.5 Plot of K_{eq} as a function of the aluminum alkyl (R) cone angle ($^\circ$) in (a) $[\text{R}_2\text{Al}(\mu\text{-OCH}_2\text{CH}_2\text{OMe})]_2$, and (b) $[\text{R}_2\text{Al}(\mu\text{-OCH}_2\text{CH}_2\text{SMe})]_2$. 32

Figure 1.6. Molecular structures of (a) $[({}^t\text{Bu})_2\text{Al}(\mu\text{-OCH}_2\text{CH}_2\text{SMe})]_2$ (1.11) and (b) $[({}^i\text{Bu})_2\text{Al}(\mu\text{-OCH}_2\text{CH}_2\text{SMe})]_2$ (1.12).

Hydrogen atoms are omitted, and only one of the disordered positions of the methyl groups attached to C(21) in compound 1.11 are shown, for clarity.

35

Figure 1.7. Space filling representations of (a) $[({}^i\text{Bu})_2\text{Al}(\mu\text{-OCH}_2\text{CH}_2\text{OMe})]_2$ (1.2), (b) $[({}^i\text{Bu})_2\text{Al}(\mu\text{-OCH}_2\text{CH}_2\text{SMe})]_2$ (1.12), (c) $[({}^i\text{Bu})_2\text{Al}(\mu\text{-OCH}_2\text{CH}_2\text{NMe}_2)]_2$ respectively showing the different steric interactions of the ether, thioether and amine methyl group with the *iso*-butyl group on aluminum.

38

Figure 1.8. Molecular structure of $[({}^t\text{Bu})_2\text{Al}(\mu\text{-OCH}_2\text{CH}_2\text{CH}_2\text{SMe})]_2$ (1.15).

Thermal ellipsoids are shown at 30% and hydrogen atoms are omitted for clarity.

39

Figure 1.9. Temperature dependence of the equilibrium constant (K_{eq}) for the conversion of the 5-coordinate to 4-coordinate forms of $[\text{Me}_2\text{Al}(\mu\text{-OCH}_2\text{CH}_2\text{OMe})]_2$ ($R = 0.995$).

41

Figure 1.10. *Ab initio* HF/3-21G(*) calculated structures of (a) five-coordinate and (b) four-coordinate isomers of $[\text{H}_2\text{Al}(\mu\text{-OCH}_2\text{CH}_2\text{OH})]_2$.

47

Figure 1.11. Dependence of the intra-molecular $\text{Al}\cdots\text{O}_{(\text{ether})}$ bond strength in $[\text{H}_2\text{Al}(\mu\text{-OCH}_2\text{CH}_2\text{OH})]_2$ as a function of the $\text{Al}\cdots\text{O}_{(\text{ether})}$ distance. Data fitted to a Lennard-Jones (12,6) potential ($\varepsilon = -64.9 \text{ kJ}\cdot\text{mol}^{-1}$ and $\sigma = 1.796 \text{ \AA}$). Values for the four-coordinate isomer of $[\text{H}_2\text{Al}(\mu\text{-OCH}_2\text{CH}_2\text{OH})]_2$, $[\text{Me}_2\text{Al}(\mu\text{-OCH}_2\text{CH}_2\text{OMe})]_2$, and $[({}^t\text{Bu})_2\text{Al}(\mu\text{-OCH}_2\text{CH}_2\text{OMe})]_2$ are included for comparison.

49

Figure 1.12. Lennard-Jones (12,6) potentials for the Al···O_(ether)

interactions in [H₂Al(μ-OCH₂CH₂OH)]₂ (i), [Me₂Al(μ-

OCH₂CH₂OMe)]₂ (ii), and [(^tBu)₂Al(μ-OCH₂CH₂OMe)]₂ (iii). 51

Chapter 2

Figure 2.1. Molecular structure of [(^tBu)₂Al(μ-O-2-C₅H₄N)]₂ (2.1).

Thermal ellipsoids shown at the 30 % level, and hydrogen atoms are omitted for clarity. 77

Figure 2.2. Molecular structure of (^tBu)₂Al(O-8-C₉H₆N) (2.3).

Thermal ellipsoids shown at the 20 % level, and hydrogen atoms are omitted for clarity. 79

Figure 2.3. A space filling representation of the "head-to-tail"

molecular packing of (^tBu)₂Al(O-8-C₉H₆N) (2.3). 80

Figure 2.4. Molecular structure of [(ⁱBu)₂Al(μ-O-8-C₉H₆N)]₂ (2.5).

Thermal ellipsoids shown at the 30 % level, and hydrogen atoms are omitted for clarity. 81

Figure 2.5. Crystal packing diagram of [(ⁱBu)₂Al(μ-O-8-C₉H₆N)]₂ (2.5). 83

Figure 2.6. Room temperature ¹H NMR spectra for

[(ⁱBu)₂Al(μ-O-8-C₉H₆N)]₂ (2.5) showing the inequivalent

iso-butyl groups and anisochronous methylene (Al-CH₂) groups. 84

Figure 2.7. Space filling diagram of [(ⁱBu)₂Al(μ-O-8-C₉H₆N)]₂

(2.5), showing the *anti* arrangement of the *iso*-butyl groups. 85

Chapter 3

Figure 3.1. Molecular structure of [(^tBu)₂Al(μ-OC₆H₄-2-OMe)]₂ (3.1).

Thermal ellipsoids are shown at the 30 % level, and all hydrogens are omitted for clarity. 101

Figure 3.2. Plot of Al-O(ether), Al-O(trans), and Al-O(cis) bond lengths (\AA) as a function of the Tolman cone angle (θ , $^{\circ}$) for the aluminum substituent (R) in $[(\text{R})_2\text{Al}(\mu\text{-OC}_6\text{H}_4\text{-2-OMe})]_2$. 103

Figure 3.3. Plot of C(11)-Al(1)-C(21), O(1)-Al(1)-O(1'), and Al(1)-O(1)-Al(1') bond angles ($^{\circ}$) as a function of the Tolman cone angle (θ , $^{\circ}$) for the aluminum substituent (R) in $[(\text{R})_2\text{Al}(\mu\text{-OC}_6\text{H}_4\text{-2-OMe})]_2$. 104

Figure 3.4. Plot of C-Al-C bond angles ($^{\circ}$) as a function of the Tolman cone angle (θ , $^{\circ}$) for the aluminum substituent (R) in $[(\text{R})_2\text{Al}(\mu\text{-OC}_6\text{H}_4\text{-2-OMe})]_2$ and $[(\text{R})_2\text{Al}(\mu\text{-Cl})]_2$. 105

Figure 3.5. Plots of (a) calculated Al-H distance (\AA) and (b) calculated Al-O(axial) and Al-O(equ.) distance (\AA) as a function of Al…O(ether) distance (\AA) for the model $[\text{H}_2\text{Al}(\mu\text{-OCH}_2\text{CH}_2\text{OH})]_2$. 107

Figure 3.6. Plot of calculated (a) H-Al-H angles ($^{\circ}$) as a function of Al…O(ether) distance (\AA) for the model $[\text{H}_2\text{Al}(\mu\text{-OCH}_2\text{CH}_2\text{OH})]_2$ and (b) Plot of calculated Al-O-Al and O-Al-O angles ($^{\circ}$). 109

Figure 3.7. Space filling diagram of $[\text{R}_2\text{Al}(\mu\text{-OC}_6\text{H}_4\text{-2-OMe})]_2$, viewed parallel to the Al_2O_2 core, showing the steric interaction of the *tert*-butyl groups. 111

Figure 3.8. Plot of Al…Al distances (\AA) as a function of the Al…O(ether) distance (\AA) (a) calculated for the model $[\text{H}_2\text{Al}(\mu\text{-OCH}_2\text{CH}_2\text{OH})]_2$ and (b) the experimental values for $[\text{R}_2\text{Al}(\mu\text{-OC}_6\text{H}_4\text{-2-OMe})]_2$. 111

Chapter 4

Figure 4.1. Molecular structure of $[(\text{BHT})\text{Al}(\text{H})(\mu\text{-OCH}_2\text{CH}_2\text{NMe}_2)]_2$

(4.2). Thermal ellisoids are given at the 30% level and hydrogen atoms are omitted for clarity.

120

Figure 4.2. Molecular structures of $[(\text{BHT})\text{Al}(\text{OCH}_2\text{CH}_2\text{OMe})(\mu\text{-OCH}_2\text{CH}_2\text{OMe})]_2$ (4.6).

Thermal ellisoids are given at the 30% level and hydrogen atoms are omitted for clarity.

122

Figure 4.3 Molecular structure of $(\text{BHT})_2\text{Al}(\mu\text{-OCH}_2\text{CH}_2\text{NMe}_2)_2\text{Li}$

(4.8). Thermal ellipsoids are shown at the 30% level and hydrogen atoms are omitted for clarity.

127

Figure 4.4. Molecular structure of $(\text{BHT})_2\text{Al}(\mu\text{-OCH}_2\text{CH}_2\text{SMe})_2\text{Li} \cdot (\text{HOCH}_2\text{CH}_2\text{SMe})$ (4.10b).

Thermal ellipsoids are shown at the 30% level and hydrogen atoms are omitted for clarity.

128

Chapter 5

Figure 5.1. Molecular structure of $(^t\text{Bu})_2\text{Al}(\text{CH}_2\text{CH}_2\text{CH}_2\text{SMe})$.

Thermal ellipsoids shown at the 30% level, and hydrogen atoms are omitted for clarity.

141

Chapter 6

Figure 6.1. Molecular structure of $[(^t\text{Bu})_2\text{Al}(\mu\text{-Cl})]_2$ (6.1).

Thermal ellipsoids are shown at the 30 % level, and all hydrogens are omitted for clarity.

150

Figure 6.2 Partial coordination sphere of Al(1) in $[(^t\text{Bu})_2\text{Al}(\mu\text{-Cl})]_2$

(6.1) showing the major (a) and minor (b) isomers.

151

Figure 6.3. Plot of Al-Cl-Al bond angle ($^{\circ}$) as a function of Cl-Al-Cl bond angle ($^{\circ}$) for dialkylaluminum chloride compounds, $[R_2Al(\mu-Cl)]_2$.

151

Figure 6.4. Plot of C-Al-C, Al-Cl-Al, and Cl-Al-Cl bond angles ($^{\circ}$) as a function of the Tolman cone angle ($\theta, ^{\circ}$) for the aluminum substituent (R) in $[(R)_2Al(\mu-Cl)]_2$.

153

Figure 6.5. Plot of Al-Cl and Al \cdots Al distances (\AA) as a function of the Tolman cone angle ($\theta, ^{\circ}$) for the aluminum substituent (R) in $[(R)_2Al(\mu-Cl)]_2$.

154

List of Tables

Chapter 1

Table 1.1. Selected bond lengths (\AA) and angles ($^\circ$) in $[\text{R}_2\text{Al}(\mu\text{-OCH}_2\text{CH}_2\text{OMe})]_2$.	17
Table 1.2. Selected bond lengths (\AA) and angles ($^\circ$) in $[\text{R}_2\text{Al}(\mu\text{-OCH}_2\text{CH}_2\text{CH}_2\text{OMe})]_2$, $\text{R} = \text{tBu}$ (1.6), Me (1.7).	22
Table 1.3. Selected room temperature solution ^{27}Al spectral data.	26
Table 1.4. Selected room temperature solution ^{13}C NMR spectral data and calculated equilibrium constants.	31
Table 1.5. Selected bond lengths (\AA) and angles ($^\circ$) in $[(\text{tBu})_2\text{Al}(\mu\text{-OCH}_2\text{CH}_2\text{SMe})]_2$ (1.11) and $[(\text{iBu})_2\text{Al}(\mu\text{-OCH}_2\text{CH}_2\text{SMe})]_2$ (1.12).	36
Table 1.6. Selected bond lengths (\AA) and angles ($^\circ$) in $[(\text{tBu})_2\text{Al}(\mu\text{-OCH}_2\text{CH}_2\text{CH}_2\text{SMe})]_2$ (1.15).	39
Table 1.7. Selected room temperature solution ^{27}Al and ^{13}C NMR spectral data and calculated equilibrium constants.	40
Table 1.8. Selected equilibrium and thermodynamic data.	42
Table 1.9. Selected enthalpies, ΔH , of Lewis acid-base complexes of aluminum.	44
Table 1.10. Structural parameters for five- and four-coordinate dimeric isomers of $[\text{H}_2\text{Al}(\mu\text{-OCH}_2\text{CH}_2\text{OH})]_n$ in comparison to experimental values.	48
Table 1.11. Lennard-Jones (12,6) potential parameters for $[\text{R}_2\text{Al}(\mu\text{-OCH}_2\text{CH}_2\text{OR}')_2]_2$.	50
Table 1.12. Summary of X-ray diffraction data for compounds in Chapter 1.	63

Chapter 2

Table 2.1. Selected bond lengths (\AA) and angles ($^\circ$) in [(^t Bu) ₂ Al(μ -O-2-C ₅ H ₄ N)] ₂ (2.1).	77
Table 2.2. Selected bond lengths (\AA) and angles ($^\circ$) in (^t Bu) ₂ Al(O-8-C ₉ H ₆ N) (2.3).	79
Table 2.3. Selected bond lengths (\AA) and angles ($^\circ$) in [R ₂ Al(μ -O-8-C ₉ H ₆ N)] ₂ = Et, ⁱ Bu (2.5).	82
Table 2.4. Summary of X-ray diffraction data for compounds in Chapter 2.	92

Chapter 3

Table 3.1. Selected bond lengths (\AA) and angles (deg) in [R ₂ Al(μ -OC ₆ H ₄ -2-OMe)] ₂ .	102
Table 3.2. Crystal data and summary of X-ray diffraction data for [(^t Bu) ₂ Al(μ -OC ₆ H ₄ -2-OMe)] ₂ .	114

Chapter 4

Table 4.1. Selected bond lengths (\AA) and angles ($^\circ$) for [(BHT)Al(H)(μ -OCH ₂ CH ₂ NMe ₂)] ₂ (4.2).	121
Table 4.2 Selected bond lengths (\AA) and angles ($^\circ$) for [(BHT)Al(OCH ₂ CH ₂ OMe)(μ -OCH ₂ CH ₂ OMe)] ₂ (4.6).	123
Table 4.3. Selected bond lengths (\AA) and angles ($^\circ$) for (BHT) ₂ Al(μ -OCH ₂ CH ₂ NMe ₂) ₂ Li (4.8).	127
Table 4.4 Selected bond lengths (\AA) and angles ($^\circ$) for (BHT) ₂ Al(μ -OCH ₂ CH ₂ SMe) ₂ LiHOCH ₂ CH ₂ SMe (4.10b).	129

Table 4.5. Bond valences for the lithium bonds in $(BHT)_2Al(\mu-OCH_2CH_2NMe_2)_2Li$ (4.8) and $(BHT)_2Al(\mu-OCH_2CH_2SMe)_2Li \cdot HOCH_2CH_2SMe$ (4.10b). Chapter 4.	130 136
Chapter 5	
Table 5.1. Selected bond lengths (\AA) and angles ($^\circ$) in $(^t\text{Bu})_2Al(CH_2CH_2CH_2SMe)$ (5.1). Table 5.2. Summary of X-ray diffraction data for $(^t\text{Bu})_2Al(CH_2CH_2CH_2SMe)$ (5.1). Chapter 6	141 145
Table 6.1. Selected bond lengths (\AA) and angles ($^\circ$) in $[(^t\text{Bu})_2Al(\mu-\text{Cl})]_2$ (6.1). Table 6.2. Crystal data and summary of X-ray diffraction data for $[(^t\text{Bu})_2Al(\mu-\text{Cl})]_2$ (6.1). Chapter 7	150 156

List of Compounds

- 1.1** $[(t\text{Bu})_2\text{Al}(\mu\text{-OCH}_2\text{CH}_2\text{OMe})]_2$
1.2 $[(i\text{Bu})_2\text{Al}(\mu\text{-OCH}_2\text{CH}_2\text{OMe})]_2$
1.3 $[(Et)_2\text{Al}(\mu\text{-OCH}_2\text{CH}_2\text{OMe})]_2$
1.4 $[(t\text{Bu})_2\text{Al}(\mu\text{-OCH}_2\text{CH}_2\text{O}^n\text{Bu})]_2$
1.5 $[\text{Me}_2\text{Al}(\mu\text{-OCH}_2\text{CH}_2\text{O}^n\text{Bu})]_2$
1.6 $[(t\text{Bu})_2\text{Al}(\mu\text{-OCH}_2\text{CH}_2\text{CH}_2\text{OMe})]_2$
1.7 $[\text{Me}_2\text{Al}(\mu\text{-OCH}_2\text{CH}_2\text{CH}_2\text{OMe})]_2$
1.8 $[(t\text{Bu})_2\text{Al}(\mu\text{-O}^n\text{Bu})]_2$
1.9 $[(i\text{Bu})_2\text{Al}(\mu\text{-O}^n\text{Bu})]_2$
1.10 $[\text{Et}_2\text{Al}(\mu\text{-O}^n\text{Bu})]_2$
1.11 $[(t\text{Bu})_2\text{Al}(\mu\text{-OCH}_2\text{CH}_2\text{SMe})]_2$
1.12 $[(i\text{Bu})_2\text{Al}(\mu\text{-OCH}_2\text{CH}_2\text{SMe})]_2$
1.13 $[\text{Et}_2\text{Al}(\mu\text{-OCH}_2\text{CH}_2\text{SMe})]_2$
1.14 $[\text{Me}_2\text{Al}(\mu\text{-OCH}_2\text{CH}_2\text{SMe})]_2$
1.15 $[(t\text{Bu})_2\text{Al}(\mu\text{-OCH}_2\text{CH}_2\text{CH}_2\text{SMe})]_2$
1.16 $[\text{Me}_2\text{Al}(\mu\text{-OCH}_2\text{CH}_2\text{CH}_2\text{SMe})]_2$
2.1 $[(t\text{Bu})_2\text{Al}(\text{O-2-C}_5\text{H}_4\text{N})]_2$
2.2 $(t\text{Bu})_2\text{Al}(\text{OCH}_2\text{-2-C}_5\text{H}_4\text{N})$
2.3 $(t\text{Bu})_2\text{Al}(\text{O-8-C}_9\text{H}_6\text{N})$
2.4 $(t\text{Bu})_2\text{Al}(\text{OCH}_2\text{-8-C}_9\text{H}_6\text{N})$
2.5 $[(i\text{Bu})_2\text{Al}(\mu\text{-O-8-C}_9\text{H}_6\text{N})]_2$
3.1 $[(t\text{Bu})_2\text{Al}(\mu\text{-OC}_6\text{H}_4\text{-2-OMe})]_2$
4.1 $[(\text{BHT})_2\text{Al}(\text{H})]_2$
4.2 $[(\text{BHT})\text{Al}(\text{H})(\mu\text{-OCH}_2\text{CH}_2\text{NMe}_2)]_2$
4.3 $[(\text{BHT})\text{Al}(\text{H})(\mu\text{-OCH}_2\text{CH}_2\text{OMe})]_2$

- 4.4** [(BHT)Al(H)(μ -OCH₂CH₂SMe)]₂
- 4.5** [(BHT)Al(OCH₂CH₂NMe₂)(μ -OCH₂CH₂NMe₂)]₂
- 4.6** [(BHT)Al(OCH₂CH₂OMe)(μ -OCH₂CH₂OMe)]₂
- 4.7** [(BHT)Al(OCH₂CH₂SMe)(μ -OCH₂CH₂SMe)]₂
- 4.8** BHT)₂Al(μ -OCH₂CH₂NMe₂)₂Li
- 4.9** (BHT)₂Al(μ -OCH₂CH₂OMe)₂Li
- 4.10** (BHT)₂Al(μ -OCH₂CH₂SMe)₂Li
- 4.10b** (BHT)₂Al(μ -OCH₂CH₂SMe)₂Li(HOCH₂CH₂SMe)
- 5.1** (^tBu)₂Al(CH₂CH₂CH₂SMe)
- 6.1** [(^tBu)₂Al(μ -Cl)]₂

Abbreviations and Glossary

Å	Angstom
Anal.	analysis
BDE	bond dissociation energy
BHT-H	2,6-di- <i>tert</i> -butyl-4-methylphenol (from the trivial name, butylated hydroxy toluene)
ⁱ Bu	<i>iso</i> -butyl, -CH ₂ CH(CH ₃) ₂
ⁿ Bu	<i>n</i> -butyl, -CH ₂ CH ₂ CH ₂ CH ₃
^t Bu	<i>tert</i> -butyl, -C(CH ₃) ₃
°C	degrees celcius
Calc'd	calculated
δ	delta, chemical shift (NMR)
D	density
°	degrees
E	heteroatom, e.g., oxygen, sulfur, nitrogen, etc.
ε	depth of the minimum of the Lennard-Jones Potential, absorption coefficient (UV/Vis)
Et	ethyl, CH ₂ CH ₃
Et ₂ O	diethylether
Eq	equation
Fc	calculated structure factor
Fo	observed structure factor
g	grams
h	hour
ΔH	change in enthalpy
IR	Infrared spectroscopy

J	Joule
K	Kelvin
K_{eq}	equilibrium constant
L	Lewis base
λ	wavelength
<i>m</i>	meta
m	medium (IR), multiplet (NMR)
MAO	methylalumoxane
Me	methyl, CH_3
mesityl	1,3,5-trimethylbenzene, $[\text{C}_6\text{H}_3(\text{CH}_3)_3]$
mg	milligram(s)
mL	milliliter(s)
mmol	millimole(s)
MP2	Møller-Plesset calculations
MS	mass spectroscopy
n	integer
NMR	nuclear magnetic spectroscopy
ppm	parts per million
py	pyridyl
quin	quintet
R	alkyl, bond distance
R_e	equilibrium bond length
ΔS	entropy
s	singlet, strong
sept	septet
θ	Tolman's cone angle, angle(s)
$V(R)$	intermolecular energy

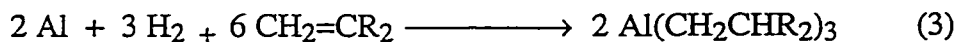
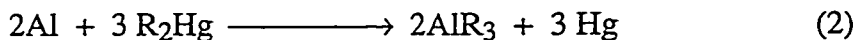
w	weak
$W_{1/2}$	width at half height, (^{27}Al NMR)
χ	mole fraction
alumoxanes	A species containing at least one bridging oxo group between two aluminum centers
bidentate	An adjective used to describe a ligand that may bond at two sites.
chelate	A metal coordination complex where one ligand coordinates at two or more points to the same metal ion.
cone angle	A steric parameter, θ , which is the apex angle of a cylindrical cone which just touches the van der Waals radii of the outermost atoms of a substituent.
ether	A type of organic compound containing the group $\text{R}'-\text{O}-\text{R}$, where R' and R are aryl or alkyl groups.
Lewis acid	A substance that can accept an electron pair to form a coordinate bond.
Lewis base	A substance that can donate an electron pair to form a coordinate bond.
thioether	A type of organic compound containing the group $\text{R}'-\text{S}-\text{R}$, where R' and R are aryl or alkyl groups.

Introduction

Aluminum is the most abundant metal in the Earth's crust and as such its chemistry has been studied for many years. The metal itself and its alloys are employed for a wide variety of uses in the building and transportation industries. Because of the diversity displayed by aluminum compounds, their applications span many disciplines, from material science and electronics to catalysis. Several applications include the use of alkoxides as precursors in sol-gel processes,¹ the halides as Lewis acid catalysts,² the hydrides as reducing agents in organic synthesis,³ and the nitrate salts as water treatment.⁴ The alkyl derivatives of aluminum play very important roles as co-catalysts or precursors to co-catalysts in Ziegler-Natta polymerization of olefins. The aluminum alkyls are representative of main group organometallic chemistry, and as such have extremely reactive metal-carbon bonds and are pyrophoric, spontaneously combusting in air.

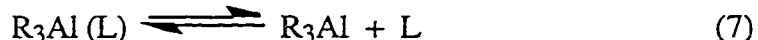
Aluminum alkyls are synthesized almost exclusively by one of four general routes:

(a) metathesis between metal alkyls and aluminum compounds (Eq. 1), (b) displacement between metal alkyls and aluminum metal (Eq. 2), (c) hydroalumination of unsaturated hydrocarbons (Eqs. 3 and 4) and (d) dehalogenation of organoaluminum sesquihalides (Eqs. 5 and 6).⁵





The Lewis acidity of aluminum alkyls is demonstrated by their propensity to form $\text{R}_3\text{Al(L)}$ addition compounds in the presence of Lewis bases (L). Traditionally, it is these four-coordinate tetrahedral complexes that have dominated the organometallic chemistry of aluminum. The chemistry surrounding these complexes involve the simple dissociative process (Eq. 7) whereby the reactivity of the compound is related to the ease of dissociation of the complex.



Other four-coordinate aluminum complexes include the bridged dimers formed from the reaction of aluminum alkyls with alcohols, thiols, or amines as seen in equation 8. The degree of oligomerization depends on the nature of E, R and R'.



With respect to the alkoxide formed from this reaction when E = O, the strength of the Al-O-Al bridge is sufficient to inhibit interchange of the bridging, (R'), and terminal, (R), substituents.⁶ It also makes cleavage of this bridge by a Lewis base quite difficult. Although electron precise (octet) four-coordinate organometallic compounds of aluminum remain the majority there are an increasing number of alkyl derivatives with coordination numbers of three, five and six.⁷ Electron deficient three-coordinate complexes of aluminum are only seen when the compound is stabilized by bulky groups such as BHT (2,6-di-*tert*-butyl-4-methylphenoxy),⁸ mesityl groups,⁹ or *bis*(trimethylsilyl)amide.¹⁰ Six-coordinate

organometallic complexes remain elusive and only a few have been published.¹¹ Five-coordinate complexes of aluminum have been fast emerging involving macrocyclic ligands like crown ethers¹² and multidentate ligands.

Interest in organoaluminum compounds as catalysts and co-catalysts has exploded since Karl Ziegler's discovery of alkene insertion reactions¹³ which formed the basis of the now giant olefin polymerization industry. Two main processes must be distinguished: (a) the synthesis of unbranched long-chain primary alcohols and alkenes exclusively using aluminum alkyls (Eq. 9), and (b) the low-pressure polymerization of ethene with $TiCl_4 - AlClEt_2$ catalysts.



The discovery that a combination of an aluminum alkyl with transition metal halide created a highly active polymerization catalyst led to the receipt by Ziegler of the Nobel Prize in 1963. Ziegler shared the Nobel Prize with Giulio Natta who had demonstrated that the stereoselective polymerization of olefins could be accomplished by the use of $TiCl_3$ in place of $TiCl_4$.¹⁴ Another important development in the advancement of organoaluminum compounds as catalysts began with the realization that the previously inactive system involving the metallocene, Cp_2MX_2 ($M = Zr, Ti$; $X = Me, \text{halide}$), and $AlMe_3$, became highly active upon addition of water. This work was noted by Long and Breslow as the water effect,¹⁵ but it wasn't until the work of Sinn, Kaminsky and co-workers that the nature of this effect was appreciated.¹⁶ Detailed investigations on the influence of water and on the reactions between water and trimethylaluminum showed that an oligomeric alumoxane, methylalumoxane (MAO), was formed.¹⁷ The presence of MAO was found to be a much more effective activator for metallocene dihalides than aluminum alkyl halides and even allows for the polymerization of propene.¹⁸ Since these significant discoveries, MAO has become the most widely used co-catalyst in industry for the metallocene catalyzed

polymerization of α -olefins. A major drawback of MAO, however, is that a large excess is needed to achieve high activity making it expensive to use, and its inherent properties such as alkyl group exchange, route dependent products and violent hydrolysis make it difficult to fully characterize and handle. This introduces opportunity for the development of new co-catalysts that can operate in the same manner, with similar or greater activities without the disadvantages that MAO presents.

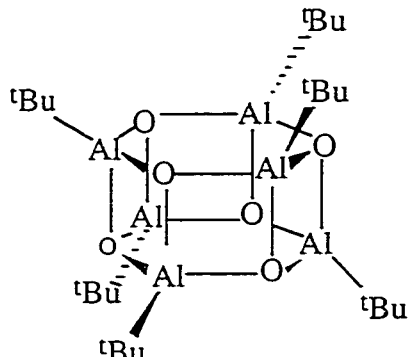
Despite its popularity and importance in the olefin polymerization industry, the exact structure of MAO and its mode of catalytic activity remains ambiguous. Alumoxanes are defined as species containing at least one bridging oxo group between two aluminum centers.¹⁹ The exact structure of MAO remains elusive due to inherent drawbacks to simple structural characterization such as the presence of multiple species and the equilibria that exists between them, alkyl group exchange, route dependent products and violent hydrolysis. Modes of characterization that have been employed to elucidate the structure and mechanism of MAO include XPS,²⁰ theoretical studies,²¹ and NMR spectroscopy.²² These suggest that the primary role of MAO is an alkide abstraction from the metallocene to produce a 14 electron, unsaturated 'cation-like' catalytic metal center (Eq 10).¹⁹



This would be the active site for a Ziegler - Natta type catalytic mechanism. The formation of a cationic metal center by MAO infers that the aluminum center in MAO must be coordinatively unsaturated and highly Lewis acidic in order for this mechanism to work. It is as this basis (the presence of a Lewis acid center) that alternative co-catalysts have been studied.^{23,24}

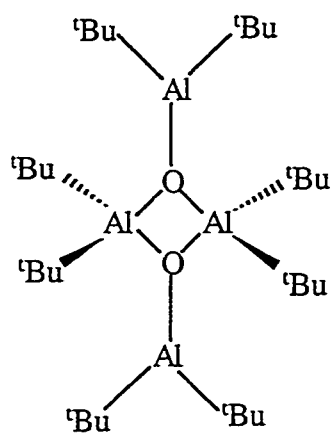
In 1993, the Barron group reported²⁵ the first conclusive evidence that alkylalumoxanes, prepared by the hydrolysis of $\text{Al}(\text{tBu}_3)$, are electron precise, three-

dimensional caged structures of formula $[({}^t\text{Bu})\text{AlO}]_n$ ($n = 6, 7, 8, 9$). An example of these compounds can be seen in (I).



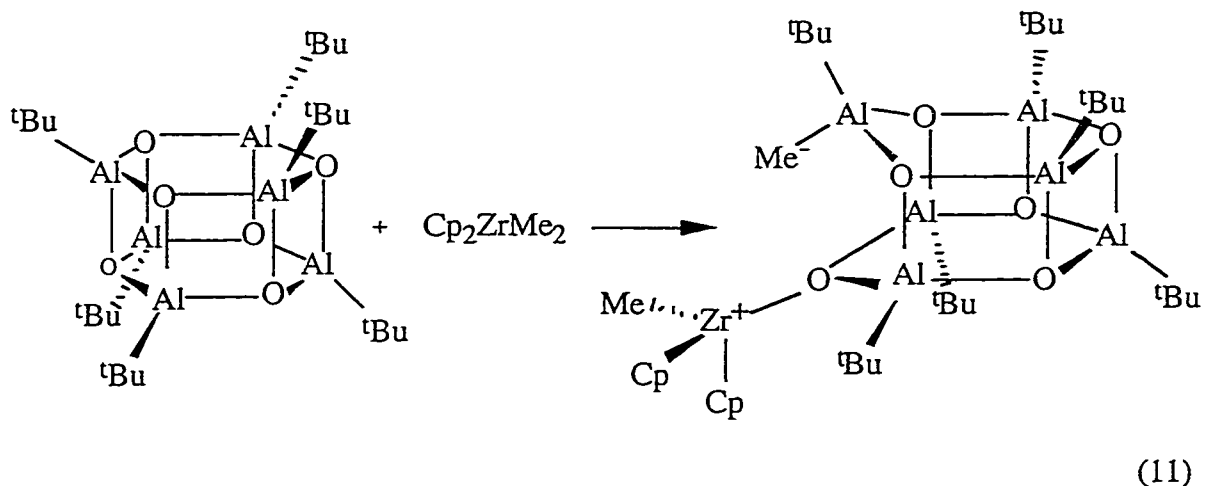
(I)

The partial hydrolysis of $\text{Al}({}^t\text{Bu}_3)$ also allows for the isolation of $[({}^t\text{Bu})_2\text{Al}\{\mu-\text{OAl}({}^t\text{Bu})_2\}]_2$ (II), which based on conventional wisdom, was expected to function as an active co-catalyst, since this compound does contain two three-coordinate, coordinatively unsaturated aluminum atoms that are suitable for alkide abstraction if Lewis acidity alone were responsible for co-catalytic activity.



(II)

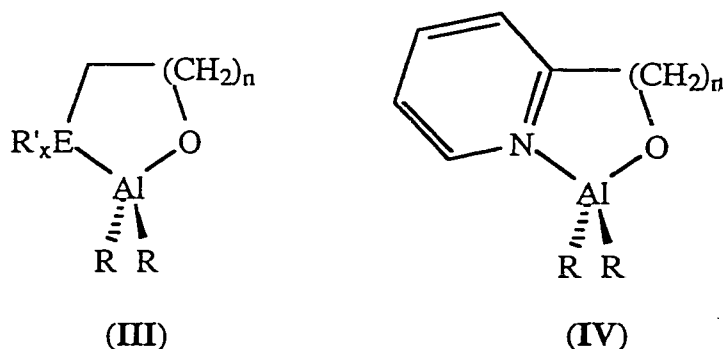
Subsequent work²⁶ shows that $[({}^t\text{Bu})_2\text{Al}\{\mu\text{-OAl}({}^t\text{Bu})_2\}]_2$ is ineffective as a co-catalyst and surprisingly, it is the caged alumoxane that reacts exothermically at room temperature with Cp_2ZrMe_2 to yield the methyl transfer product in equilibrium with the two reactants (Eq. 11).



Furthermore, all caged alumoxanes are active co-catalysts for the polymerization of ethylene. In order to explain the activity of the cage compounds the concept of Latent Lewis acidity was proposed.²⁶

Latent Lewis acidity is a term used to describe the ability of an electron precise molecule to undergo heterolytic bond cleavage to generate an electron deficient, Lewis acidic site. In the case of the caged alumoxanes, latent Lewis acidity explains co-catalytic ability and is a direct consequence of the ring strain present in the cluster. This concept is useful to explain the displayed co-catalytic activity of the electron precise cages. A system to model this property would provide insight into the latent Lewis acidity for cage compounds, especially alumoxanes. Understanding this concept will also permit the development of new and better engineered co-catalysts in the metallocene polymerization of α -olefins. It was gaining this understanding that formed the initial basis of this thesis.

To this end, general model systems of the type shown in **III** and **IV** were prepared and the steric and electronic factors that influence the formation and strength of the intramolecular coordination between the neutral donor ligands and aluminum were investigated. Several considerations were taken into account such as (i) the identity of the heteroatom used which determines electronic effects, (ii) the ring size which determines ring strain, and (iii) the steric bulk at the aluminum and the heteroatom which determines the steric effects. Each of these parameters was varied when designing these simple intramolecularly stabilized complexes. In addition to these compounds, quinolinic compounds were prepared in a similar manner to the pyridyl compounds and these offered insight into the effect that rigid ligands have on the formation of monomeric or dimeric compounds and on strength of the intramolecular coordination that results.



It was the intention of this research that the investigation of these compounds will lend a better understanding to the factors that control intramolecular coordination of neutral donor atoms to aluminum which in turn will provide insight into the ring opening reaction mechanism of caged alumoxanes.²⁶

References

- 1 D. C. Bradley, *Chem. Rev.*, 1989, **89**, 1317.
- 2 See for example: G. A. Olah, S. Kobayashi, and M. Tashior, *J. Am. Chem. Soc.*, 1972, **94**, 7448.
- 3 See for example: (a) H. C. Brown and C. J. Shoaf, *J. Am. Chem. Soc.*, 1964, **86**, 1079.
(b) E. Wilberg and E. Amberger, *Hydrides of the Elements of Main Group I-IV*, Elsevier, New York, 1971, Ch. 5.
- 4 A. Murphy, *Nature*, 1991, **350**, 223.
- 5 See for example, A. R. Barron, in *Coordination Chemistry of Aluminum*, Ed., G. H. Robinson, VCH, New York, 1993, Ch.4.
- 6 (a) E. A. Jeffery, T. Mole, and K. J. Saunders, *Can. J. Chem.*, 1968, **21**, 137.
(b) E. A. Jeffery; T. Mole, and J. K. Saunders, *Can. J. Chem.*, 1968, **21**, 649.
- 7 While four-coordinate compounds are the norm in the organometallic chemistry of aluminum, it should be noted that the coordination chemistry of aluminum is dominated by six-coordinate structures.
- 8 M. D. Healy and A.R. Barron, *Angew. Chem., Int. Ed. Engl.* 1992, **31**, 921.
- 9 J. J. Jerius, J. M. Hahn, A. F. M. M. Rahman, O. Mols, W. H. Ilsley, and J. P. Oliver, *Organometallics*, 1986, **5**, 1812.
- 10 G. M. Sheldrick and W.S. Sheldrick, *J. Chem. Soc. A*, 1969, 2279.
- 11 See for example: (a) M. D. Healy and A.R. Barron, *J. Am. Chem. Soc.*, 1989, **111**, 398.
(b) J. T. Leman and A.R. Barron, *Organometallics*, 1989, **8**, 1828.
(c) H. Noth and P. Konrad, *Chem. Ber.*, 1983, **116**, 3552.
- 12 See for example: (a) V. L. Goedken, H. Ito, and T. Ito, *J. Chem. Soc., Chem. Commun.*, 1984, 1453.
(b) G. H. Robinson and S. A. Sangokoya, *J. Am. Chem. Soc.*, 1987, **109**, 6852.

- (c) S. G. Bott, A. Alvanipour, S. D. Morley, D. A. Atwood, C. M. Means, A. W. Coleman, and J. L. Atwood, *Angew. Chem., Int. Ed. Engl.* 1987, **26**, 485.
- 13 (a) K. Ziegler, E. Holzkamp, H. Briel, and H. Martin, *Angew. Chem.*, 1955, **67**, 541.
- (b) K. Ziegler, *Angew. Chem.*, 1964, **76**, 545.
- 14 G. Natta, *Angew. Chem.*, 1956, **68**, 3936; 1964, **76**, 553.
- 15 W. P. Long and D. S. Breslow, *Liebigs Ann. Chem.*, 1975, 463.
- 16 (a) A. A. Anderson, H. G. Cordes, J. Herwig, W. Kaminsky, A. Merck, R. Mottweiler, J. Pein, H. Sinn, and H. J. Vollmer, *Angew. Chem.*, 1976, **88**, 689.
- (b) A. A. Anderson, H. G. Cordes, J. Herwig, W. Kaminsky, A. Merck, R. Mottweiler, J. Pein, H. Sinn, and H. J. Vollmer, *Angew. Chem. Int. Ed. Engl.*, 1976, **15**, 630.
- 17 H. Sinn and W. Kaminsky, *Adv. Organomet. Chem.*, 1980, **18**, 99.
- 18 M. Bochmann, *J. Chem. Soc. Dalton Trans.*, 1996, 255, and references therein.
- 19 S. Pasynkiewicz, *Polyhedron*, **9**, 429.
- 20 P. G. Gassman, M. R. Callstrom, *J. Am. Chem. Soc.*, 1987, **109**, 7875.
- 21 (a) C. A. Jolly and D. S. Marynick, *J. Am. Chem. Soc.*, 1989, **111**, 7968.
- (b) J. W. Lauher and R. Hoffman, *J. Am. Chem. Soc.*, 1976, **98**, 1729.
- 22 S. Chand, R. M. Hathorn, and T. J. Marks, *J. Am. Chem. Soc.*, 1992, **114**, 1112.
- 23 (a) A. D. Horton and A. G. Orpen, *Organometallics*, 1992, **11**, 8.
- (b) A. D. Horton and A. G. Orpen, *Organometallics*, 1991, **10**, 3910.
- (c) D. M. Amorose, R. A. Lee, and J. L. Petersen, *Organometallics*, 1991, **10**, 2191.
- (d) R. Taube, and L. Krukowka, *J. Organomet. Chem.*, 1988, **347**, C9.
- (e) J. J. Eisch, A. M. Piotrowski, S. K. Brownstein, E. J. Gabe, and F. L. Lee, *J. Am. Chem. Soc.*, 1985, **107**, 7219.

- (f) M. Bochmann and S. J. Lancaster, *J. Organomet. Chem.*, 1992, **434**, C1.
- (g) M. Bochmann and A. J. Jaggar, *J. Organomet. Chem.*, 1992, **424**, C5.
- (h) M. Bochmann, G. Karger, and A. J. Jaggar, *J. Chem. Soc., Chem. Commun.*, 1990, 1038.
- (i) M. Bochmann, A. J. Jaggar, and J. C. Nicholls, *Angew. Chem., Int. Ed. Engl.*, 1990, **29**, 780.
- (j) M. Bochmann, A. J. Jaggar, M.B. Hursthouse, and M. Mazid, *Polyhedron*, 1990, **9**, 2097.
- (k) M. Bochmann, A. J. Jaggar, M. B. Hursthouse, and M. Motevalli, *Polyhedron*, 1989, **8**, 1838.
- (l) M. Bochmann, L. M. Wilson, M. B. Hursthouse, and M. Motevalli, *Organometallics*, 1988, **7**, 1148.
- (m) M. Bochmann, L. M. Wilson, M. B. Hursthouse, and R. L. Short, *Organometallics*, 1987, **6**, 2556.
- (n) M. Bochmann and L. M. Wilson, *J. Chem. Soc., Chem. Commun.*, 1986, 1610.
- 24 (a) R. F. Jordan, *Adv. Organomet. Chem.*, 1991, **32**, 325.
- (b) Y. W. Alelyunas, R. F. Jordan, S. F. Echols, S. L. Borkowsky, and P. K. Bradley, *Organometallics*, 1991, **10**, 1406.
- (c) R. F. Jordan, D. F. Taylor, and N. C. Baenziger, *Organometallics*, 1990, **9**, 1546.
- (d) R. F. Jordan, R. E. LaPointe, P. K. Bradley, and N. Baenziger, *Organometallics*, 1989, **8**, 2892.
- (e) R. F. Jordan, *J. Chem. Educ.*, 1988, **65**, 285.
- (f) R. F. Jordan and S. F. Echols, *Inorg. Chem.*, 1987, **26**, 383.
- (g) R. F. Jordan, R. E. LaPointe, C. S. Bajgur, S. F. Echols, and R. Willett, *J. Am. Chem. Soc.*, 1987, **109**, 4111.

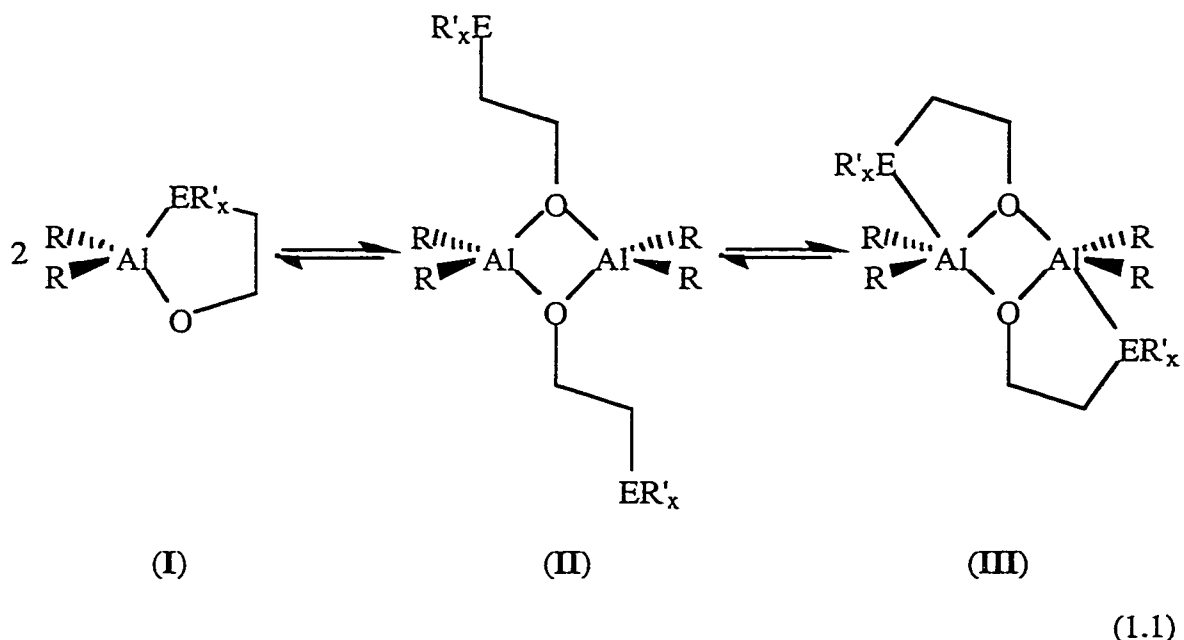
- (h) R. F. Jordan, C. S. Bajgur, W.E. Dasher, and A. L. Rheingold, *Organometallics*, 1987, **6**, 1041.
- (i) R. F. Jordan, C. S. Bajgur, R. Willett, and B.Scott, *J. Am. Chem. Soc.*, 1986, **108**, 7410.
- (j) R. Willett, W. E. Dasher, and S. F. Echols, *J. Am. Chem. Soc.*, 1986, **108**, 1718.
- (k) X. Yang, C. L. Stern, and T. J. Marks, *J. Am. Chem. Soc.*, 1991, **113**, 3623.
- (l) X. Yang, C. L. Stern, and T. J. Marks, *Organometallics*, 1991, **10**, 840.
- (l) G. G. Hlatky, R. R. Eckman, and H. W. Turner, *Organometallics*, 1992, **11**, 1413.
- (m) G. G. Hlatky, H. W. Turner, and R. R. Eckman, *J. Am. Chem. Soc.*, 1989, **111**, 2728.
- (n) H. W. Turner, G. G. Hlatky, Eur. Pat. Appl. 0 277 004, 1988.
- (o) H. W. Turner, G. G. Hlatky, Eur. Pat. Appl. 0 277 003, 1988.
- 25 (a) M. R. Mason, J. M. Smith, S. G. Bott and A. R. Barron, *J. Am. Chem. Soc.*, 1993, **115**, 4971.
- (b) C. J. Harlan, M. R. Mason, and A. R. Barron, *Organometallics*, 1994, **13**, 2957.
- 26 C. J. Harlan, S. G. Bott, and A. R. Barron, *J. Am. Chem. Soc.*, 1995, **117**, 6465.

Chapter 1

Steric Effects in Aluminum Compounds Containing Monoanionic Potentially Bidentate Ligands: Towards a Quantitative Measure of Steric Bulk

Introduction

Compounds containing various monoanionic potentially bidentate ligands are ubiquitous within the chemistry of aluminum. Although such compounds include β -diketonate ligands (e.g., acetylacetone), interest in recent years has focused on non-delocalized ligands containing both anionic and neutral Lewis base termini,¹ an example of which may be given the general formula, $[\text{O}(\text{CH}_2)_n\text{ER}'_x]^-$. Equilibria between monomeric chelate (e.g., for $n = 2$, I in Eq. 1.1) and dimeric compounds (e.g., for $n = 2$, II in Eq. 1.1) have been proposed.^{1a} In addition, there has been variable temperature NMR evidence that in solution the nonbridging heteroatoms can interact with the aluminum atoms to form tri-cyclic compounds that contain five-coordinate aluminum (e.g., for $n = 2$, III in Eq. 1.1).²



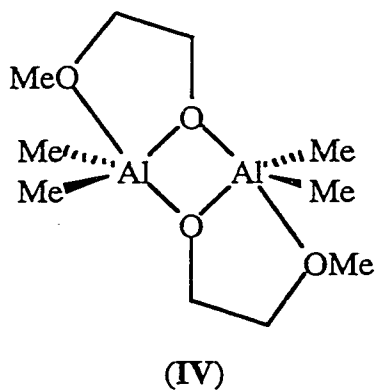
Possible factors that control the coordination about aluminum and the degree of association, and hence the position of this proposed three-way equilibrium, include: the steric bulk of the substituents at aluminum (R) and at the Lewis base donor (R'), the basicity of the neutral donor group (ER'_x) versus the anionic donor atom,³ the chelate ring size as determined by the length of the ligand's backbone (n), and the steric bulk at the ligand's α -carbon. In a series of seminal experiments, Mole⁴ demonstrated that the relative bridging ability of a series of donor groups could be determined for aluminum compounds of the general formula, $[R_2Al(\mu-X)]_n$. However, these results were not aimed at the possible formation of five-coordinate aluminum compounds. Similarly, Beachley *et al.*^{1a} have previously shown that the potential chelate ring size and relative basicity are certainly controlling factors with regard to the degree of association (i.e., the formation of **I** versus either **II** or **III**). However, no indication as to the relative formation of **II** versus **III** was given at that time. Even with the addition of several structural investigations there has been little attempt to develop a cohesive picture related to the factors controlling the proposed structural equilibria shown in Eq. 1.1.

Our initial interest in this area arose from the desire to prepare simple monomeric intramolecularly-stabilized compounds as latent Lewis acid catalysts and co-catalysts.⁵ In order for such compounds to be designed, a detailed understanding must be obtained of the factors that determine the absence or presence, and most importantly the strength of any such intramolecular interaction. Furthermore, while there is an abundance of quantitative thermodynamic data on the strength of Lewis acid-base interactions for four-coordinate aluminum, there is little information for five-coordinate compounds. In this regard compounds of the general formula $[R_2Al\{O(CH_2)_nER'_x\}]_n$, where ER'_x is a neutral donor group (e.g., ether, thioether or amine⁶) have been prepared, and it is this study that is presented herein.

Results and Discussion

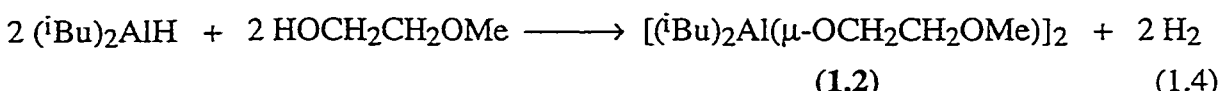
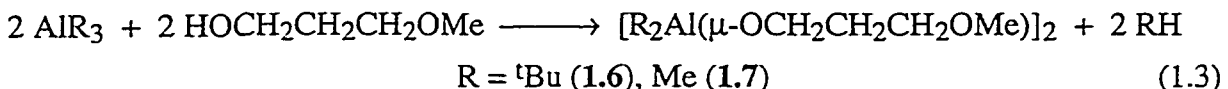
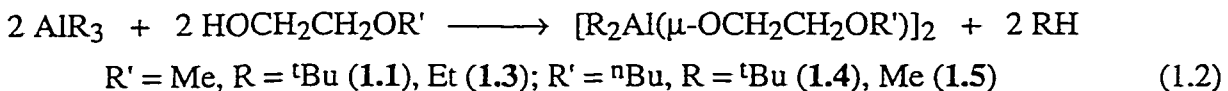
In order to investigate the trends and allow for comparisons with previously characterized compounds the following discussion is divided with respect to the ligand type.

Ether-alkoxide ligands. 2-Methoxyethanol and related ether alcohols, HO(CH₂)_nOR, represent perhaps the simplest source of chelate-bridging ligands. The alcohol terminus, upon deprotonation to the alkoxide, is a source of a stable bridging unit for aluminum,⁷ while the ether substituent can act as a Lewis base, and the carbon chain length may be varied to control the chelate ring size and bite angle.⁸ In fact, [Me₂Al(μ-OCH₂CH₂OMe)]₂ (**IV**), formed from the reaction of AlMe₃ with methoxy-ethanol, was the first aluminum compound of this general class to be crystallographically characterized.⁹



In order to ascertain the effects of the steric bulk of the substituents on aluminum, the homologous series, [R₂Al(μ-OCH₂CH₂OMe)]₂ R = ^tBu (**1.1**), ⁱBu (**1.2**), and Et (**1.3**) has been prepared. The effects of steric bulk at the Lewis base donor can be observed from the ⁿBu substituted derivatives [R₂Al(μ-OCH₂CH₂OⁿBu)]₂ R = ^tBu (**1.4**) and Me (**1.5**), while the effects of variation in the ligand backbone chain length are observed from comparison with [R₂Al(μ-OCH₂CH₂CH₂OMe)]₂, R = ^tBu (**1.6**) and Me (**1.7**).

Compounds **1.1** - **1.7** were prepared by the reaction of the appropriate ether alcohol with either AlR_3 (Eqs. 1. 2 and 1.3) or $(^i\text{Bu})_2\text{AlH}$ (Eq. 1.4).



Compounds **1.1** - **1.7** have been characterized by ^1H , ^{13}C and ^{27}Al NMR, MS, and solution molecular weight (see Experimental and below). The solid state molecular structures of compounds **1.1**, **1.2**, **1.6** and **1.7** have been determined by X-ray crystallography.

The molecular structures of $[(^t\text{Bu})_2\text{Al}(\mu\text{-OCH}_2\text{CH}_2\text{OMe})]_2$ (**1.1**) and $[(^i\text{Bu})_2\text{Al}(\mu\text{-OCH}_2\text{CH}_2\text{OMe})]_2$ (**1.2**) are shown in Figure 1.1; selected bond lengths and angles are given in Table 1.1 along with those previously reported for $[\text{Me}_2\text{Al}(\mu\text{-OCH}_2\text{CH}_2\text{OMe})]_2$ (**IV**).⁹ Both compounds **1.1** and **1.2** exist as centrosymmetric dimers with no significant intermolecular contacts. The bond lengths within the Al_2O_2 cores are similar, and the internal Al_2O_2 cycle's angles show only a slight variation, see Table 1.1. The geometry about aluminum in compounds **1.1**, **1.2**, and $[\text{Me}_2\text{Al}(\mu\text{-OCH}_2\text{CH}_2\text{OMe})]_2$ is significantly different from the tetrahedral ideal that is observed for simple alkoxide compounds, $[\text{R}_2\text{Al}(\mu\text{-OR}')]_2$,¹⁰ and is essentially that of distorted trigonal bipyramidal with the sum of the bond angles between the equatorial ligands being 354.5° in **1.1**, 355.8° in **1.2**, and 358.4° in $[\text{Me}_2\text{Al}(\mu\text{-OCH}_2\text{CH}_2\text{OMe})]_2$.

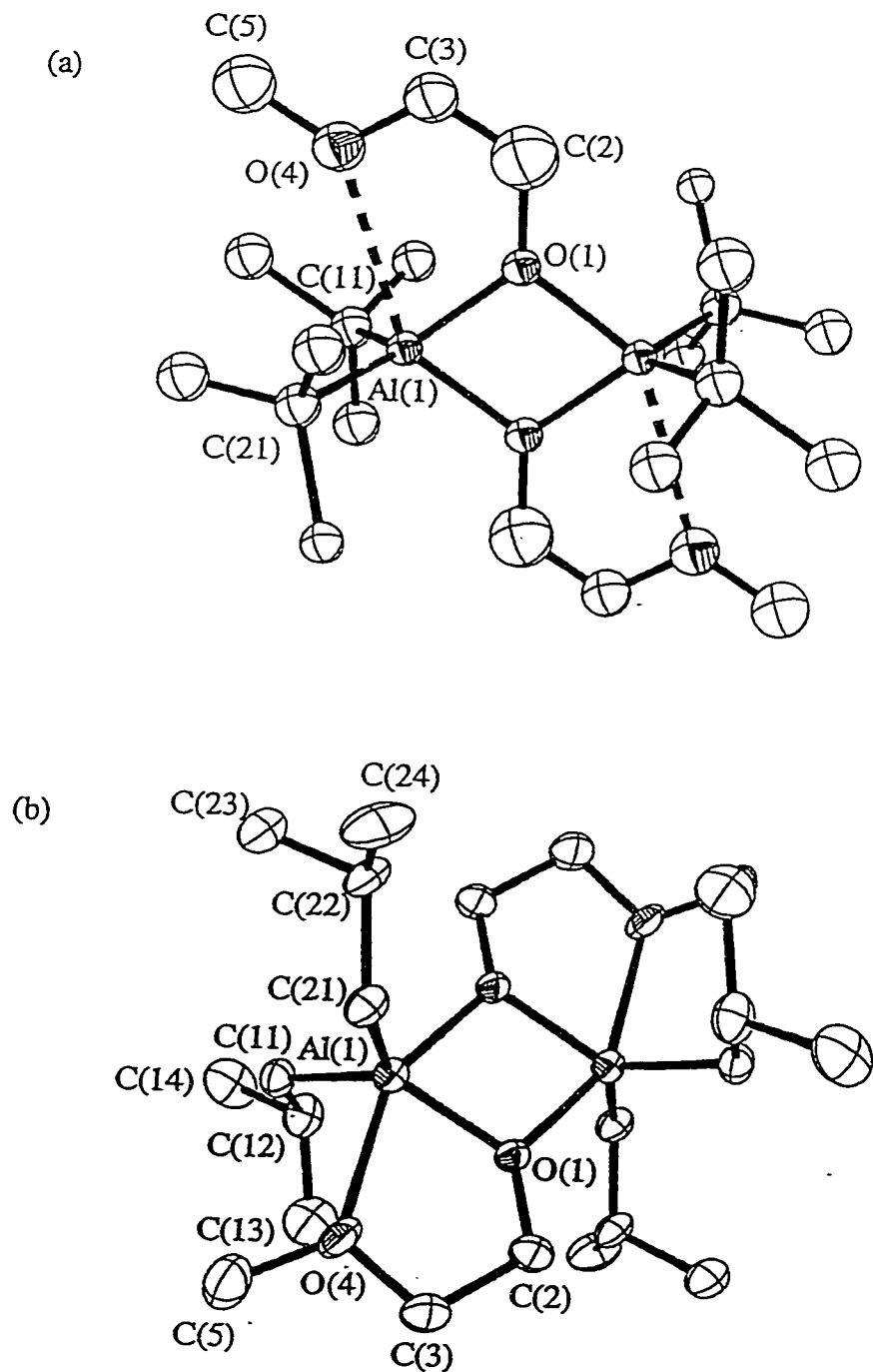


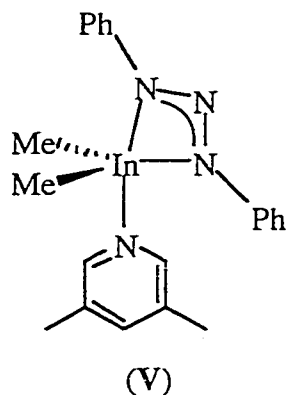
Figure 1.1. Molecular structures of (a) $[({}^t\text{Bu})_2\text{Al}(\mu-\text{OCH}_2\text{CH}_2\text{OMe})]_2$ (**1.1**) and (b) $[({}^i\text{Bu})_2\text{Al}(\mu-\text{OCH}_2\text{CH}_2\text{OMe})]_2$ (**1.2**). Hydrogen atoms are omitted; and only one set of the disordered positions of the methyl groups attached to C(11) and C(21) in compound **1.1** is shown, for clarity.

Table 1.1. Selected Bond Lengths (\AA) and Angles ($^\circ$) in $[\text{R}_2\text{Al}(\mu\text{-OCH}_2\text{CH}_2\text{OMe})]_2$.

R	^t Bu (1.1)	ⁱ Bu (1.2)	Me ^a
Al(1)-O(1)	1.82(1)	1.840(2)	1.827(3)
Al(1)-O(1a)	1.890(6)	1.909(1)	1.892(3)
Al(1)-C(11)	2.03(2)	1.974(2)	1.940(5)
Al(1)-C(21)	1.98(2)	1.975(3)	1.962(5)
Al(1)-O(4)		2.283(2)	2.269(3)
O(1)-Al(1)-O(1a)	74.8(4)	76.38(7)	76.3
O(1)-Al(1)-O(4)		75.06(9)	75.9
O(1)-Al(1)-C(11)	117.5(7)	122.8(1)	118.2(2)
O(1)-Al(1)-C(21)	119.2(8)	114.7(1)	119.4(2)
O(4)-Al(1)-C(11)		95.2(1)	92.1(2)
O(4)-Al(1)-C(21)		86.9(1)	89.3(2)
C(11)-Al(1)-C(21)	117.8(9)	117.8(9)	120.8(2)
Al(1)-O(1)-Al(1a)	105.2(6)	103.62(9)	103.7
Al(1)-O(1)-C(2)	128(2)	123.4(2)	124.6
C(3)-O(4)-C(5)	114(2)	117.1(3)	114.5

^a R. Benn, A. Rufinska, H. Lehmkul, E. Janssen, and C. Krüger, *Angew. Chem., Int. Ed. Engl.*, 1983, **22**, 779.

As a consequence of the $\text{Al}(\mu\text{-O})_2\text{Al}$ core the axial O-Al-O angle is significantly decreased from the ideal 180° (i.e., 144.1° in **1.1**, $151.41(8)^\circ$ in **2**, and 152.2° in $[\text{Me}_2\text{Al}(\mu\text{-OCH}_2\text{CH}_2\text{OMe})]_2$). A similar distortion [$137.1(2)^\circ$] is found in $\text{InMe}_2(\text{dpt})(\text{py-3,5-Me}_2)$ (**V**) in which the small *trans*-axial angle is due to the chelating 1,3-diphenyltriazenide ligand.¹¹



Despite the larger steric bulk, as defined by the Tolman cone angle,¹² of the *tert*-butyl ($\theta = 126^\circ$) and *iso*-butyl ($\theta = 108^\circ$) groups compared to methyl ($\theta = 90^\circ$), the overall structure of compounds **1.1** and **1.2** are remarkably similar to their methyl analog, $[\text{Me}_2\text{Al}(\mu\text{-OCH}_2\text{CH}_2\text{OMe})]_2$.⁹ The only significant difference between these three structures is the extent of the axial Al···O_(ether) interaction. In compound **1.2** and $[\text{Me}_2\text{Al}(\mu\text{-OCH}_2\text{CH}_2\text{OMe})]_2$ this interaction [2.283(2) and 2.269(3) Å, respectively] is longer than ordinary dative Lewis acid-base interactions (1.90 - 2.02 Å),¹³ but significantly shorter than in compound **1.1**, where the Al(1)···O(4) distance (2.74 Å) is close to the limits of a van der Waal interaction. We propose that the orientation of the ether moiety in compound **1.1** is due to a real (albeit weak) interaction, or solvation, in the solid state as opposed to being a consequence of crystal packing forces because of the following observations: (a) the similarity of the geometry about aluminum, between the above compounds (b) variable temperature NMR data (see below). As can be seen from Figure 1.2 the extent of the axial Al···O_(ether) interaction is dependent on the steric bulk of the aluminum alkyl, as measured by the Tolman cone angle (θ).¹² Similar values are observed in the structurally related 2-methoxy phenoxide compounds, $[\text{R}_2\text{Al}(\mu\text{-OC}_6\text{H}_4\text{-2-OMe})]_2$ (**VI**), reported by Oliver¹⁴ and Schumann,¹⁵ values for which are also included in Figure 1.2.

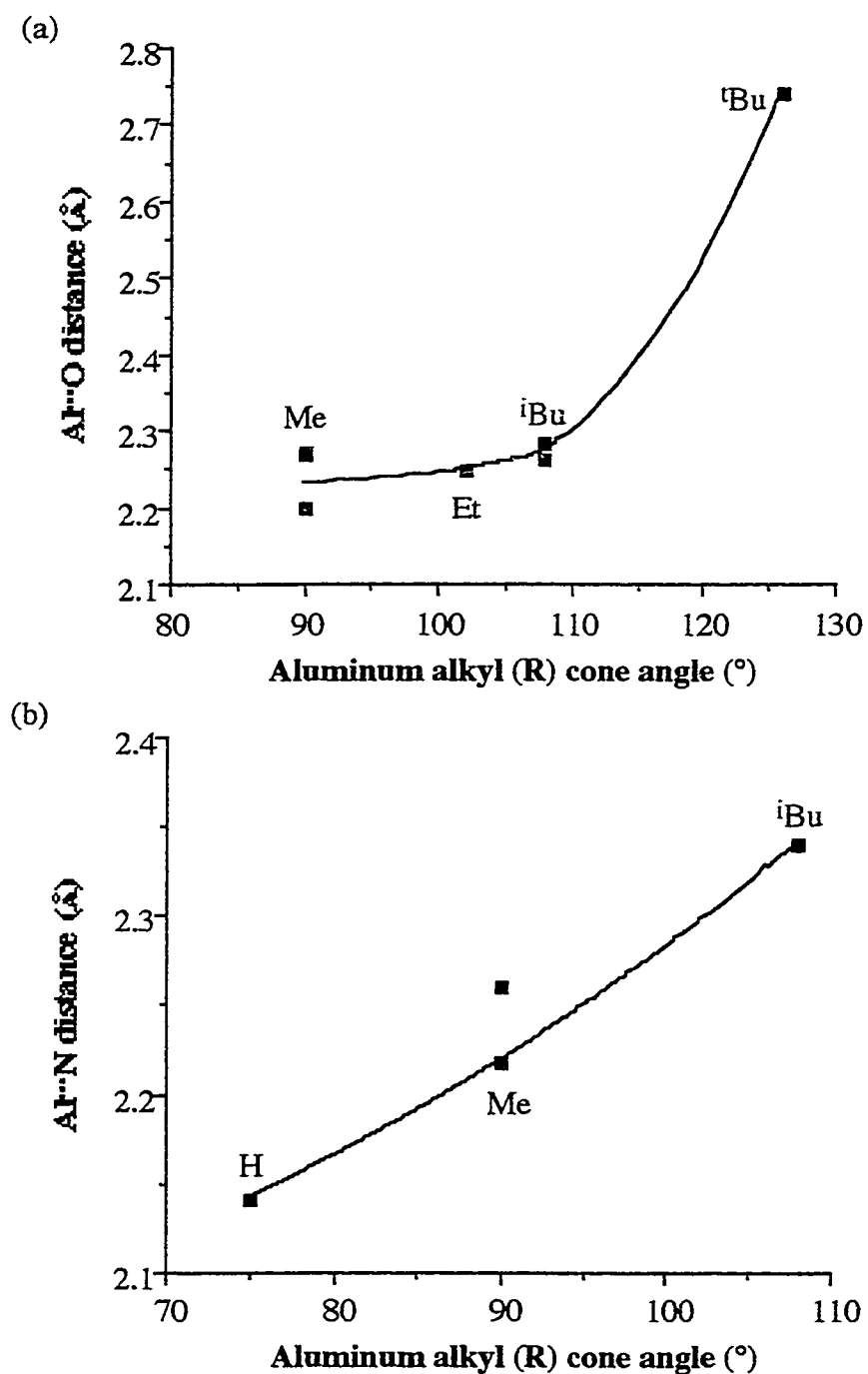
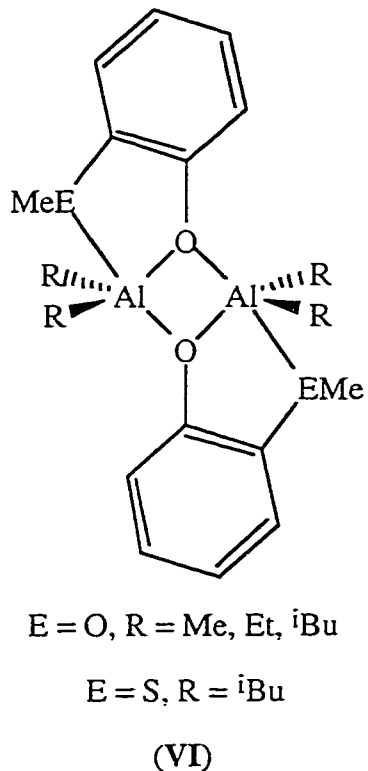


Figure 1.2. Plot of (a) the Al···O_(ether) bond distance (Å) in $[R_2Al(\mu\text{-OCH}_2CH_2OMe)]_2$ and (b) the Al···N bond distance (Å) in $[R_2Al(\mu\text{-OCH}_2CH_2NMe_2)]_2$ ⁶ as a function of the aluminum alkyl (R) cone angle (°). The value for $[R_2Al(\mu\text{-OC}_6H_4\text{-}2\text{-OMe})]_2$ and $[Me_2Al\{\mu\text{-OC(OMe)}=\text{C(H)NMe}_2\}]_2$, are shown (■) for comparison in 1.2 (a) and 1.2(b) respectively.



The extent of the $Al \cdots O_{(ether)}$ interactions only varies slightly for compounds with aluminum alkyl substituents sterically less demanding than *iso*-butyl ($\theta = 108^\circ$). This suggests that either the steric bulk of Me, Et, and *i*Bu are not as dissimilar as ordinarily envisioned, or that the $Al \cdots O$ distance is controlled by the following factors: (a) the ring strain within the AlO_2C_2 cycle, (b) the essentially p-character of the axial environment about the aluminum,¹⁶ and (c) the *trans*-influence of the bridging alkoxide ligand.¹⁷ For compounds with aluminum alkyl substituents larger than *iso*-butyl, the ether $Al \cdots O$ interaction is clearly determined by the steric repulsion between the MeO group and the two aluminum alkyls.

The molecular structures of $[({}^tBu)_2Al(\mu-OCH_2CH_2CH_2OMe)]_2$ (**1.6**) and $[Me_2Al(\mu-OCH_2CH_2CH_2OMe)]_2$ (**1.7**) are shown in Figure 1.3; selected bond lengths and angles are given in Table 1.2.

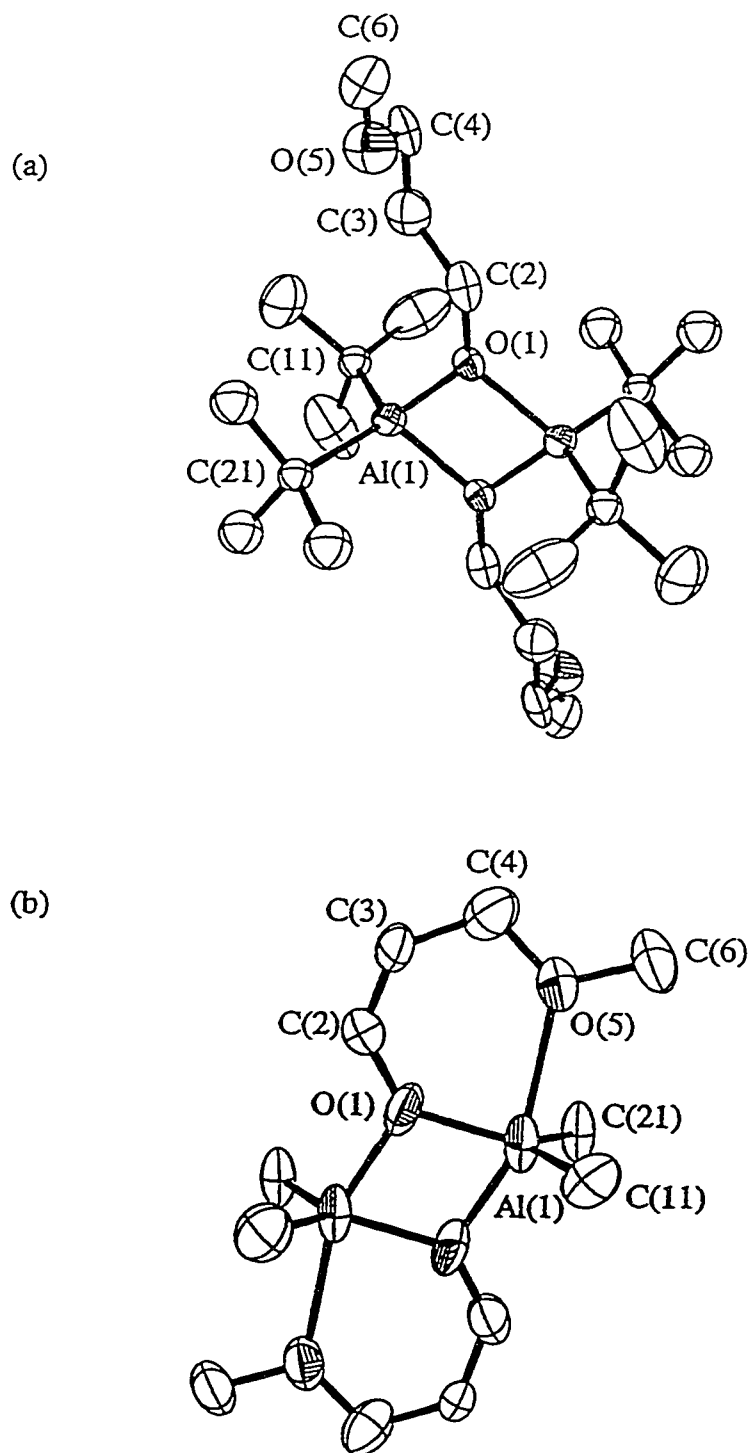


Figure 1.3. Molecular structures of (a) $[({}^t\text{Bu})_2\text{Al}(\mu\text{-OCH}_2\text{CH}_2\text{CH}_2\text{OMe})]_2$ (**1.6**) and (b) $[\text{Me}_2\text{Al}(\mu\text{-OCH}_2\text{CH}_2\text{CH}_2\text{OMe})]_2$ (**1.7**). Hydrogen atoms are omitted, and only one set of the disordered positions of the methyl groups attached to C(11) and C(21) in compound **1.6** is shown, for clarity.

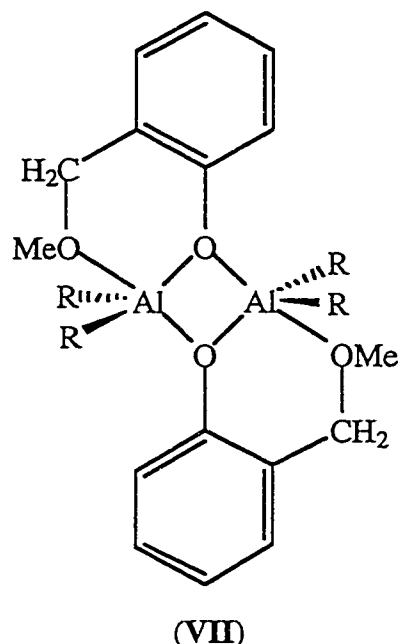
Table 1.2. Selected Bond Lengths (\AA) and Angles ($^\circ$) in $[\text{R}_2\text{Al}(\mu\text{-OCH}_2\text{CH}_2\text{CH}_2\text{OMe})]_2$,
 $\text{R} = ^t\text{Bu}$ (1.6), Me (1.7).

	$[(^t\text{Bu})_2\text{Al}(\mu\text{-OCH}_2\text{CH}_2\text{CH}_2\text{OMe})]_2$ (1.6)	$[\text{Me}_2\text{Al}(\mu\text{-OCH}_2\text{CH}_2\text{CH}_2\text{OMe})]_2$ (1.7)
Al(1)-O(1)	1.844(5)	1.78(1)
Al(1)-O(1a)	1.852(2)	1.87(2)
Al(1)-C(11)	2.005(7)	1.95(4)
Al(1)-C(21)	1.999(8)	1.96(3)
Al(1)-O(5)	n/a	2.39(2)
O(1)-Al(1)-O(1a)	78.4(2)	74.9(8)
O(1)-Al(1)-C(11)	116.7(3)	118(2)
O(1)-Al(1)-C(21)	114.1(3)	119(1)
C(11)-Al(1)-C(21)	116.2(3)	122.5(9)
O(1)-Al(1)-O(5)	n/a	83.9(7)
Al(1)-O(1)-Al(1a)	101.6(2)	105.1(8)
Al(1)-O(1)-C(2)	132.1(4)	121(1)

In contrast to $[(^t\text{Bu})_2\text{Al}(\mu\text{-OCH}_2\text{CH}_2\text{OMe})]_2$ (1.1) the structure of compound 1.6 shows no evidence for any intramolecular interaction between the ether oxygen and the aluminum center [$\text{Al}(1)\cdots\text{O}(5) > 5.1 \text{ \AA}$]. This lack of fifth ligand interaction in $[(^t\text{Bu})_2\text{Al}(\mu\text{-OCH}_2\text{CH}_2\text{CH}_2\text{OMe})]_2$ is highlighted by (a) the greater tetrahedral like coordination about Al(1) in compound $[(^t\text{Bu})_2\text{Al}(\mu\text{-OCH}_2\text{CH}_2\text{CH}_2\text{OMe})]_2$ than observed for $[\text{R}_2\text{Al}(\mu\text{-OCH}_2\text{CH}_2\text{OMe})]_2$ [R = $t\text{Bu}$ (1.1), $i\text{Bu}$ (1.2), Me], see Tables 1.1 and 1.2, and

(b) the orientation of the $\text{OCH}_2\text{CH}_2\text{CH}_2\text{OMe}$ chain away from the Al_2O_2 core, see Figure 1.3a. As can be seen from Figure 1.3b, the structure of $[\text{Me}_2\text{Al}(\mu-\text{OCH}_2\text{CH}_2\text{OMe})_2]_2$ (**1.7**) shows intramolecular interaction between the ether oxygen and the aluminum center [$\text{Al}(1)\text{-O}(5)$ 2.39(2) Å]. However, this interaction is significantly larger than that observed for $[\text{Me}_2\text{Al}(\mu-\text{OCH}_2\text{CH}_2\text{OMe})_2]$, see Tables 1.1 and 1.2.

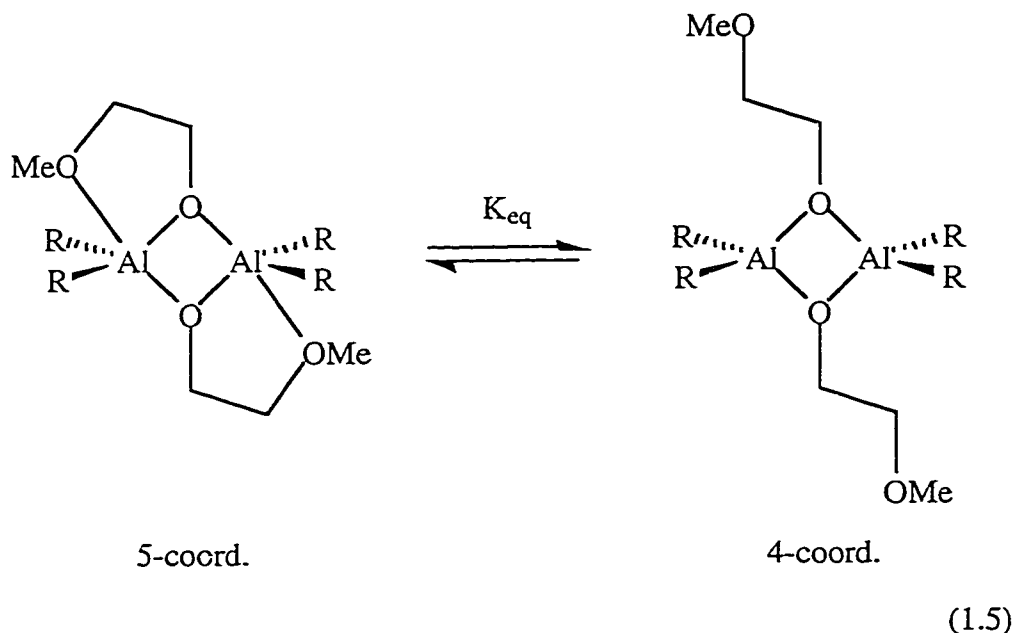
The decrease in $\text{Al}\cdots\text{O}_{\text{ether}}$ interaction upon increasing the carbon chain from C_2 in compound $[\text{R}_2\text{Al}(\mu-\text{OCH}_2\text{CH}_2\text{OMe})_2]$ to C_3 in $[\text{R}_2\text{Al}(\mu-\text{OCH}_2\text{CH}_2\text{CH}_2\text{OMe})_2]$ is in accord with the longer Al-O distances reported for $[\text{Me}_2\text{Al}(\mu-\text{OC}_6\text{H}_4-2\text{-OMe})_2]$, i.e., [**VI**, 2.198(3) Å] and $[\text{Me}_2\text{Al}(\mu-\text{OC}_6\text{H}_4-2\text{-CH}_2\text{OMe})_2]$ [**VII**, 2.572(2) Å] in which the intramolecular coordination results in 5-membered and 6-membered cycles, respectively. This difference may be due to the combination of two effects. First, an increased strain about the aluminum atom is incurred by the formation of an $\text{Al}\cdots\text{O}$ bond within a 6-membered $\text{Al}-\text{O}-\text{C}-\text{C}-\text{C}-\text{O}$ cycle in which the intra-cyclic angle would be ideally 120° , while that in 5-membered $\text{Al}-\text{O}-\text{C}-\text{C}-\text{O}$ cycle is 108° . These values may be compared to the ideal of 90° required in a trigonal bipyramidal structure between the axial and equatorial ligands.



Second, in the 6-membered ring the MeO substituent is pushed closer to the aluminum alkyl groups, resulting in increased steric repulsion and hence a longer Al···O_(ether) interaction.

The presence of dimeric alkoxide bridged structures as opposed to monomeric structures (i.e., **II** and **III** versus **I**) for the ether-alkoxides is expected since it has been previously shown that Et₂O does not cleave alkoxide bridges in compounds of the general formula, [R₂Al(μ-OR')]₂.¹⁸ From the crystallographic data the intramolecular coordination of the ether is controlled by the steric bulk on the aluminum as well as the length of the carbon back-bone (n). It is common to assume that solid state structures are representative of those in solution. However, molecular weight measurements confirm dimeric structures in solution, and it is desirable to have a probe that directly allows determination of structural information in solution, i.e., the extent of coordination of the ether moiety.

For any dimeric 2-methoxyethoxide compound the extent to which the four-coordinate isomer (4-coord.) exists relative to the five-coordinate isomer (5-coord.) is dictated by the equilibrium shown in Eq. 1.5, and can be quantified by its equilibrium constant, K_{eq} (Eq. 1.6). Similar equilibria are possible for the 3-methoxypropoxide and 2-butoxyethoxide compounds. It is desirable to answer the following questions: Is intramolecular coordination maintained in solution? If not, is there an equilibrium process between coordinated (**III**) and uncoordinated (**II**) species? How is that equilibrium, as measured by K_{eq}, affected by the chelate ring size (n), the steric bulk at the aluminum center (R) and the steric bulk of the ether ligand (R')? In order to answer these questions, the coordination number of the aluminum and hence the presence or extent of any intramolecular Al···O coordination (i.e., **II** versus **III**) must be determined by spectroscopic methods. In this regard we have investigated the solution NMR of the ether-alkoxide compounds of aluminum, [R₂Al{μ-O(CH₂)_nOR'}]₂.



$$K_{eq} = \frac{[4\text{-coord.}]}{[5\text{-coord.}]} \quad (1.6)$$

Ashe *et al.*¹⁹ have shown that the temperature-dependent equilibrium constants (K_{eq}) for equilibria between 3- and 4-coordinate boratabenzene complexes may be determined from ^{11}B NMR spectra. Similarly, the presence of four or five-coordinate aluminum may be, in principle, determined by the use of ^{27}Al NMR spectroscopy. Conventional wisdom suggests that the chemical shifts (δ) are dependent on the coordination number (6-coordinate ≈ 0 ppm; 5-coordinate ≈ 50 ppm; 4-coordinate $= 70 - 200$ ppm; 3-coordinate $= 200 - 300$ ppm), while the line width ($W_{1/2}$) is ordinarily correlated with the symmetry about aluminum.⁹ Unfortunately, counter to this simplified view, the chemical shift of a signal in the ^{27}Al NMR spectrum is also dependent on the chemical environment about aluminum, i.e., the identity of the ligand donor atoms.²⁰ In principle this issue may be mitigated through the study of a homologous series of compounds such as those discussed herein. As can be seen from Table 1.3, the ^{27}Al NMR chemical shifts for $[\text{R}_2\text{Al}(\mu\text{-OCH}_2\text{CH}_2\text{OMe})]_2$, R = ^tBu (1.1), ^iBu (1.2), and Et (1.3), and

$[\text{Me}_2\text{Al}(\mu\text{-OCH}_2\text{CH}_2\text{O}^n\text{Bu})]_2$ (**1.5**) are essentially the same within experimental error (120 - 123 ppm), and the same as the value previously reported for $[\text{Me}_2\text{Al}(\mu\text{-OCH}_2\text{CH}_2\text{OMe})]_2$ (121 ppm),⁹ suggesting that they are isostructural in solution.

Table 1.3. Selected room temperature solution ^{27}Al spectral data.

Compound	^{27}Al	
	δ (ppm)	$W_{1/2}$ (Hz)
$[(^t\text{Bu})_2\text{Al}(\mu\text{-OCH}_2\text{CH}_2\text{OMe})]_2$ (1.1)	123	4560
$[(^i\text{Bu})_2\text{Al}(\mu\text{-OCH}_2\text{CH}_2\text{OMe})]_2$ (1.2)	123	7210
$[\text{Et}_2\text{Al}(\mu\text{-OCH}_2\text{CH}_2\text{OMe})]_2$ (1.3)	120	3590
$[\text{Me}_2\text{Al}(\mu\text{-OCH}_2\text{CH}_2\text{OMe})]_2$ ^a	121	1830
$[(^t\text{Bu})_2\text{Al}(\mu\text{-OCH}_2\text{CH}_2\text{O}^n\text{Bu})]_2$ (1.4)	140	7700
$[\text{Me}_2\text{Al}(\mu\text{-OCH}_2\text{CH}_2\text{O}^n\text{Bu})]_2$ (1.5)	126	5940
$[(^t\text{Bu})_2\text{Al}(\mu\text{-OCH}_2\text{CH}_2\text{CH}_2\text{OMe})]_2$ (1.6)	134	2730
$[\text{Me}_2\text{Al}(\mu\text{-OCH}_2\text{CH}_2\text{CH}_2\text{OMe})]_2$ (1.7)	144	6560
$[(^t\text{Bu})_2\text{Al}(\mu\text{-O}^n\text{Bu})]_2$ (1.8)	137	5880
$[(^i\text{Bu})_2\text{Al}(\mu\text{-O}^n\text{Bu})]_2$ (1.9)	150	5500
$[\text{Et}_2\text{Al}(\mu\text{-O}^n\text{Bu})]_2$ (1.10)	149	4770
$[\text{Me}_2\text{Al}(\mu\text{-O}^n\text{Bu})]_2$ ^b	149	2110

^a R. Benn, A. Rufinska, H. Lehmkul, E. Janssen, and C. Krüger, *Angew. Chem., Int. Ed. Engl.*, 1983, **22**, 779.

^b J. H. Rogers, A. W. Applett, W. M. Cleaver, A. N. Tyler, and A. R. Barron, *J. Chem. Soc., Dalton Trans.*, 1992, 3179.

In contrast, $[(t\text{Bu})_2\text{Al}(\mu\text{-OCH}_2\text{CH}_2\text{O}^n\text{Bu})]_2$ (**1.4**), and $[\text{R}_2\text{Al}(\mu\text{-OCH}_2\text{CH}_2\text{CH}_2\text{OMe})]_2$, $\text{R} = t\text{Bu}$ (**1.6**), Me (**1.7**) exhibit chemical shifts within the range (149 - 137 ppm) observed for the four-coordinate compounds, $[\text{R}_2\text{Al}(\mu\text{-O}^n\text{Bu})]_2$ [$\text{R} = t\text{Bu}$ (**1.8**), $i\text{Bu}$ (**1.9**), Et (**1.10**), Me,²¹ see Experimental].

Based on this comparison and the upfield shift for compounds **1.1**, **1.2**, **1.3** and **1.5**, the aluminum centers can be implied to be five-coordinate due to the presence, to some extent, of the intramolecular coordination in solution. However, the chemical shift for compound **1.7** implies a four-coordinate species in solution which is different to that observed in the solid state. In addition, the small shift differences do not allow for any meaningful comparison, in particular of the subtle differences between the structures or the position of possible equilibria in solution. Thus, an alternative structural probe must be used and since neither the alkyl substituent at aluminum (R), nor the Lewis base, are constant, we decided to use the chemical shift of the alkoxide α -carbon (i.e., OCH_2) as the diagnostic group (see Table 1.4). It has been shown that ^1H NMR chemical shifts are not good structural probes since they are affected not only by the bonding environment of the proton, but also by shielding effects and through-space interactions.²² However, ^{13}C NMR spectral shifts are not susceptible to such shielding effects. Based upon previous results,²² an approach has been developed to measure the relative structural trends within a homologous series of compounds.

The ^{13}C NMR spectra of all complexes, $[\text{R}_2\text{Al}\{\mu\text{-O}(\text{CH}_2)_n\text{OR}'\}]_2$, show a single, sharp resonance due to the OCH_2 group over all the temperature ranges measured, indicating that equilibria is rapid on the NMR time scale. Assuming the ^{13}C NMR shift of the OCH_2 group is directly proportional to the mole fraction of the total species present as the four-coordinate isomer (4-coord.), $\chi_{4\text{-coord}}$, the ^{13}C NMR chemical shift of the OCH_2 , at a given temperature, $\delta_{(\text{obs})}$, may be used to calculate both $\chi_{4\text{-coord}}$ and $\chi_{5\text{-coord}}$, e.g., Eqs. 1.7 and 1.8, respectively.²³

$$\chi_{(4\text{-coord})} = \frac{\delta_{(\text{obs})} - \delta_{(5\text{-coord})}}{\delta_{(4\text{-coord})} - \delta_{(5\text{-coord})}} \quad (1.7)$$

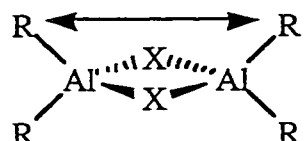
$$\chi_{(5\text{-coord})} = \frac{\delta_{(4\text{-coord})} - \delta_{(\text{obs})}}{\delta_{(4\text{-coord})} - \delta_{(5\text{-coord})}} \quad (1.8)$$

K_{eq} (Eq. 1.6) can be defined by Eq. 1.9.

$$K_{\text{eq}} = \frac{\chi_{(4\text{-coord})}}{\chi_{(5\text{-coord})}} \quad (1.9)$$

The same general method was used by Ashe *et al.*,¹⁹ however, in the present case the asymptotic values at high and low temperatures appear to be different for compounds with different alkyl substituents on aluminum (R). In addition, not all the compounds reach an asymptotic value at both temperatures. Thus, a modification of this method is needed to estimate the chemical shifts for $\delta_{(4\text{-coord})}$ and $\delta_{(5\text{-coord})}$ for compounds with each alkyl group, R.

We have previously reported²⁴ that in aluminum compounds of the general formula, $[\text{R}_2\text{Al}(\mu\text{-X})]_2$, the Al-X-Al angle is directly proportional to the steric bulk of the alkyl ligand as measured by the Tolman cone angle. This trend is as a consequence of steric repulsion between the alkyl groups on adjacent aluminum centers, i.e., **VIII**.²⁵



(VIII)

Thus, for a series of the homologous four-coordinate compounds, $[R_2Al(\mu-O^nBu)]_2$ for R = t Bu (**1.8**), i Bu (**1.9**), Et (**1.10**) and Me,²¹ the Al-O-Al angle would be proportional to the steric bulk of the alkyl ligand (R). It has been shown that ^{13}C NMR spectral shifts may be used as a probe of the C-Al-C angle in $Me_3Al(PR_3)$ complexes.^{22,26} Consequently, it stands to reason that in an analogous manner, the ^{13}C NMR chemical shift of the OCH_2 in $[R_2Al(\mu-O^nBu)]_2$ should be dependent on the Al-O-Al bond angle and hence the cone angle of the alkyl ligand. As can be seen in Figure 1.4 this is indeed observed.

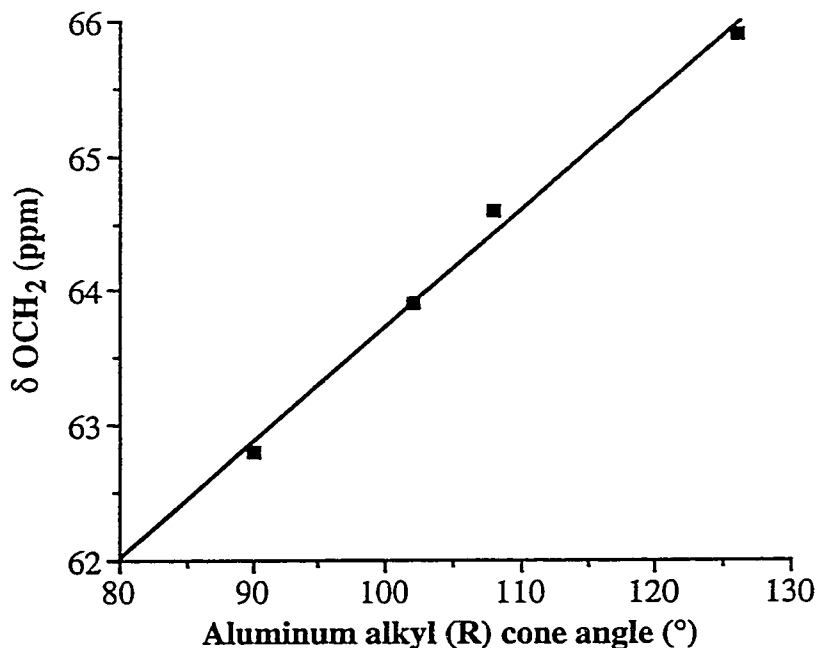


Figure 1.4. Plot of the ^{13}C NMR shift of the OCH_2 carbon as a function of the Tolman cone angle (θ , $^{\circ}$) for the aluminum substituents (R) in $[R_2Al(\mu-O^nBu)]_2$ (Line fit = 0.992).

The ^{13}C NMR chemical shift values for OCH_2 in $[R_2Al(\mu-O^nBu)]_2$ may be used as a good estimates for the values of $\delta_{(4\text{-coord})}$ in $[R_2Al\{\mu-O(CH_2)_nOR'\}]_2$, $[R_2Al\{\mu-O(CH_2)_nSR'\}]_2$ and $[R_2Al\{\mu-O(CH_2)_nNR'2\}]_2$ ⁶ since the high temperature values for the

tert-butyl derivatives are close to that of $[(^t\text{Bu})_2\text{Al}(\mu-\text{O}^n\text{Bu})]_2$ (1.8). In contrast, the lack of suitable model compounds for the five-coordinate structures of $[\text{R}_2\text{Al}\{\mu-\text{O}(\text{CH}_2)_n\text{OR}'\}]_2$, $[\text{R}_2\text{Al}\{\mu-\text{O}(\text{CH}_2)_n\text{SR}'\}]_2$ and $[\text{R}_2\text{Al}\{\mu-\text{O}(\text{CH}_2)_n\text{NR}'_2\}]_2$ ⁶ requires a different estimate of the value of $\delta_{(5\text{-coord})}$ for each alkyl substituent. At the lowest temperatures for Me and Et derivatives the ^{13}C NMR chemical shift values reach an asymptote. As per Ashe *et al.*,¹⁹ we propose that these values can be used directly. However the ^iBu and ^tBu derivatives do not reach an asymptote, so assuming the Al-O-Al bond angle and therefore ^{13}C NMR chemical shift for OCH_2 in five-coordinate compounds is linearly dependent on the steric bulk of R, then an estimate of the asymptotic values for ^iBu and ^tBu derivatives may be made from the extrapolation of the values of Me and Et compounds. Therefore, the ^{13}C NMR chemical shift values for $[\text{R}_2\text{Al}(\mu-\text{O}^n\text{Bu})]_2$ may be used for the four-coordinate chemical shift [i.e., $\delta_{(4\text{-coord})}$], and the extrapolation of the low temperature data for the Me and Et compounds gives the five-coordinate chemical shift limit [i.e., $\delta_{(5\text{-coord})}$]. Based on these data K_{eq} values may be calculated. This approach may be generally applied to a number of systems.

From the values in Table 1.4, it is clear that as expected the equilibrium (Eq. 1.5) is shifted towards the dissociation of the neutral Lewis base termini (OR') with increased steric bulk at the aluminum center (R). The correlation of K_{eq} with the cone angle (θ) for the aluminum alkyl (R) in $[\text{R}_2\text{Al}(\mu-\text{OCH}_2\text{CH}_2\text{OMe})]_2$ is shown in Figure 1.5a, and should be compared to the relationship of the Al...O_(ether) bond distance with cone angle shown in Figure 1.2. Similarly, an increased steric bulk of the ether ligand (R'), also results in a shift in the equilibrium towards dissociation of the ether ligand. Thus, the K_{eq} observed for $[\text{R}_2\text{Al}(\mu-\text{OCH}_2\text{CH}_2\text{O}^n\text{Bu})]_2$ (R = Me, ^tBu) is greater than for the analogous compounds $[\text{R}_2\text{Al}(\mu-\text{OCH}_2\text{CH}_2\text{OMe})]_2$. An increase in the potential chelate ring size (i.e., from n = 2 in $[\text{R}_2\text{Al}(\mu-\text{OCH}_2\text{CH}_2\text{OMe})]_2$ to n = 3 in $[\text{R}_2\text{Al}(\mu-\text{OCH}_2\text{CH}_2\text{CH}_2\text{OMe})]_2$) results in a general increase in the K_{eq} , consistent with the increased Al...O_(ether) distance, see above.

Based on the above results we can show that the ether moiety of the ether-alkoxide ligand in $[R_2Al\{\mu-O(CH_2)_nOR'\}]_2$ is an insufficiently strong Lewis base to cleave the $Al(\mu-OR)_2Al$ unit. However, the ether oxygen complexes to the aluminum forming a 5-coordinate center in which the extent of coordination in the solid state is controlled by the steric bulk of the aluminum alkyls and the ether substituent, and the chelate ring size.

Table 1.4. Selected room temperature solution ^{13}C NMR spectral data and calculated equilibrium constants.

Compound	^{13}C , Al-O <u>CH₂</u>	K_{eq}^a
$[(tBu)_2Al(\mu-OCH_2CH_2OMe)]_2$ (1.1)	64.7	4.00
$[(iBu)_2Al(\mu-OCH_2CH_2OMe)]_2$ (1.2)	60.1	0.236
$[Et_2Al(\mu-OCH_2CH_2OMe)]_2$ (1.3)	59.5	0.176
$[Me_2Al(\mu-OCH_2CH_2OMe)]_2$ ^b (1.4)	58.8	0.160
$[(tBu)_2Al(\mu-OCH_2CH_2O^nBu)]_2$ (1.4)	65.5	> 14.0
$[Me_2Al(\mu-OCH_2CH_2O^nBu)]_2$ (1.5)	59.6	0.450
$[(tBu)_2Al(\mu-OCH_2CH_2CH_2OMe)]_2$ (1.6)	64.1	\approx 4.0
$[Me_2Al(\mu-OCH_2CH_2CH_2OMe)]_2$ (1.7)	61.1	\approx 1.7
$[(tBu)_2Al(\mu-O^nBu)]_2$ (1.8)	65.9	n/a
$[(iBu)_2Al(\mu-O^nBu)]_2$ (1.9)	64.6	n/a
$[Et_2Al(\mu-O^nBu)]_2$ (1.10)	63.9	n/a
$[Me_2Al(\mu-O^nBu)]_2$ ^c	62.8	n/a

^a Equilibrium constant, $K_{eq} = [4\text{-coord.}]/[5\text{-coord.}]$.

^b R. Benn, A. Rufinska, H. Lehmkul, E. Janssen, and C. Krüger, *Angew. Chem., Int. Ed. Engl.* 1983, **22**, 779.

^c J. H. Rogers, A. W. Applett, W. M. Cleaver, A. N. Tyler, and A. R. Barron, *J. Chem. Soc., Dalton Trans.*, 1992, 3179.

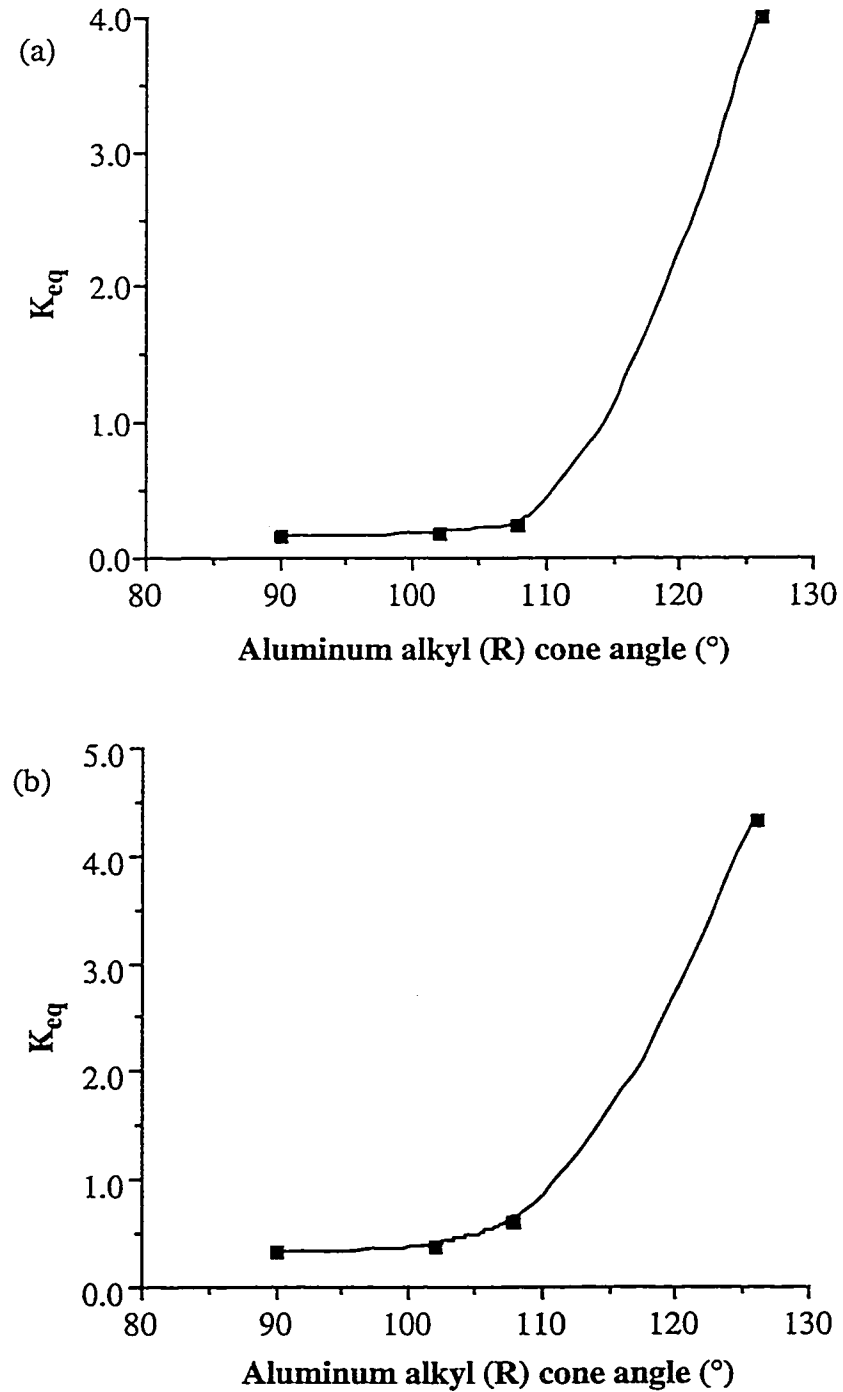
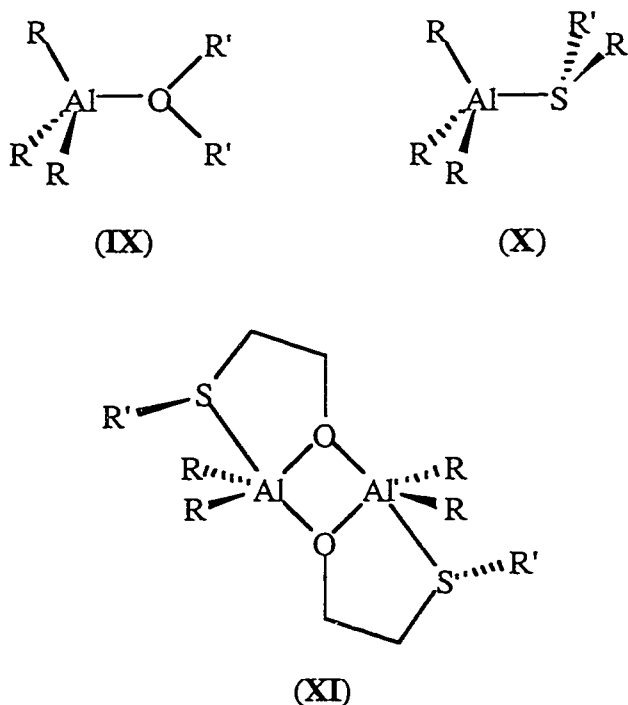


Figure 1.5 Plot of K_{eq} as a function of the aluminum alkyl (R) cone angle (°) in (a) $[R_2Al(\mu-OCH_2CH_2OMe)]_2$, and (b) $[R_2Al(\mu-OCH_2CH_2SMe)]_2$.

Thioether-alkoxide ligands. Thioether complexes of aluminum are ordinarily weaker than their ether analogs,²⁷ and as such represent a suitable comparison to the 2-methoxyethoxide compounds to investigate the effects of a weaker Lewis base donor ligand. However, while thioether complexes of aluminum are isoelectronic to their ether donor analogs, there are a number of differences that may alter the stability and structure of complexes to aluminum. The radius of sulfur (1.85 Å) is significantly larger than oxygen (1.40 Å) resulting in a concomitant increase in Al-E bond length, i.e., Al-S = 2.19 - 2.52 Å versus Al-O = 1.69 - 2.00 Å.²⁸ In addition, while the hybridization at oxygen in R₂O approximates to sp² resulting in a planar geometry in an aluminum complex (e.g., **IX**), the hybridization about sulfur in R₂S results in a pyramidal geometry in the Lewis acid-base complex (e.g., **X**). One consequence of this difference is an increased steric interaction between the alkyl substituent on the thioether (R') and the substituents on the aluminum (R), i.e., **XI** in comparison to **IV**.²⁹



In order to ascertain the effects of the Lewis base donor atom we have prepared the homologous series, $[R_2Al(\mu-OCH_2CH_2SMe)]_2$ R = t^3Bu (**1.11**), i^3Bu (**1.12**), Et (**1.13**), and Me (**1.14**), as a comparison to compounds **1.1 - 1.3** and $[Me_2Al(\mu-OCH_2CH_2OMe)]_2$. The effect of variation in the ligand backbone chain length is observed as compared with $[R_2Al(\mu-OCH_2CH_2CH_2SMe)]_2$, R = t^3Bu (**1.15**) and Me (**1.16**). Compounds **1.11 - 1.16** were prepared and characterized in a manner similar to that employed for their ether analogs (see Experimental). In addition the solid state molecular structures of compounds **1.11**, **1.12** and **1.15** have been determined by X-ray crystallography.

The molecular structures of $[(t^3Bu)_2Al(\mu-OCH_2CH_2SMe)]_2$ (**1.11**) and $[(i^3Bu)_2Al(\mu-OCH_2CH_2SMe)]_2$ (**1.12**) are shown in Figure 1.6; selected bond lengths and angles are given in Table 1.5. The large Al(1)…S(4) distance ($\approx 5.5 \text{ \AA}$), and the orientation of the thioether moieties, and thus the sulfur's lone pairs, in $[(t^3Bu)_2Al(\mu-OCH_2CH_2SMe)]_2$ (**1.11**), are clearly indicative of the lack of an interaction between Al(1) and S(4). This is supported by the distorted tetrahedral geometry about aluminum in compound **1.11** (see Table 1.5) which is typical of alkoxide compounds, $[(t^3Bu)_2Al(\mu-OR)]_2$.³⁰ In contrast, the orientation of the thioether ligands and the Al(1)…S(4) distance (2.95 \AA) in the *iso*-butyl compound (**1.12**) are consistent with some form of bonding interaction. The presence of a fifth coordination site in $[(i^3Bu)_2Al(\mu-OCH_2CH_2SMe)]_2$ is also indicated by the geometry about Al(1) which is essentially that of a distorted trigonal bipyramidal. However, the Al…S interaction is presumably very weak since it is significantly longer than the range observed for simple Lewis acid-base complexes ($2.515 - 2.718 \text{ \AA}$).³¹ Furthermore, if one assumes an increase in covalent radius of between 0.45 and 0.52 \AA in going from oxygen to sulfur, and using the Al-O distance of $2.283(2) \text{ \AA}$ observed in $[(i^3Bu)_2Al(\mu-OCH_2CH_2OMe)]_2$ (**1.2**), a value of $2.74 - 2.80 \text{ \AA}$ would be expected for the Al-S distance in $[(i^3Bu)_2Al(\mu-OCH_2CH_2SMe)]_2$.

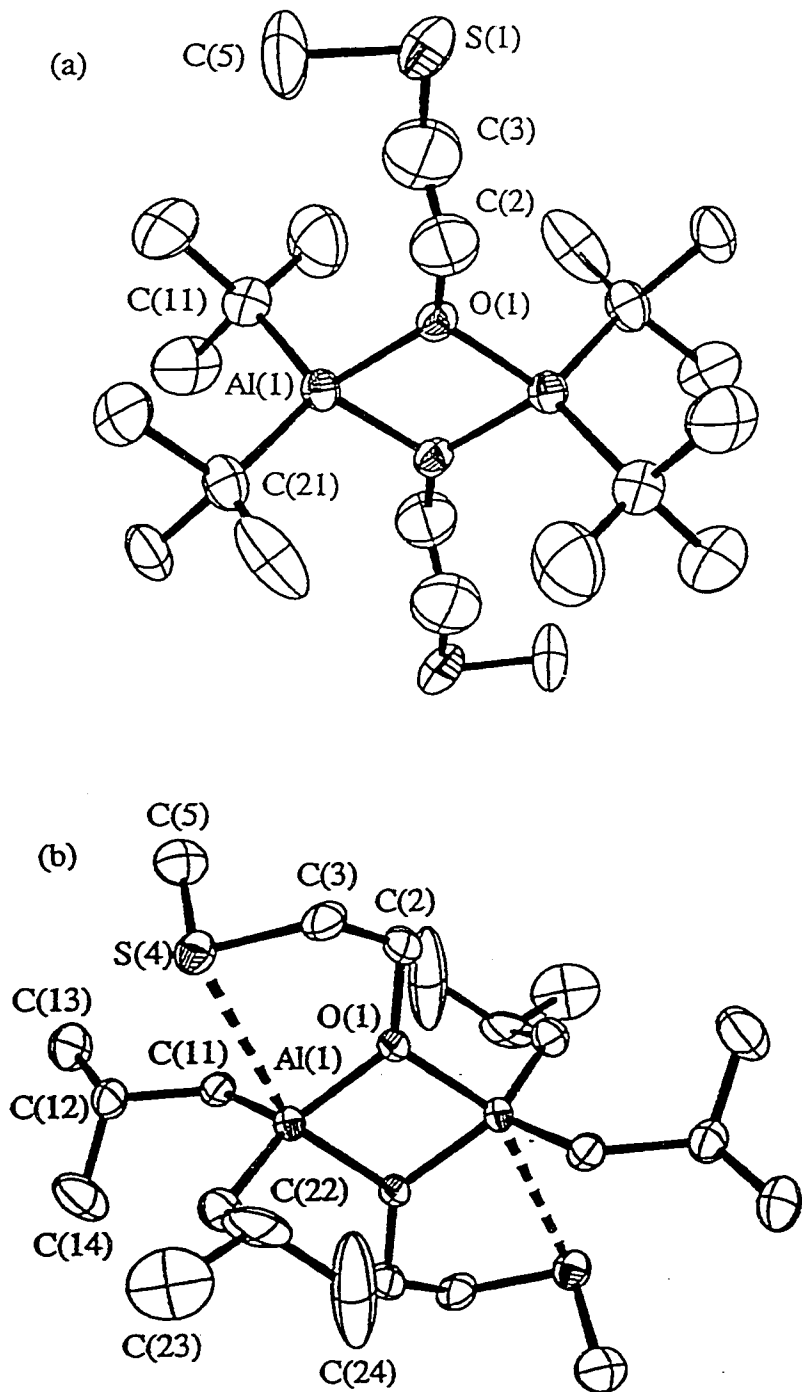


Figure 1.6. Molecular structures of (a) $[(i\text{Bu})_2\text{Al}(\mu\text{-OCH}_2\text{CH}_2\text{SMe})]_2$ (**1.11**) and (b) $[(i\text{Bu})_2\text{Al}(\mu\text{-OCH}_2\text{CH}_2\text{SMe})]_2$ (**1.12**). Hydrogen atoms are omitted, and only one set of the disordered positions of the methyl groups attached to C(21) in compound **1.11** is shown, for clarity.

Table 1.5. Selected Bond Lengths (\AA) and Angles ($^\circ$) in $[(\text{tBu})_2\text{Al}(\mu\text{-OCH}_2\text{CH}_2\text{SMe})]_2$ (**1.11**) and $[(\text{iBu})_2\text{Al}(\mu\text{-OCH}_2\text{CH}_2\text{SMe})]_2$ (**1.12**).

	$[(\text{tBu})_2\text{Al}(\mu\text{-OCH}_2\text{CH}_2\text{SMe})]_2$ (1.11)	$[(\text{iBu})_2\text{Al}(\mu\text{-OCH}_2\text{CH}_2\text{SMe})]_2$ (1.12)
Al(1)-O(1)	1.852(3)	1.841(2)
Al(1)-O(1a)	1.851(2)	1.888(1)
Al(1)-C(11)	1.994(9)	1.973(4)
Al(1)-C(21)	1.984(9)	1.969(4)
Al(1)…S(4)	n/a	2.95(1)
O(1)-Al(1)-O(1a)	78.8(1)	77.31(8)
O(1)-Al(1)-C(11)	113.8(2)	117.2(1)
O(1)-Al(1)-C(21)	114.1(3)	120.2(2)
O(1)-Al(1)-S(4)		
C(11)-Al(1)-C(21)	116.8(3)	118.6(2)
C(11)-Al(1)-S(4)		
Al(1)-O(1)-Al(1a)	101.2(2)	102.7(1)
Al(1)-O(1)-C(2)	131.1(4)	132.8(2)
C(4)-S(5)-C(6)	99.9(6)	101.8(2)

Clearly, the observed Al…S interaction in compound **1.12** is significantly lengthened, being almost a solvation interaction rather than a well defined dative covalent bond. As was observed for the ether derivatives (see above) the extent of the axial Al…S(thioether) interaction is dependent on the steric bulk of the aluminum alkyl; increased steric bulk

results in weaker interactions. However, there also appears to be a dependence on the ligand geometry. Thus, whereas the O-C-C-S unit is planar in $[(^{\text{t}}\text{Bu})_2\text{Al}(\mu\text{-OC}_6\text{H}_4\text{-2-SMe})]_2$ (*cf.*, VI),¹⁴ presumably as a consequence of π -delocalization with the aromatic ring, it is nonplanar in $[(^{\text{t}}\text{Bu})_2\text{Al}(\mu\text{-OCH}_2\text{CH}_2\text{SMe})]_2$. While this change did not appear to greatly affect the relative Al…O interactions in the ether derivatives, the pyramidal geometry about the thioether sulfur means that the change in configuration of the O-C-C-S unit results in the methyl group on the sulfur exhibiting a greater steric repulsion from the aluminum alkyl substituents. This is exhibited by the relative position of the thioether methyl group, C(5), and the *iso*-butyl group, C(11) - C(14), is clearly seen in Figure 1.7a and b. In comparing the thioether ligands to their ether analogs, $[\text{R}_2\text{Al}(\mu\text{-OCH}_2\text{CH}_2\text{EMe})]_2$, it is clear that the Al…E interactions are both influenced by the steric bulk of the aluminum alkyls substituents. This also is apparent in the amine analog⁶ as is seen in Figure 1.7c. The sp^3 hybridization at nitrogen in an aluminum complex results in an increased steric interaction between the alkyl substituent on the amine (R') and the substituents on the aluminum (R). However, while the Al-S distances are expected to be longer than the analogous Al-O distances, the observed structures of compounds of the type $[\text{R}_2\text{Al}(\mu\text{-OCH}_2\text{CH}_2\text{SMe})]_2$ suggests that the orientation of the substituents on the Lewis base also plays an important role.

The molecular structure of $[(^{\text{t}}\text{Bu})_2\text{Al}(\mu\text{-OCH}_2\text{CH}_2\text{CH}_2\text{SMe})]_2$ (**1.15**) is shown in Figure 1.8; selected bond lengths and angles are given in Table 1.6. As with $[(^{\text{t}}\text{Bu})_2\text{Al}(\mu\text{-OCH}_2\text{CH}_2\text{CH}_2\text{OMe})]_2$ (**1.7**) the structure of compound **1.15** shows no evidence for any intramolecular interaction between the thioether sulfur and the aluminum center [Al(1)…S(5) > 5.5 Å]. This lack of fifth ligand interaction is confirmed by the tetrahedral-like coordination about Al(1). The ^{27}Al NMR spectral shifts for compounds **1.11** - **1.16** are to lower field than their ether analogs (Table 1.7 and 1.3, respectively), suggesting a more dissociated complex, i.e., 4-coordinate rather than 5-coordinate. This is supported by the K_{eq} values determined from the ^{13}C data, see Table 1.7.

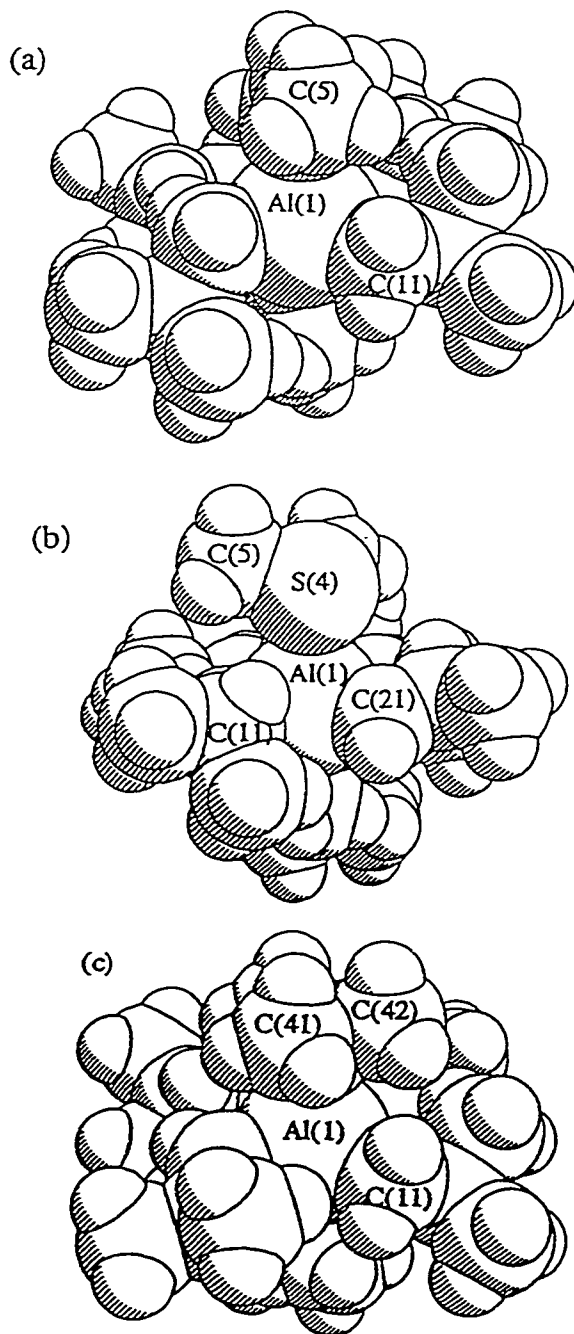


Figure 1.7. Space filling representations of (a) $[({}^i\text{Bu})_2\text{Al}(\mu-\text{OCH}_2\text{CH}_2\text{OMe})]_2$ (**1.2**), (b) $[({}^i\text{Bu})_2\text{Al}(\mu-\text{OCH}_2\text{CH}_2\text{SMe})]_2$ (**1.12**), (c) $[({}^i\text{Bu})_2\text{Al}(\mu-\text{OCH}_2\text{CH}_2\text{NMe}_2)]_2$ respectively showing the different steric interactions of the ether, thioether and amine methyl group with the *i*so-butyl group on aluminum.

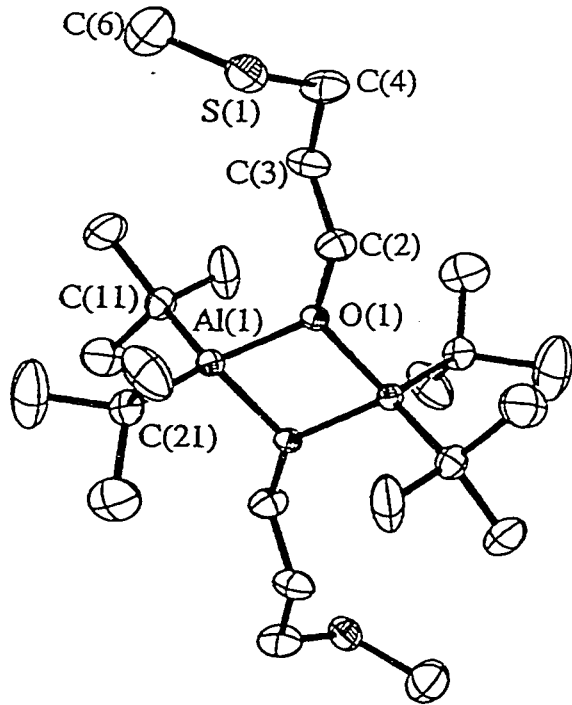


Figure 1.8. Molecular structure of $[(\text{tBu})_2\text{Al}(\mu\text{-OCH}_2\text{CH}_2\text{CH}_2\text{SMe})]_2$ (**1.15**). Thermal ellipsoids are shown at 30% and hydrogen atoms are omitted for clarity.

Table 1.6. Selected Bond Lengths (\AA) and Angles ($^\circ$) in $[(\text{tBu})_2\text{Al}(\mu\text{-OCH}_2\text{CH}_2\text{CH}_2\text{SMe})]_2$ (**1.15**).

Al(1)-O(1)	1.857(2)	Al(1)-C(11)	1.998(3)
Al(1)-C(21)	2.006(3)	O(1)-C(2)	1.459(3)
S(5)-C(4)	1.761(4)	S(5)-C(6)	1.733(5)
O(1)-Al(1)-O(1a)	78.6(1)	O(1)-Al(1)-C(11)	115.1(1)
O(1)-Al(1)-C(21)	114.1(1)	C(11)-Al(1)-C(21)	117.8(1)
Al(1)-O(1)-Al(1a)	101.40(8)	Al(1)-O(1)-C(2)	132.1(2)
C(4)-S(5)-C(6)	101.4(2)		

As with the ether donor ligands, the thioether moiety is an insufficiently strong Lewis base to cleave the $\text{Al}(\mu\text{-OR})_2\text{Al}$ unit, and the equilibrium (*c.f.*, Eq. 1.5) is shifted towards the dissociation of the neutral Lewis base termini (SMe) with increased steric bulk at the aluminum center (R) and increase in the potential chelate ring size (n). The variation of K_{eq} with the cone angle (θ) for the aluminum alkyl (R) in $[\text{R}_2\text{Al}(\mu\text{-OCH}_2\text{CH}_2\text{SMe})]_2$ is shown in Figure 1.5b, and should be compared to the relationship observed for $[\text{R}_2\text{Al}(\mu\text{-OCH}_2\text{CH}_2\text{OMe})]_2$ (Figure 1.5a). The increased K_{eq} for the sulfur analog which indicates a shift towards more dissociated complexes (*i.e.*, **II** versus **III**) for the sulfur versus oxygen donor ligands is consistent with both the increased covalent radius and hybridization of sulfur, discussed above.

Table 1.7. Selected room temperature solution ^{27}Al and ^{13}C NMR spectral data and calculated equilibrium constants.

Compound	^{27}Al		$^{13}\text{C}^{\text{a}}$	K_{eq}^{b}
	δ (ppm)	$W_{1/2}$ (Hz)		
$[(\text{tBu})_2\text{Al}(\mu\text{-OCH}_2\text{CH}_2\text{SMe})]_2$ (1.11)	142	5280	64.5	4.33
$[(\text{iBu})_2\text{Al}(\mu\text{-OCH}_2\text{CH}_2\text{SMe})]_2$ (1.12)	146	6950	60.3	0.605
$[\text{Et}_2\text{Al}(\mu\text{-OCH}_2\text{CH}_2\text{SMe})]_2$ (1.13)	134	5410	59.1	0.370
$[\text{Me}_2\text{Al}(\mu\text{-OCH}_2\text{CH}_2\text{SMe})]_2$ (1.14)	142	3440	58.5	0.324
$[(\text{tBu})_2\text{Al}(\mu\text{-OCH}_2\text{CH}_2\text{CH}_2\text{SMe})]_2$ (1.15)	138	5220	65.1	≈ 8.1
$[\text{Me}_2\text{Al}(\mu\text{-OCH}_2\text{CH}_2\text{CH}_2\text{SMe})]_2$ (1.16)	153	5130	64.4	≈ 5.1

^a Al-OCH_2 .

^b Equilibrium constant, $K_{\text{eq}} = [\text{4-coord.}]/[\text{5-coord.}]$.

Determination of Intramolecular Bond Dissociation Energies. The bond dissociation energies (BDEs) for Lewis acid-base complexes of aluminum have previously been determined from the temperature dependence of the equilibrium constant, K_{eq} (i.e., Eq. 1.10).



Given the temperature dependence of the equilibrium constants for the intramolecular coordination complexes described above, it is reasonable to propose that the enthalpy (ΔH) and entropy (ΔS) for the reaction shown in Eq. 1.5 should be associated with the bond dissociation energy of the intramolecular Lewis acid-base coordination.³²

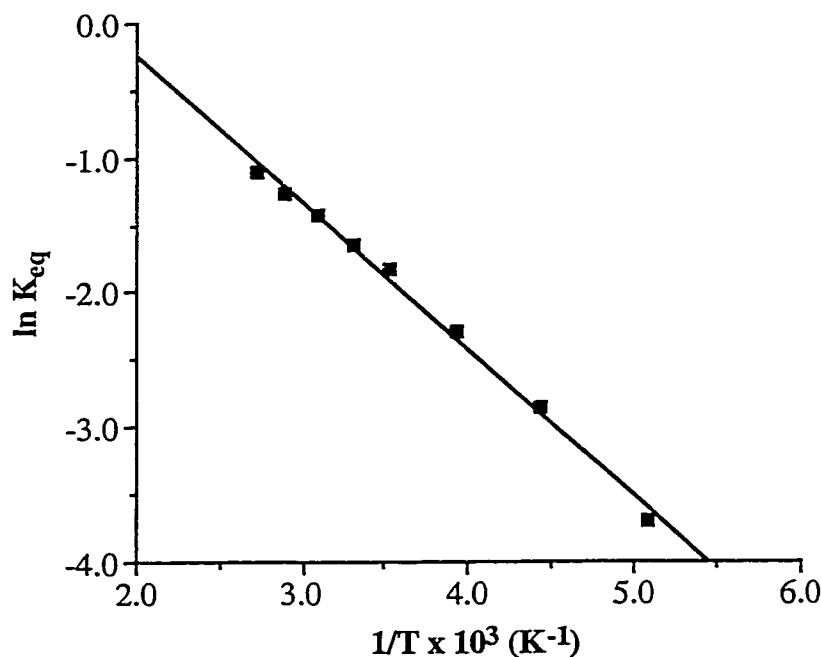


Figure 1.9. Temperature dependence of the equilibrium constant (K_{eq}) for the conversion of the 5-coordinate to 4-coordinate forms of $[\text{Me}_2\text{Al}(\mu-\text{OCH}_2\text{CH}_2\text{OMe})_2]$ ($R = 0.995$).

The temperature dependence of the equilibrium constants for compounds **1.1**, **1.11**, **1.14**, $[(t\text{Bu})_2\text{Al}(\mu\text{-OCH}_2\text{OCH}_2\text{NMe}_2)]_2^6$, $[\text{Me}_2\text{Al}(\mu\text{-OCH}_2\text{CH}_2\text{OMe})]_2^9$, and $[\text{Me}_2\text{Al}(\mu\text{-OCH}_2\text{CH}_2\text{NMe}_2)]_2^1$ was measured, and the ΔH and ΔS values were determined from the appropriate van't Hoff plots, e.g., Figure 1.9.³³ All calculated ΔH and ΔS values are given in Table 1.8, along with the calculated values for ΔG at 298 K. It should be noted that the values calculated directly from the van't Hoff plots are for a single intramolecular interaction, i.e., half the value for the reaction shown in Eq. 1.5. However, since a comparison with monomeric Lewis acid-base complexes is required, the value per intramolecular bond is used in all Tables and the following discussion.

Table 1.8. Selected equilibrium and thermodynamic data.

Compound	K_{eq}^{a} @ 298 K	ΔH (kJ.mol ⁻¹) ^b	ΔS (J.K ⁻¹ .mol ⁻¹) ^b	ΔG @ 298 K (kJ.mol ⁻¹)
$[\text{Me}_2\text{Al}(\mu\text{-OCH}_2\text{CH}_2\text{OMe})]_2^{\text{c}}$	0.179	9.1(6)	16(2)	4.3
$[\text{Me}_2\text{Al}(\mu\text{-OCH}_2\text{CH}_2\text{SMe})]_2$ (1.14)	0.456	13.2(2)	37.7(5)	1.9
$[\text{Me}_2\text{Al}(\mu\text{-OCH}_2\text{CH}_2\text{NMe}_2)]_2^{\text{d}}$	0.275	7.4(5)	14(2)	3.2
$[(t\text{Bu})_2\text{Al}(\mu\text{-OCH}_2\text{CH}_2\text{OMe})]_2$ (1.1)	4.236	5.2(4)	29(1)	-3.4
$[(t\text{Bu})_2\text{Al}(\mu\text{-OCH}_2\text{CH}_2\text{SMe})]_2$ (1.11)	4.972	4.94(2)	29.9(1)	-3.9
$[(t\text{Bu})_2\text{Al}(\mu\text{-OCH}_2\text{CH}_2\text{NMe}_2)]_2^{\text{e}}$	2.766	2.3(1)	16.2(5)	-2.5

^a Equilibrium constant, $K_{\text{eq}} = [4\text{-coord.}]/[5\text{-coord.}]$; ^b Error given in parenthesis.

^c For synthesis and characterization, see: R. Benn, A. Rufinska, H. Lehmkul, E. Janssen, and C. Krüger, *Angew. Chem., Int. Ed. Engl.*, 1983, **22**, 779.

^d For synthesis and characterization, see: O. T. Beachley, Jr., and K. C. Racette, *Inorg. Chem.*, 1976, **15**, 2110.

^e For synthesis and characterization see reference 6.

As would be expected for a dissociative process, ΔS is positive ($14 - 38 \text{ J.K}^{-1}.\text{mol}^{-1}$) for all the compounds measured. Furthermore, consistent with the intramolecular nature of the reaction these values are significantly smaller than those reported for the dissociation of a Lewis base from a four-coordinate aluminum complex, e.g., for the reaction shown in Eq. 1.10 ($\Delta S = 160 - 240 \text{ J.K}^{-1}.\text{mol}^{-1}$).³⁴ The ΔH values for the *tert*-butyl derivatives are approximately half those of the methyl compounds, i.e., $[(\text{iBu})_2\text{Al}(\mu\text{-OCH}_2\text{CH}_2\text{OMe})]_2$ (1.1) versus $[\text{Me}_2\text{Al}(\mu\text{-OCH}_2\text{CH}_2\text{OMe})]_2$. This is in line with the expected steric interaction between the alkyl substituent on aluminum (R) and those on the Lewis base (R'). Based upon a comparison of the appropriate Al-O, Al-S and Al-N⁶ bond lengths for Lewis base donors with those of typical aluminum complexes, it is obviously expected that the intramolecular bonds should be weaker. However, what is unexpected is that the ΔH values are almost an order of magnitude smaller than those of complexes of four-coordinate aluminum with comparable Lewis bases (Table 1.9).^{27,35,36,38} In addition, the relative bond strength (Al-S > Al-O > Al-N) is in the contrary order to that expected, e.g., Al-N (125.5 kJ.mol⁻¹ for $\text{Me}_3\text{Al-NMe}_3$) > Al-O (84.9 kJ.mol⁻¹ for $\text{Me}_3\text{Al-OMe}_2$) > Al-S (75.7 kJ.mol⁻¹ for $\text{Me}_3\text{Al-SMe}_2$).²⁶

These results prompt the following questions: *why are these intramolecular coordinate bonds so weak and why is the relative order of the intramolecular bond strengths Al-S > Al-O > Al-N?*

Towards a quantitative measure of steric bulk. The concept of steric bulk was first developed by Hofmann in 1872³⁷ to explain differences in reactivity in organic chemistry. However, it was the work of Meyer in 1894 that provided the first quantifiable steric effect.³⁸ Subsequently researchers were able to provide a rationalization of reactivity in organic systems by the recognition of steric effects.³⁹ In inorganic and particularly organometallic systems the quantification of steric effects has been standardized by the work of Tolman (See Appendix A).^{12,40} Subsequently, there have

been several developments towards providing quantification of steric bulk,⁴¹ in particular thermodynamic values for the destabilization of a molecule due to steric interactions.⁴²

Table 1.9. Selected enthalpies, ΔH , of Lewis acid-base complexes of aluminum.

Donor atom	Compound	ΔH (kJ.mol ⁻¹)	reference
oxygen	AlMe ₃ (OMe ₂)	84.9	a
	AlMe ₃ (OEt ₂)	84.5	a
	AlBr ₃ (OEt ₂)	152.7	b
	AlMe ₂ (BHT)(OEt ₂)	63.8	c
	[Me ₂ Al(μ-OCH ₂ CH ₂ OMe)] ₂	9.1	d
	[(^t Bu) ₂ Al(μ-OCH ₂ CH ₂ OMe)] ₂ (1)	5.2	d
sulfur	AlMe ₃ (SMe ₂)	75.7	e
	AlMe ₃ (SEt ₂)	70.3	e
	AlCl ₃ (SMe ₂)	126.7	b
	AlCl ₃ (SEt ₂)	125.1	b
	AlBr ₃ (SEt ₂)	128.0	b
	[Me ₂ Al(μ-OCH ₂ CH ₂ SMe)] ₂ (1.14)	13.2	d
	[(^t Bu) ₂ Al(μ-OCH ₂ CH ₂ SMe)] ₂ (1.11)	4.9	d

^a C. H. Henrickson, D. Duffy, and D. P. Eyman, *Inorg. Chem.*, 1968, **7**, 1047.

^b E. N. Guryanova, I. P. Goldstein, and I. P. Romm, *Donor-Acceptor Bond*, Wiley, New York, 1975.

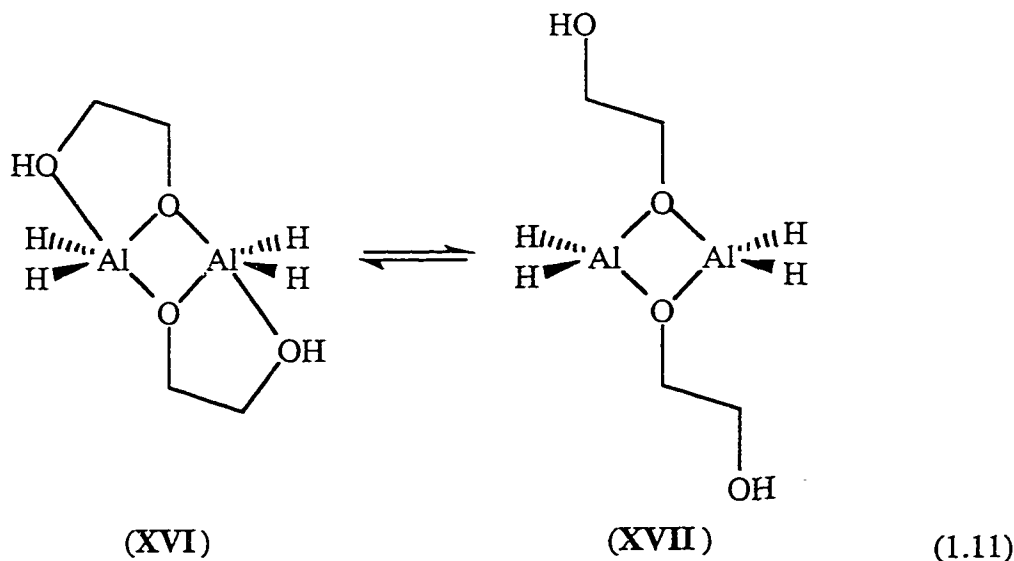
^c M. B. Power, J. R. Nash, M. D. Healy, and A. R. Barron, *Organometallics*, 1992, **11**, 1830.

^d This work.

^e C. H. Henrickson, and D. P. Eyman, *Inorg. Chem.*, 1967, **6**, 1461.

Clearly the presence of weak Lewis acid-base interactions in the dimeric dialkylaluminum compounds $[R_2Al\{\mu-O(CH_2)_nER'_x\}]_2$ ($n = 2, 3$; $ER'_x = OR', SR', NR'_2$) is related to steric hindrance, however, we posed the question as to whether it is possible to use the BDE data to provide a quantitative measure of steric repulsion.

In order to understand the relative stability of five- and four-coordinate isomers of $[R_2Al\{\mu-O(CH_2)_nER'_x\}]_2$, *ab initio* calculations at the HF/3-21G(*) level have been performed (see Experimental) on the model compound, $[H_2Al(\mu-OCH_2CH_2OH)]_2$ as both the five- and four-coordinate isomers; designated as $[H_2Al(\mu-OCH_2CH_2OH)]_2$ (XVI) and $[H_2Al(\mu-OCH_2CH_2OH)]_2$ (XVII).



The optimized calculated structural parameters for each model are given in Table 1.10, and the structures are shown in Figure 1.10. For both dimeric isomers the calculated Al-H distances are comparable to those determined experimentally.⁴³ As can be seen from Table 1.10, the Al-O distance and O-Al-O and Al-O-Al angles in the dimers are within experimental error of the ranges reported from X-ray diffraction studies.

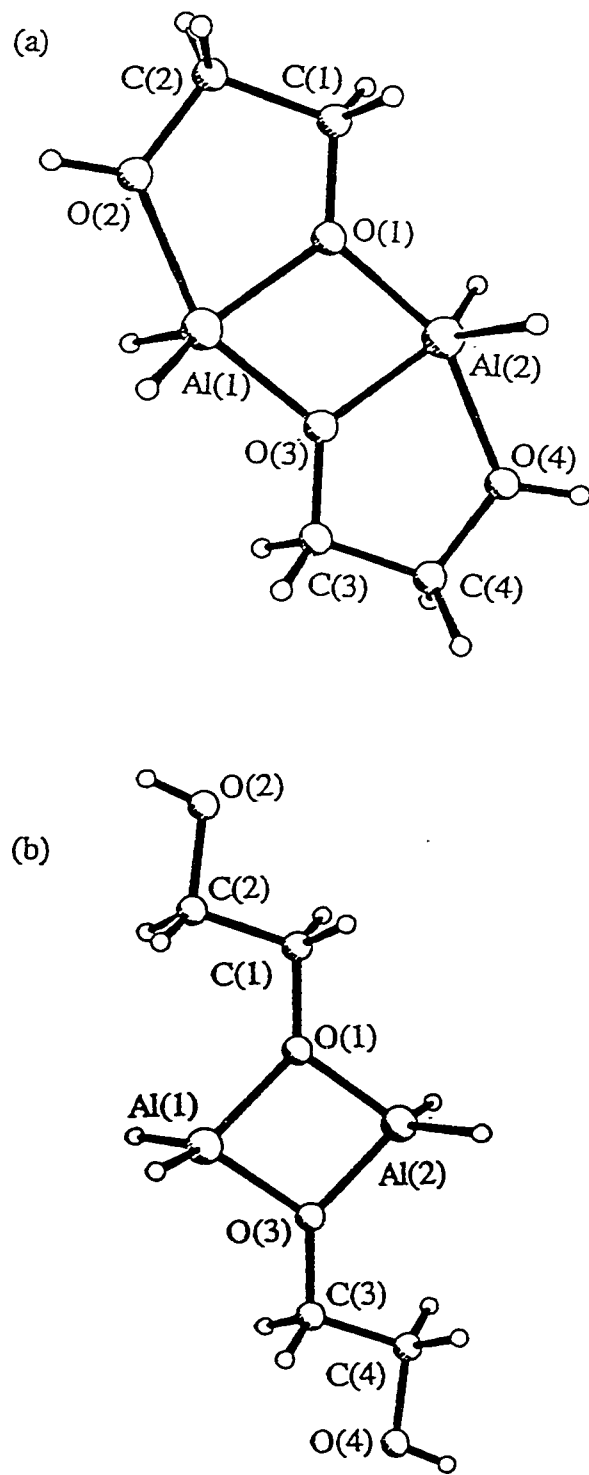


Figure 1.10. *Ab initio* HF/3-21G(*) calculated structures of (a) five-coordinate and (b) four-coordinate isomers of $[H_2Al(\mu-OCH_2CH_2OH)]_2$.

Table 1.10. Structural parameters for five- and four-coordinate dimeric isomers of $[H_2Al(\mu-OCH_2CH_2OH)]_n$ in comparison to experimental values.^a

	five-coordinate dimer		four-coordinate dimer	
	calculated	experimental ^b	calculated	experimental ^c
Al-O	1.839, 1.894	1.827(3), 1.892(3)	1.833	1.844(5) - 1.860(3)
Al---O _(ether)	2.019	2.269(3)		
Al-H	1.622	1.56(2), 1.60(2) ^d	1.597	n/a
O-Al-O'	76.2	76.3	81.8	78.4(2) - 78.9(1)
O-Al-O _(ether)	77.1	75.9		
O-Al-H	121.0	118.2(2), 119.4(2)	112.6	113.8(2) - 116.7(3)
O _(ether) -Al-H	93.3	92.1(2), 89.3(2)		
H-Al-H	117.6	120.8(2)	118.8	116.2(3) - 117.8(1)
Al-O-Al'	103.8	103.7	98.2	101.1(1) - 101.6(2)
Al-O-C	127.3	124.6	135.0, 126.0	131.0(4) - 132.1(4)

^a Distances in Å, angles in °.

^b $[Me_2Al(\mu-OCH_2CH_2OMe)]_2$ from, R. Benn, A. Rufinska, H. Lehmkul, E. Janssen, and C. Krüger, *Angew. Chem., Int. Ed. Engl.* 1983, **22**, 779.

^c Compounds **1.6**, **1.11**, **1.15**, and $[(^tBu)_2Al(\mu-OCH_2CH_2NMe_2)]_2$.⁶

^d for $H_2Al(\mu-OCH_2CH_2NMe_2)_2$.⁶

This is in line with a previous suggestion that the Al_2O_2 core is relatively insensitive to steric effects of the bridging alkoxide,²¹ and indicates that the 3-21G(*) level faithfully models the overall geometry.⁴⁴ However, it should be noted that the calculated Al-O_(ether) bond (2.019 Å) is significantly shorter than that in $[Me_2Al(\mu-OCH_2CH_2OMe)]_2$ [2.269(3) Å].⁹

The total energies of the model compounds were determined at the MP2/3-21G(*) level for the optimized structures. The five-coordinate compound $[H_2Al(\mu-$

$\text{OCH}_2\text{CH}_2\text{OH})_2$ is stabilized by $-129.8 \text{ kJ}\cdot\text{mol}^{-1}$ with respect to the four-coordinate compound $[\text{H}_2\text{Al}(\mu\text{-OCH}_2\text{CH}_2\text{OH})_2]_2$, i.e., Eq. 1.11. This stabilization is equivalent to $64.9 \text{ kJ}\cdot\text{mol}^{-1}$ per Al-O bond breaking reaction, i.e., the bond dissociation energy (BDE) of the intramolecular Al-O(ether) interaction, *c.f.*, Eq. 1.5. This calculated bond energy is in the expected range for a Lewis acid-base interaction to aluminum. The stabilization energy follows the expected series $\text{H} >> \text{Me} > {}^t\text{Bu}$ while the bond lengths follow the reverse (but also expected) trend. It is unclear, however, as to why the calculated value of the bond dissociation energy for $[\text{H}_2\text{Al}(\mu\text{-OCH}_2\text{CH}_2\text{OH})_2]_2$ is considerably greater than the experimental values for compound **1.1** and $[\text{Me}_2\text{Al}(\mu\text{-OCH}_2\text{CH}_2\text{OMe})_2]^9$. It is to this variation that we must look for an explanation of the surprisingly weak intramolecular Al-O(ether) interactions. As was noted above, the calculated Al-O(ether) distance for $[\text{H}_2\text{Al}(\mu\text{-OCH}_2\text{CH}_2\text{OH})_2]_2$ is significantly shorter than that of compounds **1.1**, **1.2**, and $[\text{Me}_2\text{Al}(\mu\text{-OCH}_2\text{CH}_2\text{OMe})_2]^9$ (see Tables 1.9 and 1.1). It is possible that the Al-O(ether) bond strength is simply a function of Al-O(ether) bond length. In this regard the optimized geometries and total energies were calculated by *ab initio* methods MP2/3-21G(*) as a function of Al…O(ether) distance for $[\text{H}_2\text{Al}(\mu\text{-OCH}_2\text{CH}_2\text{OH})_2]_2$.

A comparison of the compounds **1.1** and $[\text{Me}_2\text{Al}(\mu\text{-OCH}_2\text{CH}_2\text{OH})_2]^9$ relative to the four-coordinate dimer, $[\text{H}_2\text{Al}(\mu\text{-OCH}_2\text{CH}_2\text{OH})_2]_2$, allows for the determination of the bond dissociation energy of the intramolecular Al-O(ether) interaction as a function of Al…O(ether) distance in $[\text{H}_2\text{Al}(\mu\text{-OCH}_2\text{CH}_2\text{OH})_2]_2$, see Figure 1.11. The data in Figure 1.11 has the appearance of an intermolecular energy curve, and can be fitted to a Lennard-Jones (12,6) potential in the form shown in Eq. 1.12, where ε is the depth of the minimum ($-64.9 \text{ kJ}\cdot\text{mol}^{-1}$) of the curve and σ (1.796 \AA) is derived from the equilibrium bond distance (R_e), Eq. 1.13.

$$\text{BDE}_R = 4\varepsilon \left[\left(\frac{\sigma}{R} \right)^{12} - \left(\frac{\sigma}{R} \right)^6 \right] \quad (1.12)$$

$$R_e = 2^{1/6}\sigma \quad (1.13)$$

Based on a simplistic view of the relationship between bond strength and bond length, it may be expected the decreased Al-O(ether) bond strengths in compound **1.1** and $[\text{Me}_2\text{Al}(\mu\text{-OCH}_2\text{CH}_2\text{OMe})]_2$ are as a consequence of the steric interactions and thus increased Al-O(ether) distance. However, it should be noted that the experimental values for compound **1.1** and $[\text{Me}_2\text{Al}(\mu\text{-OCH}_2\text{CH}_2\text{OMe})]_2$ (shown in Figure 1.11) do not fit the calculated Lennard-Jones (12,6) potential for $[\text{H}_2\text{Al}(\mu\text{-OCH}_2\text{CH}_2\text{OH})]_2$.

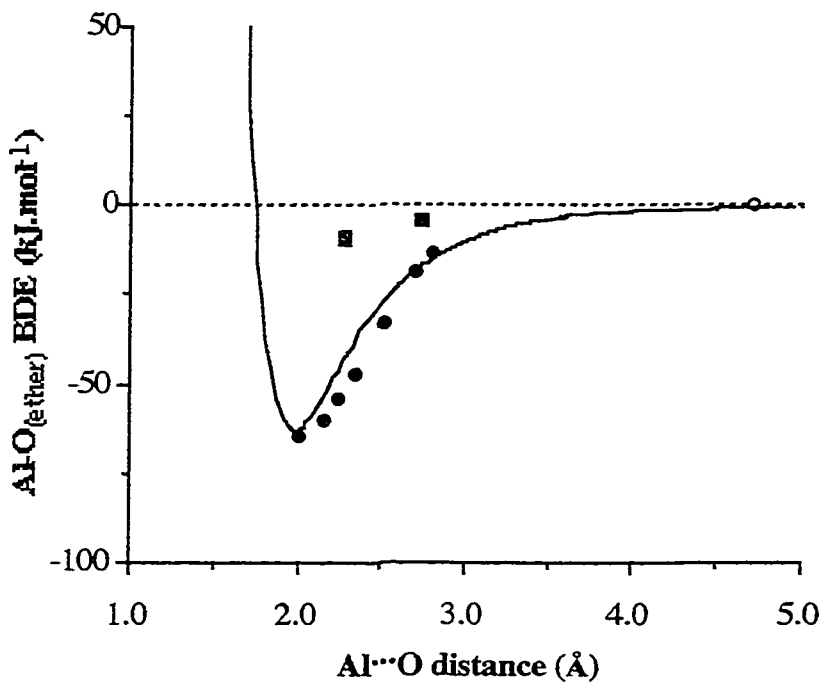


Figure 1.11. Dependence of the calculated intramolecular Al...O(ether) bond strength in $[\text{H}_2\text{Al}(\mu\text{-OCH}_2\text{CH}_2\text{OH})]_2$ (●) as a function of the Al...O(ether) distance. Data fitted to a Lennard-Jones (12,6) potential ($\varepsilon = -64.9 \text{ kJ.mol}^{-1}$ and $\sigma = 1.796 \text{ \AA}$). Values for the four-coordinate isomer of $[\text{H}_2\text{Al}(\mu\text{-OCH}_2\text{CH}_2\text{OH})]_2$ (○), $[\text{Me}_2\text{Al}(\mu\text{-OCH}_2\text{CH}_2\text{OMe})]_2$ (■), and $[(^{\text{t}}\text{Bu})_2\text{Al}(\mu\text{-OCH}_2\text{CH}_2\text{OMe})]_2$ (■) are included for comparison.

Based upon the bond energies (ΔH_{Al-O}) and Al-O(ether) distances determined for compound **1.1** and $[Me_2Al(\mu-OCH_2CH_2OMe)]_2$, the appropriate Lennard-Jones (12,6) potentials may be determined for each compound, see Figure 1.12 and Table 1.11. Using these Lennard-Jones (12,6) potentials a semi-quantitative measure of the steric bulk of methyl and *tert*-butyl groups may be obtained.

Table 1.11. Lennard-Jones (12,6) potential parameters for $[R_2Al(\mu-OCH_2CH_2OR')]_2$.

Compound	ϵ (kJ.mol ⁻¹)	σ (Å)
$[H_2Al(\mu-OCH_2CH_2OH)]_2$	-64.9	1.796
$[Me_2Al(\mu-OCH_2CH_2OMe)]_2$	-9.08	2.021
$[(^tBu)_2Al(\mu-OCH_2CH_2OMe)]_2$ (1)	-5.15	2.447

If one considers the structure of the model compound, $[H_2Al(\mu-OCH_2CH_2OH)]_2$, to be absent of steric interactions between the substituents on either the aluminum or the ether oxygen, then the substitution of the hydrogens on aluminum and oxygen with methyl groups will result in an increase in repulsive force between the aluminum and ether oxygen.⁴⁵ This is estimated to be *ca.* 65 kJ.mol⁻¹ (see Figure 1.12, A). In order to relieve the repulsive forces between the Al-CH₃ and O-CH₃ groups, the Al-O(ether) bond lengthens to a new equilibrium value (Figure 1.12, B). The result of the substitution of hydrogen with methyl is therefore to lengthen and weaken the Lewis acid-base interaction. In a similar manner, substitution of the aluminum methyl groups with *tert*-butyl groups results in the destabilization of the structure found for $[Me_2Al(\mu-OCH_2CH_2OMe)]_2$ by *ca.* 28 kJ.mol⁻¹ (see Figure 1.12, C), with a subsequent bond lengthening to the equilibrium value observed for compound **1.1** (Figure 1.12, D). Thus,

in total, the substitution of the aluminum hydrogen groups with *tert*-butyl groups, and ether hydrogen with a methyl group, results in the destabilization of the "ideal" structure calculated for $[H_2Al(\mu-OCH_2CH_2OH)]_2$ by *ca.* 200 kJ.mol⁻¹.

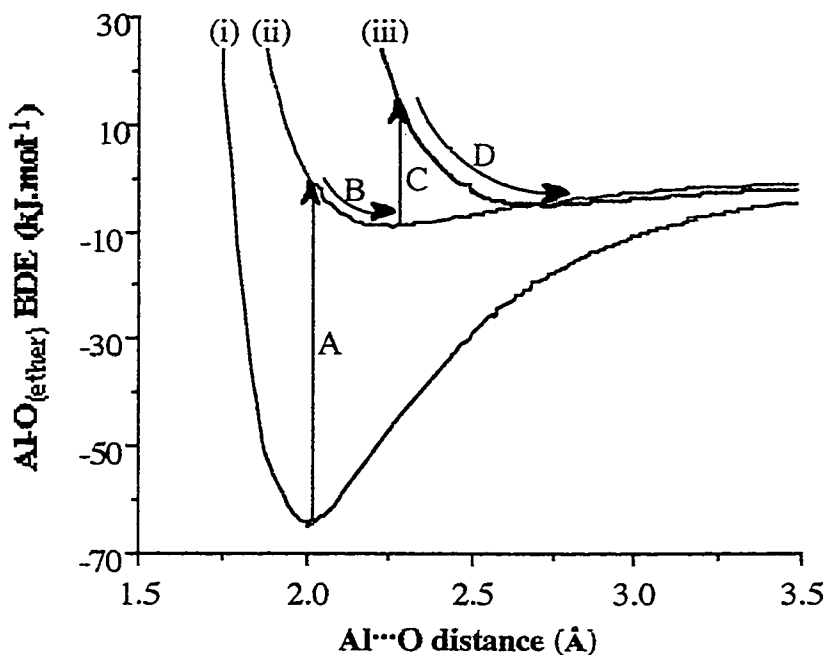


Figure 1.12. Lennard-Jones (12,6) potentials for the $Al \cdots O_{\text{ether}}$ interactions in $[H_2Al(\mu-OCH_2CH_2OH)]_2$ (i), $[Me_2Al(\mu-OCH_2CH_2OMe)]_2$ (ii), and $[(^t\text{Bu})_2Al(\mu-OCH_2CH_2OMe)]_2$ (iii). For an explanation of labels see text.

As would be expected the repulsive interaction is significantly increased for the substitution of methyl with *tert*-butyl (i.e., $[Me_2Al(\mu-OCH_2CH_2OMe)]_2$) versus compound (1.1), however, it is surprising that the substitution of hydrogen with methyl (i.e., $[H_2Al(\mu-OCH_2CH_2OH)]_2$ versus $[Me_2Al(\mu-OCH_2CH_2OMe)]_2$) is also a significant effect. This result suggests that the steric effects of alkyl groups such as methyl should not be ignored in considering both structural and thermodynamic data as compared to the idealized model compounds commonly used in higher level computations. Based on the above discussion it is possible to rationalize the experimental results for the thioether and

amine ligands and answer the questions posed above. The apparent weakness of the intramolecular coordinate bonds in $[R_2Al(\mu-OCH_2CH_2ER'x)]_2$ is clearly due to the steric repulsion between the alkyl groups on aluminum and the substituents on the Lewis base. Therefore the bond strengths of the fifth coordination ligand are actually very low.

The relative order of the intramolecular bond strengths Al-S > Al-O > Al-N may be explained by a consideration of the effects of increased steric bulk at the aluminum and heteroatom. Thus, the steric destabilization that occurs from the substitution of hydrogens with methyl groups is dependent on the initial ligand-ligand distance. Since the radius for sulfur (1.84 Å) is significantly larger than for oxygen (1.40 Å) the ligands will be at a greater distance apart and consequently in order to overcome the inter-ligand repulsion, the Al-S bond doesn't have to relax as far as the equivalent Al-O(ether) bond, resulting in a smaller weakening of the Al-S bond relative to the analogous oxygen system. In contrast, the radii of oxygen and nitrogen (1.5 Å) are similar and therefore would expect similar effects for specific alkyl substitution. However, the sp^3 hybridization about nitrogen results in increased steric interaction between the alkyl substituents on the amine and the alkyl groups on aluminum. Thus for any given substitution (i.e., H with Me) the amine complex must relax further than the ether complex, resulting in a greater decrease in the Al-E bond strength.

Conclusions

A range of dialkylaluminum compounds have been prepared with bi-functional ligands of the general formula $[R_2Al\{\mu-O(CH_2)_nER'x\}]_2$, where n is 2 or 3, $ER'x$ is OR' , SR' or NR'_2 ,⁶ and R is tBu , iBu , Et or Me. All these compounds (in the absence of steric hindrance at the α -carbon) are dimeric species where the interaction of the non-bridged heteroatoms (E) to form five-coordinate aluminum center is an equilibrium in solution. Equilibrium constants (where $K_{eq} = [4\text{-coord.}]/[5\text{-coord.}]$) have been determined from ^{13}C NMR measurements and are found to be controlled by the following factors: Increase

in the length of ligand back-bone (n), the steric bulk of the alkyl substituents on aluminum (R) and/or on the heteroatom donor (R'), all result in greater dissociation of the neutral Lewis base donor. The extent of coordination of the fifth ligand is also dependent on the identity of the heteroatom donor (E).

Determination of the enthalpy associated with the equilibrium shows that the fifth ligand is only weakly bound. In fact, the bond dissociation energies (5.2 - 13.2 kJ.mol⁻¹) are in the range expected for solvation rather than formation of stable Lewis acid-base interactions. However, *ab initio* calculations on the model system, [H₂Al(μ-OCH₂CH₂OH)]₂, indicates that, in the absence of steric interactions, the strength of the fifth ligand should be comparable to Lewis acid-base complexes in four-coordinate compounds. We have found that this discrepancy is due to inter-ligand steric repulsion, and may be used as a thermodynamic measure of steric bulk. Although an increased effect of steric bulk in five-coordinate compounds as compared to four-coordinate compounds is not unexpected due to the smaller in the inter-ligand (X-Al-X) bond angles in the former, the dramatic difference between hydrogen and methyl is unexpected. Consequently, this indicates that the commonly held assumption that hydrogen atoms may simulate larger alkyl groups in calculations is invalid.

Experimental Section

Mass spectra were obtained on a Finnigan MAT 95 mass spectrometer operating with an electron beam energy of 70 eV for EI mass spectra. IR spectra (4000 - 400 cm⁻¹) were obtained using an Nicolet 760 FT-IR infrared spectrometer. IR samples were prepared as Nujol mulls between KBr plates unless otherwise stated. NMR spectra were obtained on Bruker AM-250, AM-300 and Avance 200 spectrometers using (unless otherwise stated) d₆-benzene solutions. Chemical shifts are reported relative to internal solvent resonances (¹H and ¹³C), and external [Al(H₂O)₆]³⁺ (²⁷Al). Elemental analysis were performed using a Perkin Elmer Magna 400 ICP Atomic Emission Spectrometer.

All compounds were digested in concentrated nitric acid to enable analysis. *Caution:* *Digestion of organoaluminum compounds in acidic solutions should be undertaken with care.* Microanalyses were performed by Oneida Research Services, Inc., Whitesboro, NY. Molecular weight measurements were made in CH₂Cl₂ with the use of an instrument similar to that described by Clark.⁴⁶ The synthesis of Al(^tBu)₃ was performed according to a modification of the literature method.⁴⁷ AlMe₃, AlEt₃, Al(ⁱBu)₃ and (ⁱBu)₂AlH were generously donated by Akzo Nobel. HOCH₂CH₂OMe and HOCH₂CH₂CH₂OMe were obtained from Aldrich and were used without further purification.

[(^tBu)₂Al(μ-OCH₂CH₂OMe)]₂ (1.1). To a cooled (-78 °C) hexane (50 mL) solution of Al(^tBu)₃ (1.50 g, 7.58 mmol) was added HOCH₂CH₂OCH₃ (1.9 mL, 7.58 mmol) with stirring. The reaction was allowed to warm to room temperature and stirred overnight. After filtering the supernatent was concentrated and cooled to -22 °C. The resulting white crystals were collected by filtration. Several crops were obtained by subsequent recooling of the filtrate. Yield: *ca* 76%. Mp: 123 - 125 °C. Analysis (calc., %): Al, 13.3 (12.5). MS (EI, %): *m/z*: 375 (2M⁺ - ^tBu, 100), 216 (M⁺, 60), 159 (M⁺ - ^tBu, 60), 57 (^tBu, 100). IR (cm⁻¹): 2724 (w), 2689 (w), 1259 (m), 1125 (w), 1067 (s), 1024 (s, br), 911 (m), 721 (m), 617 (m), 587 (m), 561 (m). ¹H NMR (CDCl₃): δ 3.68 [4H, t, *J*(H-H) = 4.8 Hz, OCH₂], 2.97 [6H, s, OCH₃], 2.88 [4H, t, *J*(H-H) = 4.8 Hz, OCH₂], 1.24 [36H, s, C(CH₃)₃]. ¹³C NMR (CDCl₃): δ 72.2 (OCH₃), 64.7 (OCH₂), 60.0 (OCH₂), 32.9 [C(CH₃)₃]. ²⁷Al NMR (C₇H₈/C₆D₆): δ 123 (W_{1/2} = 4560 Hz).

[(ⁱBu)₂Al(μ-OCH₂CH₂OMe)]₂ (1.2). Prepared in a similar manner to compound **1.1**, but using (ⁱBu)₂AlH (1.81 g, 12.7 mmol) and HOCH₂CH₂OCH₃ (0.97g, 12.7 mmol). Yield: *ca* 40%. Mp: 76 - 78 °C. Analysis (calc., %): C, 59.0 (61.0); H, 11.3 (11.6). MS (EI, %): *m/z* 375 (2M⁺ - ⁱBu, 100), 159 (M⁺ - ⁱBu, 7), 57 (ⁱBu, 20), 43 (ⁱBu - Me, 75). Molecular weight determination: 431 (432). IR (KBr pellet, cm⁻¹): 2939 (s), 2863 (s),

2776 (w), 2601 (w), 1460 (s), 1372 (m), 1265 (m), 1116 (s), 1183 (s), 645 (s). ^1H NMR (C_6D_6): δ 3.52 [4H, t, $J(\text{H-H}) = 5.2$ Hz, OCH_2], 2.95 [6H, s, OCH_3], 2.86 [4H, t, $J(\text{H-H}) = 5.2$ Hz, OCH_2], 2.01 [2H, m, $J(\text{H-H}) = 6.6$ Hz, CHCH_3], 1.25 [12H, d, $J(\text{H-H}) = 6.6$ Hz, CH_3], 0.12 [4H, d, $J(\text{H-H}) = 7.0$, CH_2]. ^{13}C NMR (C_6D_6): δ 71.4 (OCH_3), 60.0 (OCH_2), 58.4 (OCH_2), 29.4 [$\text{C}(\text{CH}_3)_3$], 26.9 (CH). ^{27}Al NMR (C_7H_8 , C_6D_6): δ 123 ($W_{1/2} = 7210$ Hz).

[$\text{Et}_2\text{Al}(\mu\text{-OCH}_2\text{CH}_2\text{OMe})_2$]₂ (1.3). Prepared in a similar manner to compound **1.1**, but using AlEt_3 (1.45g, 12.7 mmol) and $\text{HOCH}_2\text{CH}_2\text{OCH}_3$ (0.97g, 12.7 mmol). Yield: ca 60%. Mp: 38 - 40 °C. Analysis (calc., %): C, 51.2 (52.5); H, 10.3 (10.7). MS (EI, %): m/z 291 (2M⁺-Et, 100), 261(2M⁺ - 2Et, 18), 247 (2M⁺ - 2Et - Me, 10), 131 (M⁺ - Et, 10), 103 (M⁺ - 2Et, 5), 45 (CH_2OMe , 20). IR (cm⁻¹): 1372 (s), 1238 (w), 1195 (w), 1020 (m), 1077 (s), 1021(m), 986 (m), 923 (m), 655 (s). ^1H NMR (C_6D_6): δ 3.48 [4H, t, $J(\text{H-H}) = 5.2$ Hz, OCH_2], 2.94 [6H, s, OCH_3], 2.82 [4H, t, $J(\text{H-H}) = 5.2$ Hz, CH_2OMe], 1.39 [8H, t, $J(\text{H-H}) = 8.2$ Hz, AlCH_2], 0.15 [12H, q, $J(\text{H-H}) = 8.2$ Hz, CH_3]. ^{13}C NMR (C_6D_6): δ 71.3(OCH_3), 59.5 (OCH_2), 57.9 (OCH_2), 10.3 (Al- CH_2CH_3). ^{27}Al NMR (C_7H_8 , C_6D_6): δ 120 ($W_{1/2} = 3590$ Hz).

[($t\text{Bu}$)₂ $\text{Al}(\mu\text{-OCH}_2\text{CH}_2\text{O}^n\text{Bu})_2$]₂ (1.4). Prepared in a similar manner to compound **1.1**, but using $\text{Al}(t\text{Bu})_3$ (1.58 g, 7.9 mmol) and $\text{HOCH}_2\text{CH}_2\text{O}^n\text{Bu}$ (1.04 mL, 7.9 mmol). Yield: 71 %. Mp: < 25 °C. MS (EI, %): m/z 459 (2M⁺ - $t\text{Bu}$, 60), 399 (2M⁺ - $\text{OCH}_2\text{CH}_2\text{O}^n\text{Bu}$, 10), 201 (M⁺ - $t\text{Bu}$, 50), 117 ($\text{OCH}_2\text{CH}_2\text{O}^n\text{Bu}$, 25), 57 ($t\text{Bu}$, 80). IR (cm⁻¹): 2689 (m), 1383 (s), 1302 (s), 1260 (m), 1070 (s), 935 (m), 911 (m), 812 (m), 738 (w), 626 (m). ^1H NMR (C_6D_6): δ 3.81 [4H, t, $J(\text{H-H}) = 5.0$ Hz, OCH_2], 3.23 [4H, t, $J(\text{H-H}) = 7.5$ Hz, OCH_2], 3.14 [4H, t, $J(\text{H-H}) = 5.0$ Hz, OCH_2], 1.45 [4H, tt, $J(\text{H-H}) = 7.5$ Hz, OCH_2CH_2], 1.26 [36H, s, $\text{C}(\text{CH}_3)_3$], 1.21 (4H, m, $\text{OCH}_2\text{CH}_2\text{CH}_2$), 0.81 [6H, t, $J(\text{H-H}) = 7.5$ Hz, CH_3]. ^{13}C NMR (C_6D_6): δ 71.7 (OCH_2), 70.8 (OCH_2), 65.5 (OCH_2), 32.6

$[\text{C}(\text{CH}_3)_3]$, 31.8 (OCH_2CH_2), 19.8 ($\text{OCH}_2\text{CH}_2\text{CH}_2$), 14.4 (CH_3). ^{27}Al NMR (C_7H_8 , C_6D_6): δ 140 ($W_{1/2} = 7700$ Hz).

[$\text{Me}_2\text{Al}(\mu\text{-OCH}_2\text{CH}_2\text{O}^n\text{Bu})_2$]₂ (1.5). Prepared in a similar manner to compound **1.1**, but using AlMe_3 (2.23 g, 31.0 mmol) and $\text{HOCH}_2\text{CH}_2\text{O}^n\text{Bu}$ (3.66 g, 31.0 mmol). Yield: *ca* 60%. Mp. < 25 °C. MS (EI, %): *m/z* 333 (2M⁺ - Me, 35), 261 (2M⁺ - 2Me - $n\text{Bu}$, 25), 117 [$\text{OCH}_2\text{CH}_2\text{O}^n\text{Bu}$, 25]. IR (neat, cm^{-1}): 2883 (s, br), 1465 (s), 1383 (m), 1357 (s), 1301 (w), 1260 (m), 1234 (m), 1096 (s, br), 912 (m), 804 (m), 686 (s, br). 569 (m). ^1H NMR (C_6D_6): δ 3.50 [4H, t, $J(\text{H-H}) = 5.1$ Hz, OCH_2], 3.27 [4H, t, $J(\text{H-H}) = 7.1$ Hz, OCH_2], 2.95 [4H, t, $J(\text{H-H}) = 5.1$ Hz, OCH_2], 1.39 [4H, tt, $J(\text{H-H}) = 7.1$ Hz, OCH_2CH_2], 1.14 [4H, tt, $J(\text{H-H}) = 7.1$, $\text{OCH}_2\text{CH}_2\text{CH}_2$], 0.80 [6H, t, $J(\text{H-H}) = 7.1$ Hz, CH_3], -0.47 (12H, s, Al- CH_3). ^{13}C NMR (C_6D_6): δ 71.0 (OCH_2), 69.3 (OCH_2), 59.6 (OCH_2), 31.1 (OCH_2CH_2), 19.6 ($\text{OCH}_2\text{CH}_2\text{CH}_2$), 14.3 (CH_3), -10.0 (Al CH_3). ^{27}Al NMR (C_7H_8 , C_6D_6): δ 126 ($W_{1/2} = 5940$ Hz).

[($t\text{Bu}$)₂ $\text{Al}(\mu\text{-OCH}_2\text{CH}_2\text{CH}_2\text{OMe})_2$]₂ (1.6). Prepared in a similar manner to compound **1.1**, but using $\text{Al}(t\text{Bu})_3$ (2.1 g; 10.7 mmol) and $\text{HOCH}_2\text{CH}_2\text{CH}_2\text{OCH}_3$ (0.97 g, 10.7 mmol). Mp. 146 - 148 °C. Analysis (calc., %): Al, 10.5 (11.7). MS (%): *m/z* 403 (2M⁺ - $t\text{Bu}$, 100), 173 (M⁺ - $t\text{Bu}$, 20), 73 [$\text{OCH}_2\text{CH}_2\text{CH}_2\text{OMe}$, 75], 57 ($t\text{Bu}$, 16). IR (cm^{-1}): 2721 (w), 2675 (w), 1302 (w), 1262 (m), 1092 (s, br), 1017 (s, br), 797 (s), 716 (m), 643 (w), 589 (w). ^1H NMR (CD_2Cl_2): δ 4.02 [4H, t, $J(\text{H-H}) = 7.5$ Hz, OCH_2], 3.01 (4H, m, OCH_2), 2.97 (6H, s, OCH_3), 1.91 (4H, m, $\text{CH}_2\text{CH}_2\text{CH}_2$), 1.25 [36H, s, $\text{C}(\text{CH}_3)_3$]. ^{13}C NMR (CD_2Cl_2): 68.9 (OCH_3), 64.1 (OCH_2), 58.7 (OCH_2), 34.4 ($\text{CH}_2\text{CH}_2\text{CH}_2$), 32.4 [$\text{C}(\text{CH}_3)_3$]. ^{27}Al NMR ($\text{C}_7\text{H}_8/\text{C}_6\text{D}_6$): δ 134 ($W_{1/2} = 2730$ Hz).

[$\text{Me}_2\text{Al}(\mu\text{-OCH}_2\text{CH}_2\text{CH}_2\text{OMe})_2$]₂ (1.7). Prepared in a similar manner to compound **1.1**, but using AlMe_3 (0.84 g, 11.8 mmol) $\text{HOCH}_2\text{CH}_2\text{CH}_2\text{OCH}_3$ (1.06g, 11.8

mmol). Yield: *ca* 40%. Mp: 85 - 87 °C. MS (EI, %): *m/z* 277 (2M⁺ - Me, 80), 131 (M⁺ - Me, 75). IR (neat, cm⁻¹): 2901 (s, br), 1478 (s), 1457 (s), 1386 (s), 1268 (m), 1797 (m), 1084 (s, br), 899 (w), 798 (m, br), 467 (m). ¹H NMR (C₆D₆): δ 3.63 [4H, t, *J*(H-H) = 5.6 Hz, OCH₂], 3.03 [4H, t, *J*(H-H) = 5.6 Hz, OCH₂], 2.97 (6H, s, OCH₃), 1.46 [4H, quintet, *J*(H-H) = 5.6 Hz, CH₂CH₂CH₂], -0.48 [12H, s, Al-CH₃]. ¹³C NMR (C₆D₆): 70.4 (OCH₃), 61.1 (OCH₂), 59.0 (OCH₂), 32.1 (CH₂CH₂CH₂), -10.0 (br, Al-CH₃). ²⁷Al NMR (C₇H₈, C₆D₆): δ 144 (*W*_{1/2} = 6560 Hz).

[(^tBu)₂Al(μ-OⁿBu)]₂ (1.8). Prepared in a similar manner to compound **1.1**, but using Al(^tBu)₃ (2.37 g, 12.0 mmol) and ⁿBuOH (1.1 mL, 12.0 mmol). Yield: *ca* 70%. Mp: 90 - 92 °C. Analysis (calc., %): C, 67.0 (67.2); H, 12.1 (12.7). MS (EI, %): *m/z* 371 (2M⁺ - ^tBu, 55), 315 (2M⁺ - 2^tBu, 10), 257 (2M⁺ - 3^tBu, 7), 59 [(CH₂)₂OCH₃, 100]. IR (cm⁻¹): 2904 (s, br), 1449 (s), 1388 (s), 1075 (m), 1029 (m), 809 (m), 722 (m), 635 (m), 594 (m). ¹H NMR (C₆D₆): δ 3.77 [4H, t, *J*(H-H) = 8.3 Hz, OCH₂], 1.65 [4H, m, *J*(H-H) = 7.3 Hz, OCH₂CH₂], 1.25 [36H, s, C(CH₃)₃], 1.00 [4H, m, *J*(H-H) = 7.3 Hz, OCH₂CH₂CH₂], 0.74 [6H, t, *J*(H-H) = 7.3 Hz, CH₃]. ¹³C NMR (C₆D₆): 65.9 (OCH₂), 36.3 (OCH₂CH₂), 32.4 [C(CH₃)₃], 19.1 (OCH₂CH₂CH₂), 14.1 (CH₃). ²⁷Al NMR (C₇H₈, C₆D₆): δ 137 (*W*_{1/2} = 5880 Hz).

[(ⁱBu)₂Al(μ-OⁿBu)]₂ (1.9). Prepared in a similar manner to compound **1.1**, but using (ⁱBu)₂AlH (4.69 g, 32 mmol) and ⁿBuOH (1.5 mL, 16 mmol). Yield: *ca* 80%. Mp: 134 - 135 °C. Analysis (calc., %): C, 67.7 (67.2); H, 12.8 (12.7). MS (EI, %): *m/z* 387 (2M⁺ - ⁱBu, 12), 315 (2M⁺ - 2ⁱBu, 8), 85 (AlⁱBu, 5). IR (cm⁻¹): 2899 (s, br), 1456 (s), 1374 (s), 1316 (w), 1259 (m), 1068 (m), 1042 (m), 800 (m), 670 (m), 616 (w). ¹H NMR (C₆D₆): NMR (C₆D₆): δ 3.96 (4H, m, OCH₂), 2.20 [2H, sept, *J*(H-H) = 6.6, CH(CH₃)₂], 1.89 (4H, m, OCH₂CH₂), 1.32 (4H, m, OCH₂CH₂CH₂), 1.26 [12H, d, *J*(H-H) = 7.0 Hz, CH(CH₃)], 1.24 [12H, d, *J*(H-H) = 7.0 Hz, CH(CH₃)], 0.98 [6H, t, *J*(H-H) = 7.4,

$\text{CH}_2\text{CH}_3]$, 0.39 [4H, d, $J(\text{H-H}) = 7.0$, Al- CH_2]. ^{13}C NMR (C_6D_6): 64.6 (OCH_2), 35.7 (OCH_2CH_2), 29.7 [$\text{CH}(\text{CH}_3)_2$], 29.6 [$\text{CH}(\text{CH}_3)_2$], 24.8 (CH_2CH), 19.7 ($\text{OCH}_2\text{CH}_2\text{CH}_2$), 14.4 (CH_3). ^{27}Al NMR (C_7H_8 , C_6D_6): δ 150 ($W_{1/2} = 5500$ Hz).

[Et₂Al(μ -OⁿBu)]₂ (1.10). Prepared in a similar manner to compound **1.1**, but using AlEt₃ (2.505 g, 22 mmol) and ⁿBuOH (2.0 mL, 22 mmol). After removal of all volatiles under vacuum, the remaining liquid was distilled under vaccum. Yield: *ca.* 70%. Analysis (calc., %): C 59.7 (60.7), H 11.8 (12.1). MS (EI, %): *m/z* 287 (2M⁺ - Et, 100), 259 (2M⁺ - ⁿBu, 80), 201 (2M⁺ - ⁿBu - 2Et, 40), 56 (AlEt, 80). IR (neat, cm^{-1}): 2909 (s, br), 1465 (s), 1406 (s), 1258 (s), 1196 (m), 1065 (s, br), 921 (w), 903 (m), 858 (m), 641 (s, br). ^1H NMR (C_6D_6): δ 3.52 [4H, t, $J(\text{H-H}) = 7.0$ Hz, OCH_2], 1.46 (4H, m, OCH_2CH_2), 1.23 [12H, t, $J(\text{H-H}) = 8.3$ Hz, Al- CH_2CH_3], 1.16 (4H, m, $\text{OCH}_2\text{CH}_2\text{CH}_2$), 0.77 [6H, t, $J(\text{H-H}) = 7.3$ Hz, CH_2CH_3], 0.13 [8H, q, $J(\text{H-H}) = 8.2$ Hz, Al- CH_2]. ^{13}C NMR (C_6D_6): 63.9 (OCH_2), 35.4 (OCH_2CH_2), 19.4 ($\text{OCH}_2\text{CH}_2\text{CH}_2$), 14.1 (CH_3), 9.4 (Al- CH_2CH_3), -0.17 (Al- CH_2). ^{27}Al NMR (C_7H_8 , C_6D_6): δ 149 ($W_{1/2} = 4770$ Hz).

[(^tBu)₂Al(μ -OCH₂CH₂SMe)]₂ (1.11). To a solution of HOCH₂CH₂SMe (1.47 g, 15.9 mmol) in hexane (50 mL) was added Al(^tBu)₃ (3.16 g, 15.9 mmol) at -78 °C. The mixture was allowed to warm to room temperature and stirred overnight. Filtration, reduction of the solvent under vacuum, and cooloing to -20 °C resulted in the formation of colorless crystals. Yield: *ca.* 80 %. Mp: 150 - 152 °C. Analysis (calc., %): C, 55.6 (56.8); H, 10.1 (10.8). MS (EI, %): *m/z*: 407 (2M⁺ - ^tBu, 60), 133 (M⁺ - 2 ^tBu, 80), 75 (^tBu, 100). Molecular weight determination: 459 (464). IR (cm^{-1}): 2964 (m), 2921 (m), 2828 (m), 684 (w), 1261 (s), 1090 (s), 810 (s), 611 (w). ^1H NMR (C_6D_6): δ 3.92 [4H, t, $J(\text{H-H}) = 7.5$ Hz, OCH_2], 1.66 (6H, s, SCH₃), 2.59 [4H, t, $J(\text{H-H}) = 7.5$ Hz, SCH₂], 1.16 [36H, s, C(CH₃)₃]. ^{13}C NMR (C_6D_6): δ 15.9 (SCH₃), 64.5 (OCH_2), 36.4 (SCH₂), 32.4 [C(CH₃)₃]. ^{27}Al NMR ($\text{C}_7\text{H}_8/\text{C}_6\text{D}_6$): δ 142 ($W_{1/2} = 5280$ Hz).

[(*i*Bu)₂Al(μ-OCH₂CH₂SMe)]₂ (1.12). Prepared in a similar manner to compound **1.11**, but using (*i*Bu)₂AlH (1.64g, 11.5 mmol) and HOCH₂CH₂SMe (1.06g, 11.5mmol). Yield: *ca* 30%. Mp. 33 - 35 °C. Analysis (calc., %): C, 56.6 (56.8); H 10.7 (10.8). MS (EI, %): *m/z* 407 (2M⁺ - *i*Bu, 100), 177 (M⁺ - *i*Bu, 7), 389 (M⁺ - *i*Bu - Me, 25), 75 (OCH₂CH₂S, 55). IR (neat, cm⁻¹): 2603 (w), 1404 (w), 1311 (w), 1375 (s), 1293 (w), 1019 (m), 958 (m), 817 (m), 836 (w), 676 (s). ¹H NMR (C₆D₆): δ 3.62 [4H, t, *J*(H-H) = 6.1 Hz, OCH₂], 2.32 [4H, t, *J*(H-H) = 6.1 Hz, SCH₂], 2.02 [2H, m, *J*(H-H) = 6.6 Hz, *J*(H-H) = 7.0 Hz, CH(CH₃)₂], 1.59 [6H, s, SCH₃], 1.19 [12H, d, *J*(H-H) = 6.6 Hz, C(CH₃)₂], 0.26 [4H, d, *J*(H-H) = 7.0 Hz, Al-CH₂]. ¹³C NMR (C₆D₆): δ 60.3 (OCH₂), 36.5 (SCH₂), 29.1 [C(CH₃)₂], 26.8 (CH), 14.9 (SCH₃). ²⁷Al NMR (C₇H₈, C₆D₆): δ 146 (W_{1/2} = 6950 Hz).

[Et₂Al(μ-OCH₂CH₂SMe)]₂ (1.13). Prepared in a similar manner to compound **1.11**, but using AlEt₃ (2.62g, 23.0 mmol) and HOCH₂CH₂SCMe (2.12g, 23.0 mmol). Removal of solvent yields a viscous oil. Yield: *ca* 60%. MS (EI, %): *m/z* 351 (2M⁺, 15), 323 (2M⁺ - Et, 100), 147 (M⁺-Et, 10). IR (neat, cm⁻¹): 2898 (s, br), 1409 (s), 1381 (m), 1196 (s), 1064 (s, br), 1425 (s), 916 (m), 836 (s), 944 (m), 620 (s, br). ¹H NMR (C₆D₆): δ 3.47 [4H, t, *J*(H-H) = 5.5 Hz, OCH₂], 1.55 [6H, s, SCH₃], 2.18 [4H, t, *J*(H-H) = 5.5 Hz, SCH₂], 1.29 [12H, t, *J*(H-H) = 8.1 Hz, Al-CH₂CH₃], 0.18 [8H, q, *J*(H-H) = 8.1 Hz, Al-CH₂]. ¹³C NMR (C₆D₆): δ 59.1 (OCH₂), 36.7 (SCH₂), 14.1 (SCH₃), 10.4 (Al-CH₂CH₃). ²⁷Al NMR (C₇H₈, C₆D₆): δ 134 (W_{1/2} = 5410 Hz).

[(Me)₂Al(μ-OCH₂CH₂SMe)]₂ (1.14). Prepared in a similar manner to compound **1.11**, but using AlMe₃ (1.24g, 17.2mmol) and HOCH₂CH₂SMe (1.59g, 17.2 mmol). Yield: *ca* 70% Mp. 85 - 87 °C. MS (EI, %): *m/z* 281 (2M⁺ - Me, 60), 221 (2M⁺ - CH₂CH₂SMe, 30), 131 (M⁺ - Me, 20), 75 (CH₂CH₂SMe, 100). Molecular weight

determination: 306 (296). IR (neat, cm^{-1}): 2965 (s), 2899 (w), 2366 (m), 1263 (s), 1096 (s), 1024 (s), 804 (s), 871 (w), 691 (w). ^1H NMR (C_6D_6): δ 3.41 [4H, t, $J(\text{H-H}) = 5.4$ Hz, OCH_2], 1.47 (6H, s, SCH_3), 2.09 [4H, t, $J(\text{H-H}) = 5.4$ Hz, SCH_2], -0.36 (12H, s, Al- CH_3). ^{13}C NMR (C_6D_6): δ 58.5 (OCH_2), 37.2 (SCH_2), 13.9 (SCH_3), -10.0 (br, Al- CH_3). ^{27}Al NMR (C_7H_8 , C_6D_6): δ 142 ($W_{1/2} = 3440$ Hz).

[($t\text{Bu}$)₂Al(μ -OCH₂CH₂CH₂SMe)]₂ (1.15). Prepared in the same manner as compound **1.11**, but using Al($t\text{Bu}$)₃ (3.16g, 15.96 mmol) and HOCH₂CH₂CH₂SMe (1.695 g, 15.96 mmol). Yield: *ca.* 80 %. Mp: 110 - 112 °C. MS (EI, %): *m/z*: 435 (2M⁺ - $t\text{Bu}$, 100), 189 (M⁺ - $t\text{Bu}$, 10), 147 (M⁺ - 2 $t\text{Bu}$, 20), 106 (OCH₂CH₂SMe, 20). Molecular weight determination: 496 (492). IR (cm^{-1}): 2961 (m), 2908 (w), 2826 (w), 1264 (s), 1096 (s), 1018 (s), 805 (s), 682 (w). ^1H NMR (C_6D_6): δ 3.88 [4H, t, $J(\text{H-H}) = 7.0$ Hz, OCH_2], 2.00 [4H, t, $J(\text{H-H}) = 7.0$ Hz, SCH_2], 1.87 (2H, m, CH₂CH₂CH₂), 1.71 (6H, s, SCH_3), 1.24 [36H, s, C(CH₃)₃]. ^{13}C NMR (C_6D_6): δ 65.1 (OCH_2), 33.0 (SCH_2), 32.4 [C(CH₃)₃], 30.1 (SCH_3), 15.6 (CH₂CH₂CH₂). ^{27}Al NMR ($\text{C}_7\text{H}_8/\text{C}_6\text{D}_6$): δ 138 ($W_{1/2} = 5220$ Hz).

[Me₂Al(μ -OCH₂CH₂CH₂SMe)]₂ (1.16). Prepared in the same manner as compound **1.11**, but using AlMe₃ (0.698g, 9.7 mmol) and HOCH₂CH₂CH₂SMe (1.03g, 9.7 mmol). Yield: *ca.* 40%. MS (EI, %): *m/z* 309 (2M⁺ - Me, 100), 235 (2M⁺ - CH₂CH₂CH₂SMe, 70), 147 (M⁺ - Me, 55), 105 (OCH₂CH₂CH₂SMe, 30), 89 (CH₂CH₂CH₂SMe, 60). IR (neat, cm^{-1}): 2919 (s, br), 1479 (m), 1436 (s), 1393 (w), 1279 (m), 1196 (s), 1052 (s, br), 872 (w), 692 (s, br), 497 (m). ^1H NMR (C_6D_6): δ 3.80 [4H, t, $J(\text{H-H}) = 7.4$ Hz, OCH_2], 2.11 [4H, $J(\text{H-H}) = 6.8$ Hz, SCH_2], 1.79 (4H, m, CH₂CH₂CH₂), 1.75 (6H, s, SCH_3), -0.52 (12H, s, Al-CH₃). ^{13}C NMR (C_6D_6): 64.4 (OCH₂), 31.8 (SCH_2), 30.3 (SCH_3), 15.6 (CH₂CH₂CH₂), -8.7 (Al-CH₃). ^{27}Al NMR ($\text{C}_7\text{H}_8/\text{C}_6\text{D}_6$): δ 153 ($W_{1/2} = 5133$ Hz).

Equilibrium Studies. Since, a variation in ^{13}C NMR shifts for the α -carbon (OCH_2) is observed between different solvents, the same solvent (toluene-d₈) was used for all the variable temperature NMR measurements. Although the equilibrium constant is concentration independent, care was taken to ensure similar concentrations were used for all samples (0.1 - 1.0 mM). All the samples were heated to the appropriate temperature within the NMR spectrometer, and the ^{13}C NMR spectra was collected. Constancy of the spectrum was taken as evidence for the attainment of equilibrium. The temperature of the NMR spectrometer probe was calibrated using the chemical shifts of ethylene glycol.⁴⁸ This process was repeated for a minimum of 6 temperatures over a minimum temperature range of 80 K. Alternate points on the $\ln K_{\text{eq}}$ versus $1/T$ plot were obtained during upward and downward passages over the temperature range spanned. Because both sets of points fell on the same line, we consider that equilibration was achieved. The temperature dependence of the equilibrium constant, K_{eq} , allows for the determination of the ΔH and ΔS for the conversion of 5-coordinatespecies to 4-coordinate species . A summary of calculated values is given in Table 1.8.

Crystallographic Studies. Crystals of compounds **1.1**, **1.2**, **1.6**, **1.11**, **1.12**, **1.15** were sealed in a glass capillaries under argon. Crystal and data collection and solution details are given in Table 1.12. Standard procedures in our laboratory have been described previously.⁴⁹ Data were collected on either an Enraf-Nonius CAD-4 or Rigaku four-circle diffractometer equipped with graphite monochromated Mo-K α radiation ($\lambda = 0.71073 \text{ \AA}$) and corrected for Lorentz and polarization effects. The structures were solved by using direct methods (using SHELXS-86⁵⁰), and difference Fourier synthesis and refined using full-matrix least squares.⁵¹ Scattering factors were taken from the usual source.⁵² No variation of $w(|F_0| - |F_c|)$ versus $|F_0|$ or $(\sin \theta/\lambda)$ was observed.

Computational Methods. *Ab initio* on all electron molecular orbital (MO) calculations were performed using the GAUSSIAN 92⁵³ suite of programs. Initial optimization of all structures was carried out at the Hartree-Fock level with the STO-3G basis set.⁵⁴ The results from these studies were used as the initial guess for optimization using the 3-21G(*) basis set.⁵⁵ To determine the relative energy of each species with electron correlation included, second-order Møller-Plesset (MP2) calculations were performed.⁵⁶

Table 1.12. Summary of X-ray Diffraction Data.

Compound	$[(t\text{Bu})_2\text{Al}(\mu\text{-OCH}_2\text{CH}_2\text{OMe})]_2$ (1.1)	$[(i\text{Bu})_2\text{Al}(\mu\text{-OCH}_2\text{CH}_2\text{OMe})]_2$ (1.2)
empir. formula	$\text{C}_{22}\text{H}_{50}\text{Al}_2\text{O}_4$	$\text{C}_{22}\text{H}_{50}\text{Al}_2\text{O}_4$
cryst size, mm	0.22 x 0.25 x 0.28	0.12 x 0.31 x 0.34
cryst system	monoclinic	triclinic
space group	$\text{P}2_1/\text{n}$	$\text{P}\bar{1}$
<i>a</i> , Å	8.9670(8)	8.6257(9)
<i>b</i> , Å	8.9127(7)	9.597(1)
<i>c</i> , Å	17.703(1)	10.0584(9)
α , deg		69.894(8)
β , deg	99.460(7)	88.889(8)
γ , deg		65.659(8)
V, Å ³	1395.6(2)	705.1(1)
Z	2	1
D(calcd), g/cm ³	1.029	1.019
μ , cm ⁻¹	1.20	1.19
temp, K	298	298
2θ range, deg	2.0 - 44.0	3.0 - 50.0
no. collected	1970	2477
no. ind	1844	2477
no. obsd	668 ($ F_o > 5.0\sigma F_o $)	1738 ($ F_o > 6.0\sigma F_o $)
weighting scheme	$w^{-1} = 0.04(F_o)^2 + \sigma(F_o)^2$	$w^{-1} = 0.04(F_o)^2 + \sigma(F_o)^2$
R	0.1345	0.0475
R _w	0.1480	0.0475
largest diff peak, eÅ ⁻³	0.55	0.24

Table 1.12 contd.

Compound	$[(t\text{Bu})_2\text{Al}(\mu\text{-OCH}_2\text{CH}_2\text{CH}_2\text{OMe})]_2$ (1.6)	$[\text{Me}_2\text{Al}(\mu\text{-OCH}_2\text{CH}_2\text{CH}_2\text{OMe})]_2$ (1.7)
empir. formula	$\text{C}_{24}\text{H}_{54}\text{Al}_2\text{O}_4$	$\text{C}_{12}\text{H}_{30}\text{Al}_2\text{O}_4$
cryst size, mm	0.12 x 0.14 x 0.61	0.21 x 0.24 x 0.32
cryst system	monoclinic	monoclinic
space group	P2 ₁ /c	C2
a, Å	9.372(1)	12.425(3)
b, Å	18.745(3)	9.6446(2)
c, Å	8.459(2)	7.754(2)
α , deg		
β , deg	100.37(2)	104.15(2)
γ , deg		
V, Å ³	1461.8(5)	901.1(3)
Z	2	2
D(calcd), g/cm ³	1.046	1.077
μ , cm ⁻¹	1.18	1.65
temp, K	298	298
2θ range, deg	3.0 - 44.0	4.0 - 40.0
no. collected	1968	682
no. ind	1848	319
no. obsd	857 ($ F_o > 6.0\sigma F_o $)	251 ($ F_o > 6.0\sigma F_o $)
weighting scheme	$w^{-1} = 0.04(F_o)^2 + \sigma(F_o)^2$	$w^{-1} = 0.04(F_o)^2 + \sigma(F_o)^2$
R	0.0664	0.103
R _w	0.0668	0.228
largest diff peak, eÅ ⁻³	0.25	0.37

Table 1.12, contd.

Compound	$[(t\text{Bu})_2\text{Al}(\mu\text{-OCH}_2\text{CH}_2\text{SMe})]_2$ (1.11)	$[(i\text{Bu})_2\text{Al}(\mu\text{-OCH}_2\text{CH}_2\text{SMe})]_2$ (1.12)
empir. formula	$\text{C}_{22}\text{H}_{50}\text{Al}_2\text{O}_2\text{S}_2$	$\text{C}_{22}\text{H}_{50}\text{Al}_2\text{O}_2\text{S}_2$
cryst size, mm	0.18 x 0.24 x 0.29	0.09 x 0.21 x 0.32
cryst system	triclinic	monoclinic
space group	$\bar{\text{P}}\bar{1}$	$\text{P}2_1/\text{c}$
<i>a</i> , Å	8.529(1)	8.4518(6)
<i>b</i> , Å	9.1211(9)	17.913(2)
<i>c</i> , Å	10.689(1)	9.8953(6)
α , deg	67.168(8)	
β , deg	80.302(9)	100.755(5)
γ , deg	73.495(9)	
<i>V</i> , Å ³	733.2(1)	1471.8(2)
<i>Z</i>	1	2
D(calcd), g/cm ³	1.052	1.003
μ , cm ⁻¹	2.46	2.43
temp, K	298	298
2θ range, deg	3.0 - 50.0	3.0 - 50.0
no. collected	2566	2844
no. ind	2566	2667
no. obsd	1637 ($ F_o > 6.0\sigma F_o $)	1647 ($ F_o > 6.0\sigma F_o $)
weighting scheme	$w^{-1} = 0.04(F_o)^2 + \sigma(F_o)^2$	$w^{-1} = 0.04(F_o)^2 + \sigma(F_o)^2$
R	0.0999	0.0487
R_w	0.1354	0.0489
largest diff peak, eÅ ⁻³	0.87	0.28

Table 1.12, contd.

Compound	$[(t\text{Bu})_2\text{Al}(\mu-\text{OCH}_2\text{CH}_2\text{CH}_2\text{SMe})]_2$ (1.15)
empir. formula	$\text{C}_{24}\text{H}_{54}\text{Al}_2\text{O}_2\text{S}_2$
cryst size, mm	0.15 x 0.21 x 0.42
cryst system	monoclinic
space group	$\text{P}2_1/\text{c}$
<i>a</i> , Å	8.787(2)
<i>b</i> , Å	15.990(2)
<i>c</i> , Å	10.964(1)
α , deg	
β , deg	95.17(1)
γ , deg	
<i>V</i> , Å ³	1534.2(4)
<i>Z</i>	2
D(calcd), g/cm ³	1.067
μ , cm ⁻¹	2.38
temp, K	298
2θ range, deg	3.0 - 50.0
no. collected	2976
no. ind	2800
no. obsd	1667 ($ F_o > 6.0\sigma F_o $)
weighting scheme	$w^{-1} = 0.04(F_o)^2 + \sigma(F_o)^2$
R	0.0417
R _w	0.0548
largest diff peak, eÅ ⁻³	0.25

References

- 1 See for example, (a) O. T. Beachley, Jr., and K. C. Racette, *Inorg. Chem.*, 1976, **15**, 2110, and references therein.
 (b) D. A. Atwood, F. P. Gabbai, J. Lu, M. P. Remington, D. Rutherford, and M. P. Sibi, *Organometallics*, 1996, **15**, 2308.
 (c) M. R. P. van Vliet, G. van Koyen, M. A. Rotteveel, M. Schrap, K. Vrieze, B. Kojic-Prodic, A. L. Spek, and A. J. M. Duisenberg, *Organometallics*, 1986, **5**, 1389.
 (d) C. Jones, F. C. Lee, G. A. Koutsantonis, M. G. Gardiner, and C. L. Raston, *J. Chem. Soc., Dalton Trans.*, 1996, **829**.
 (e) M. P. Hogerheide, M. Wesseling, J. T. B. H. Jastrzebski, J. Boersma, H. Kooijman, A. L. Spek, and G. van Koten, *Organometallics*, 1995, **14**, 4483.
 (f) S. T. Dzugan and V. L. Goedken, *Inorg. Chim. Acta.*, 1988, **154**, 169.
 (g) M. R. P. van Vliet, P. Buysingh, G. van Koyen, K. Vrieze, B. Kojic-Prodic, and A. L. Spek, *Organometallics*, 1985, **4**, 1701.
- 2 R. Kumar, M. L. Sierra, and J. P. Oliver, *Organometallics*, 1994, **13**, 4285.
- 3 In the present case the anionic donor atom is oxygen, however, other Group 16 or Group 14 and 15 donor atoms are also possible.
- 4 (a) E. A. Jeffery, T. Mole, and K. J. Saunders, *Can. J. Chem.*, 1968, **21**, 137.
 (b) E. A. Jeffery; T. Mole, and J. K. Saunders, *Can. J. Chem.*, 1968, **21**, 649.
- 5 We have previously proposed the term latent Lewis acidity to describe the cage-opening reactions of alkylalumoxane compounds, see (a) C. J. Harlan, S. G. Bott, and A. R. Barron, *J. Am. Chem. Soc.*, 1995, **117**, 6465.
 (b) Y. Koide, S. G. Bott, and A. R. Barron, *Organometallics*, 1996, **15**, 2213.
 (c) Y. Koide, S. G. Bott, and A. R. Barron, *Organometallics*, 1996, **15**, 5514.
- 6 J. A. Francis, C. N. McMahon, and A. R. Barron, submitted for publication.
- 7 D. C. Bradley, R. C. Mehrotra, and P. D. Gaur, in *Metal Alkoxides*, Academic Press, New York, 1978.

- 8 The theoretical chelate bite angle for planar five- and six-membered cycles are 108° and 120°, respectively.
- 9 R. Benn, A. Rufinska, H. Lehmkul, E. Janssen, and C. Krüger, *Angew. Chem., Int. Ed. Engl.* 1983, **22**, 779.
- 10 See for example, (a) A. Haaland and O. Stokkeland, *J. Organomet. Chem.*, 1975, **94**, 345.
(b) R. H. Cayton, M. H. Chisholm, E. R. Davidson, V. F. DiStas, P. Du, and J. C. Huffmann, *Inorg. Chem.*, 1991, **30**, 1020.
(c) C. L. Aitken and A. R. Barron, *J. Chem. Cryst.*, 1996, **26**, 293.
- 11 J. T. Leman, H. A. Roman, and A. R. Barron, *Organometallics*, 1993, **12**, 2988.
- 12 C. A. Tolman, *Chem. Rev.*, 1977, **77**, 313.
- 13 See for example, (a) A. Haaland, S. Samdal, O. Stokkeland, and J. Weidlein, *J. Organomet. Chem.*, 1977, **134**, 165.
(b) J. L. Atwood and G. D. Stucky, *J. Am. Chem. Soc.*, 1967, **89**, 5362.
(c) V. Srinivas, J. de Mel, and J. P. Oliver, *Organometallics*, 1989, **8**, 827.
(d) A. F. M. M. Rahman, K. F. Siddiqui, and J. P. Oliver, *J. Organomet. Chem.* 1987, **319**, 161.
- 14 D. G. Hendershot, M. Barber, R. Kumar, and J. P. Oliver, *Organometallics*, 1991, **10**, 3302.
- 15 H. Schumann, M. Frick, B. Heymer, and F. Girgsdies, *J. Organomet. Chem.*, 1996, **512**, 117.
- 16 T. A. Albright, J. K. Burdett, and M. H. Whangbo, *Orbital Interactions in Chemistry*, Wiley, New York, 1985, Chapter 14, p 273.
- 17 T. C. Appleton, H. C. Clark, and L. E. Manzer, *Coord. Chem. Rev.*, 1973, **10**, 335.
- 18 (a) M. D. Healy, J. W. Ziller, and A. R. Barron, *J. Am. Chem. Soc.*, 1990, **112**, 2949.

- (b) M. D. Healy, M. B. Power, and A. R. Barron, *J. Coord. Chem.*, 1990, **21**, 363.
- ¹⁹ A. J. Ashe, III, J. W. Kampf, and J. R. Waas, *Organometallics*, 1997, **16**, 163.
- ²⁰ See for example, A. R. Barron, *Polyhedron* 1995, **14**, 3197.
- ²¹ J. H. Rogers, A. W. Applett, W. M. Cleaver, A. N. Tyler, and A. R. Barron, *J. Chem. Soc., Dalton Trans.*, 1992, 3179.
- ²² A. R. Barron, *J. Chem. Soc., Dalton Trans.*, 1988, 3047.
- ²³ J. Sandström, *Dynamic NMR Spectroscopy*, Academic Press, London, 1982.
- ²⁴ J. A. Francis, C. N. McMahon, and A. R. Barron, *J. Chem. Cryst.*, 1997, **27**, 167.
- ²⁵ For a detailed explanation, see Chapter 6.
- ²⁶ D. A. Wierda and A. R. Barron, *Polyhedron*, 1989, **8**, 831.
- ²⁷ For example, the dissociation enthalpies, ΔH of the adduct $\text{AlMe}_3(\text{OEt}_2)$ is 84.5 $\text{kJ}\cdot\text{mol}^{-1}$ compared to 70.2 $\text{kJ}\cdot\text{mol}^{-1}$ for $\text{AlMe}_3(\text{SEt}_2)$, see (a) C. H. Henrickson, and D. P. Eyman, *Inorg. Chem.*, 1967, **6**, 1461.
(b) C. H. Henrickson, D. Duffy, and D. P. Eyman, *Inorg. Chem.*, 1968, **7**, 1047.
- ²⁸ A. Haaland, *Coordination Chemistry of Aluminum*, Ed. Robinson G. H., VCH, New York, 1993, Ch. 1.
- ²⁹ See for example, (a) S. L. Stoll, S. G. Bott, and A. R. Barron, *J. Chem. Soc., Dalton Trans.*, 1997, 1315.
(b) M. A. Banks, O. T. Beachley, Jr., H. J. Gysling, and H. R. Luss, *Organometallics*, 1990, **9**, 1979.
(c) W. Uhl, M. Layh, G. Becker, K. W. Klinkhammer, and T. Hildenbrand, *Chem. Ber.*, 1992, **125**, 1547.
- ³⁰ C. N. McMahon, S. G. Bott, and A. R. Barron, *J. Chem. Soc., Dalton Trans.*, 1997, 3129.
- ³¹ See for example, (a) A. Weiss, R. Plass, and A. Weiss, *Z. Anorg. Allg. Chem.*, 1956, **283**, 390.

- (b) G. H. Robinson, H. Zhang, and J. L. Atwood, *Organometallics*, 1987, **6**, 887.
- (c) N Burford, B. W. Royan, R. E. v. H. Spence, and R. D. Rogers, *J. Chem. Soc., Dalton Trans.*, 1990, 2111.
- 32 It should be noted that this assumes that solvation of the 4-coord. and 5-coord. isomers of $[R_2Al(\mu-OCH_2CH_2ER'_x)]_2$ are not significantly different.
- 33 Unfortunately re-equilibration of the solution results is too rapid to allow the enthalpy (ΔH^\ddagger) and entropy (ΔS^\ddagger) of activation to be determined from an appropriate Eyring plot.
- 34 (a) M. B. Power, J. R. Nash, M. D. Healy, and A. R. Barron, *Organometallics*, 1992, **11**, 1830.
(b) M. B. Power, J. W. Ziller, and A. R. Barron, *Organometallics*, 1993, **12**, 4908.
- 35 It is worth noting that the sign of the calculated value for ΔG at 298 K, correlates well with the position of the equilibrium (K_{eq}) at 298 K.
- 36 The observed values are towards the low end of typical O-H \cdots N hydrogen bonds (4 - 40 kJ.mol $^{-1}$), see (a) G. C. Pimentel, and A. L. McClellan, *The Hydrogen Bond*, Freeman, San Francisco, 1960.
(b) M. D. Joesten, and L. J. Schaad, *Hydrogen Bonding*, Dekker, New York, 1974.
- 37 A. W. Hofmann, *Chem. Ber.*, 1872, **5**, 704.
- 38 V. Meyer, *Chem. Ber.*, 1894, **27**, 510.
- 39 For a review of the early developments of steric effects in organic chemistry see, H. S. Mosher and T. T. Tidwell, *J. Chem. Educ.*, 1990, **67**, 9.
- 40 C. A. Tolman, *J. Am. Chem. Soc.*, 1970, **92**, 2953.
- 41 For a recent review see, D. White and N. J. Coville, *Adv. Organomet. Chem.* 1994, **36**, 95.
- 42 See for example, (a) T. L. Brown, *Inorg. Chem.*, 1992, **31**, 1286.
(b) B. Staskun, *J. Org. Chem.*, 1981, **46**, 1643.

- (c) M. N. Golovin, M. M. Rahman, J. Belmonte, and W. P. Giering, *Organometallics*, 1985, **4**, 1981.
- 43 A.R. Barron and G. Wilkinson, *Polyhedron*, 1986, **5**, 1897.
- 44 A.R. Barron, K. D. Dobbs, and M. M. Fralch, *J. Am. Chem. Soc.*, 1991, **113**, 39. and references therein.
- 45 For an alternative approach to quantification of repulsion forces see, (a) M.-G. Choi and T. L. Brown, *Inorg. Chim. Acta*, 1992, **198**, 823.
(b) M.-G. Choi, and T. L. Brown, *Inorg. Chem.*, 1993, **32**, 1548.
- 46 E. P. Clark, *Ind. Eng. Chem. Anal. Ed.*, 1941, **13**, 820.
- 47 (a) W. Uhl, *Z. Anorg. Allg. Chem.*, 1989, **570**, 37.
(b) H. Lehmkuhl, O. Olbrysche, and H. Nehl, *Liebigs Ann. Chem.*, 1973, 708.
(c) H. Lehmkuhl, and O. Olbrysche, *Liebigs Ann. Chem.*, 1973, 715.
- 48 (a) A. L. van Geet, *Anal. Chem.*, 1968, **40**, 2227.
(b) H. J. Gordon, and R. A. Ford, *The Chemists Companion*, Wiley, New York, 1972.
- 49 M. R. Mason, J. M. Smith, S. G. Bott and A. R. Barron, *J. Am. Chem. Soc.*, 1993, **115**, 4971
- 50 G. M. Sheldrick, *Acta Crystallogr.*, 1990, **A46**, 467.
- 51 MolEN - Enraf-Nonius. MolEN, An interactive Structure Solution Procedure; Enraf-Nonius, Delft, Netherlands, 1990.
- 52 *International Tables for X-Ray Crystallography*, Kynoch Press, Birmingham, 1974, vol. 4.
- 53 *Gaussian 92/DFT, Revision G.2*, M. J. Frisch, G. W. Trucks, H. B. Schlegel, P. M. W. Gill, B. G. Johnson, M. W. Wong, J. B. Foresman, M. A. Robb, M. Head-Gordon, E. S. Replogle, R. Gomperts, J. L. Andres, K. Raghavachari, J. S. Binkley,

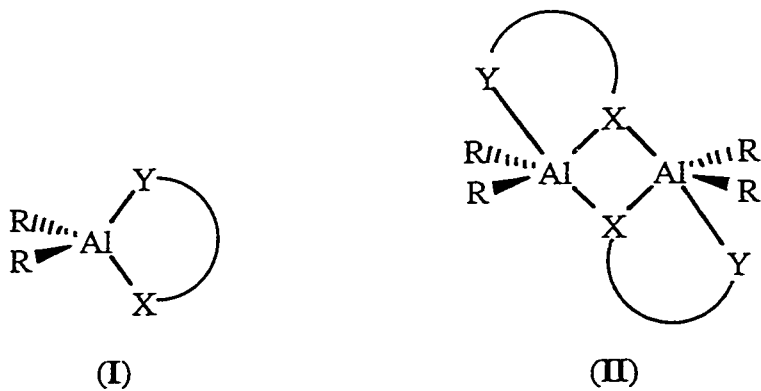
- C. Gonzalez, R. L. Martin, D. J. Fox, D. Defrees, J. J. Baker, J. J. P. Stewart, and J. A. Pople, Gaussian, Inc., Pittsburgh PA, 1993.
- 54 A. R. Barron, unpublished results.
- 55 (a) First-row elements: J. S. Binkley, J. A. Pople, and W. J. Hehre, *J. Am. Chem. Soc.*, 1980, **102**, 939.
(b) Second-row elements: W. J. Pietro, M. M. Franci, W. J. Hehre, D. J. DeFrees, J. A. Pople, and J. S. Binkley, *J. Am. Chem. Soc.*, 1982, **104**, 5039.
- 56 (a) C. Møller and M. S. Plesset, *Phys. Rev.*, 1934, **46**, 618.
(b) J. S. Binkley and J. A. Pople, *Int. J. Quantum Chem.*, 1975, **9**, 229.

Chapter 2

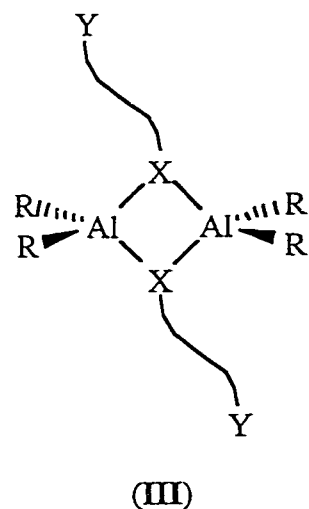
Aluminum Compounds Containing Bidentate Ligands: Chelate Ring Size and Rigid Conformation Effects

Introduction

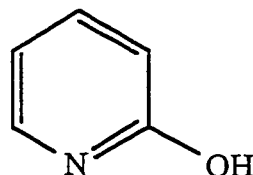
Given the results described in chapter 1, it is of interest to develop an understanding of the geometric rather than steric or electronic factors that control the extent of oligomerization and coordination number at the aluminum center in compounds with non-delocalized ligands containing both anionic and neutral Lewis base termini; in particular, what controls the relative stability of a monomer **I** versus a dimer **II**.¹



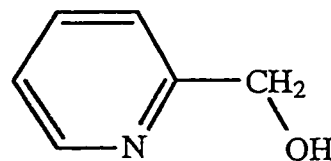
Compounds of this general type are known with a wide range of substituents, e.g., $X = O, S, NR', CH_2$; $Y = OR', SR', NR'_2$, where $R' = \text{alkyl}$.² The studies described in Chapter 1 have shown that the strength of bonding at the fifth coordination site in **(II)** is highly dependent on the steric bulk of the substituents at aluminum (R) and the neutral Lewis base donor (R').¹ However, in the case of alkoxide-based ligands (i.e., $X = O$) increased steric bulk does not result in the formation of a monomer **(I)**; a 4-coordinate dimer is formed instead **(III)**. Based on these results it would appear that the Lewis base termini ($Y = \text{ether or thioether}$) are insufficiently basic to cleave the $\text{Al}(\mu\text{-O})_2\text{Al}$ core of a dimeric alkoxide to give monomeric chelate compounds.



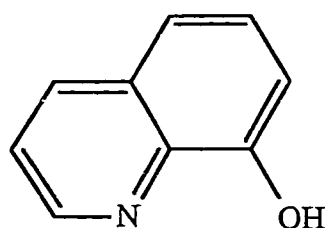
A similar effect has been previously observed for aluminum aryloxides,³ and it has been demonstrated that pyridine and related ligands react with oligomeric aluminum compounds to yield monomers. Thus, use of pyridine (and quinoline⁴) based ligands (**IV** - **VII**) should result in the formation of monomeric compounds given sufficient steric bulk at aluminum.



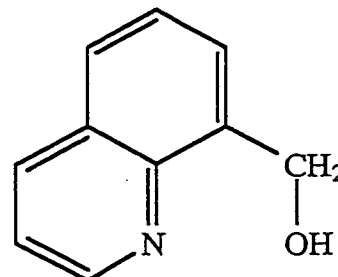
(IV)



(V)



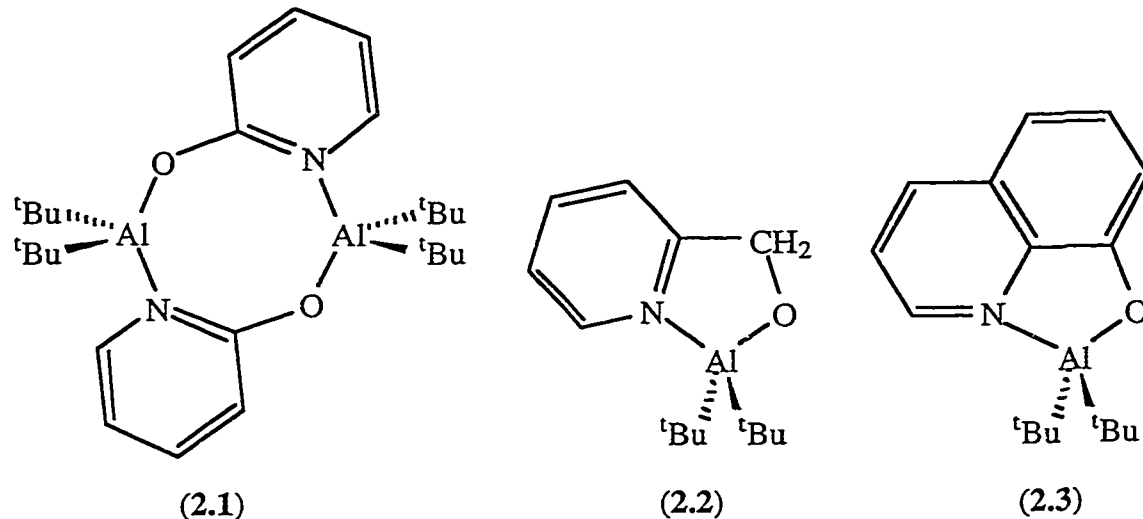
(VI)

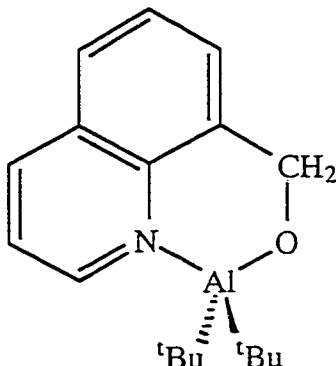


(VII)

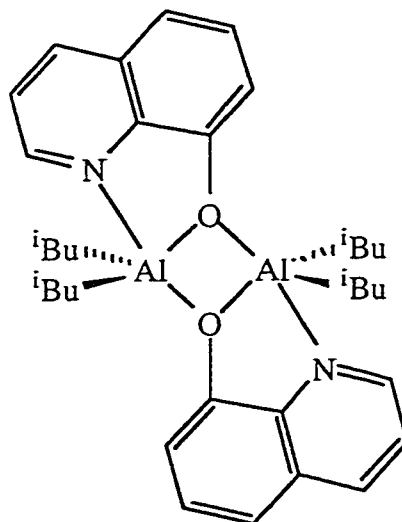
Results and Discussion

Reaction of $\text{Al}(\text{tBu})_3$ with 2-hydroxypyridine (**IV**), 2-pyridinemethanol (**V**), 8-hydroxyquinoline (**VI**), and 8-quinolinemethanol (**VII**) yields $[(\text{tBu})_2\text{Al}(\mu\text{-O-2-C}_5\text{H}_4\text{N})]_2$ (**2.1**), $(\text{tBu})_2\text{Al}(\text{OCH}_2\text{-2-C}_5\text{H}_4\text{N})$ (**2.2**), $(\text{tBu})_2\text{Al}(\text{O-8-C}_9\text{H}_6\text{N})$ (**2.3**) and $(\text{tBu})_2\text{Al}(\text{OCH}_2\text{-8-C}_9\text{H}_6\text{N})$ (**2.4**), respectively. The *iso*-butyl derivative of **2.3**, $[(\text{iBu})_2\text{Al}(\mu\text{-O-8-C}_9\text{H}_6\text{N})]_2$ (**2.5**), is prepared in an analogous manner. Compounds **2.1** - **2.5** have been characterized by ^1H , ^{13}C and ^{27}Al NMR, and MS weight (see Experimental). The ^{27}Al NMR spectra for compounds **2.1** - **2.4** all consist of a broad resonance ($\delta = 120$ - 140 ppm) indicative of a four-coordinate aluminum in a C_2AlON coordination environment.⁵ In contrast, the ^{27}Al NMR spectrum for $[(\text{iBu})_2\text{Al}(\mu\text{-O-8-C}_9\text{H}_6\text{N})]_2$ (**2.5**) ($\delta = 81$ ppm) is similar to that observed for other five-coordinate compounds with $\text{C}_2\text{AlO}_2\text{N}$ coordination.^{1,2} Compounds **2.3** and **2.5** are both yellow in color with an associated absorbance in the visible spectrum [$\lambda = 384$ nm (**2.3**), 375 nm (**2.5**)], which appears to be essentially independent of the coordination about aluminum. Similar spectra have been observed for other quinoline compounds of aluminum.⁶ The solid state molecular structures of compounds **2.1**, **2.3** and **2.5** have been determined by X-ray crystallography.





(2.4)



(2.5)

The molecular structure of $[({}^t\text{Bu})_2\text{Al}(\mu\text{-O-2-C}_5\text{H}_4\text{N})]_2$ (**2.1**) is shown in Figure 2.1; selected bond lengths and angles are given in Table 2.1. Compound **2.1** exists as a centrosymmetric molecule in which both the oxygen and nitrogen donor atoms of the hydroxypyridine ligands bridge the two $\text{Al}({}^t\text{Bu})_2$ moieties, resulting in an eight membered $\text{Al}_2\text{O}_2\text{C}_2\text{N}_2$ cyclic core. The $\text{Al}(1)\text{-O}(2)$ and $\text{Al}(1)\text{-N}(1)$ bond lengths [1.774(5) and 1.991(2) Å, respectively] are shorter than the range expected for simple Lewis acid-base complexes (2.0 - 2.1 Å).⁷ Although the pyridine rings are stacked in the crystal lattice, the inter-ring distance (> 4.5 Å) is greater than that expected for any significant electronic interaction (i.e., 3.4 Å).⁸

As a bridging ligand, hydroxypyridine is isolobal to carboxylate, and the structure of compound **2.1** is similar to those observed for $[\text{R}_2\text{Al}(\mu\text{-O}_2\text{CR}')]_2$.⁹ In fact, the ligand bite distance [$\text{Al}(1)\cdots\text{Al}(1a) = 4.14$ Å] is within the range previously observed for alkylaluminum carboxylates [3.26 - 4.46 Å].^{9,10} Furthermore, as with the carboxylate analogs, the eight-membered ring in $[({}^t\text{Bu})_2\text{Al}(\mu\text{-O-2-C}_5\text{H}_4\text{N})]_2$ adopts a chair-like conformation (**VIII**).

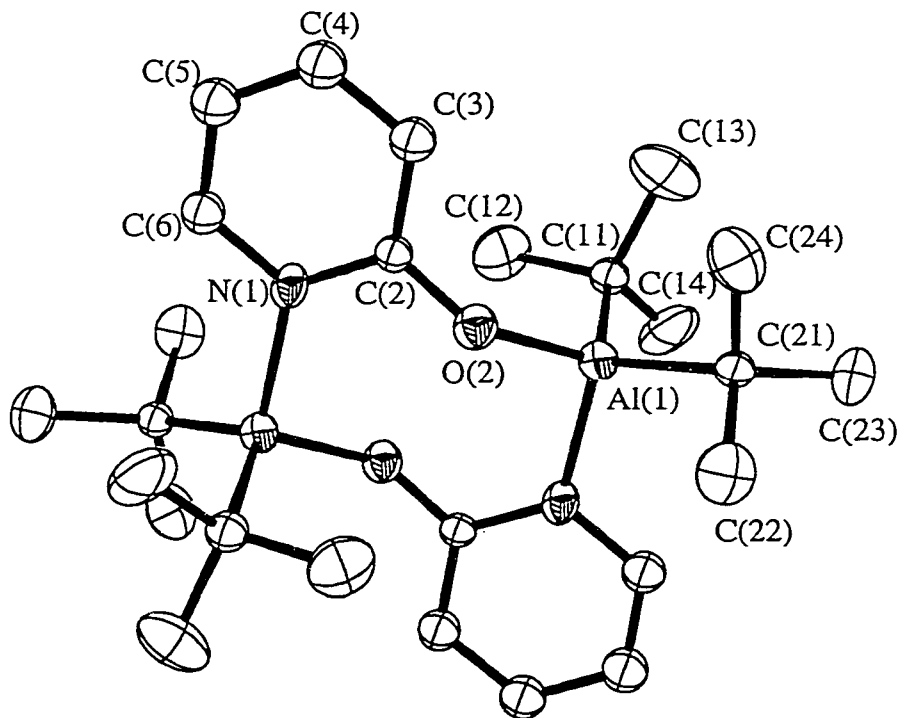
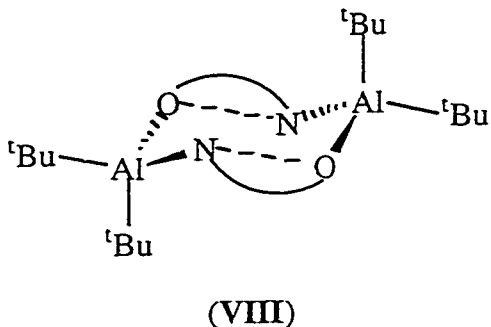


Figure 2.1. Molecular structure of $[(\text{tBu})_2\text{Al}(\mu\text{-O-2-C}_5\text{H}_4\text{N})]_2$ (2.1). Thermal ellipsoids are shown at the 30 % level, and hydrogen atoms are omitted for clarity.

Table 2.1. Selected Bond Lengths (\AA) and Angles ($^\circ$) in $[(\text{tBu})_2\text{Al}(\mu\text{-O-2-C}_5\text{H}_4\text{N})]_2$ (2.1).

Al(1)-O(2)	1.774(5)	Al(1)-N(1a)	1.991(2)
Al(1)-C(11)	1.963(8)	Al(1)-C(21)	1.990(8)
O(2)-C(2)	1.296(9)		
O(2)-Al(1)-N(1a)	102.4(1)	O(2)-Al(1)-C(11)	113.3(3)
O(2)-Al(1)-C(21)	104.8(3)	C(11)-Al(1)-C(21)	120.3(3)
C(11)-Al(1)-N(1a)	106.1(2)	C(21)-Al(1)-N(1a)	108.5(2)
Al(1)-O(2)-C(2)	140.0(4)		



Similar chair-like conformations have been observed for the gallium diphenylphosphinate compounds $[R_2Ga(\mu-O_2PPh_2)]_2$.¹¹ The puckering of the $Al_2O_2C_2N_2$ ring may be considered to be as a result of folding of the eight-membered ring along the two inter-ligand O···N vectors. The extent of folding (θ_{ring}) is defined as the angle between the AlON planes and the $O_2C_2N_2$ plane. It has been demonstrated that there exists a correlation between the extent of the puckering of the $Al_2O_4C_2$ ring in aluminum carboxylates with the steric bulk of the carboxylate alkyl substituent, R.⁹ However, in the absence of steric interactions, the "ideal" folding angle (θ_{ring}) should be *ca.* 130 °. The fold angle in $[(t\text{-Bu})_2Al(\mu-O-2-C_5H_4N)]_2$ (2.1) (127.4 °) is consistent with the hydroxypyridine ligand being sterically similar to formate, $[O_2CH]^-$.

The molecular structure of $(t\text{-Bu})_2Al(O-8-C_9H_6N)$ (2.3) is shown in Figure 2.2; selected bond lengths and angles are given in Table 2.2. Unlike $[R_2Al(\mu-O-8-C_9H_6N)]_2$ ($R = t\text{-Bu}$, Et, see below), compound 2.3 exists as a monomer with no significant inter-molecular contacts. The $Al(1)\text{-O}(1)$ and $Al(1)\text{-N}(1)$ bond lengths [1.806(4) and 1.974(6) Å, respectively] are typical of such interactions,¹² while the coordination about aluminum is distorted from an ideal tetrahedral geometry due to the small bite angle of the 8-quinolinol ligand [85.3(2)°].

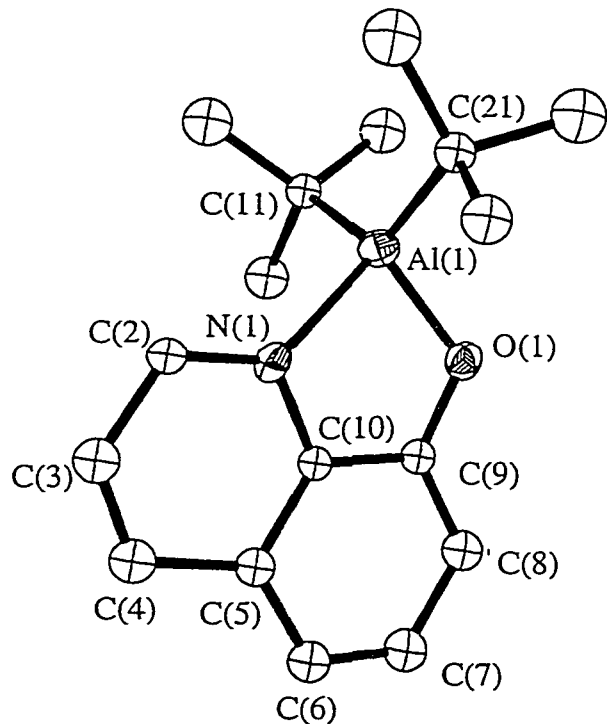
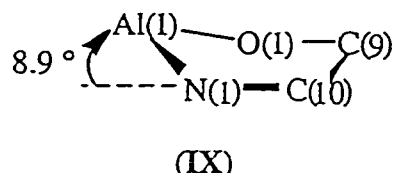


Figure 2.2. Molecular structure of $(\text{tBu})_2\text{Al}(\text{O}-8-\text{C}_9\text{H}_6\text{N})$ (2.3). Thermal ellipsoids are shown at the 20 % level, and hydrogen atoms are omitted for clarity.

Table 2.2. Selected Bond Lengths (\AA) and Angles ($^\circ$) in $(\text{tBu})_2\text{Al}(\text{O}-8-\text{C}_9\text{H}_6\text{N})$ (2.3).

Al(1)-O(1)	1.806(4)	Al(1)-N(1)	1.979(3)
Al(1)-C(11)	1.974(6)	Al(1)-C(21)	1.937(6)
O(1)-C(9)	1.327(5)		
O(1)-Al(1)-N(1)	85.3(2)	O(1)-Al(1)-C(11)	112.2(2)
O(1)-Al(1)-C(21)	111.1(2)	N(1)-Al(1)-C(11)	106.4(2)
N(1)-Al(1)-C(21)	112.1(2)	C(11)-Al(1)-C(21)	123.2(2)
Al(1)-O(1)-C(9)	114.5(3)	Al(1)-N(1)-C(2)	132.2(3)
Al(1)-N(1)-C(10)	108.6(3)	C(2)-N(1)-C(10)	119.1(4)

Although the 8-quinolinol moiety is planar, the Al(1)-N(1)-C(10)-C(9)-O(1) ring is puckered (**IX**) as demonstrated by the aluminum being 0.15 Å out of the N(1)-C(10)-C(9)-O(1) plane, presumably in order to minimize the ring strain.



It is interesting to note that despite the extended π -system the crystal packing of compound **2.3** is not dominated by $\pi \cdots \pi$ stacking interactions. Instead, the molecules of are stacked "head-to-tail" (see Figure 2.3) such that the 8-quinolinol's π system is sandwiched between the *tert*-butyl groups of adjacent molecules.

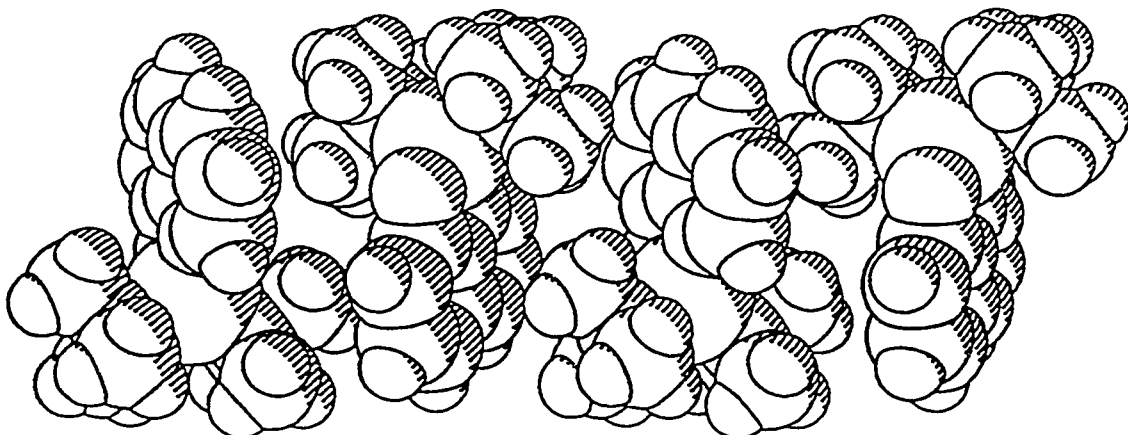


Figure 2.3. A space filling representation of the "head-to-tail" molecular packing of $(^t\text{Bu})_2\text{Al}(\text{O}-8-\text{C}_9\text{H}_6\text{N})$ (**2.3**).

The molecular structure of $[(^t\text{Bu})_2\text{Al}(\mu-\text{O}-8-\text{C}_9\text{H}_6\text{N})]_2$ (**2.5**) is shown in Figure 2.4; selected bond lengths and angles are given in Table 2.3 along with the corresponding

values for the previously reported ethyl analog, $[\text{Et}_2\text{Al}(\mu\text{-O-8-C}_9\text{H}_6\text{N})]_2$.¹³ Both compounds are dimeric being bridged by the oxygens of the chelating 8-quinolate ligands. A fifth coordination site on each aluminum is filled by interaction with the nitrogen atom of a 8-quinolate ligand. The Al(1)-N(1) distance [2.124(7) Å] is somewhat longer than a typical Al-N Lewis acid base interaction, however, it is similar to that observed for $[\text{Et}_2\text{Al}(\mu\text{-O-8-C}_9\text{H}_6\text{N})]_2$ [2.136(9) Å] and is consistent with the axial coordination to the trigonal bipyramidal aluminum, N(1)-Al(1)-O(8a) = 151.5(2)°.

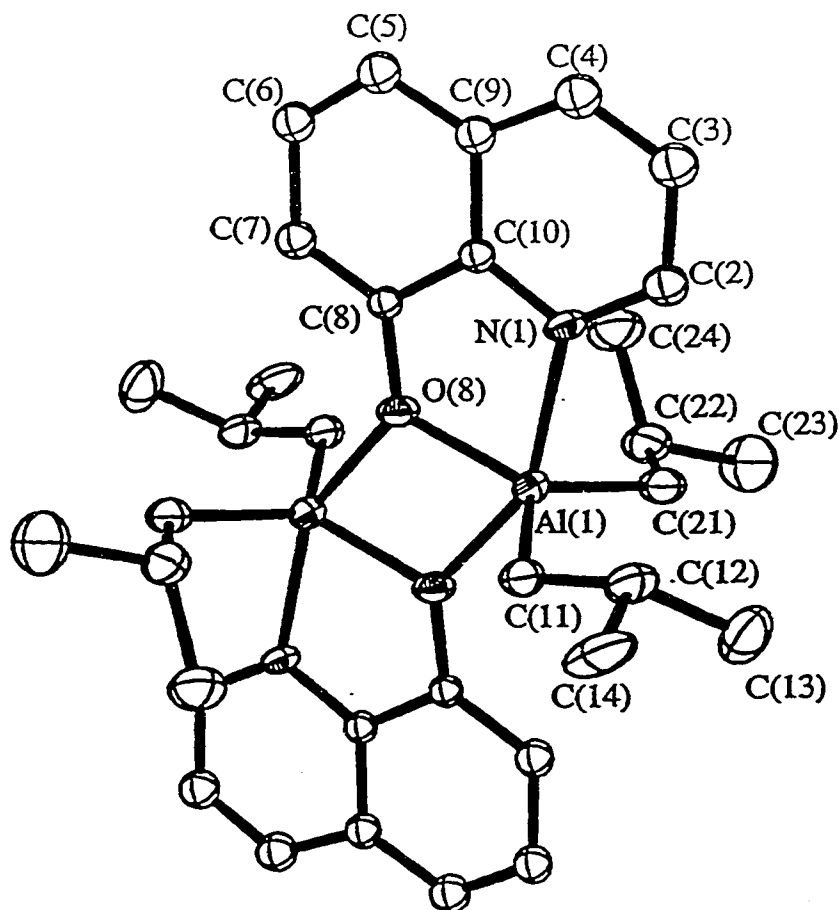


Figure 2.4. Molecular structure of $[(\text{iBu})_2\text{Al}(\mu\text{-O-8-C}_9\text{H}_6\text{N})]_2$ (2.5). Thermal ellipsoids are shown at the 30 % level, and hydrogen atoms are omitted for clarity.

Table 2.3. Selected Bond Lengths (\AA) and Angles ($^\circ$) in $[\text{R}_2\text{Al}(\mu\text{-O-8-C}_9\text{H}_6\text{N})]_2$.

	$[(^i\text{Bu})_2\text{Al}(\mu\text{-O-8-C}_9\text{H}_6\text{N})]_2$ (2.5)	$[\text{Et}_2\text{Al}(\mu\text{-O-8-C}_9\text{H}_6\text{N})]_2$. ^a
Al(1)-O(8)	1.879(4)	1.868(9), 1.863(9)
Al(1)-O(8a)	2.003(3)	2.002(9), 1.99(1)
Al(1)-N(1)	2.124(7)	2.136(9), 2.12(1)
Al(1)-C(11)	1.983(7)	1.94(1), 1.99(1)
Al(1)-C(21)	1.975(6)	1.94(1), 1.93(1)
O(8)-C(8)	1.364(8)	1.37(1), 1.36(1)
O(8)-Al(1)-N(1)	79.3(2)	79.0(4), 79.4(4)
O(8)-Al(1)-O(8a)	72.2(2)	72.4(4), 72.7(4)
O(1)-Al(1)-C(11)	114.7(2)	114.7(5), 119.5(5)
O(1)-Al(1)-C(21)	120.5(3)	120.4(5), 120.5(5)
N(1)-Al(1)-O(8a)	151.5(2)	151.2(4), 152.1(4)
N(1)-Al(1)-C(11)	96.4(3)	93.9(4), 94.3(5)
N(1)-Al(1)-C(21)	96.0(3)	97.5(5), 96.0(5)
C(11)-Al(1)-O(8a)	96.6(3)	97.0(5), 98.3(5)
C(11)-Al(1)-C(21)	124.7(3)	124.9(6), 120.0(5)
C(21)-Al(1)-O(8a)	97.2(3)	98.0(5), 99.1(5)
Al(1)-O(8)-Al(1a)	107.8(2)	107.5(4), 107.3(4)

^a S. T. Dzugan and V. L. Goedken, *Inorg. Chem. Acta.*, 1988, **154**, 169.

The increased cone angle of the *iso*-butyl compared to an ethyl ligand, the similarity in bond lengths and angles between compound 2.5 and $[\text{Et}_2\text{Al}(\mu\text{-O-8-C}_9\text{H}_6\text{N})]_2$ is perhaps surprising. The increased bulk of the *iso*-butyl ligand occurs at the β -carbon while the van der Waal radii (*ca.* 1.7 Å) of the blade-like 8-quinolate ligands should only experience significant steric repulsion with increased substitution at the aluminum alkyl's α -carbon, i.e., *iso*-propyl and *tert*-butyl. This is clearly observed from the molecular structure of $(^t\text{Bu})_2\text{Al}(\text{O-8-C}_9\text{H}_6\text{N})$ (2.3). The aromatic rings in compound 2.5 are stacked in the crystal lattice (Figure 2.5), with an inter-ring distance of *ca.* 3.8 Å and exhibits significant π interaction..

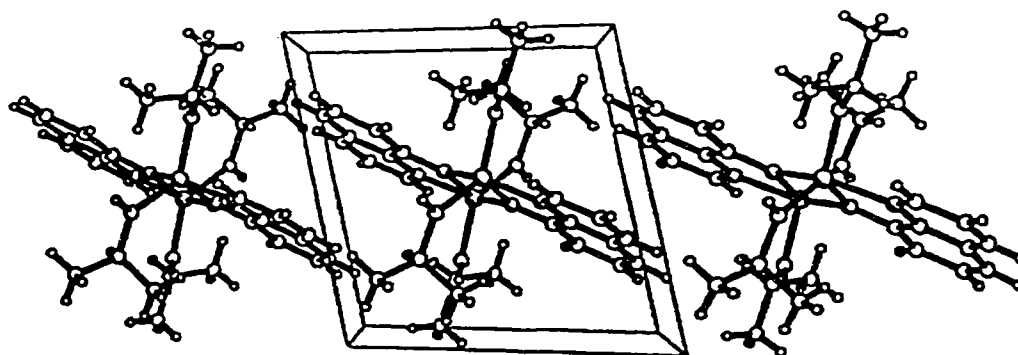


Figure 2.5. Crystal packing diagram of $[(^t\text{Bu})_2\text{Al}(\mu\text{-O-8-C}_9\text{H}_6\text{N})]_2$ (2.5).

The room temperature solution ^1H NMR spectrum of compound 2.5 (Figure 2.6) shows the presence of inequivalent *iso*-butyl groups, but only a single set of resonances for the quinoline ligand. The presence of anisochronous methylene (Al-CH_2) groups indicates that there is hindered rotation about the Al-C bonds. Dzugan and Goedken previously observed a similar inequivalence of the ethyl groups in the ^1H NMR spectrum of $[\text{Et}_2\text{Al}(\mu\text{-O-8-C}_9\text{H}_6\text{N})]_2$.¹³ Their explanation for this inequivalence involved the dissociation of the quinoline's nitrogen from the axial site on the aluminum and re-coordination in an equatorial manner. However, such a reorganization of the aluminum

coordination sphere would require the "bite angle" of the quinoline to change from $79.3(2)^\circ$ to $114 - 120^\circ$, clearly an unfavorable geometry. Furthermore, as is discussed below, the dissociation of the quinoline nitrogen is disfavored due to significant geometric strain. Based upon the solid state structure we propose an alternative explanation for the observed inequivalence of the *iso*-butyl (and ethyl) groups in $[R_2Al(\mu-O-8-C_9H_6N)]_2$.

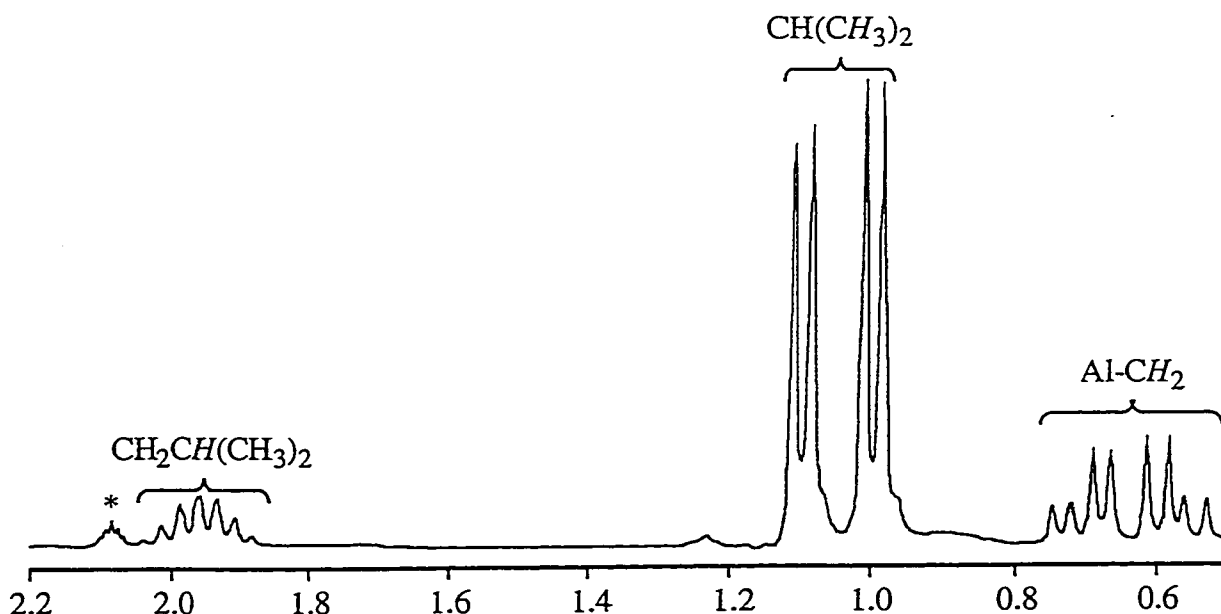


Figure 2.6. Room temperature 1H NMR spectra for $[(^i\text{Bu})_2\text{Al}(\mu-\text{O}-8-\text{C}_9\text{H}_6\text{N})]_2$ (2.5) showing the inequivalent iso-butyl groups and anisochronous methylene (Al-CH_2) groups.

As is seen from Figure 2.4, the *iso*-butyl groups on each aluminum center are positioned *anti* with respect to each other (i.e., X). This orientation allows for minimization of steric interactions between the quinoline and the *iso*-butyl groups (Figure 2.7), as compared to either of the two possible *syn* arrangements (**XI** and **XII**).

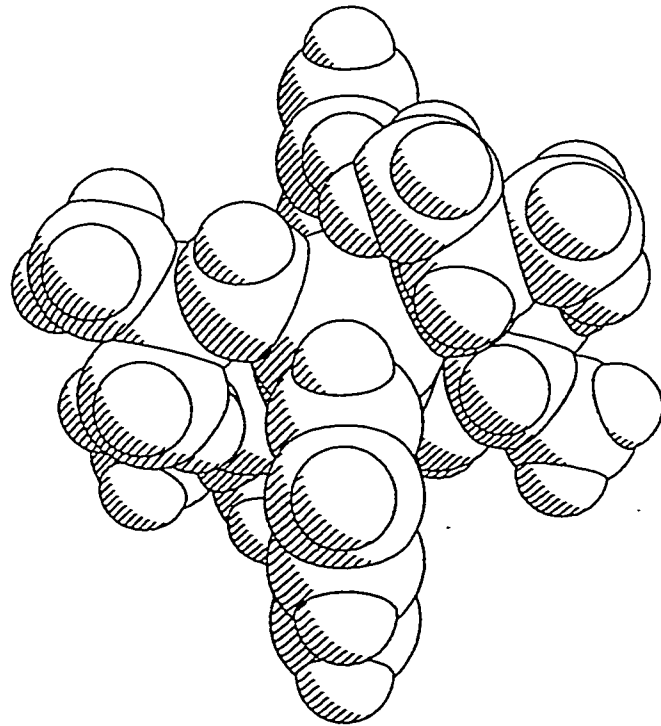
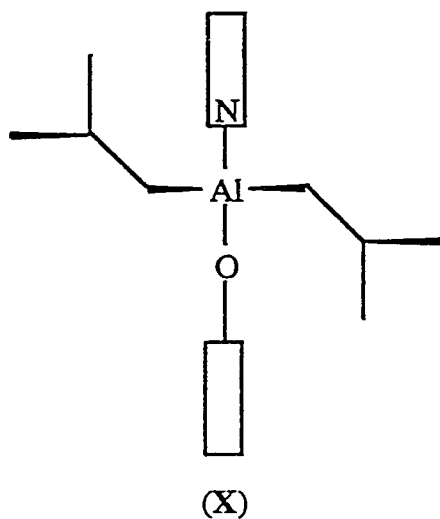
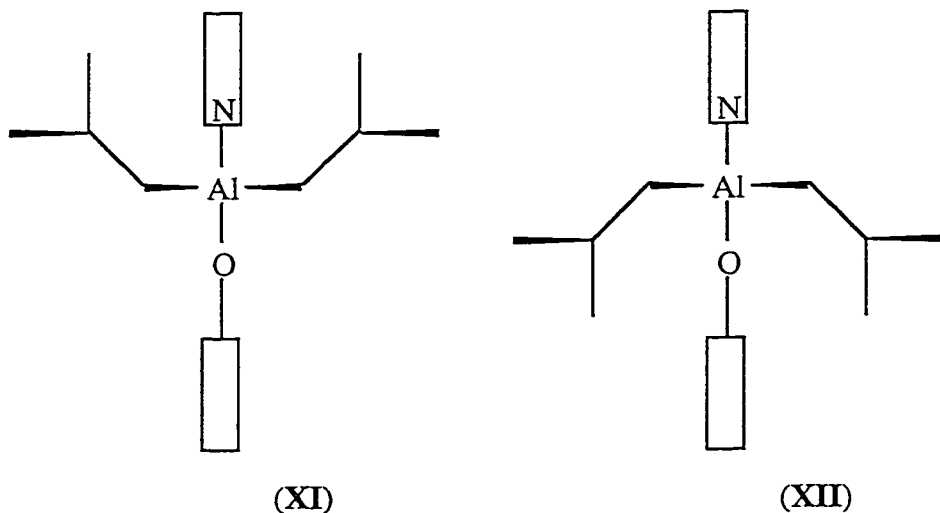


Figure 2.7. Space filling diagram of $[(i\text{Bu})_2\text{Al}(\mu-\text{O}-8\text{-C}_9\text{H}_6\text{N})]_2$ (2.5), showing the *anti* arrangement of the *iso*-butyl groups.

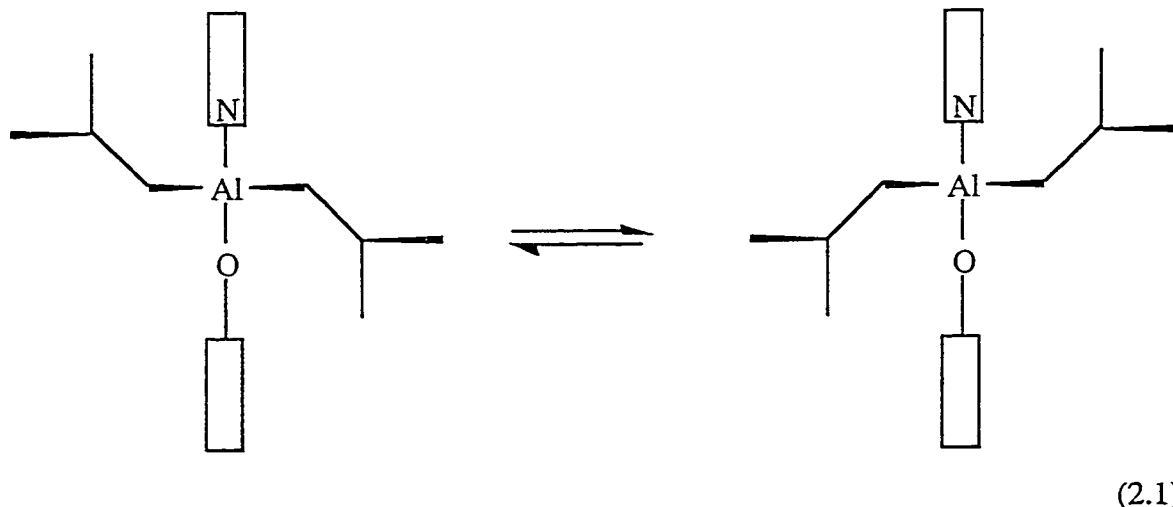
In the *syn* isomers the *iso*-butyl groups are either both next to the nitrogen containing ring (XI) or closer to the all-carbon ring and have a small inter *iso*-butyl distance (XII).





In the *anti* conformation the *iso*-butyl groups would be magnetically inequivalent, i.e., one *iso*-butyl is close to the nitrogen containing ring [C(21) - C(24) in Figure 2.4], while the other is closer to the all-carbon ring [C(11) - C(14) in Figure 2.4], thus explaining the observed room temperature ^1H NMR spectrum. In addition, the presence of a single set of resonances for the quinoline ligand indicates that the molecular structure of compound 2.5 retains its C_2 symmetry, i.e., the *anti* isomer. Although the dimeric molecule of $[\text{R}_2\text{Al}(\mu\text{-O-8-C}_9\text{H}_6\text{N})]_2$ has a center of symmetry, each of the aluminum centers are chiral, thus enantiomeric forms of the *anti* isomer are possible. If we assume that the *anti* form is the only stable conformation, then the two enantiomers may be in a interconverting equilibrium (Eq. 2.1). The anisochronous nature of the methylene groups (see Figure 2.6) indicates that at room temperature this exchange does not occur or is slow on the NMR time scale, however, at higher temperatures such an exchange could occur. This is indeed observed. Heating a NMR sample causes the coalescence of the signals due to the inequivalent *iso*-butyl groups. The activation energy for this process has been determined from the ^1H NMR data [$\Delta G^\ddagger = 68.5(4)$ kJ.mol $^{-1}$]. Given the discussion below on the geometric strain of dissociating the quinoline ligand, it is unlikely that the process in Eq. 1 involves cleavage of the Al-N bond, but involves

rotation about the Al-C bond. The value measured, therefore, is rather large for such a process, probably due to the presence of C-H \cdots ring interactions.



Monomer Versus Dimer: Rigid Conformation Effects.

We have shown in Chapter 1 that for dimeric aluminum compounds with non-delocalized ligands containing both anionic and neutral Lewis base termini (**II**, where X = O, S, NR', CH₂; Y = OR', SR', NR'₂), that an increase in the steric bulk of the aluminum alkyl substituents (R) results in dissociation of the neutral Lewis base, i.e., **III**. Why then in the case of the pyridine and quinoline derived ligands are monomeric compounds (*c.f.*, **I**) formed?

The simplest explanation of the monomeric nature of compounds **2.2 - 2.4** would be that the increased basicity of the pyridine and quinoline derived ligands enables cleavage of the Al₂O₂ core. However, while pyridine ($pK_b \approx 9$) is more basic than Et₂O ($pK_b = 17.6$) it is actually less basic than trimethylamine ($pK_b = 4.21$) or ammonia ($pK_b = 4.76$). Thus, based on a basicity argument, compounds of the type $[(R)_2Al\{\mu-O(CH_2)_nNMe_2\}]_2$ would be expected to be monomeric, which they are not.¹ Therefore, basicity cannot be the reason for compounds **2.2 - 2.4** being monomeric, and other factors

need to be considered. An alternative explanation could involve the shape of the pyridine and quinoline derived ligands. Both classes of ligand are "blade-like", which allows them to fit between other substituents. In this regard they should have lower steric bulk than a tertiary amine derivative and again on these grounds $[(R)_2Al\{\mu-O(CH_2)_nNMe_2\}]_2$ would also be expected to be monomeric. Therefore, the shape cannot be the controlling difference. An explanation more consistent with the observations described above is as follows.

As an example, consider the structure of $[(^iBu)_2Al(\mu-O-8-C_9H_6N)]_2$ (**2.5**) shown in Figure 2.4. If the steric bulk of the aluminum alkyl groups is increased such that inter-ligand repulsion is increased, then the Al-N bond will lengthen (weaken), and eventually dissociate. In order for this to happen, one of two things would have to occur. First, the O(8)-C(8)-C(10) angle would have to increase significantly, or second, the quinoline ligand would have to rotate about the O(8)-C(8) axis. Clearly, the former is limited by the rigid geometry about the sp^2 carbon, C(8). A consideration of a space filling model of compound **2.5** suggests that the latter possibility is to be equally disfavored. Thus, the quinoline's nitrogen cannot readily dissociate from the aluminum. However, formation of a monomeric compound (i.e., compound **2.3**) does allow for relief of all inter-ligand steric hindrance. Similar rationalization may be used for compounds **2.2** and **2.4**. Thus, we propose that the formation of monomeric structures for compounds **2.2 - 2.4** is associated with the rigid conformation of the pyridine and quinoline ligands.

Conclusion

The formation of monomeric structures for compounds **2.2 - 2.4** is associated with the rigid conformation of the pyridine and quinoline ligands and not upon the basicity of the chelating ligand. Consequently, the stability of monomeric versus dimeric structures in this system depends upon a combination of factors: the steric bulk at the aluminum, the rigidity of the ligand, and the ring size formed by the chelating ligand.

Experimental Section

General experimental procedures were carried out as described in Chapter 1. The synthesis of Al(^tBu)₃ was performed according to a literature method.¹⁴ 2-Hydroxypyridine, 2-pyridinemethanol, 8-hydroxyquinoline, and 8-quinolinemethanol were obtained from Aldrich and were used without further purification. 8-Quinolinol was prepared from the reduction of 8-quinolincarboxylic acid by lithium aluminum hydride.¹⁵

[(^tBu)₂Al(O-2-C₅H₄N)]₂ (2.1). Al(^tBu)₃ (3.16 g, 15.96 mmol) was dissolved in hexane (50 mL) and cooled to -78 °C. 2-hydroxypyridine (1.52 g, 15.9 mmol) was added dropwise and upon completion, the mixture was allowed to warm to room temperature and stirred overnight. The resulting mixture was then filtered and the solid product was recrystallized in toluene. Yield: *ca.* 60 %. Mp. 205 - 207 °C. MS (EI, %): *m/z* 413 (2M⁺ - ^tBu, 60), 357 (2M⁺ - ^tBu - H₂C=CMe₂, 10), 235 (M⁺, 8), 178 (M⁺ - ^tBu, 30), 121 (M⁺ - 2 ^tBu, 10), 77 (C₅H₄N, 100), 57 (^tBu, 20). IR (cm⁻¹): 1094 (s), 1023 (s), 1261 (m), 800 (s), 1507 (m), 1622 (m), 2824 (w), 1447 (w), 651 (m), 478 (m), 406 (m). ¹H NMR (C₆D₆): δ 8.18 [2H, d, *J*(H-H) = 5.0 Hz, 6-CH], 7.12 [2H, dd, *J*(H-H) = 5.0 Hz, 4-CH], 7.35 [2H, d, *J*(H-H) = 7.0 Hz, 3-CH], 6.55 [2H, dd, *J*(H-H) = 7.0 Hz, 5-CH], 1.59 [36H, s, C(CH₃)]. ¹³C NMR (C₆D₆): δ 169.6 (OC), 145.9 (6-CH), 140.7 (4-CH), 121.5 (5-CH), 117.0 (3-CH), 34.3 [C(CH₃)₃]. ²⁷Al NMR (C₇H₈, C₆D₆): δ 129 (W_{1/2} = 4176 Hz).

(^tBu)₂Al(OCH₂-2-C₅H₄N) (2.2). Prepared in an analogous manner to compound 1 using Al(^tBu)₃ (5.44 g, 27.5 mmol) and 2-pyridylmethanol (3.00 g, 27.5 mmol). Yield: 55%. Mp. 143 - 145 °C. ICP Analysis (calc): Al, 11.7±0.02% (10.8%). MS (EI, %): *m/z* 192 (M⁺ - ^tBu, 35), 135 (M⁺ - 2 ^tBu, 28), 57 (^tBu, 100). IR (cm⁻¹): 1609 (w), 1574 (w), 1260 (m), 1087 (s), 1059 (s), 1020 (s), 800 (s), 927 (s), 679 (w), 636 (w). ¹H NMR (C₆D₆): δ 7.97 [1H, d, *J*(H-H) = 5.0 Hz, 6-CH], 6.68 [1H, m, dd, *J*(H-H) = 7.5 Hz, 5-

*CH], 6.30 [1H, dd, $J(H-H) = 5.0$ Hz, 4-*CH*], 6.26 [1H, d, $J(H-H) = 7.5$ Hz, 3-*CH*], 5.07 [2H, s, O*CH*₂], 1.29 [18H, s, C(CH₃)₃]. ¹³C NMR (C₆D₆): δ 145.6 [6-*CH*], 139.2 [4-*CH*], 122.5 [5-*CH*], 120.7 [3-*CH*], 67.7 [O*CH*₂], 32.2 [C(CH₃)₃]. ²⁷Al NMR (C₇H₈, C₆D₆): δ 124 ($W_{1/2} = 5836$ Hz).*

(tBu)₂Al(O-8-C₉H₆N) (2.3). Prepared in an analogous manner to compound **1** using Al(tBu)₃ (5.44 g, 27.5 mmol) and 8-hydroxyquinoline (3.98 g, 27.5 mmol). Yellow crystals resulted after placing the reaction mixture in the freezer (-25 °C). Yield: 50 %. Mp: 89 - 91 °C. MS (EI, %): *m/z*: 285 (M⁺, 20), 228 (M⁺ - tBu, 35), 171 (M⁺ - 2 tBu, 50), 57 (tBu, 20). IR (cm⁻¹): 1261 (s), 1094 (s), 1019 (s), 802 (s), 2965 (m), 2827 (m). ¹H NMR (C₆D₆): δ 7.77 [1H, d, $J(H-H) = 5.0$ Hz, 2-*CH*], 7.39 [1H, d, $J(H-H) = 10.0$ Hz, 7-*CH*], 7.17 [1H, dd, $J(H-H) = 5.0$ Hz, 3-*CH*], 6.65 [1H, dd, $J(H-H) = 10.0$ Hz, $J(H-H) = 5.0$ Hz, 6-*CH*], 6.47 [1H, d, $J(H-H) = 5.0$ Hz, 4-*CH*], 6.44 [1H, d, $J(H-H) = 5.0$ Hz, 5-*CH*], 1.18 [18H, s, C(CH₃)₃]. ¹³C NMR (C₆D₆): δ 159.9 (OC), 143.9 (2-*CH*), 140.8 (4-*CH*), 132.1 (5-*CH*), 121.6 (3-*CH*), 114.8 (7-*CH*), 113.5 (6-*CH*), 33.3 [C(CH₃)₃], 30.3 [C(CH₃)₃]. ²⁷Al NMR (C₇H₈/C₆D₆): δ 138 ($W_{1/2} = 4638$ Hz). UV-vis (λ , 8.77 × 10⁻⁴ M, CHCl₃): 384 ($\epsilon = 2264$ L mol⁻¹ cm⁻¹).

(tBu)₂Al(OCH₂-8-C₉H₆N) (2.4). Prepared in an analogous manner to compound **1** using Al(tBu)₃ (5.44 g, 27.5 mmol) and (8-quinoline)methanol (4.37 g, 27.5 mmol). Yield: 30 %. Mp. 118 - 120 °C. MS (EI, %): *m/z*: 299 (M⁺, 5), 242 (M⁺ - tBu, 100), 185 (M⁺ - 2 tBu, 20), 57 (tBu, 20). IR (cm⁻¹): 1592 (w), 1508 (w), 1456 (w), 1262 (m), 1088 (s), 1022 (s), 799 (s), 677 (w), 648 (w), 591 (w). ¹H NMR (C₆D₆): δ 8.43 [1H, d, $J(H-H) = 5.0$ Hz, 2-*CH*], 7.34 [1H, d, $J(H-H) = 10.0$ Hz, 7-*CH*], 6.99 (1H, m, 4-*CH*), 6.97 (1H, m, 6-*CH*), 6.92 (1H, m, 5-*CH*), 6.47 [1H, dd, $J(H-H) = 7.5$ Hz, $J(H-H) = 5.0$ Hz, 3-*CH*], 5.52 (2H, s, O*CH*₂), 1.30 [18H, S, C(CH₃)₃]. ¹³C NMR (C₆D₆): δ 147.7 (2-*CH*), 142.4

(4-CH), 130.0 (5-CH), 127.1 (6-CH), 120.2 (3-CH), 103.0 (7-CH), 67.3 (CH_2O), 32.5 [$\text{C}(\text{CH}_3)_3$], 31.5 [$\text{C}(\text{CH}_3)_3$]. ^{27}Al NMR ($\text{C}_7\text{H}_8/\text{C}_6\text{D}_6$): δ 132 ($\text{W}_{1/2} = 2720$ Hz).

[$(^{\text{i}}\text{Bu})_2\text{Al}(\mu\text{-O-8-C}_9\text{H}_6\text{N})]_2$ (2.5). Prepared in an analogous manner to compound **2.1** using $\text{HAL}(^{\text{i}}\text{Bu})_2$ (2.94 g, 20.7 mmol) and 8-hydroxyquinoline (3.00 g, 20.7 mmol). Yellow crystals resulted after placing the reaction mixture in the freezer (-25 °C). Yield: 70 %. Mp: 89 - 91 °C. MS (EI, %): m/z : 285 (M^+ , 5), 228 ($\text{M}^+ - ^{\text{i}}\text{Bu}$, 100), 172 ($\text{M}^+ - 2$ ^iBu , 90), 57 (^iBu , 7). IR (cm^{-1}): 2960 (m), 1255 (s), 1096 (s), 1019 (s), 804 (s), 743 (w), 691 (w), 661 (w). ^1H NMR (C_6D_6): δ 8.70 [2H, d, $J(\text{H-H}) = 4.5$ Hz, 2-CH], 7.50 [2H, d, $J(\text{H-H}) = 7.8$ Hz, 7-CH], 7.26 [2H, dd, $J(\text{H-H}) = 4.5$ Hz, 3-CH], 6.82 [2H, dd, $J(\text{H-H}) = 7.8$ Hz, 6-CH], 6.66 [2H, d, $J(\text{H-H}) = 4.5$ Hz, 4-CH], 6.64 [2H, d, $J(\text{H-H}) = 4.5$ Hz, 5-CH], 2.02 [2H, sept, $J(\text{H-H}) = 6.7$ Hz, CH], 1.16 [6H, d, $J(\text{H-H}) = 6.6$ Hz, CH_3], 1.06 [6H, d, $J(\text{H-H}) = 6.3$ Hz, CH_3], 0.78 [2H, d, $J(\text{H-H}) = 6.1$ Hz, Al- CH_2], 0.69 [2H, d, $J(\text{H-H}) = 6.1$ Hz, Al- CH_2]. ^{13}C NMR (C_6D_6): δ 160.0 (OC), 144.9 (2-CH), 138.8 (4-CH), 129.9 (5-CH), 121.9 (3-CH), 114.5 (7-CH), 113.0 (6-CH), 29.7 [$\text{CH}(\text{CH}_3)_2$], 28.8 [$\text{CH}(\text{CH}_3)_2$], 27.2 [$\text{CH}(\text{CH}_3)_2$], 1.75 (Al- CH_2). ^{27}Al NMR ($\text{C}_7\text{H}_8/\text{C}_6\text{D}_6$): δ 81 ($\text{W}_{1/2} = 7500$ Hz). UV-vis (λ , 3.51×10^{-4} M, CHCl_3): 375 ($\epsilon = 2330$ L mol $^{-1}$ cm $^{-1}$).

Crystallographic Studies. Crystals of compounds **2.1**, **2.3** and **2.5** were sealed in glass capillaries under argon and mounted on the goniometer of a Enraf-Nonius CAD-4 automated diffractometer at the University of North Texas, using Mo-K α radiation with a graphite monochromator. A summary of cell parameters, data collection, and structure solution is given in Table 2.4. Scattering factors were taken from reference 16.

Table 2.4. Summary of X-ray diffraction data.

Compound	$[(t\text{Bu})_2\text{Al}(\mu\text{-O-2-C}_5\text{H}_4\text{N})]_2$ (2.1)	$(t\text{Bu})_2\text{Al}(\text{O-8-C}_9\text{H}_6\text{N})$ (2.3)
empir. formula	$\text{C}_{26}\text{H}_{44}\text{Al}_2\text{N}_2\text{O}_2$	$\text{C}_{17}\text{H}_{24}\text{AlNO}$
cryst size, mm	0.07 x 0.09 x 0.42	0.14 x 0.17 x 0.42
cryst system	triclinic	monoclinic
space group	$\bar{\text{P}1}$	$\text{P}2_1/\text{c}$
a , Å	7.986(2)	10.763(2)
b , Å	9.187(1)	12.579(1)
c , Å	11.620(1)	13.443(1)
α , °	111.889(9)	
β , °	96.13(1)	105.15(1)
γ , °	107.78(1)	
V , Å ³	729.4(2)	1756.8(4)
Z	1	4
D(calcd), g/cm ³	1.071	1.079
μ , cm ⁻¹	1.17	1.07
temp, K	298	298
2θ range, °	3.0 - 44.0	3.0 - 44.0
no. collected	1793	2415
no. ind	1793	2286
no. obsd	867 ($ F_o > 6.0\sigma F_o $)	638 ($ F_o > 6.0\sigma F_o $)
weighting scheme	$\omega^{-1} = 0.04(F_o)^2 + \sigma(F_o)^2$	$\omega^{-1} = 0.04(F_o)^2 + \sigma(F_o)^2$
R	0.0576	0.0326
R_w	0.0609	0.0401
largest diff peak, eÅ ⁻³	0.26	0.10

Table 2.4, contd.

Compound	$[(^i\text{Bu})_2\text{Al}(\mu\text{-O-8-C}_9\text{H}_6\text{N})]_2$
	(2.5)
empir. formula	$\text{C}_{34}\text{H}_{48}\text{Al}_2\text{N}_2\text{O}_2$
cryst size, mm	0.09 x 0.09 x 0.31
cryst system	triclinic
space group	$\bar{\text{P}1}$
<i>a</i> , Å	9.288(1)
<i>b</i> , Å	9.854(2)
<i>c</i> , Å	10.288(1)
α , °	68.46(1)
β , °	85.58(1)
γ , °	76.67(2)
<i>V</i> , Å ³	852.2(4)
<i>Z</i>	1
D(calcd), g/cm ³	1.112
μ , cm ⁻¹	1.11
temp, K	298
2θ range, °	3.0 - 44.0
no. collected	2090
no. ind	2090
no. obsd	1012 ($ F_o > 6.0\sigma F_{\text{o}} $)
weighting scheme	$\omega^{-1} = 0.04(F_o)^2 + \sigma(F_o)^2$
R	0.0589
R_w	0.0608
largest diff peak, eÅ ⁻³	0.35

References.

- 1 J. A. Francis, C. N. McMahon, S. G. Bott, and A. R. Barron, *Organometallics*, in press.
- 2 (a) O. T. Beachley, Jr. and K. C. Racette, *Inorg. Chem.*, 1976, **15**, 2110.
(b) D. A. Atwood, F. P. Gabbai, J. Lu, M. P. Remington, D. Rutherford, and M. P. Sibi, *Organometallics*, 1996, **15**, 2308.
(c) M. R. P. van Vliet, G. van Koyen, M. A. Rotteveel, M. Schrap, K. Vrieze, B. Kojic-Prodic, A. L. Spek, and A. J. M. Duisenberg, *Organometallics*, 1986, **5**, 1389.
(d) C. Jones, F. C. Lee, G. A. Koutsantonis, M. G. Gardiner, and C. L. Raston, *J. Chem. Soc., Dalton Trans.*, 1996, 829.
(e) M. P. Hogerheide, M. Wesseling, J. T. B. H. Jastrzebski, J. Boersma, H. Kooijman, A. L. Spek and G. van Koten, *Organometallics*, 1995, **14**, 4483.
(f) S. T. Dzugan and V. L. Goedken, *Inorg. Chem. Acta.*, 1988, **154**, 169.
(g) R. Kumar, M. L. Sierra, and J. P. Oliver, *Organometallics*, 1994, **13**, 4285.
(h) R. Benn, A. Rufinska, H. Lehmkul, E. Janssen, and C. Krüger, *Angew. Chem., Int. Ed. Engl.*, 1983, **22**, 779.
(i) H. Schumann, M. Frick, B. Heymer, and F. Girgsdies, *J. Organomet. Chem.*, 1996, **512**, 117.
(j) F. H. van der Steen, G. P. M. van Mier, A. L. Spek, J. Kroon, and G. van Koten, *J. Am. Chem. Soc.*, 1991, **113**, 5742.
(k) M. L. Sierra, V. S. J. de Mel, and J. P. Oliver, *Organometallics*, 1989, **8**, 2486.
- 3 M. D. Healy, M. B. Power, and A. R. Barron, *Coord. Chem. Rev.*, 1994, **130**, 63.
- 4 (a) J. P. Phillips, *Chem. Rev.*, 1956, **56**, 271.
(b) F. Papadimitrakopoulos and X. M. Zhang, *Synth. Met.*, 1997, **85**, 1221.
(c) K. A. Higginson, X. M. Zhang, and F. Papadimitrakopoulos, *Chem. Mater.*, 1998, **10**, 1017.

- 5 A. R. Barron, *Polyhedron*, 1995, **14**, 3197.
- 6 F. Papadimitrakopoulos, X. M. Zhang, D. L. Thomsen, III, and K. A. Higginson, *Chem. Mater.*, 1996, **8**, 1363.
- 7 See for example, (a) K. M. Nykerk and D. P. Eyman, D. P., *Inorg. Chem.*, 1967, **6**, 1461.
(b) G. H. Robinson, H. Zhang, and J. L. Atwood, *J. Organomet. Chem.*, 1987, **331**, 153.
(c) D. W. Goebel, J. L. Hencher, and J. P. Oliver, *Organometallics*, 1983, **2**, 746.
(d) A. Almennigen, G. Gundersen, T. Haugen, and A. Haaland, *Acta Chem. Scand.*, 1972, **26**, 3928.
(e) J. L. Atwood, S. K. Seale, and D. H. Roberts, *J. Organomet. Chem.*, 1973, **51**, 105.
- 8 Pauling, L., *The Nature of the Chemical Bond*; Cornell University Press; Itaca, NY, 1960; Chapter 7.
- 9 C. E. Bethley, C. L. Aitken, Y. Koide, C. J. Harlan, S. G. Bott, and A. R. Barron, *Organometallics*, 1997, **16**, 329.
- 10 (a) P. Sobota, M. O. Mustafa, J. Utko, and T. Lis, *J. Chem. Soc., Dalton Trans.*, 1990, 1809.
(b) Y. Koide and A. R. Barron, *Organometallics*, 1995, **14**, 4026.
(c) Y. Koide, S. G. Bott, and A. R. Barron, *Organometallics*, 1996, **15**, 2213.
- 11 (a) F. E. Hahn and B. Schneider, *Z. Naturforsch. B*, 1990, **45**, 134.
(b) C. C. Landry, A. Hynes, A. R. Barron, I. Haiduc, and C. Silvestru, *Polyhedron*, 1996, **15**, 391.
- 12 Y. Kushi and Q. Fernando, *J. Am. Chem. Soc.*, 1970, **92**, 91.
- 13 Dzugan S. T., and Goedken, V. L., *Inorg. Chem. Acta.*, 1988, **154**, 169.
- 14 W. Uhl, *Z. Anorg. Allg. Chem.*, 1989, **570**, 37.

- 15 M. Uchida, M. Chihiro, S. Morita, T. Kanbe, H. Yamashita, K. Yamasaki, Y. Yabuuchi, and K. Nakagawa, *Chem. Pharm. Bull.*, 1989, **37**, 2109.
- 16 *International Tables for X-Ray Crystallography*, Kynoch Press, Birmingham, 1974, vol. 4.

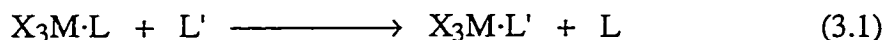
Chapter 3

Are Intramolecularly Stabilized Compounds of Aluminum Suitable Structural Models of the S_N2 Transition State?

Introduction

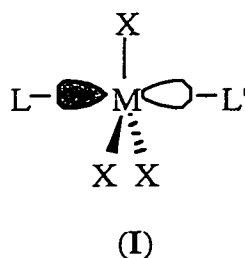
In 1928 Christopher Ingold proposed a convenient nomenclature (i.e., S_N2 versus S_N1) to differentiate the intimate mechanistic details of nucleophilic substitution reactions in organic chemistry.¹ These terms are still in common usage in organic chemistry and for many reactions in inorganic chemistry.² However, the ability of metals (and some non-metal elements) to have an expanded coordination environment requires an additional differentiation of reaction pathways, especially with regard to ligand substitution reactions in coordination compounds. Thus, ligand substitution is commonly divided into two distinct reaction mechanisms. Dissociation of a ligand prior to association of a new ligand (i.e., a S_N1 reaction) is termed dissociative (D). Conversely, reactions involving association of a new ligand prior to dissociation of the outgoing ligand are termed associative (A) or interchange (I) reaction. These latter mechanisms are dependent on whether a transition state (I) or intermediate (A) are involved. While associative reactions have no analog in organic chemistry, an interchange reaction (I) is equivalent to a S_N2 reaction.²

Lewis base exchange reactions of Group 13 Lewis acid-base complexes (Eq. 3.1) are isolobal to nucleophilic substitutions in organic chemistry and are hence probably the closest analogs in inorganic chemistry.

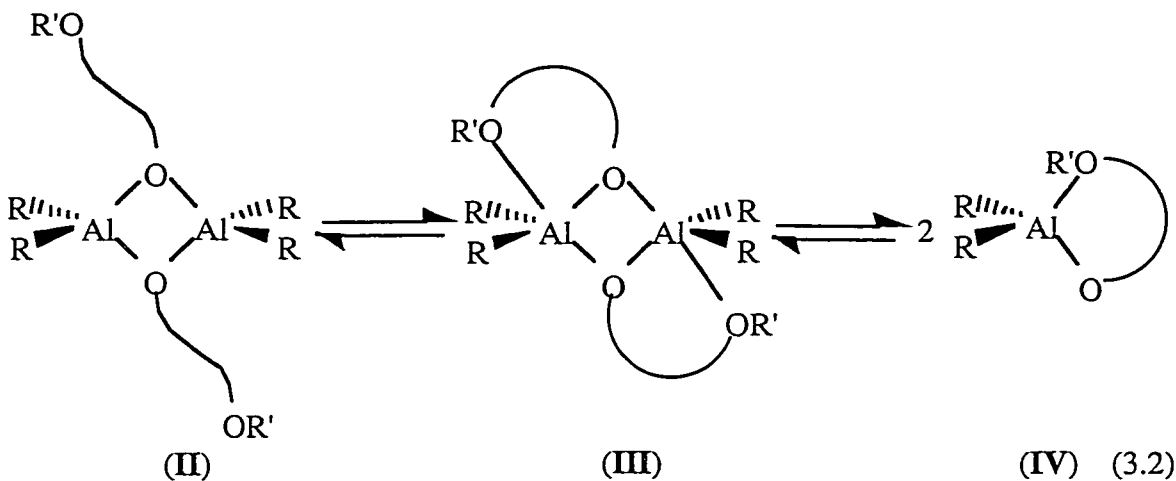


M = Al, Ga, In; X = alkyl, halide; L, L' = ether, amine, etc.

Ligand exchange in Group 13 Lewis acid-base complexes are generally dissociative (D),³ but when the ligands have sufficiently low steric bulk, or with the larger metals, interchange (I) (or associative (A)) mechanisms have been observed.⁴ In the latter case, as with a S_N2 reaction, the transition state (intermediate for A mechanism) is a five-coordinate trigonal bipyramidal species. In this geometry the incoming and outgoing ligands are mutually *trans* and share a p-orbital (I); the remaining ligands lie in the equatorial coordination sites.

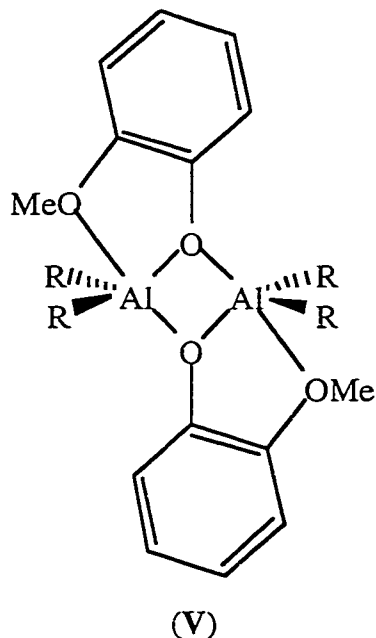


Whereas five-coordinate compounds of carbon are highly unstable, five-coordinate compounds of the Group 13 metals are widely known (see Chapters 1 and 2).⁵ In fact, compounds containing bidentate-bridging ligands (in particular those of aluminum with ligands such as ether-alkoxides) display the reverse of the normal trend, i.e., five-coordinate compounds are often more stable than four-coordinate compounds.⁶ For such compounds the cleavage of a four-coordinate dimer (**II**), via a five-coordinate dimer (**III**), to give two four-coordinate monomers (**IV**) may be considered to be an example of a S_N2 reaction (Eq. 3.2). The stability of five-coordinate compounds of aluminum (i.e., **III**) allows the possibility that such compounds are structural representations of the S_N2 (**I**) transition state (or A intermediate).⁶ However, despite several proposals⁶ it is worth asking the question, *are these compounds really suitable geometric models for S_N2 transition state?* In order to provide an answer a combined crystallographic-theoretical study of a homologous series of dimeric five-coordinate dialkylaluminum compounds with bi-functional ligands (*cf.*, **III**), was undertaken.



The extent of intra-molecular coordination (e.g., the Al…O bond distance in **III**) has been shown to be dependent on a number of factors, including: the steric bulk of the substituents at aluminum (R) and the Lewis base donor (R') (see Chapter 1),⁷ the basicity of the neutral donor group, and the chelate ring size (as determined by the length of the carbon backbone),⁷ substitution at the ligand's α -carbon,⁸ the geometry at the bridging ligand,⁹ and the rigidity of the ligand backbone (see Chapters 1 and 2).¹⁰ The easiest parameter to vary in a systematic manner is the steric bulk of the substituents at aluminum. In this regard, the Al…O distance decreases with decreased steric bulk of R. Conversely it should be possible to use the steric bulk of the substituent on aluminum (as determined by the Tolman cone angle¹¹) to control the Al…O distance and hence the geometry about aluminum (e.g., R = Me, Et, ⁱBu, ^tBu). Such a systematic variation should provide a geometric model of the structural changes that occur along the reaction profile as it moves towards the transition state for ligand substitution.

In choosing a simple system for study we needed one in which all the compounds in the series are amenable to crystallographic study (i.e., crystallizable solids) and may be compared with a simple theoretical model compound.



In this regard, the compounds $[R_2Al(\mu-OC_6H_4-2-OMe)]_2$ (V, R = Me, Et, *i*Bu) had already been prepared, by Oliver¹² and Schumann,¹³ and thus in order to complete the series only the *tert*-butyl homologue, $[({}^t\text{Bu})_2Al(\mu-OC_6H_4-2-OMe)]_2$, was required. Furthermore, these compounds may be compared to the model compound, $[H_2Al(\mu-OCH_2CH_2OH)]_2$.⁷

Results and Discussion

Synthesis and Characterization of $[({}^t\text{Bu})_2Al(\mu-OC_6H_4-2-OMe)]_2$. Reaction of $Al({}^t\text{Bu})_3$ ¹⁴ with 2-methoxyphenol results in the formation of $[({}^t\text{Bu})_2Al(\mu-OC_6H_4-2-OMe)]_2$ (3.1) (see Experimental). Although the mass spectrum of $[({}^t\text{Bu})_2Al(\mu-OC_6H_4-2-OMe)]_2$ (3.1) does not show peaks due to a dimer, the ^{27}Al NMR spectrum (δ 45 ppm) is within the range previously observed for dimeric five-coordinate compounds.¹⁵ The dimeric structure was confirmed by X-ray crystallography.

The molecular structure of $[({}^t\text{Bu})_2Al(\mu-OC_6H_4-2-OMe)]_2$ is shown in Figure 3.1; selected bond lengths and angles are given in Table 3.1 along with those of the methyl, ethyl and *iso*-butyl analogs.

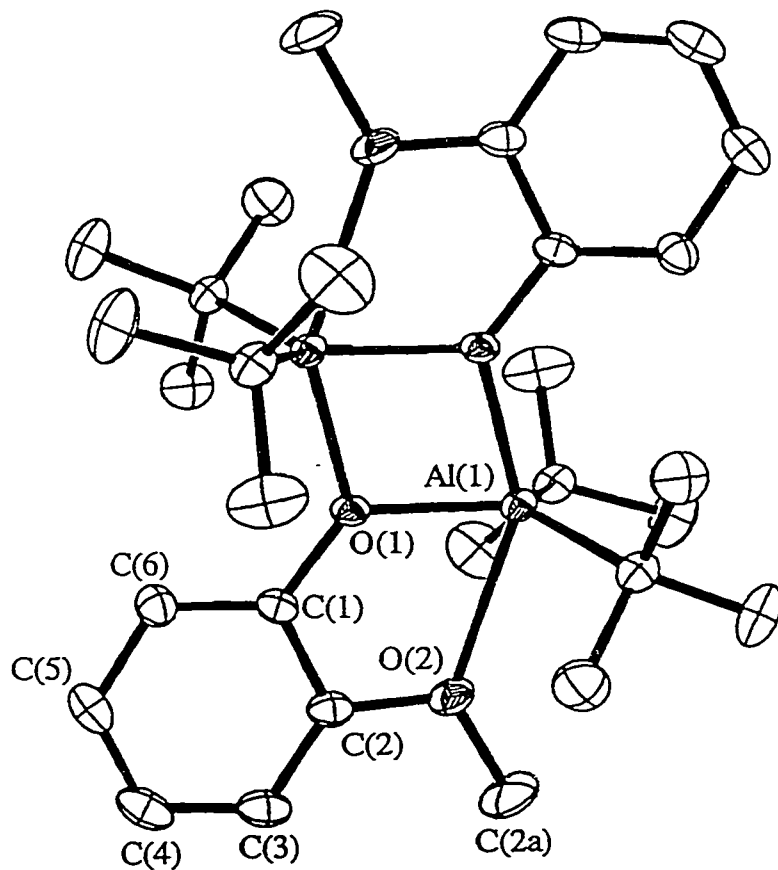


Figure 3.1. Molecular structure of $[(\text{tBu})_2\text{Al}(\mu-\text{OC}_6\text{H}_4-2\text{-OMe})]_2$ (3.1). Thermal ellipsoids are shown at the 30 % level, and all hydrogens are omitted for clarity.

The molecular structure of $[(\text{tBu})_2\text{Al}(\mu-\text{OC}_6\text{H}_4-2\text{-OMe})]_2$ consists of discrete centrosymmetric dimers with no close inter-molecular contacts. The coordination geometry about the aluminum is that of a distorted trigonal bipyramidal; $\text{O}(2)\text{-Al}(1)\text{-O}(1') = 148.3(1)^\circ$ and $\Sigma(\text{X}_{\text{eq}}\text{-Al}\text{-X}_{\text{eq}}) = 357.1(2)^\circ$. The Al-C bond distances [2.042(4) and 2.040(4) Å] are slightly longer than those reported for the Me, Et and iBu analogs [1.950(4) - 1.972(2) Å, see Table 3.1], consistent with the increased steric bulk of the *tert*-butyl groups. All the bond lengths and angles associated with the ligands are within the ranges expected.¹⁶

Table 3.1. Selected bond lengths (\AA) and angles (deg) in $[\text{R}_2\text{Al}(\mu\text{-OC}_6\text{H}_4\text{-2-OMe})]_2$.

Parameter ^a	Me ^b	Et ^c	ⁱ Bu ^c	^t Bu ^d
Al(1)-O(1)	1.858(2)	1.859(1)	1.861(1)	1.876(2)
Al(1)-O(1')	1.938(2)	1.952(1)	1.950(1)	1.966(2)
Al(1)-O(2)	2.198(3)	2.249(1)	2.267(1)	2.390(3)
Al(1)-C(11)	1.950(4)	1.957(2)	1.972(2)	2.040(4)
Al(1)-C(21)	1.956(3)	1.952(2)	1.966(2)	2.042(4)
Al(1)…Al(1')	3.015(2)	3.018(2)	3.023(8)	3.048(2)
O(1)-Al(1)-O(1')	74.8(1)	73.3(1)	75.00(6)	75.0(1)
O(1)-Al(1)-O(2)	75.83(9)	75.2(1)	75.01(6)	73.3(1)
O(1)-Al(1)-C(11)	121.7(1)	118.0(1)	120.3(1)	116.4(1)
O(1)-Al(1)-C(21)	116.8(1)	117.5(1)	115.1(1)	114.2(1)
O(2)-Al(1)-O(1')	150.6(9)	150.4(1)	150.1(1)	148.3(1)
O(2)-Al(1)-C(11)	92.2(1)	90.0(1)	93.3(1)	88.9(1)
O(2)-Al(1)-C(21)	92.6(1)	93.0(1)	93.1(1)	90.0(1)
C(11)-Al(1)-C(21)	120.5(2)	123.2(2)	123.9(1)	126.6(2)
Al(1)-O(1)-Al(1')	105.1(1)	104.7(1)	105.00(6)	105.0(1)

^a Where numbering schemes in the original references differ, atom numbers have been made to be consistent with those of $[(\text{tBu})_2\text{Al}(\mu\text{-OC}_6\text{H}_4\text{-2-OMe})]_2$ (3.1).

^b D. G. Hendershot, M. Barber, R. Kumar, and J. P. Oliver, *Organometallics*, 1991, **10**, 3302.

^c H. Schumann, M. Frick, B. Heymer, and F. Girgsdies, *J. Organomet. Chem.*, 1996, **512**, 117.

^d This work.

Effect on Molecular Geometry of the Alkyl Substituent (R) in $[R_2Al(\mu-OC_6H_4-2-OMe)]_2$. As expected the Al-O_(ether) distance [Al(1)-O(2) = 2.390(3) Å] in $[(^tBu)_2Al(\mu-OC_6H_4-2-OMe)]_2$ (**3.1**) is longer than those found in the less sterically hindered aluminum alkyls, see Table 3.1. In fact, as is shown in Figure 3.2, there is a near linear trend between the Al-O_(ether) distances and the Tolman cone angle (θ)¹¹ of the aluminum alkyl substituents. As expected, increased steric hindrance at aluminum results in an increase in the Al-O_(ether) bond distance, i.e., decrease in the bonding interaction.⁷ Although clearly a lesser effect, the Al-O bond distances *cis* [Al-O_(cis) = Al(1)-O(1)] and *trans* [Al-O_(trans) = Al(1)-O(1')] to the ether ligand [O(2)] also show an increase in bond length with increased steric bulk, see Figure 3.2.

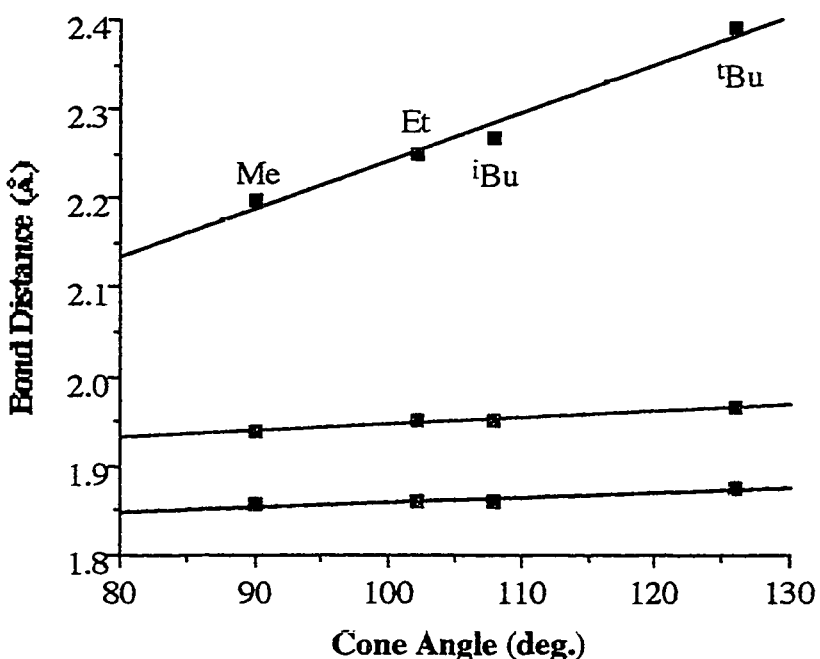


Figure 3.2. Plot of Al-O_(ether) (■), Al-O_(trans) (■), and Al-O_(cis) (■) bond lengths (Å) as a function of the Tolman cone angle (θ , °) for the aluminum substituent (R) in $[(R)_2Al(\mu-OC_6H_4-2-OMe)]_2$.

The geometry about the aluminum also appears to show a near linear dependence on the steric bulk of the alkyl groups. However, in this case only the C(11)-Al(1)-C(21) angle is significantly affected. As is shown in Figure 3.3, there is an increase in the C(11)-Al(1)-C(21) angle with increased steric bulk of the aluminum alkyl.

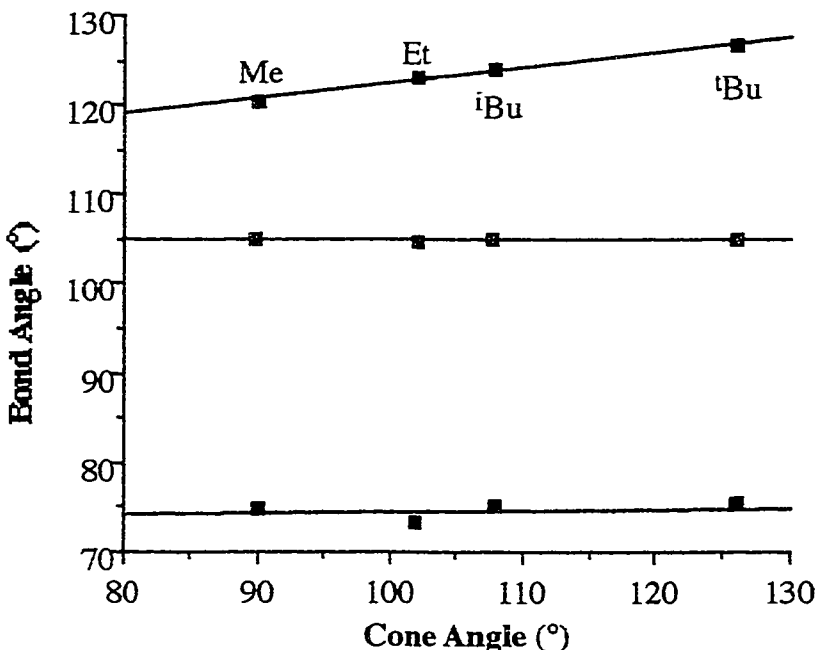


Figure 3.3. Plot of C(11)-Al(1)-C(21) (□), O(1)-Al(1)-O(1') (■), and Al(1)-O(1)-Al(1') (■) bond angles (°) as a function of the Tolman cone angle (θ , °) for the aluminum substituent (R) in $[(R)_2\text{Al}(\mu\text{-OC}_6\text{H}_4\text{-2-OMe})_2]$.

While this may be expected based upon mutual steric repulsion of the alkyl substituents, this actually follows a trend opposite to that observed for four-coordinate dimeric aluminum compounds (see Figure 3.4), where the decrease in C-Al-C angle is as a consequence of increased *trans*-dimer interaction, see below.¹⁷ There appears to be almost no effect of increased steric bulk of the aluminum alkyl on either the O(1)-Al(1)-O(1') or Al(1)-O(1)-Al(1') bond angles, see Figure 3.3. This suggests the Al_2O_2 core is

invariant with changes in the steric bulk of the aluminum alkyl and consequently the Al-O_(ether) interaction as mentioned in Chapter 1.

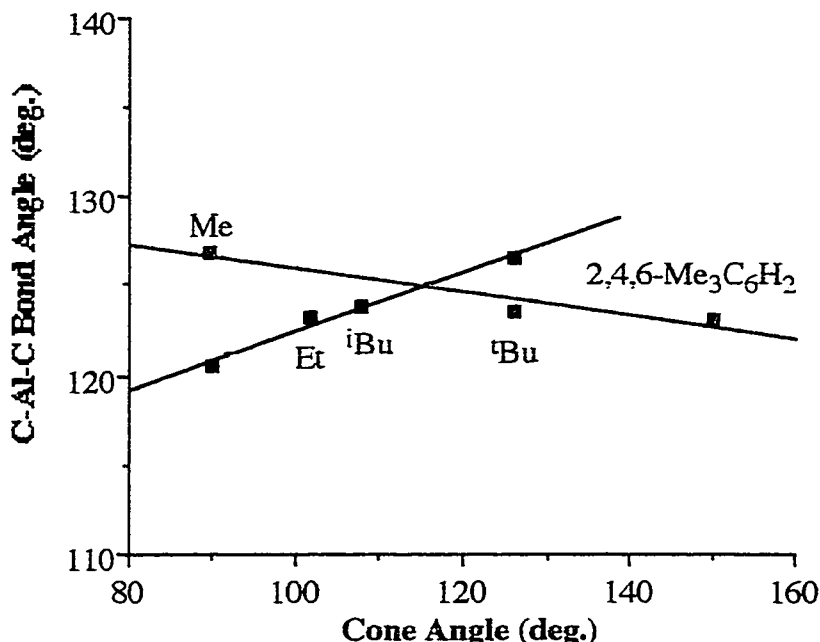
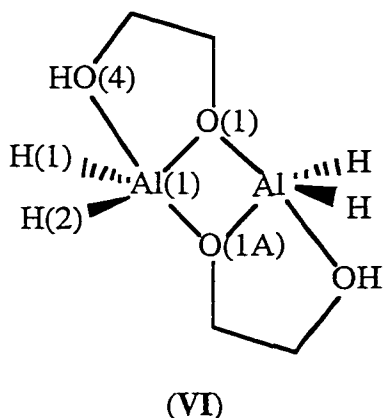


Figure 3.4. Plot of C-Al-C bond angles ($^{\circ}$) as a function of the Tolman cone angle (θ , $^{\circ}$) for the aluminum substituent (R) in $[(R)_2\text{Al}(\mu\text{-OC}_6\text{H}_4\text{-2-OMe})_2]$ (■) and $[(R)_2\text{Al}(\mu\text{-Cl})_2]$ (■).

Ab Initio Calculations on the Model Compound $[\text{H}_2\text{Al}(\mu\text{-OCH}_2\text{CH}_2\text{OH})_2]$. *Ab initio* calculations at the HF/3-21G(*) level have been performed on the model compound, $[\text{H}_2\text{Al}(\mu\text{-OCH}_2\text{CH}_2\text{OH})_2]$ (**VI**).⁷ In order to determine the structural changes that would occur during the formation of the Al-O_(ether) bond, additional structure optimization and total energy calculations were performed for a series of model compounds derived from $[\text{H}_2\text{Al}(\mu\text{-OCH}_2\text{CH}_2\text{OH})_2]$ with regular increases in the Al...O_(ether) distance, see Experimental. If one considers the model reaction shown in Eq. 3.2, there are a number of geometric changes expected as one moves along the reaction coordinate from a four-coordinate dimer (**II**) towards five-coordinate

intermediate (**III**). In general these are faithfully reproduced by the calculations on $[H_2Al(\mu-OCH_2CH_2OH)]_2$.



The Al-H(1) and Al-H(2) bond distances are expected to decrease with decreased Al···O(4) distance, due to a change from tetrahedral (sp^3) to equatorial trigonal bipyramidal (sp^2) hybridization about aluminum. Such a trend is not observed from the calculations on $[H_2Al(\mu-OCH_2CH_2OH)]_2$, instead Al-H(1) and Al-H(2) bond distances increase with decreased Al···O(4) distance, see Figure 3.5a. The equatorial Al-O bond distance, Al-O(1), which is positioned *cis* to the "incoming" donor ligand, see Figure 3.5b (■) also decreases as the Al···O(4) distance becomes greater. Below an Al···O(4) distance of 2.2 Å the Al···O(1) decreases significantly, consistent with the change in hybridization at aluminum. Given the trend observed for the Al-H(1) and Al(H2) distances, it is perhaps better to rationalize the trend by considering that the equatorial oxygen (O1) is actually a bridging alkoxide and with an increased ether oxygen bonding interaction [i.e., decreased Al···O(4) distance] the previously symmetric Al_2O_2 , becomes significantly asymmetric. This asymmetric bridging alkoxide may be considered to consist of a strong covalent bond, Al(1)-O(1) and a weaker dative bond, Al(1)-O(1A).¹⁸

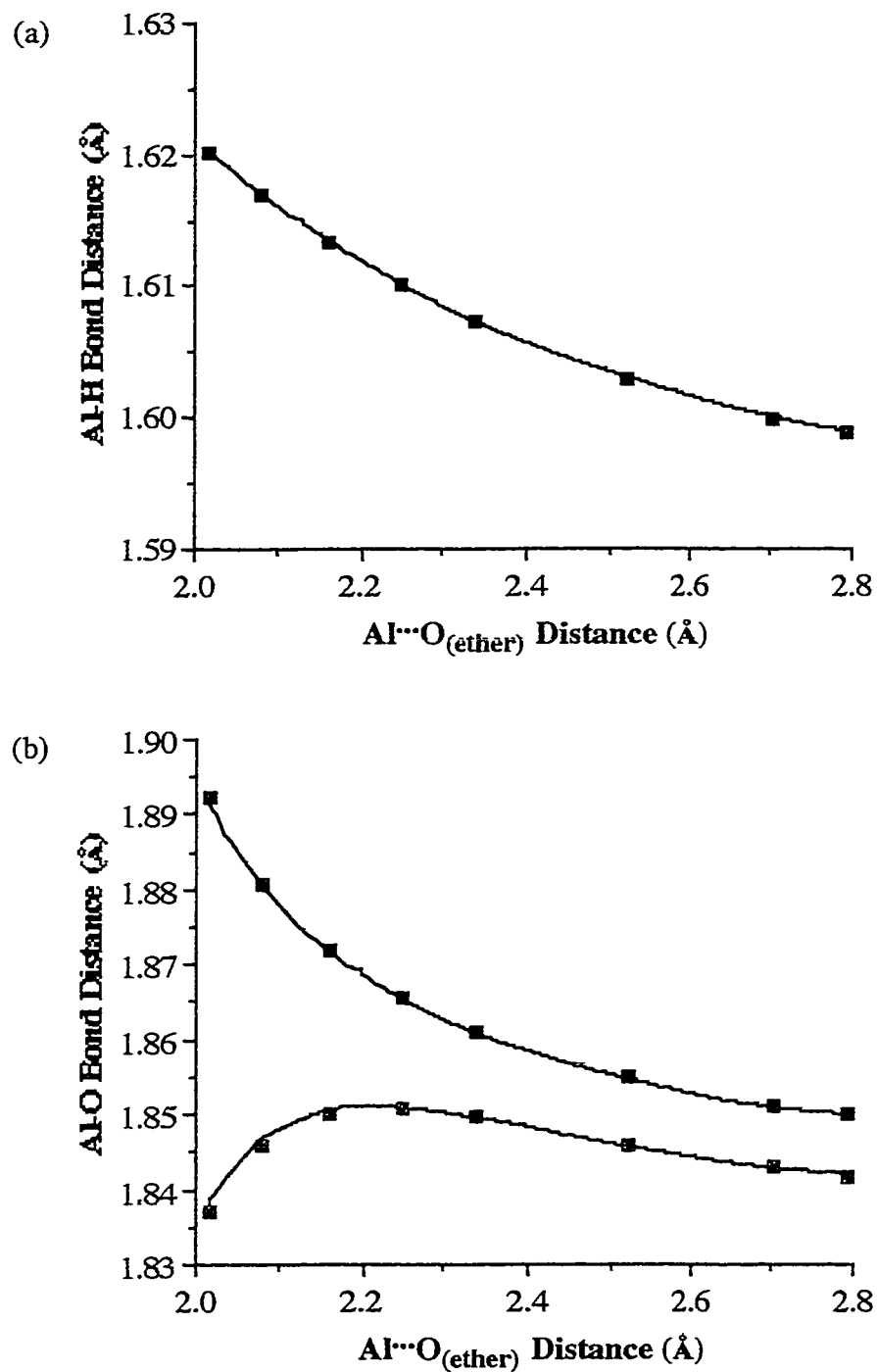


Figure 3.5. Plots of (a) calculated Al-H distance (Å) and (b) calculated Al-O_(axial) (■) and Al-O_(equ.) (■) distance (Å) as a function of Al···O_(ether) distance (Å) for the model $[H_2Al(\mu-OCH_2CH_2OH)]_2$.

The Al-O(1A) bond which is trans to the incoming donor ligand undergoes a significant increase in length with decreased Al···O(4) distance, see Figure 3.5b (■). This trend is consistent with (a) an increase in p-character in the Al···O(1A) bond, (b) increased *trans*-influence of the ether ligand, and (c) the cleavage of the Al₂O₂ dimer. This trend is also consistent with donation of the ether's oxygen lone pair into the Al-O anti-bonding orbital, however, this leads to the same general bonding picture given in I.

We have previously reported that for dimeric [R₂M(μ-X)]₂ compounds of the Group 13 metals, the X-M-X and M-X-M angles are inversely dependent.¹⁶ This trend is also observed for [H₂Al(μ-OCH₂CH₂OH)]₂ as a function of Al···O(ether) distance, see Figure 3.6a. As expected the O-Al-O angle increases with decreased Al···O(ether) distance; from the value found for dimeric alkoxides with four-coordinate aluminum to near the ideal of 90° for a trigonal bipyramidal geometry. The change in the H-Al-H angle upon increased ether donation [decreased Al···O(ether) distance] is counter to that expected from a simplistic tetrahedral (109.5°) to trigonal bipyramidal (120°) geometry change (Figure 3.6b). However, we have previously shown that in dimeric [R₂M(μ-X)]₂ compounds the R-Al-R angle is between 120 - 130° (depending on the identity of R) as a consequence of the small angle within the M₂X₂ cycle.¹⁶ Upon coordination of a fifth ligand (ether oxygen in the present case) the R-Al-R angle appears to decrease (see Figure 3.6b).

Are Intramolecularly Stabilized Compounds of Aluminum Suitable Structural Models of the S_N2 Transition State? As discussed above, there are a number of changes in the structure of a dimeric aluminum alkoxide that are expected upon coordination of a fifth ligand and the subsequent cleavage of the dimer (II - IV in Eq. 3.2).

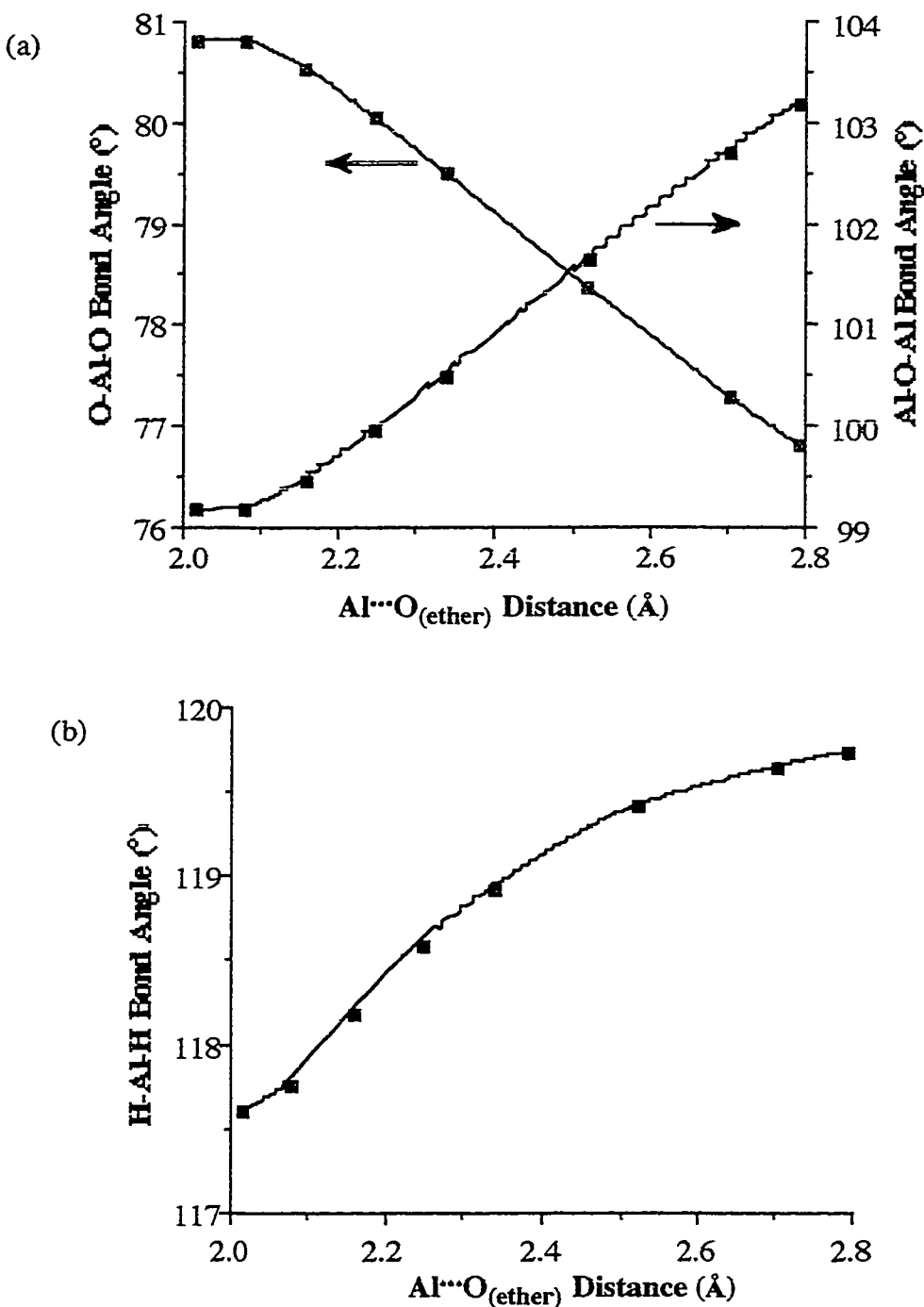
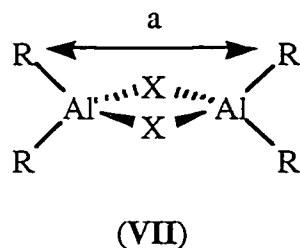


Figure 3.6. Plot of calculated (a) H-Al-H angles (°) as a function of Al^{...}O_(ether) distance (Å) for the model [H₂Al(μ-OCH₂CH₂OH)]₂ and (b) Plot of calculated Al-O-Al (■) and O-Al-O (■) angles (°).

In general all of the expected trends are faithfully reproduced in the model system $[H_2Al(\mu-OCH_2CH_2OH)]_2$, suggesting that these model systems are suitable structural models of the S_N2 transition state. The "real" system, $[R_2Al(\mu-OC_6H_4-2-OMe)]_2$, does not appear to conform to the required trends. Although the variation in the O-Al-O, Al-O-Al and R-Al-R angles as a function of Al...O(ether) distance reasonably reproduced the calculated trends, the variation in bond lengths are not such a good match. The experimental Al-O(_{cis}) bond lengths are all larger than the calculated values, but they do at least follow the correct trend. In fact, if the experimental data is extrapolated it does fit with calculated data. But, the experimental Al-O(_{trans}) follows the opposite trend than that expected. Thus, increased Al...O(ether) donation results in a shorter (stronger) Al-O(_{trans}) bond!

We have observed that the structures of $[R_2M(\mu-X)]_2$ ($M = Al, Ga, In; X =$ halide, alkoxide, amide, etc.) are controlled by the inter-ligand steric repulsion, in particular between the alkyl groups on the adjacent aluminum atoms, i.e., "a" in VII (see Chapter 6).¹⁶



The extent of this repulsion may be observed in the space filling diagram of $[(^tBu)_2Al(\mu-OC_6H_4-2-OMe)]_2$, Figure 3.7.

This effect is highlighted by comparing the Al...Al intra-molecular distances determined experimentally for $[R_2Al(\mu-OC_6H_4-2-OMe)]_2$ in comparison to the values calculated for the model system $[H_2Al(\mu-OCH_2CH_2OH)]_2$ (Figure 3.8).

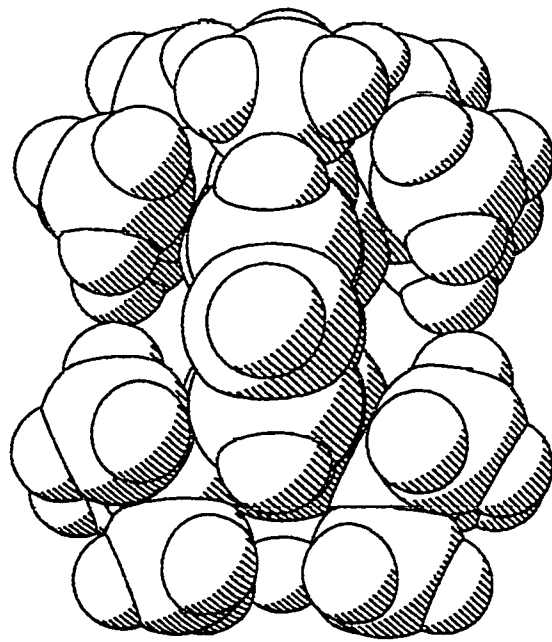


Figure 3.7. Space filling diagram of $[R_2Al(\mu-OC_6H_4-2-OMe)]_2$, viewed parallel to the Al_2O_2 core, showing the steric interaction of the *tert*-butyl groups.

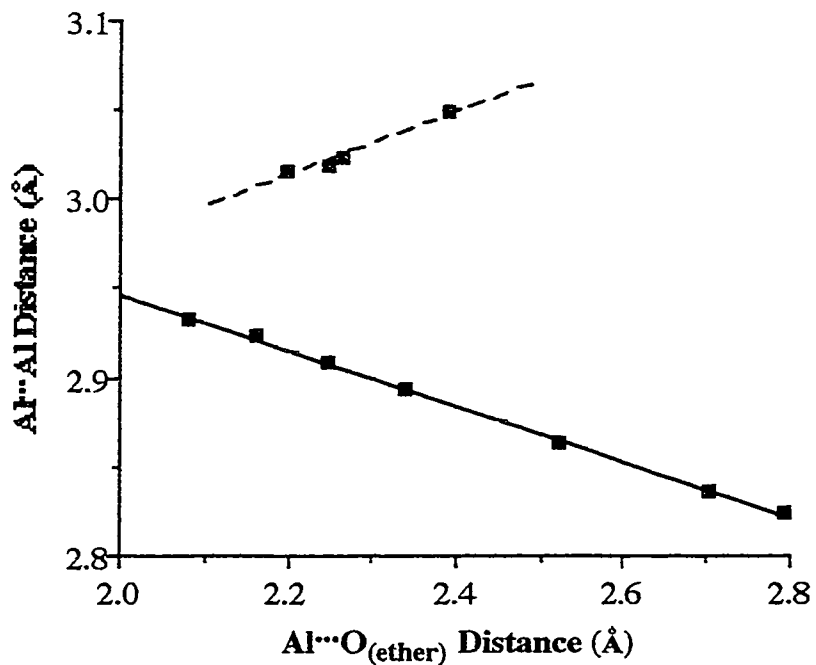


Figure 3.8. Plot of Al-Al distances (Å) as a function of the Al-O(ether) distance (Å) (a) calculated for the model $[H_2Al(\mu-OCH_2CH_2OH)]_2$ (◻) and (b) the experimental values for $[R_2Al(\mu-OC_6H_4-2-OMe)]_2$ (■).

This latter is better expressed as decreased Al···Al distance resulting from the increased steric bulk (cone angle) of the aluminum alkyl; i.e., Me < Et < ⁱBu < ^tBu. The calculated model system follows the expected trend, i.e., shorter Al···O_(ether) distances result in an increased Al···Al distance associated with the breaking the dimeric unit. In contrast, the experimentally determined values for [R₂Al(μ-OC₆H₄-2-OMe)]₂ show a decrease in the Al···Al distance with a shorter Al···O_(ether) distances.

Conclusion

We have investigated the question as to whether intramolecularly stabilized compounds of aluminum are suitable structural models of the S_N2 transition state. We have shown that in the absence of steric considerations, i.e., the model compound [H₂Al(μ-OCH₂CH₂OH)]₂, such compounds faithfully describe the structural changes that occur in the S_N2 cleavage of dimeric aluminum compounds, Eq. 3.2. Unfortunately, real compounds are not such good models. Angular changes appear to follow the correct trends, however, the bond distances are controlled by the steric bulk of the aluminum alkyl substituents rather than the coordination of the fifth ligand.

Experimental Section

General experimental procedures were carried out as described in Chapter 1. 2-Methoxyphenol was obtained from Aldrich and used without further purification.

[(^tBu)₂Al(μ-OC₆H₄-2-OMe)]₂. To a cooled (-78 °C) solution of Al(^tBu)₃ (1.0 mL, 3.9 mmol) in hexane (50 mL) was added a solution of 2-methoxyphenol (0.49 g, 3.9 mmol) in hexane (50 mL). The mixture was allowed warm to room temperature as it was stirred overnight. Filtration followed by cooling to -21 °C resulted in the formation of colorless crystals. Yield: 0.79 g, 75%. Mp. 114 - 115 °C. MS (EI, %): *m/z* 264 (M⁺, 20), 207 (M⁺ - ^tBu, 75), 150 (M⁺ - 2 ^tBu, 72), 57 (^tBu, 30). IR (cm⁻¹): 1603 (m), 1501 (s),

1388 (w), 1280 (w), 1255 (s), 1111 (m), 768 (m), 748 (s). ^1H NMR (C_6D_6): δ 7.12 [1H, d, $J(\text{H-H}) = 7.6$ Hz, OCH], 6.82 [2H, dd, $J(\text{H-H}) = 7.6$ Hz, $J(\text{H-H}) = 8.0$ Hz, 4-CH], 6.56 [2H, dd, $J(\text{H-H}) = 7.6$ Hz, $J(\text{H-H}) = 8.0$ Hz, 5-CH], 6.27 [2H, d, $J(\text{H-H}) = 8.2$ Hz, 6-CH], 3.23 (6H, s, OCH₃), 1.17 [36H, s, C(CH₃)₃]. ^{13}C NMR (C_6D_6): δ 122 (6-CH), 120 (3-CH), 119 (5-CH), 110 (4-CH), 56.9 (OCH₃), 30.9 [C(CH₃)₃]. ^{27}Al NMR (C_6D_6 , C₇H₈): 45 ($W_{1/2} = 3050$ Hz).

Crystallographic Studies. A crystal of [(tBu)₂Al(μ-OC₆H₄-2-OMe)]₂ was sealed in a glass capillary under argon and mounted on the goniometer of a Rigaku four-circle diffractometer using Mo-K α radiation with a graphite monochromator. Data collection and cell determinations were performed in a manner previously described,¹⁹ using the $\theta/2\theta$ scan technique. Pertinent details are given in Table 3.2. The structure was solved by direct methods (SHELX86).²⁰ The model was refined using full-matrix least squares techniques. Hydrogen atoms were included and constrained to 'ride' upon the appropriate atoms [$d(\text{C-H}) = 0.95$ Å, $U(\text{H}) = 1.3 B_{eq}(\text{C})$]. A summary of cell parameters, data collection, and structure solution is given in Table 3.2. Scattering factors were taken from the usual reference.²¹

Table 3.2. Crystal data and summary of X-ray diffraction data for $[(^t\text{Bu})_2\text{Al}(\mu\text{-OC}_6\text{H}_4\text{-2-OMe})]_2$.

Compound	$[(^t\text{Bu})_2\text{Al}(\mu\text{-OC}_6\text{H}_4\text{-2-OMe})]_2$.
empir. formula	$\text{C}_{30}\text{H}_{50}\text{Al}_2\text{O}_4$
cryst size, mm	0.20 x 0.35 x 0.36
cryst system	monoclinic
space group	$\text{P}2_1/c$
a , Å	8.984(3)
b , Å	17.205(2)
c , Å	10.636(5)
α , deg	
β , deg	109.53(3)
γ , deg	
V , Å ³	1549.4(5)
Z	2
D(calcd), g/cm ³	
μ , cm ⁻¹	1.20
temp, K	298
2θ range, deg	4.6-45.0
no. collected	2183
no. ind	2035
no. obsd	1532($ F_o > 4.0\sigma F_o $)
weighting scheme	$w^{-1} = 0.04(F_o)^2 + \sigma(F_o)^2$
R	0.069
R_w	0.175
largest diff peak, eÅ ⁻³	0.43

References

- 1 C. K. Ingold and E. Rothstein, *J. Chem. Soc.*, 1928, 1217.
- 2 (a) J. D. Atwood, *Inorganic and Organometallic Reaction Mechanisms*, VCH, New York, 2nd Ed., 1997.
(b) K. F. Purcell and J. C. Kotz, *Inorganic Chemistry*, Holt-Saunders, Philadelphia, 1977.
- 3 (a) M. B. Power, J. R. Nash, M. D. Healy, and A. R. Barron, *Organometallics*, 1992, **11**, 1830.
(b) W. L. Buddle and M. F. Hawthorne, *Inorg. Chem.*, 1965, **4**, 1741.
(c) A. H. Cowley and J. H. Mills, *J. Am. Chem. Soc.*, 1969, **91**, 2910.
- 4 See for example, J. B. DeRoos and J. P. Oliver, *Inorg. Chem.*, 1965, **4**, 1741.
- 5 See for example, A. Haaland, in *Coordination Chemistry of Aluminum*, Ed., G. H. Robinson, VCH, New York, 1993.
- 6 See for example, (a) O. T. Beachley, Jr, and K. C. Racette, *Inorg. Chem.*, 1976, **15**, 2110, and references therein.
(b) D. A. Atwood, F. P. Gabbai, J. Lu, M. P. Remington, D. Rutherford, and M. P. Sibi, *Organometallics*, 1996, **15**, 2308.
(c) M. R. P. van Vliet, G. van Koyen, M. A. Rotteveel, M. Schrap, K. Vrieze, B. Kojic-Prodic, A. L. Spek, and A. J. M. Duisenberg, *Organometallics*, 1986, **5**, 1389.
(d) C. Jones, F. C. Lee, G. A. Koutsantonis, M. G. Gardiner, and C. L. Raston, *J. Chem. Soc., Dalton Trans.*, 1996, 829.
(e) M. P. Hogerheide, M. Wesseling, J. T. B. H. Jastrzebski, J. Boersma, H. Kooijman, A. L. Spek, and G. van Koten, *Organometallics*, 1995, **14**, 4483.
(f) S. T. Dzugan and V. L. Goedken, *Inorg. Chem. Acta.*, 1988, **154**, 169.
(g) M. R. P. van Vliet, P. Buysingh, G. van Koyen, K. Vrieze, B. Kojic-Prodic, and A. L. Spek, *Organometallics*, 1985, **4**, 1701.
(h) R. Kumar, M. L. Sierra, and J. P. Oliver, *Organometallics*, 1994, **13**, 4285.

- (i) R. Benn, A. Rufinska, H. Lehmkul, E. Janssen, and C. Krüger, *Angew. Chem., Int. Ed. Engl.*, 1983, **22**, 779.
- 7 J. A. Francis, C. N. McMahon, S. G. Bott, and A. R. Barron, submitted for publication.
- 8 C. N. McMahon, S. G. Bott, and A. R. Barron, submitted for publication.
- 9 C. N. McMahon, J. A. Francis, S. G. Bott, and A. R. Barron, *J. Chem. Soc., Dalton Trans.*, 1998, 3305.
- 10 J. A. Francis, S. G. Bott, and A. R. Barron, *J. Chem. Soc., Dalton Trans.*, 1998, 3305.
- 11 C. A. Tolman, *Chem. Rev.*, 1977, **77**, 313.
- 12 D. G. Hendershot, M. Barber, R. Kumar, and J. P. Oliver, *Organometallics*, 1991, **10**, 3302.
- 13 H. Schumann, M. Frick, B. Heymer, and F. Girgsdies, *J. Organomet. Chem.*, 1996, **512**, 117.
- 14 (a) W. Uhl, *Z. Anorg. Allg. Chem.*, 1989, **570**, 37.
(b) H. Lehmkuhl, O. Olbrysch, and H. Nehl, *Liebigs Ann. Chem.*, 1973, 708.
(c) H. Lehmkuhl and O. Olbrysch, *Liebigs Ann. Chem.*, 1973, 715.
- 15 See for example, A. R. Barron, *Polyhedron*, 1995, **14**, 3197, and references therein.
- 16 See for example, (a) K. Lindstrom and F. Osterberg, *Can. J. Chem.*, 1980, **58**, 815.
(b) M. Nethaji, V. Pattabhi, and G. R. Desiraju, *Acta Crystallogr., Sect. C*, 1988, **44**, 275.
(c) R. Velavan, P. Sureshkumar, K. Sivakumar, and S. Natarajan, *Acta Crystallogr., Sect. C*, 1995, **51**, 1131.
(d) H. Krupitsky, Z. Stein, and I. Goldberg, *J. Inclusion Phenom.*, 1995, **20**, 211.
(e) I. Goldberg, H. Krupitsky, Z. Stein, Y. Hsiou, and C. E. Strouse, *Supramolecular Chemistry*, 1994, **4**, 203.

- 17 C. N. McMahon, J. A. Francis, and A. R. Barron, *J. Chem. Cryst.*, 1997, **27**, 167.
- 18 A detailed discussion of the various bonding modes of alkoxides has been presented previously, see reference 5.
- 19 M. R. Mason, J. M. Smith, S. G. Bott, and A. R. Barron, *J. Am. Chem. Soc.*, 1993, **115**, 4971.
- 20 G. M. Sheldrick, *Acta Crystallogr.*, 1990, **A46**, 467.
- 21 *International Tables for X-Ray Crystallography*, Kynoch Press, Birmingham, 1974, vol. 4.

Chapter 4

Sterically Crowded Aryloxides of Aluminum: Intramolecular Coordination of Bidentate Ligands

Introduction

We have previously shown in Chapter 1 that non-delocalized ligands containing both anionic and neutral Lewis base termini such as $[\text{O}(\text{CH}_2)_n\text{ER}'_x]^-$, where E is oxygen, sulfur or nitrogen, react with aluminum alkyls to produce dimeric compounds. These compounds may have four- or five-coordinate aluminum centers depending on the steric bulk of the substituent on the aluminum and the heteroatom, in addition to the identity of the heteroatom itself.¹ Although these compounds are useful to understand the effect of steric bulk and heteroatom on the strength of the intramolecular interaction that forms, they are not models for latent Lewis acidity (see Introduction). This is because the cleavage of the intramolecular bond results in a four-coordinate aluminum center that is itself not Lewis acidic as indicated by the lack of reactivity of these compounds with external Lewis bases.² To circumvent this problem, monomeric compounds with intramolecular coordination sites must be made. The energy barrier necessary to cleave the dimeric structure and produce a monomer has been calculated³ to be about 254 kJ mol⁻¹. In order to overcome this large barrier a sufficiently bulky group must be employed on the aluminum.

Previous work in the Barron group has focused on the sterically demanding aryloxide, 2,6-di-*tert*-butyl-4-methylphenol (BHT-H from the trivial name butylated hydroxy toluene) to stabilize otherwise inaccessible monomeric compounds by inhibition of oligomerization.^{4,5} This bulky ligand has been used to synthesize highly Lewis acidic three-coordinate compounds in order to study their structure, bonding and reactivity without the hindrance of oligomerization.⁴ For the following studies, BHT was chosen as the substituent on the aluminum not only for its steric bulk but also because the coordination sphere of aluminum would then closely mimic that in the alumoxanes. The

following outlines the attempt to synthesize potentially latent Lewis acidic aluminum compounds with ligands containing both anionic and neutral Lewis base termini using BHT as the substituents on the aluminum.

Results and Discussion

The reaction of an excess of $(\text{BHT})_2\text{Al}(\text{H})(\text{Et}_2\text{O})$ (prepared via the reaction of BHT-H and NaAlH_4 , see experimental) with $\text{HO}(\text{CH}_2)_2\text{EMe}_x$ ($\text{E} = \text{O}, \text{S}$, $x = 1$; $\text{E} = \text{N}$, $x = 2$) yields a mixture of products that may be characterized by ^1H spectroscopy. Unreacted starting material, $(\text{BHT})_2\text{Al}(\text{H})(\text{Et}_2\text{O})$, and BHT-H are found in all samples, while a third product is also formed irrespective of the starting alcohol. This third product may be separated from the reaction mixture by selective recrystallization from dichloromethane. Its ^1NMR spectrum shows that the ratio of BHT groups to an aluminum hydride is 2:1; IR spectroscopy confirms the presence of an aluminum hydride ($\nu_{\text{Al}-\text{H}} = 1844 \text{ cm}^{-1}$).⁶ The mass spectrum shows peaks due to $2 \text{ M}^+ - 2 \text{ Me}$ ($m/z = 684$) and $\text{M}^+ - \text{Me}$ ($m/z = 451$), consistent with the dimer $[(\text{BHT})_2\text{Al}(\text{H})]_2$ (**4.1**). Formation of $[(\text{BHT})_2\text{Al}(\text{H})]_2$ is presumably due to the dimerization of the starting material after the Et_2O ligand is eliminated in solution. Compound **4.1** can be identified in the NMR spectra of each reaction mixture where $(\text{BHT})_2\text{Al}(\text{H})(\text{Et}_2\text{O})$ is the reagent in excess.

Based upon spectroscopic and X-ray analysis, the products synthesized containing the functionalized alkoxide are $[(\text{BHT})\text{Al}(\text{H})(\mu-\text{OCH}_2\text{CH}_2\text{EMe}_x)]_2$, where $\text{EMe}_x = \text{NMe}_2$ (**4.2**), OMe (**4.3**), and SMe (**4.4**). The aluminum hydride stretch is seen at 1828 cm^{-1} for compound **4.4** which is consistent with a terminal hydride, and the dimeric nature of compound **4.2** is confirmed by the X-ray crystallography. It is interesting to note that in compound **4.3**, two sets of methylene triplets are seen in the ^1H NMR spectra, unlike compounds **4.2** and **4.4** where only one set of triplets is seen.

The molecular structure of $[(\text{BHT})\text{Al}(\text{H})(\mu-\text{OCH}_2\text{CH}_2\text{NMe}_2)]_2$ (**4.2**), is shown in Figure 4.1; selected bond lengths and angles are given in Table 4.1. Compound **4.2** exists

as a tri-cyclic centrosymmetric dimer with the neutral donor forming an intramolecular coordination with the aluminum center. As is expected, this intramolecular interaction occurs on the less sterically crowded side of the aluminum atom, i.e., it forms on the Al-H(1) side rather than the side to which BHT bonds. The geometry about each aluminum atom is a distorted trigonal bipyramidal with O(1) and N(4) occupying the axial positions [$O(1)-Al(1)-N(4) = 154.9^\circ$] and H(1), O(1') and O(11) defining the equatorial sites. The sum of the bond angles between the equatorial ligands is 360.2° . The distortion about the aluminum center results from the planarity of the Al_2O_2 core. The bond length of the intramolecular coordination is 2.196 Å and that of the terminal Al-H is 1.61 Å that is comparable to the values obtained for similar dimeric terminal aluminum hydrides.⁴

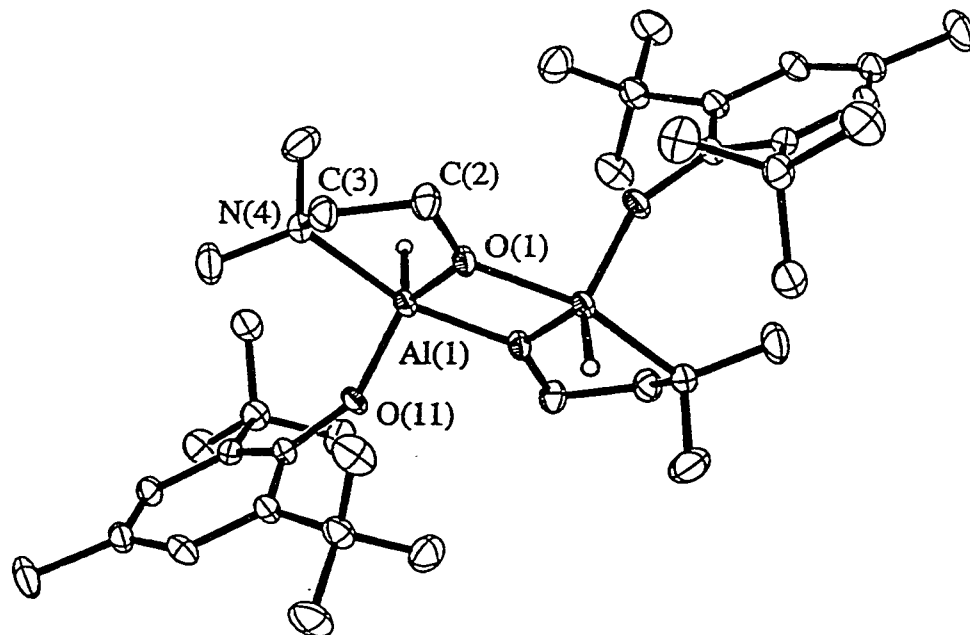


Figure 4.1. Molecular structure of $[(BHT)Al(H)(\mu-OCH_2CH_2NMe_2)]_2$ (4.2). Thermal ellipsoids are given at the 30% level and hydrogen atoms are omitted for clarity.

Table 4.1. Selected bond lengths (\AA) and angles ($^\circ$) for $[(\text{BHT})\text{Al}(\text{H})(\mu\text{-OCH}_2\text{CH}_2\text{NMe}_2)]_2$ (4.2).

Al(1)-O(1)	1.913(3)	Al(1)-N(4)	2.196(4)
Al(1)-O(11)	1.744(3)	Al(1)-O(1')	1.832(3)
Al(1)-H(1)	1.61(2)		
O(11)-Al(1)-O(1')	125.2(2)	O(11)-Al(1)-O(1)	95.8(1)
O(1')-Al(1)-O(1)	74.8(1)	O(11)-Al(1)-N(4')	99.5(1)
O(1')-Al(1)-N(4')	80.1(1)	O(1)-Al(1)-N(4')	154.9(1)
Al(1')-O(1)-Al(1)	105.1(1)	O(1)-Al(1)-H(1)	99(1)
O(11)-Al(1)-H(1)	117(1)	O(1')-Al(1)-H(1)	118(1)
N(4')-Al(1)-H(1)	92(1)		

If the reaction of $(\text{BHT})_2\text{Al}(\text{H})(\text{Et}_2\text{O})$ with $\text{HO}(\text{CH}_2)_2\text{EMe}_x$ is carried out in a stoichiometric manner in an exact 1:1 ratio, three products are seen by NMR spectroscopy. The minor products are BHT-H, and $[(\text{BHT})\text{Al}(\text{H})(\mu\text{-OCH}_2\text{CH}_2\text{EMe}_x)]_2$ (4.2 - 4.4), while the major products are the dimeric structures $[(\text{BHT})\text{Al}(\text{OCH}_2\text{CH}_2\text{EMe}_x)(\mu\text{-OCH}_2\text{CH}_2\text{EMe}_x)]_2$ [$\text{EMe}_x = \text{NMe}_2$ (4.5), OMe (4.6) and SMe (4.7)]. Compounds 4.5 - 4.7 may be separated by selective recrystallization from dichloromethane or by washing with pentane, a solvent in which $[(\text{BHT})\text{Al}(\text{H})(\mu\text{-OCH}_2\text{CH}_2\text{EMe}_x)]_2$ is insoluble. The dimeric structure of the major product is verified by the X-ray crystallographic structure of compound 4.6.

The molecular structure of $[(\text{BHT})\text{Al}(\text{OCH}_2\text{CH}_2\text{OMe})(\mu\text{-OCH}_2\text{CH}_2\text{OMe})]_2$ (4.6) shown in Figure 4.2, selected bond lengths and angles are given in Table 4.2. As with compound 4.2, compound 4.6 is a tri-cyclic centrosymmetric dimer with the neutral donor

ligand forming an intramolecular bond with the aluminum atom. Also like compound 4.2, the geometry at the aluminum atoms approximates trigonal bipyramidal with the chelating neutral oxygen O(4) and the bridging oxygen O(1) occupying the axial positions.

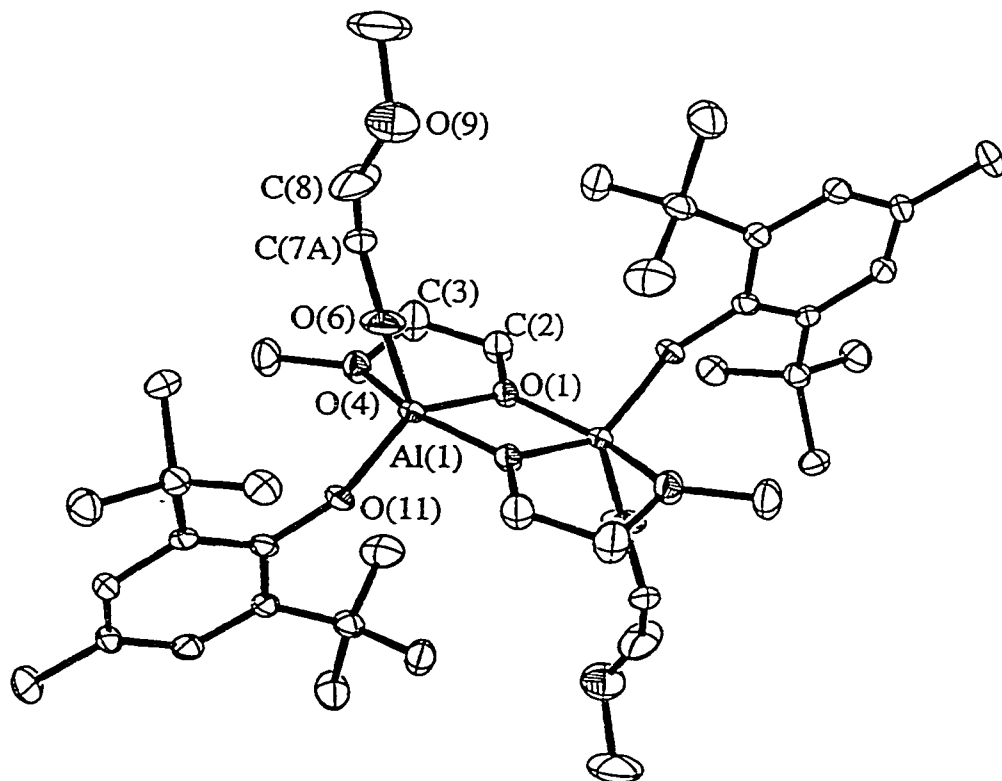


Figure 4.2. Molecular structures of $[(\text{BHT})\text{Al}(\text{OCH}_2\text{CH}_2\text{OMe})(\mu\text{-OCH}_2\text{CH}_2\text{OMe})]_2$ (4.6). Thermal ellipsoids are given at the 30% level and hydrogen atoms are omitted for clarity.

As with compound 4.2, the five-membered ring formed from the chelation of the neutral donor ligand exhibits twisting due to the planarity of the Al_2O_2 core. The length of the intramolecular coordination, $\text{Al}(1)\text{-O}(4)$, is $[2.025(3) \text{ \AA}]$ indicative of a stronger interaction than that seen in $[(\text{iBu})_2\text{Al}(\mu\text{-OCH}_2\text{CH}_2\text{OMe})]_2$ $[\text{Al}(1)\text{-O}(4)] = 2.283 \text{ \AA}$.

This difference may be due to low steric bulk of the terminal alkoxide or to the changed electronic environment around the aluminum from AlO_3C_2 to AlO_5 or to a combination of both factors. The terminal ligand possesses "slinky" type disorder⁷ of the C-C-O-C chain and the solvent molecule, CH_2Cl_2 demonstrates rotational disorder.

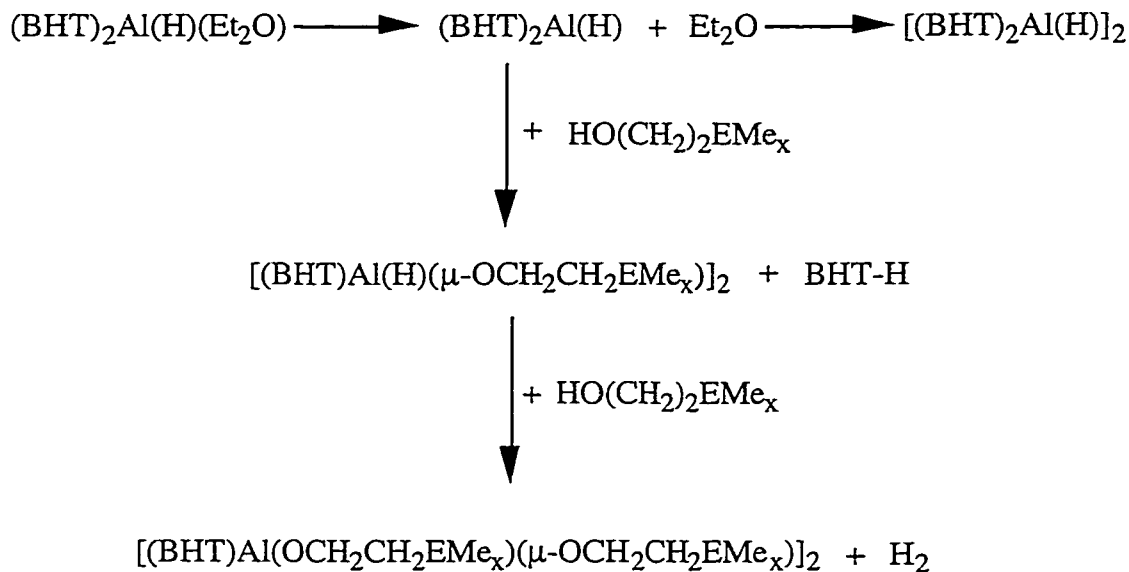
Table 4.2 Selected bond lengths (\AA) and angles ($^\circ$) for $[(\text{BHT})\text{Al}(\text{OCH}_2\text{CH}_2\text{OMe})(\mu-\text{OCH}_2\text{CH}_2\text{OMe})]_2$ (4.6).

Al(1)-O(1)	1.874(3)	Al(1)-O(11)	1.730(3)
Al(1)-O(4)	2.025(3)	Al(1)-O(6)	1.704(3)
Al(1)-O(1')	1.844(3)		
O(1)-Al(1)-O(4)	152.6(1)	O(1)-Al(1)-O(6)	103.4(2)
O(1)-Al(1)-O(11)	97.5(1)	O(1)-Al(1)-O(1')	75.0(1)
O(4)-Al(1)-O(6)	92.8(2)	O(4)-Al(1)-O(11)	94.8(1)
O(4)-Al(1)-O(1')	78.4(1)	O(6)-Al(1)-O(11)	116.0(2)
O(6)-Al(1)-O(1')	112.8(2)	O(11)-Al(1)-O(1')	131.0(2)
Al(1)-O(1)-Al(1')	104.9(1)	Al(1)-O(1)-C(2)	133.2(3)
Al(1)-O(6)-C(7A)	146.4(5)	Al(1)-O(6)-C(7B)	151.5(5)
Al(1)-O(11)-C(11)	159.3(3)		

Based on the above observations, it can be seen that the reactions of $(\text{BHT})_2\text{Al}(\text{H})(\text{Et}_2\text{O})$ with the bifunctional, potentially chelating alcohols, $\text{HO}(\text{CH}_2)_2\text{EMe}_x$ ($\text{E} = \text{O}, \text{S}, x = 1; \text{E} = \text{N}, x = 2$), proceed as shown in Scheme 4.1. The initial reaction involves the protolysis of the BHT ligand in preference to the hydride. The unexpected elimination of the BHT-H rather than hydrogen is presumably due to the greater basicity of

the aryloxide oxygen than the aluminum hydride. We have observed similar decreases in basicity of aluminum alkyls in the presence of oxygen donor ligands.⁸ The resulting mono-BHT compound dimerizes through the alkoxide oxygen to give $[(\text{BHT})\text{Al}(\text{H})(\mu-\text{OCH}_2\text{CH}_2\text{EMe}_x)]_2$ (4.2 - 4.4). Reaction with further equivalents of $\text{HO}(\text{CH}_2)_2\text{EMe}_x$ does result in hydrogen elimination, forming $[(\text{BHT})\text{Al}(\text{OCH}_2\text{CH}_2\text{EMe}_x)(\mu-\text{OCH}_2\text{CH}_2\text{EMe}_x)]_2$ (4.5 - 4.7). This reaction scheme is stoichiometrically controlled because in the presence of excess $(\text{BHT})_2\text{Al}(\text{H})(\text{Et}_2\text{O})$, only the $[(\text{BHT})\text{Al}(\text{H})(\mu-\text{OCH}_2\text{CH}_2\text{EMe}_x)]_2$ (4.2 - 4.4) is formed.

Unfortunately, in all cases, the presence of only a single BHT does not preclude the formation of a dimer as we had hoped. In provide sufficient steric bulk to form a monomer containing potentially a bridging anionic oxygen, two BHT groups are needed.⁴

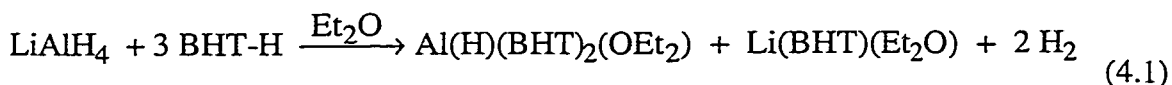


Scheme 4.1. Reaction scheme for $(\text{BHT})_2\text{Al}(\text{H})(\text{Et}_2\text{O})$ with $\text{HO}(\text{CH}_2)_2\text{EMe}_x$.

In order to overcome this problem and to produce the potential latent Lewis acid, $(\text{BHT})_2\text{Al}(\mu-\text{OCH}_2\text{CH}_2\text{EMe}_x)]_2$, $\text{Al}(\text{BHT})_3$ was used as the starting material.

Unfortunately, the results of the reactions of $\text{Al}(\text{BHT})_3$ with $\text{HOCH}_2\text{CH}_2\text{EMe}_x$ were inconclusive by NMR spectroscopy.

Lithium Aluminates. Traditionally, $(\text{BHT})_2\text{Al}(\text{H})(\text{Et}_2\text{O})$ has been synthesized from the reaction of LiAlH_4 with BHT-H.² The lithium side product, $\text{Li}(\text{BHT})(\text{Et}_2\text{O})$ (Eq. 4.1) was separated by multiple recrystallization steps. However, we have found that it is extremely difficult to completely separate the lithium salt from the desired product, (Eq. 4.1).



Although not previously an issue,³ our initial synthetic attempt to prepare $(\text{BHT})_2\text{Al}[\text{O}(\text{CH}_2)_2\text{EMe}_x]$ resulted in the isolation of a series of lithium aluminates.

If the reaction mixture formed from the reaction between LiAlH_4 with BHT-H is reacted with $\text{HO}(\text{CH}_2)_2\text{EMe}_x$ ($E = O, S, x = 1; E = N, x = 2$), then the only compounds that may be isolated are the lithium aluminates, $(\text{BHT})_2\text{Al}(\mu\text{-OCH}_2\text{CH}_2\text{EMe}_x)_2\text{Li}$. Compounds $(\text{BHT})_2\text{Al}(\mu\text{-OCH}_2\text{CH}_2\text{NMe}_2)_2\text{Li}$ (4.8), $(\text{BHT})_2\text{Al}(\mu\text{-OCH}_2\text{CH}_2\text{OMe})_2\text{Li}$ (4.9), $(\text{BHT})_2\text{Al}(\mu\text{-OCH}_2\text{CH}_2\text{SMe})_2\text{Li}$ (4.10a) have all been isolated and the presence of lithium in each was confirmed by a standard flame test. In addition, where an excess of $\text{HO}(\text{CH}_2)_2\text{SMe}$ is employed the solvate, $(\text{BHT})_2\text{Al}(\mu\text{-OCH}_2\text{CH}_2\text{SMe})_2\text{Li}(\text{HOCH}_2\text{CH}_2\text{SMe})$ (4.10b), is also isolated. The monomeric structure of compound 4.8 to 4.10 were verified by mass spectroscopy which showed peaks due to M^+ and $M^+ - \text{BHT}$ and the structures of these compounds are verified by the X-ray molecular structure of compounds 4.8 and 4.10b. The monomeric structures of 4.9, and 4.10 were shown through mass spectroscopy.

The molecular structure of $(\text{BHT})_2\text{Al}(\mu\text{-OCH}_2\text{CH}_2\text{NMe}_2)_2\text{Li}$ (4.8) and $(\text{BHT})_2\text{Al}(\mu\text{-OCH}_2\text{CH}_2\text{SMe})_2\text{Li}(\text{HOCH}_2\text{CH}_2\text{SMe})$ (4.10b) are shown in Figures 4.3

and 4.4 respectively; selected bond lengths and angles are given in Tables 4.3 and 4.4.

Compounds **4.8** and **4.10b** form monomeric structures with a central AlO_2Li core. The geometry at the aluminum center is distorted from tetrahedral due to the presence of the four membered AlO_2Li cycle. The co-ordination geometry around the lithium atom approximates to tetrahedral in compound **4.8**, but it is more distorted than that around the aluminum due to the large N(4)-Li(1)-N(9) angle (117.7°). In compound **4.10b**, the presence the ligand adduct on lithium, however changes the geometry around the lithium and it becomes five-coordinate, distorted trigonal pyramidal. Although X-ray data was collected for compounds **4.9** and **4.10**, their structures could not be refined to satisfactory values and the lithium atoms were not located, however the geometry of the ligands indicate that they are *iso*-structural to compound **4.8**. Other spectroscopic methods such as NMR and MS support this claim.

Several lithium aluminates may be found in the literature, most of which exhibit a similar AlO_2Li core.^{5,9} In these cases, however, the lithium is coordinated to either ether or THF molecules and this results in a three-coordinate, distorted trigonal planar arrangement. A tetrahedral geometry for lithium is seen in the dimer $[(\text{salpanAl})(\text{Li}(\text{THF}))_2]_2$ made by Atwood et al.¹⁰ but because the ligand attached to the lithium was not chelating, the geometry about the lithium was not as distorted as seen in compounds **4.8** and **4.10b**. In compound $\text{LiAl}[\text{OC}(\text{Ph})(\text{CF}_3)_2]_4$,¹¹ AlO_2Li core is similar as is seen in the other lithium aluminates, but the lithium is actually chelated by CF_3 substituents on the ligand and the geometry about the lithium atom becomes highly distorted. The geometry is uniquely six-coordinate and distorted from octahedral to trigonal prismatic. As in compounds **4.8** and **4.10b**, the presence of the lithium atom stabilizes the monomer in this fluorinated compound. The lithium aluminates **4.8** and **4.10b** and $\text{LiAl}[\text{OC}(\text{Ph})(\text{CF}_3)_2]_4$,¹¹ may be considered as an aluminum anion, chelating the lithium or as a neutral covalent compound.

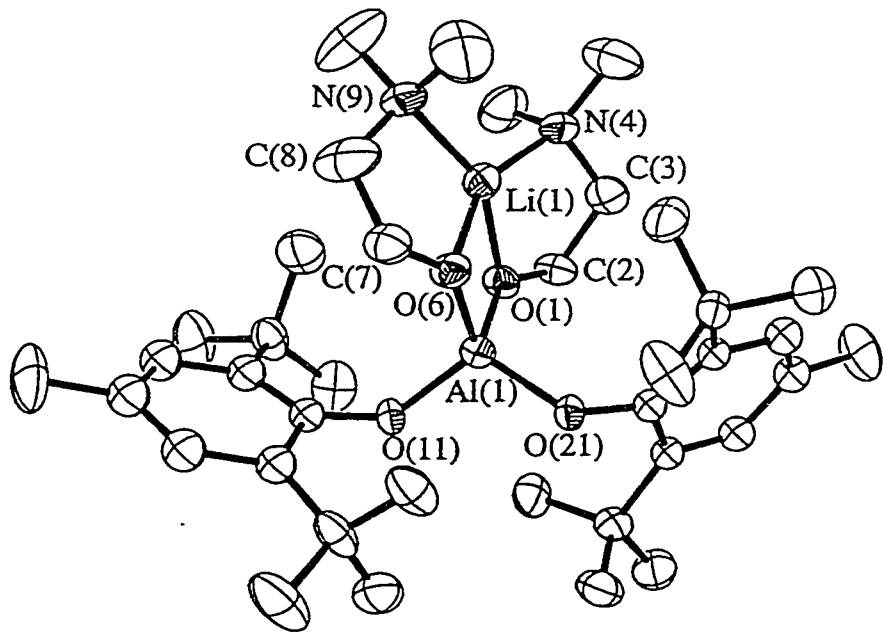


Figure 4.3 Molecular structure of $(\text{BHT})_2\text{Al}(\mu\text{-OCH}_2\text{CH}_2\text{NMe}_2)_2\text{Li}$ (4.8). Thermal ellipsoids are shown at the 30% level and hydrogen atoms are omitted for clarity.

Table 4.3. Selected bond lengths (\AA) and angles ($^\circ$) for $(\text{BHT})_2\text{Al}(\mu\text{-OCH}_2\text{CH}_2\text{NMe}_2)_2\text{Li}$ (4.8).

Al(1)-O(1)	1.730(5)	Al(1)-O(21)	1.741(5)
Al(1)-O(11)	1.735(5)	Li(1)-O(1)	1.970(4)
Al(1)-O(6)	1.736(5)	Li(1)-O(6)	1.980(3)
Li(1)-N(4)	2.130	Li(1)-N(9)	2.150(5)
O(11)-Al(1)-O(21)	109.4(2)	O(11)-Al(1)-O(1)	117.0(2)
O(1)-Al(1)-O(6)	92.1(2)	O(11)-Al(1)-O(6)	110.3(2)
O(1)-Al(1)-N(9)	153.4(7)	O(1)-Al(1)-O(21)	110.3(2)
O(1)-Li(1)-O(6)	78.8(5)	O(6)-Li(1)-N(4)	154.3(7)
O(1)-Li(1)-N(4)	84.1(5)	O(6)-Li(1)-N(9)	84.5(5)
N(4)-Li(1)-N(9)	117.7(6)		

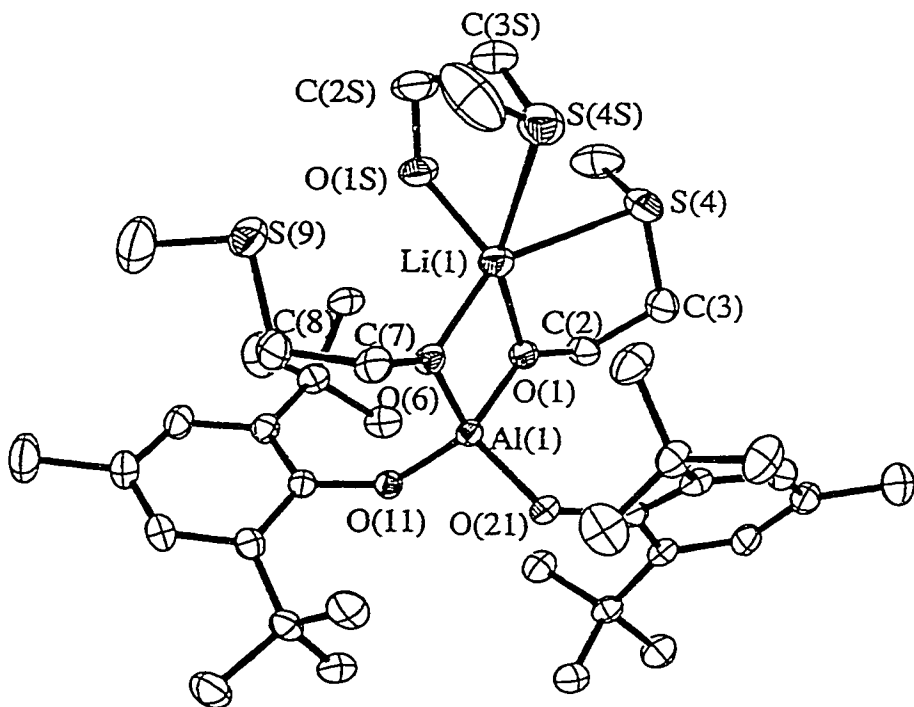


Figure 4.4. Molecular structure of $(\text{BHT})_2\text{Al}(\mu\text{-OCH}_2\text{CH}_2\text{SMe})_2\text{Li}(\text{HOCH}_2\text{CH}_2\text{SMe})$ (4.10b). Thermal ellipsoids are shown at the 30% level and hydrogen atoms are omitted for clarity.

The coordination of the lithium cation is stabilized in the structure by formation of bonds with both the anionic oxygens as well as the neutral donor ligands. Bond valence theory describes the valence of atoms in a molecule and offers the ability to measure their bonding potential^{12,13} i.e., it infers the extent to which each bond contributes to the stability of an atom or ion and the sum of the bond valences at each atom is equal to the atomic valence. Each individual bond valence may be calculated from equation 4.2, where s is the bond valence, R is the experimentally determined bond length, and R_0 (the length of a bond of unit valence) and B are empirically determined parameters.

Table 4.4 Selected bond lengths (\AA) and angles ($^\circ$) for $(\text{BHT})_2\text{Al}(\mu-\text{OCH}_2\text{CH}_2\text{SMe})_2\text{LiHOCH}_2\text{CH}_2\text{SMe}$ (**4.10b**).

Al(1)-O(1)	1.747(3)	Al(1)-O(21)	1.746(2)
Al(1)-O(11)	1.736(3)	Li(1)-O(1)	1.982(8)
Al(1)-O(6)	1.753(3)	Li(1)-O(6)	2.004(7)
Li(1)-O(1S)	1.932(8)		
O(11)-Al(1)-O(21)	108(8)	O(11)-Al(1)-O(1)	121.0(5)
O(1)-Al(1)-O(6)	91.0(3)	O(11)-Al(1)-O(6)	111.3(2)
O(1)-Al(1)-O(21)	109.2(2)	O(1)-Li(1)-O(6)	77.3(3)
O(6)-Li(1)-O(1S)	108.7(4)	O(1)-Li(1)-O(1S)	128.1(5)

$$s = 10 \left[\frac{-(R - R_0)}{B} \right] \quad (4.2)$$

The calculated bond valences for the bonds to lithium and aluminum for compounds **4.8** and **4.10b** are presented in Table 4.5. In both compounds the aluminum is nearly equally stabilized by all four oxygen donors. This is in accord with the theories that Haaland have postulated.¹⁴ In compound **4.8**, the lithium is stabilized as much as, if not slightly more by the nitrogen atoms than the oxygen atoms. This may be due to the fact that the oxygens are also bonded to aluminum. In the case of compound **4.10b**, the stabilization of the lithium is primarily by the oxygens and the sulfur donors contribute only 13.6% to the overall stability. This is obviously due to the weak association that the sulfur atoms have with the lithium and the fact that sulfur is a much softer base than oxygen. In the case of

$\text{LiAl}[\text{OC(Ph)}(\text{CF}_3)_2]_4$,¹¹ the lithium atom is stabilized far more by the flourines causing the C-F bonds to weaken.¹²

Table 4.5. Bond valences^a for the lithium bonds in $(\text{BHT})_2\text{Al}(\mu-\text{OCH}_2\text{CH}_2\text{NMe}_2)_2\text{Li}$ (4.8) and $(\text{BHT})_2\text{Al}(\mu-\text{OCH}_2\text{CH}_2\text{SMe})_2\text{Li}\cdot\text{HOCH}_2\text{CH}_2\text{SMe}$ (4.10b).

	(4.8)		(4.10b)
Li(1)-O(1)	0.246	Li(1)-O(1)	0.238
Li(1)-O(6)	0.245	Li(1)-O(6)	0.227
Li(1)-N(9)	≈ 0.254	Li(1)-O(1S)	0.264
Li(1)-N(4)	≈ 0.254	Li(1)-S(4S)	≈ 0.14
		Li(1)-S(4)	≈ 0.14
Al(1)-O(1)	0.798	Al(1)-O(1)	0.763
Al(1)-O(6)	0.785	Al(1)-O(6)	0.751
Al(1)-O(11)	0.787	Al(1)-O(11)	0.785
Al(1)-O(21)	0.775	Al(1)-O(21)	0.765

^a Bond valences were calculated from equation 4.2 where for Li-O bonds, $R_0 = 1.292$, $B = 0.48$ and for Al-O bonds, $R_0 = 1.644$, $B = 0.38$.⁶

Conclusions

These studies have shown that the reaction of $(\text{BHT})_2\text{Al}(\text{H})(\text{Et}_2\text{O})$ with bifunctional alcohols, $\text{HO}(\text{CH}_2)_n\text{ER}'_x$, produce species that dimerize through the anionic oxygen on the ligands. The formation of the *bis*-aryloxide compounds is precluded due to the preferential elimination of the BHT ligand over the hydride. The formation of dimeric rather than

monomeric structures is presumably due to the inability of only one BHT-H ligand to overcome the energy barrier³ present in the formation of a monomeric structure.

Monomeric compounds could be synthesized as lithium aluminates formed from starting material that was made using LiAlH₄. These compounds show that the presence of a lithium atom stabilizes the monomeric *bis*-aryloxide compounds.

Experimental Section

General experimental procedures were carried out as described in Chapter 1. The synthesis of (BHT)₂Al(H)(Et₂O) was performed according to a literature method³ substituting LiAlH₄ with NaAlH₄ in order to avoid contamination with lithium.

Reaction of (BHT)₂Al(H)(Et₂O) and HOCH₂CH₂NMe₂ (3:1). To a solution of (BHT)₂Al(H)(Et₂O) (1.50 g, 2.8 mmol) in CH₂Cl₂ (50 mL) was added HOCH₂CH₂NMe₂ (0.08 g, 0.93 mmol), dropwise. The mixture was allowed to stir overnight, after which time all volatiles were removed under vacuum and the residue was characterized by ¹H NMR. The ¹H NMR showed a mixture of BHT-H, [(BHT)Al(H)(μ-OCH₂CH₂NMe₂)₂], excess (BHT)₂Al(H)(Et₂O) and [(BHT)₂Al(H)]₂. The mixture was then recrystallized from dichloromethane to give very few colorless crystals of [(BHT)Al(H)(μ-OCH₂CH₂NMe₂)₂]. The supernatant was then placed in the freezer and another crop of colorless crystals were isolated and characterized as [(BHT)₂Al(H)]₂.

[(BHT)₂Al(H)]₂ (4.1). Mp: 233 - 234 °C. MS (EI, %): *m/z* 684 (2M⁺- 2Me, 15), 451 (M⁺ - Me, 25), 205 (BHT - Me, 100). IR (cm⁻¹): 2740 (w), 1741 (m), 1393 (s), 1265 (s), 942 (s), 901 (s), 871(m), 778 (m), 640 (m). ¹H NMR (C₆D₆): δ 7.11 [8H, s, m-CH], 4.26 [2H, s, AlH], 2.20 [12H, s, CH₃], 1.46 [72H, s, C(CH₃)₃]. ¹³C NMR (C₆D₆): δ 152.6 (CO), 127.0 (CH), 35.5 [C(CH₃)₃], 32.3 [C(CH₃)₃], 21.7 (CH₃Ar).

[(BHT)Al(H)(μ -OCH₂CH₂NMe₂)]₂ (4.2). ¹H NMR (C₆D₆): δ 7.22 [4H, s, m-CH], 4.26 [2H, s, AlH], 3.71 [4H, t, *J*(H-H) = 5.7 Hz, OCH₂], 2.36 [4H, t, *J*(H-H) = 5.7 Hz, CH₂N], 2.30 [6H, s, CH₃], 1.36 [12H, s, N(CH₃)₂], 1.53 [36H, s, C(CH₃)₃].

Reaction of (BHT)₂Al(H)(Et₂O) and HOCH₂CH₂OMe (3:1). To a solution of (BHT)₂Al(H)(Et₂O) (1.50 g, 2.8 mmol) in dichloromethane (50 mL) was added HOCH₂CH₂OMe (0.07 g, 0.93 mmol) dropwise manner at room temperature. The mixture was allowed to stir overnight, filtered, and then the volatiles were removed *in vacuo*. The resultant solid was then characterized by ¹H NMR which showed a mixture of [(BHT)Al(H)(μ -OCH₂CH₂OMe)]₂, BHT-H, [(BHT)₂Al(H)]₂, and excess BHT₂Al(H)(Et₂O).

[(BHT)Al(H)(μ -OCH₂CH₂OMe)]₂ (4.3). ¹H NMR (C₆D₆): δ 7.20 [4H, s, m-CH], 4.26 [2H, s, AlH], 3.64 [4H, t, *J*(H-H) = 6.0 Hz, OCH₂], 3.10 [4H, t, *J*(H-H) = 6.0 Hz, CH₂O], 3.11 [6H, s, OCH₃], 2.42 [6H, s, CH₃], 1.59 [36H, s, C(CH₃)₃].

Reaction of BHT₂Al(H)(Et₂O) and HOCH₂CH₂SMe (3:1). To a solution of (BHT)₂Al(H)(Et₂O) (2.0 g, 3.7 mmol in dichloromethane (50 mL) was added HOCH₂CH₂SMe (0.11 g, 1.2 mmol) dropwise at room temperature. The mixture was allowed to stir overnight, filtered, and then dried *in vacuo*. The resultant solid was then characterized by ¹H NMR which showed a mixture of the following compounds: (BHT)Al(H)(μ -OCH₂CH₂SMe)]₂, BHT-H, [BHT₂Al(H)]₂, and excess BHT₂Al(H)(Et₂O).

(BHT)Al(H)(μ -OCH₂CH₂SMe)]₂ (4.4). Mp: 115 - 117 °C. IR (cm⁻¹): 1828 (w) (ν , Al-H), 1250 (s), 1116 (m), 886 (m), 871 (m), 666 (w), 625 (w). ¹H NMR (C₆D₆): δ 7.19 [4H, s, m-CH], 3.53 [4H, t, *J*(H-H) = 5.4 Hz, OCH₂], 2.36 [6H, s, OCH₃], 1.92 [4H, t, *J*(H-H) = 5.4 Hz, CH₂O], 1.72 [36H, s, C(CH₃)₃], 1.35 [6H, s, CH₃]. ¹³C NMR

(C₆D₆): δ 139.7 (CO), 126.5 (CH), 36.1 (SCH₂), 32.4 [C(CH₃)₃], 30.8 [C(CH₃)₃], 21.7 (CH₃Ar), 12.9 (SCH₃)

[(BHT)Al(OCH₂CH₂NMe₂)(μ-OCH₂CH₂NMe₂)]₂ (4.5) To a solution of (BHT)₂Al(H)(Et₂O) (1.15 g, 2.1 mmol) in dichloromethane (50 mL) was added HOCH₂CH₂NMe₂ (0.19 g, 2.1 mmol) dropwise at room temperature. The mixture was allowed to stir overnight, filtered, and then placed in the freezer for crystallization. Very few colorless crystals were isolated and were insufficient for complete characterization. ¹H NMR (C₆D₆): δ 6.94 [4H, s, m-CH], 3.28 [4H, t, J(H-H) = 5.1 Hz, OCH₂], 2.13 [6H, s, CH₃], 1.86 [8H, t, J(H-H) = 5.1 Hz, CH₂N], 1.68 [24H, s, N(CH₃)₂] 1.34 [36H, s, C(CH₃)₃].

[(BHT)Al(OCH₂CH₂OMe)(μ-OCH₂CH₂OMe)]₂ (4.6) To a solution of (BHT)₂Al(H)(Et₂O) (1.75 g, 3.2 mmol) in dichloromethane (50 mL) was added HOCH₂CH₂OMe (0.25 g, 3.2 mmol) in a dropwise manner at room temperature. The mixture was allowed to stir overnight, filtered, and then placed in the freezer for crystallization. Colorless crystals then precipitated. Yield: ca10%. Mp. 163 - 166 °C. MS (EI, %): *m/z* 573 (2M⁺-BHT, 100), 529 (2M⁺ - BHT - OCH₂, 50), 396 (M⁺, 15), 353 (2M⁺ - 2BHT, 10), 205 (BHT - Me, 15). IR (cm⁻¹): 2719 (w), 1265 (m), 1157 (w), 1050 (m, br), 927 (w), 866 (w), 804 (w), 722 (w), 666 (w). ¹H NMR (C₆D₆): δ 7.28 [4H, s, m-CH], 3.66 [4H, t, J(H-H) = 4.6 Hz, OCH₂], 3.34 [4H, J(H-H) = 4.2 Hz, OCH₂], 2.98 [4H, t, J(H-H) = 4.6 Hz, CH₂O], 2.94 [6H, s, ArCH₃], 2.80 [4H, J(H-H) = 4.2 Hz, OCH₂], 2.73 [6H, s, OCH₃], 2.39 [6H, s, OCH₃], 1.82 [36 H, s, C(CH₃)₃].

Reaction of BHT₂Al(H)(Et₂O) and HO(CH₂)₂SMe (1:1). To a solution of (BHT)₂Al(H)(Et₂O) (1.50 g, 2.8 mmol) in dichloromethane (50 mL) was added HO(CH₂)₂SMe (.026 g, 2.8 mmol) in a dropwise manner at room temperature. The

mixture was allowed to stir overnight and reduced to dryness in vacuo. ^1H NMR revealed a mixture of $[(\text{BHT})\text{Al}(\text{OCH}_2\text{CH}_2\text{SMe})(\mu\text{-OCH}_2\text{CH}_2\text{SMe})]_2$, BHT-H and compound 4.3. Compound 4.3 was isolated as residue by washing the mixture with pentane.

$[(\text{BHT})\text{Al}(\text{OCH}_2\text{CH}_2\text{SMe})(\mu\text{-OCH}_2\text{CH}_2\text{SMe})]_2$ (4.7). ^1H NMR (C_6D_6): δ 7.25 [4H, s, m- CH , 3.73 [8H, t, $J(\text{H}-\text{H}) = 7.0$ Hz, OCH_2], 2.33 [6H, s, CH_3], 1.99 [8H, t, $J(\text{H}-\text{H}) = 7.0$ Hz, CH_2S], 1.68 [36H, s, $\text{C}(\text{CH}_3)_3$] 1.38 [6H, s, SCH_3].

$(\text{BHT})_2\text{Al}(\mu\text{-OCH}_2\text{CH}_2\text{NMe}_2)_2\text{Li}$ (4.8). To a mixture of $\text{Li}(\text{BHT})(\text{OEt}_2)$ and $(\text{BHT})_2\text{Al}(\text{H})(\text{Et}_2\text{O})$ (1.5 g, 2.8 mmol) dissolved in hexane (50 mL), was added $\text{HOCH}_2\text{CH}_2\text{NMe}_2$ (0.25 g, 2.8 mmol). The mixture was allowed to stir overnight, filtered and placed at -22 °C where colorless crystals precipitated. Yield: 80%. Mp. 152 - 154 °C. MS (EI, %): m/z 648 (M^+ , 5), 429 ($\text{M}^+ - \text{BHT}$, 100), 340 ($\text{M}^+ - \text{BHT} - \text{O}(\text{CH}_2)_2\text{NMe}_2$, 40), 205 (BHT - Me, 15). IR (cm^{-1}): 1829 (w), 1262 (s), 1163 (w), 1116 (m), 1026 (m), 945 (w), 898 (w), 870 (w), 804 (m), 780 (w), 719 (m). ^1H NMR (C_6D_6): δ 7.26 [4H, s, m- CH], 3.54 [4H, t, $J(\text{H}-\text{H}) = 5.3$ Hz, OCH_2], 2.36 [6H, s, Ar- CH_3], 1.78 [4H, t, $J(\text{H}-\text{H}) = 5.3$ Hz, CH_2N], 1.73 [36H, s, $\text{C}(\text{CH}_3)_3$], 1.61 [12H, s, $\text{N}(\text{CH}_3)_2$]. ^{27}Al NMR (C_7H_8 , C_6D_6): δ 43 ($W_{1/2} = 897$ Hz).

$(\text{BHT})_2\text{Al}(\mu\text{-OCH}_2\text{CH}_2\text{OMe})_2\text{Li}$ (4.9). To a mixture of $\text{Li}(\text{BHT})(\text{OEt}_2)$ and $(\text{BHT})_2\text{Al}(\text{H})(\text{Et}_2\text{O})$ (1.5 g, 2.8 mmol) dissolved in hexane (50 mL), was added $\text{HOCH}_2\text{CH}_2\text{OMe}$ (0.21 g, 2.8 mmol). The mixture was allowed to stir overnight, filtered and placed at -22 °C where colorless crystals precipitated. Yield: 81%. Mp. 74 - 75 °C. MS (EI, %): m/z 622 (M^+ , 10), 547 ($\text{M}^+ - \text{O}(\text{CH}_2)_2\text{OMe}$, 5), 403 ($\text{M}^+ - \text{BHT}$, 100), 205 (BHT - Me, 65), 57 (tBu, 100). IR (cm^{-1}): 2730 (w), 1378 (s), 1265 (m), 1157 (w), 1091 (m), 932 (w), 860 (w), 799 (m), 722 (m), 482 (s). ^1H NMR (C_6D_6): δ 7.28 [4H, s, m- CH], 3.62 [4H, t, $J(\text{H}-\text{H}) = 4.8$ Hz, OCH_2], 2.80 [4H, t, $J(\text{H}-\text{H}) = 4.8$ Hz, CH_2O], 2.62

[6H, s, OCH₃], 2.37 [6H, s, ArCH₃], 1.73 [36H, s, C(CH₃)₃]. ²⁷Al NMR (C₇H₈, C₆D₆): δ 44 (W_{1/2} = 996 Hz).

(BHT)₂Al(μ-OCH₂CH₂SMe)₂Li (4.10). To a mixture of Li(BHT)(OEt₂) and (BHT)₂Al(H)(Et₂O) (1.5 g, 2.8 mmol) dissolved in hexane (50 mL), was added HO(CH₂)₂SMe (0.26 g, 2.8 mmol). The mixture was allowed to stir overnight, filtered and placed at -22 °C where colorless crystals precipitated. Yield: 78%. Mp. 189 - 190 °C. MS (EI, %): *m/z* 654 (M⁺, 10), 435 (M⁺ - BHT, 100), 343 (M⁺ - BHT - O(CH₂)₂SMe, 10), 205 (BHT - Me, 65). IR (cm⁻¹): 2719 (w), 1285 (w), 1234 (m), 1198 (w), 1111 (m), 855 (m), 804 (w), 784 (m), 722 (w), 661 (m). ¹H NMR (C₆D₆): δ 7.20 [4H, s, m-CH], 3.51 [4H, t, *J*(H-H) = 5.1 Hz, OCH₂], 2.32 [6H, s, CH₃], 1.97 [4H, t, *J*(H-H) = 5.1 Hz, CH₂S], 1.70 [36H, s, C(CH₃)₃], 1.36 [6H, s, SCH₃]. ²⁷Al NMR (C₇H₈, C₆D₆): δ 50 (W_{1/2} = 1744 Hz).

Table 4.6. Summary of X-ray Diffraction Data.

Compound	$[(\text{BHT})\text{Al}(\text{H})(\mu-\text{OCH}_2\text{CH}_2\text{NMe}_2)]_2$ (4.2)	$[(\text{BHT})\text{Al}(\text{OCH}_2\text{CH}_2\text{OMe})(\mu-\text{OCH}_2\text{CH}_2\text{OMe})]_2$ (4.6)
empir. formula	$\text{C}_{40}\text{H}_{72}\text{Al}_2\text{Cl}_2\text{N}_2\text{O}_4$	$\text{C}_{44}\text{H}_{78}\text{Al}_2\text{Cl}_4\text{O}_{10}$
cryst system	monoclinic	triclinic
space group	$\text{P}2_1/\text{n}$	$\bar{\text{P}}\bar{1}$
a , Å	12.002(2)	8.622(2)
b , Å	15.805(3)	11.135(2)
c , Å	12.936(3)	14.351(3)
α , deg		70.83(3)
β , deg	105.41(3)	86.67(3)
γ , deg		87.86(3)
V , Å ³	2365.6(8)	1298.9(4)
Z	2	1
D(calcd), g/cm ³	1.18	1.231
μ , cm ⁻¹	0.33	0.31
temp, K	223	223
2θ range, deg	4 - 45	3.0 - 50.0
no. collected	3258	3608
no. ind	3088	3396
no. obsd	$668(F_o > 5.0\sigma F_o)$	$1738 (F_o > 6.0\sigma F_o)$
weighting scheme	$w^{-1} = 0.04(F_o)^2 + \sigma(F_o)^2$	$w^{-1} = 0.04(F_o)^2 + \sigma(F_o)^2$
R	0.0587	0.062
R_w	0.147	0.0.165
largest diff peak, eÅ ⁻³	0.45 / -0.40	0.41 / -0.33

Table 4.6. contd.

Compound	$(BHT)_2Al(\mu-OCH_2CH_2NMe_2)_2Li$ (4.8)	$(BHT)_2Al(\mu-OCH_2CH_2SMe)_2Li(HOCH_2CH_2SMe)$ (4.10b)
empir. formula	$C_{38}H_{66}AlLiN_2O_4$	$C_{39}H_{68}AlLiO_5S_3$
cryst system	orthorhombic	triclinic
space group	Pbcn	$\bar{P}\bar{1}$
<i>a</i> , Å	18.039(4)	15.451(3)
<i>b</i> , Å	20.915(4)	13.711(3)
<i>c</i> , Å	21.918(4)	11.409(2)
α , deg		96.03(3)
β , deg		106.10(3)
γ , deg		101.32(3)
<i>V</i> , Å ³	8269(3)	2244.1(8)
<i>Z</i>	8	2
D(calcd), g/cm ³	1.042	1.106
μ , cm ⁻¹	0.085	0.22
temp, K	223	223
2θ range, deg	4 - 55	4 - 45
no. collected	5915	5713
no. ind	5915	5451
no. obsd	$668(F_o > 5.0\sigma F_o)$	$1738 (F_o > 6.0\sigma F_o)$
weighting scheme	$w^{-1} = 0.04(F_o)^2 + \sigma(F_o)^2$	$w^{-1} = 0.04(F_o)^2 + \sigma(F_o)^2$
R	0.082	0.054
R _w	0.181	0.0.147
largest diff peak, eÅ ⁻³	0.26 / -0.34	0.47 / -0.32

References

- 1 J. A. Francis, C. N. McMahon, S. G . Bott, and A. R. Barron, submitted for publication.
- 2 For further discussion, see Chapter 1.
- 3 A. R. Barron, unpublished results.
- 4 M. D. Healy, M. B. Power, and A. R. Barron, *Coordination Chemistry Reviews*, 1994, **130**, 63.
- 5 M. B. Power, S. G. Bott, J. L. Atwood and A. R. Barron, *J. Am. Chem. Soc.*, 1990, **112**, 3446.
- 6 M. D. Healy, M. R. Mason, P. W. Gravelle, S. G. Bott, and A. R. Barron, *J. Chem. Soc. Dalton Trans.*, 1193, 441, and references therein.
- 7 C. L. Aitken and A. R. Barron, *J. Chem. Cryst.*, 1996, **26**, 297.
- 8 M. D. Healy, J. W. Ziller, and A. R. Barron, *Organometallics*, 1991, **10**, 597.
- 9 A. G. Avent, W. Y. Chen, C. Eaborn, I. B. Gorrell, P. B. Hitchcock, and J. D. Smith, *Organometallics*, 1996, **15**, 4343.
- 10 D. A. Atwood and D. Rutherford, *Inorg. Chem.*, 1995, **34**, 4008.
- 11 T. Barbarich, S. T. Handy, S. M. Miller, O. P. Anderson, P. A. Grieco, and S. H. Strauss, *Organometallics*, 1996, **15**, 3776.
- 12 T. Barbarich, *Fluoroalkoxide Aluminates as Weakly Coordinating Anions. Significant O-H...F-C Hydrogen Bonding*, Ph.D thesis, Colorado State University, 1998.
- 13 M. O'Keefe, A. Navrotsky, *Structure and Bonding in Crystals Vol II*, Academic Press, 1981, Chapter 1.
- 14 See for example, A. Haaland in *Coordination Chemistry of Aluminum*, Ed., G. H. Robinson, VCH, New York, 1993, Ch.1.

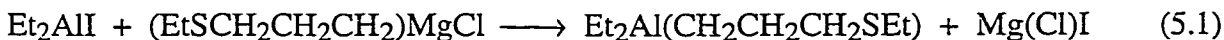
Chapter 5

Hydroalumination of H₂C=CHCH₂SMe: Synthesis and Molecular Structure of (tBu)₂Al(CH₂CH₂CH₂SMe)

Introduction

Intramolecular coordination in organometallic compounds of Group 2, 12, and 13 metals has been studied in some detail. Of particular interest is the enhanced stability and increased volatility of intramolecularly coordinated compounds as compared to their more usual organometallic analogs for applications in metal organic chemical vapor deposition (MOCVD).¹ Compounds of the Group 13 metals are known with nitrogen,² phosphorus,³ oxygen,⁴ sulfur,⁵ and halogen⁶ donor ligands. An excellent and comprehensive review has been recently published.⁷

The most general synthesis for intramolecularly coordinated compounds involves the reaction of a substituted Grignard or lithium reagent with a metal halide.⁷ For example, the aluminum alkyl, Et₂Al(CH₂CH₂CH₂SEt) has been prepared via the Grignard either preformed (Eq. 5.1) or *in-situ* (Eq. 5.2).⁵



As an alternative approach we have investigated employing the reaction of aluminum hydrides with substituted olefins, e.g., allyl-alkyl thioethers. A similar method has already been demonstrated for the synthesis of magnesium-ether⁸ and gallium-amine^{1a} compounds.

Hydroalumination of olefins has been well studied⁹ with respect to the synthesis of AlEt₃, and long chain alcohols.¹⁰ However, besides the early work by Natta and co-workers,¹¹ relatively few reports have studied hydroalumination of substituted olefins.¹²

Results and Discussion

Hydroalumination of H₂C=CHCH₂SMe with [(tBu)₂Al(μ-H)]₃ (prepared by a modification of a literature method, see Experimental) yields (tBu)₂Al(CH₂CH₂CH₂SMe) (5.1). Although analogous intramolecular coordination has been shown to allow the preparation of air stable organo-aluminum compounds, compound (tBu)₂Al(CH₂CH₂CH₂SMe) decomposes (albeit slowly) in the presence of oxygen. Although crystalline, (tBu)₂Al(CH₂CH₂CH₂SMe) is a low melting solid (37 - 39 °C).

The ²⁷Al NMR spectrum of (tBu)₂Al(CH₂CH₂CH₂SMe) (5.1) is consistent with a four coordinate aluminum ($\delta = 156$ ppm).¹³ Unfortunately, the mass spectrum of (tBu)₂Al(CH₂CH₂CH₂SMe) (5.1) does not allow for definitive assignment of a monomeric (chelate) or oligomeric structure. However, the monomeric nature of (tBu)₂Al(CH₂CH₂CH₂SMe) (5.1) has been confirmed by X-ray crystallography.

The molecular structure of (tBu)₂Al(CH₂CH₂CH₂SMe) is shown in Figure 5.1; selected bond lengths and angles are given in Table 5.1. The structure consists of discreet monomers in which the thioether-alkyl ligand acts as a chelate ligand. The Al-S interaction [2.511(2) Å] is towards the short end of the range observed for simple Lewis acid-base complexes (2.515 - 2.718 Å).¹⁴ Furthermore, it is significantly shorter than observed for other intra-molecular coordination compounds, 2.78 - 2.95 Å.¹⁵ The coordination about aluminum is highly distorted from tetrahedral. In fact, the sum of the C-Al-C angles (351 °) is closer to that expected for a trigonal planar environment (i.e., 360 °) rather than the base of a tetrahedral environment (328.5 °).

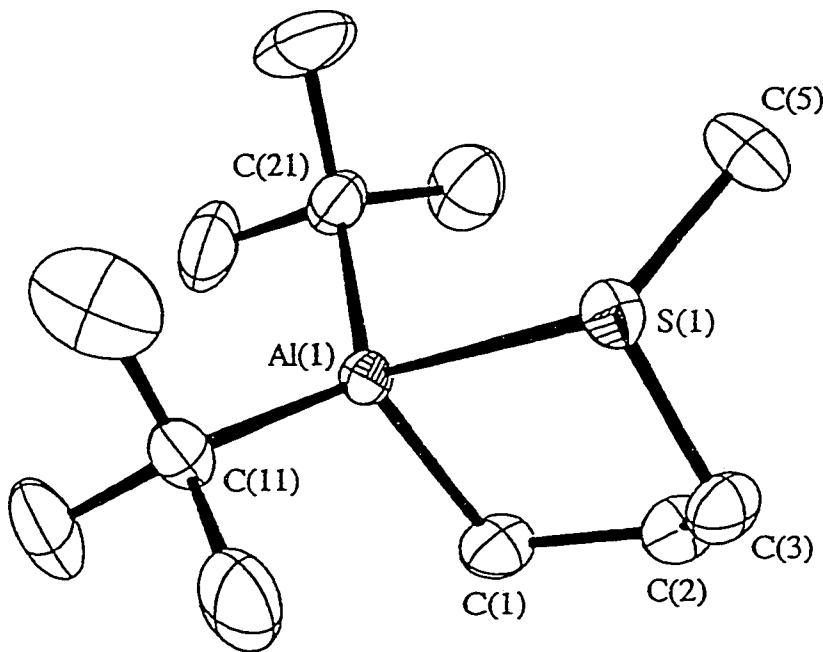
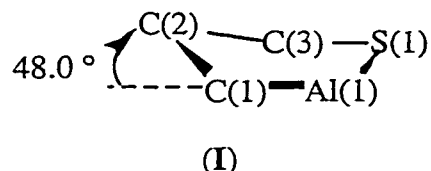


Figure 5.1. Molecular structure of $(^t\text{Bu})_2\text{Al}(\text{CH}_2\text{CH}_2\text{CH}_2\text{SMe})$ (5.1). Thermal ellipsoids shown at the 30% level, and hydrogen atoms are omitted for clarity.

Table 5.1. Selected Bond Lengths (\AA) and Angles ($^\circ$) in $(^t\text{Bu})_2\text{Al}(\text{CH}_2\text{CH}_2\text{CH}_2\text{SMe})$.

Al(1)-S(1)	2.511(2)	Al(1)-C(1)	1.991(5)
Al(1)-C(11)	1.989(5)	Al(1)-C(21)	1.996(5)
S(1)-C(3)	1.828(5)	S(1)-C(5)	1.807(5)
S(1)-Al(1)-C(1)	88.1(1)	S(1)-Al(1)-C(11)	100.2(1)
S(1)-Al(1)-C(21)	110.8(2)	C(1)-Al(1)-C(11)	115.4(2)
C(1)-Al(1)-C(21)	114.8(2)	C(11)-Al(1)-C(21)	120.8(2)
Al(1)-S(1)-C(3)	91.5(2)	Al(1)-S(1)-C(5)	111.2(2)
C(3)-S(1)-C(5)	101.3(2)	Al(1)-C(1)-C(2)	111.9(3)
C(1)-C(2)-C(3)	111.1(4)	C(2)-C(3)-S(1)	111.8(3)

The coordination of the aluminum is therefore best described as capped trigonal planar or trigonal bipyramidal with a vacant coordination site. A similar coordination geometry was observed for the dialkyl indium chloride polymer, $[(^t\text{Bu})_2\text{In}(\mu\text{-Cl})]_\infty$.¹⁶ As was previously observed for $(^t\text{Bu})_2\text{Al}(\text{SCH}_2\text{CH}_2\text{NR}_2)$ ($\text{R} = \text{Me}$ and Et),¹⁷ the five membered cycle in $(^t\text{Bu})_2\text{Al}(\text{CH}_2\text{CH}_2\text{CH}_2\text{SMe})$ is puckered, with C(3) twisted out of the plane (I), presumably in order to minimize the ring strain.



The synthesis of $(^t\text{Bu})_2\text{Al}(\text{CH}_2\text{CH}_2\text{CH}_2\text{SMe})$ via a hydroalumination reaction suggests that this method may provide a general approach to intramolecular coordinated compounds of aluminum.

In order to test the latent Lewis acidity of $(^t\text{Bu})_2\text{Al}(\text{CH}_2\text{CH}_2\text{CH}_2\text{SMe})$, it was reacted with Cp_2ZrMe_2 on a small scale in an NMR tube with C_6D_6 as the solvent. Upon mixing, the solution turned a dark green color and the ^1H NMR indicated the formation of $[\text{Cp}_2\text{Zr}(\mu\text{-S})]_2$ whose Cp resonance is known ($\delta = 6.23$ ppm).¹⁸ This compound is also formed from the reaction of $(^t\text{Bu})_2\text{Al}(\text{SCH}_2\text{CH}_2\text{NR}_2)$ ¹⁹ with Cp_2ZrMe_2 .

Conclusion

As an alternative synthetic approach, we have investigated employing the reaction of aluminum hydrides with substituted olefins, e.g., allyl-alkyl thioethers. The hydroalumination of substituted olefins proved successful and this method may be used as a general method to synthesize intramolecular coordinated complexes of aluminum.²⁰

Experimental Section

General experimental procedures were carried out as described in Chapter 1. The synthesis of $\text{Al}(\text{tBu})_3$ and $\text{AlH}_3\cdot\text{NMe}_3$ were performed according to previously described methods.^{21,22} $\text{H}_2\text{C}=\text{CHCH}_2\text{SMe}$ was obtained from Aldrich and were used without further purification.

$[(\text{tBu})_2\text{Al}(\mu-\text{H})]_3$. To a solution of $\text{AlH}_3\cdot\text{NMe}_3$ (1.0 g, 11.2 mmol), in toluene (50 mL) was added a solution of $\text{Al}(\text{tBu})_3$ (5.63 mL, 22.4 mmol) in toluene (50 mL). The mixture was then refluxed for one hour and taken to dryness *in vacuo*. The white product was then recrystallized in toluene to give a white crystalline solid. Yield: *ca.* 75%. The product was spectroscopically identical to that reported previously.²³

$(\text{tBu})_2\text{Al}(\text{CH}_2\text{CH}_2\text{CH}_2\text{SMe})$ (5.1). To a solution of $\text{H}_2\text{C}=\text{CHCH}_2\text{SMe}$ (0.81 g, 9.2 mmol) in toluene (50 mL) was added a solution of $[(\text{tBu})_2\text{Al}(\mu-\text{H})]_3$ (1.30 g, 9.2 mmol) in toluene. The mixture was then left to stir overnight and was then taken to dryness *in vacuo*. The resultant oil was then crystallized at -22 °C from toluene. Yield: *ca* 74%. Mp: 37 - 39 °C. MS (EI, %): *m/z*: 89 (MeSC_3H_6 , 60), 84 [$\text{Al}(\text{tBu})_3$, 18], 57 (tBu , 18). IR (cm^{-1}): 2934 (s, br), 2827 (s, br), 1465 (s), 1424 (m), 1188 (s), 999 (m), 886 (s), 661 (m), 456 (s). ^1H NMR (C_6D_6): δ 2.06 [2H, t, $J(\text{H}-\text{H})$ = 6.0 Hz, MeSCH_2], 1.66 [2H, m, $J(\text{H}-\text{H})$ = 7.0 Hz, $J(\text{H}-\text{H})$ = 6.0 Hz, $\text{MeSCH}_2\text{CH}_2$], 1.43 (3H, s, SCH_3), 1.18 [18H, s, $\text{C}(\text{CH}_3)_3$], 0.16 [2H, t, $J(\text{H}-\text{H})$ = 7.0 Hz, $\text{Al}-\text{CH}_2$]. ^{13}C NMR (C_6D_6): δ 42.7 (SCH_3), 31.6 [$\text{C}(\text{CH}_3)_3$], 25.7 (MeSCH_2), 15.3 ($\text{MeSCH}_2\text{CH}_2$), 1.8 ($\text{Al}-\text{CH}_2$). ^{27}Al NMR (CDCl_3): δ 156 ($W_{1/2}$ = 3570 Hz).

Crystallographic Studies. A crystal of $(\text{tBu})_2\text{Al}(\text{CH}_2\text{CH}_2\text{CH}_2\text{SMe})$ (5.1) was sealed in a glass capillary under argon. Crystal and data collection and solution details are given in Table 5.2. Standard procedures in our laboratory have been described

previously.²⁴ Data were collected on an Enraf-Nonius CAD-4 diffractometer equipped with graphite monochromated Mo-K α radiation ($\lambda = 0.71073 \text{ \AA}$) and corrected for Lorentz and polarization effects, but not for adsorption. The structure was solved by using direct methods (SHELXS-86²⁵), and difference Fourier synthesis and refined using full-matrix least squares.²⁶ Hydrogen atoms were placed in calculated positions based, where appropriate on observed methyl H positions [$U_{\text{iso}} = 1.3U_{(\text{C})}$]. Neutral-atom scattering factors were taken from the usual source.²⁷ Refinement of positional and anisotropic thermal parameters led to convergence, see Table 5.2. Final atomic positional parameters and isotropic thermal coefficients are given in Table 5.3.

Table 5.2. Summary of X-ray Diffraction Data.

Compound	(<i>t</i> Bu) ₂ Al(CH ₂ CH ₂ CH ₂ SMe)
empir. formula	C ₁₂ H ₂₇ AlS
cryst size, mm	0.09 x 0.10 x 0.11
cryst system	monoclinic
space group	P2 ₁ /n
<i>a</i> , Å	6.6357(5)
<i>b</i> , Å	13.630(1)
<i>c</i> , Å	16.959(1)
β, deg	95.416(6)
V, Å ³	1527.0(2)
Z	4
D(calcd), g/cm ³	1.002
μ, cm ⁻¹	2.31
temp, K	298
2θ range, °	3.0 - 45.0
no. collected	2286
no. ind	2093
no. obsd	1350 ($ F_o > 6.0\sigma F_o $)
weighting scheme	$w^{-1} = 0.04(F_o)^2 + \sigma(F_o)^2$
R	0.0412
R _w	0.0503
largest diff peak, eÅ ⁻³	0.21

References

- 1 See for example, (a) H. Schumann, U. W. Hartmann, and W. Wassermann, *Polyhedron*, 1990, **9**, 353.
 (b) W. S. Rees, Jr., C. R. Caballero, and W. Hesse, *Angew. Chem.*, 1992, **104**, 786.
 (c) W. S. Rees, Jr., D. and A. Moreno, *J. Chem. Soc., Chem. Commun.*, 1991, 1759.
- 2 (a) G. Bähr and G. E. Müller, *Chem. Ber.*, 1955, **88**, 251.
 (b) L. Pohl, M. Hostalek, H. Schumann, U. Hartmann, W. Wassermann, A. Brugers, G. K. Hövel, and P. Balk, *J. Cryst. Growth*, 1991, **107**, 309.
 (c) H. Schumann, T. D. Seuss, O. Just, R. Weinmann, H. Hemling, and F. H. Görlitz, *J. Organomet. Chem.*, 1994, **479**, 171.
 (d) S. J. Rettig, A. Storr, and J. Trotter, *Can. J. Chem.*, 1975, **53**, 58.
 (e) M. J. Henderson, C. H. L. Kennard, C. L. Raston, and G. Smith, *J. Chem. Soc., Chem. Commun.*, 1990, 1203.
 (f) R. A. Fischer, J. Behm, and T. Priermeier, *J. Organomet. Chem.*, 1992, **429**, 65.
 (g) P. Jutzi and M. Bangel, *J. Organomet. Chem.*, 1994, **480**, C18.
- 3 (a) G. Müller, J. Lachmann, and A. Rufinska, *Organometallics*, 1992, **11**, 2970.
 (b) G. Müller and J. Lachmann, *Z. Naturforsch.*, 1993, **48B**, 1544.
- 4 G. B. Deacon, R. N. M. Smith, and D. Tunaley, *J. Organomet. Chem.*, 1976, **114**, C1.
- 5 G. Bäher, and G. E. Müller, *Chem. Ber.*, 1955, **88**, 1765.
- 6 (a) O. T. Beachley, Jr., M. R. Churchill, J. C. Pazik, and J. W. Ziller, *Organometallics*, 1986, **5**, 1814.
 (b) M. A. Petrie, P. P. Power, H. V. Rasika Dias, K. Ruhlandt-Senge, K. M. Waggoner, and R. J. Wehmschulte, *Organometallics*, 1993, **12**, 1086.
- 7 G.-J. M. Gruter, G. P. M. van Klink, O. S. Akkerman, and F. Bickelhaupt, *Chem. Rev.*, 1995, **95**, 2405.

- 8 J. Angermund, B. Bogdanovic, G. Koppetsch, C. Krüger, R. Mynott, M. Schwickardi, and Y.-H. Tsay, *Z. Naturforsch.*, 1986, **41B**, 455.
- 9 See for example, (a) J. J. Eisch, and M. W. Foxton, *J. Org. Chem.*, 1971, **36**, 3520.
(b) K. W. Egger, *Helvetica Chim. Acta*, 1972, **55**, 1502.
(c) J. J. Eisch, and R. Husk, *J. Organomet. Chem.*, 1974, **64**, 41.
(c) M. Montury, and J. Goré, *Tetrahedron Lett.*, 1980, **21**, 51.
- 10 See for example, (a) K. Ziegler, H.-G. Gellert, H. Lehmkuhl, W. Pfohl, and K. Zosel, *Justus Liebigs Ann. Chem.*, 1960, **629**, 1.
(b) A. F. Zhigach, A. F. Popov, L. D. Vishnevskii, and N. N. Korneev, *Khim. Prom.*, 1961, 249.
- 11 G. Natta, P. Pino, G. Mazzanti, P. Longi, and F. Bernardini, *J. Am. Chem. Soc.*, 1959, **81**, 2561.
- 12 G. Sonnek, H. Reinheckel and K.-G. Baumgarten, *J. Prakt. Chem.*, 1976, **318**, 756.
- 13 See for example, A. R. Barron, *Polyhedron*, 1995, **14**, 3197.
- 14 See for example, (a) A. Weiss, R. Plass, and A. Weiss, *Z. Anorg. Allg. Chem.*, 1956, **283**, 390.
(b) G. H. Robinson, H. Zhang, and J. L. Atwood, *Organometallics*, 1987, **30**, 2633.
(c) N. Burford, B. W. Royan, R. E. v. H. Spence, and R. D. Rogers, *J. Chem. Soc., Dalton Trans.*, 1990, 2111.
- 15 D. G. Hendershot, M. Barber, R. Kumar, and J. P. Oliver, *Organometallics*, 1991, **10**, 3302.
- 16 S. L. Stoll, S. G. Bott, and A. R. Barron, *Polyhedron*, 1997, **16**, 1763.
- 17 C. N. McMahon, J. A. Francis, S. G. Bott, and A. R. Barron, submitted for publication.
- 18 W. E. Piers, L. Koch, D. S. Ridge, L. R. Macgillivray, and M. Zaworotko, *Organometallics*, 1992, **11**, 3148.

- 19 C. N. McMahon, J. A. Francis, S. G. Bott, and A.R. Barron, *J. Chem. Soc., Dalton Trans.*, 1999, **1**, 67.
- 20 G. Sonnek, H. Reinheckel, and K.-G. Baumgarten, *J. Prakt. Chem.*, 1976, **318**, 756.
- 21 (a) W. Uhl, *Z. Anorg. Allg. Chem.*, 1989, **570**, 37.
(b) H. Lehmkuhl, O. Olbrysch, and H. Nehl, *Liebigs Ann. Chem.*, 1973, 708.
(c) H. Lehmkuhl and O. Olbrysch, *Liebigs Ann. Chem.*, 1973, 715.
- 22 J. K. Ruff and M. F. Hawthorne, *J. Am. Chem. Soc.*, 1960, **82**, 2141.
- 23 W. Uhl, *Z. anorg. Allg. Chem.*, 1989, **570**, 37.
- 24 M. R. Mason, J. M. Smith, S. G. Bott, and A. R. Barron, *J. Am. Chem. Soc.*, 1993, **115**, 4971.
- 25 G. M. Sheldrick, *Acta Crystallogr.*, 1990, **A46**, 467.
- 26 MolEN - Enraf-Nonius. MolEN, An interactive Structure Solution Procedure; Enraf-Nonius, Delft, Netherlands, 1990.
- 27 *International Tables for X-Ray Crystallography*, Kynoch Press, Birmingham, **1974**, vol. 4.

Chapter 6

Molecular Structure of $[({}^t\text{Bu})_2\text{Al}(\mu\text{-Cl})]_2$

Introduction

During the last decade the Barron Group has been interested in the steric and electronic effects controlling the structures of Group 13 compounds.¹ Recent investigations have centered on determining the consequences imposed on the geometry in dimeric dialkylaluminum and dialkylgallium compounds, $[(\text{R})_2\text{M}(\mu\text{-X})]_2$ ($\text{M} = \text{Al}, \text{Ga}$) by the steric bulk of the substituents at either the Group 13 metal or bridging hetero-atom.^{2,3} Although these studies have revealed a number of trends, the steric interactions between the alkyl substituent on the Group 13 metal and on the hetero-atom bridge have been found to obviate clear relationships. In order to overcome these difficulties compounds without alkyl substituents at the bridge atom have been investigated. The most suitable class for study are the dimeric chloride compounds.

While several examples of alkylaluminum dichlorides, $[(\text{R})(\text{Cl})\text{Al}(\mu\text{-Cl})]_2$, have been structurally characterized,⁴ and a few dialkylaluminum chlorides of the type, $[(\text{R})(\text{R}')\text{Al}(\mu\text{-Cl})]_2$,⁵ only three previous examples of $[(\text{R})_2\text{Al}(\mu\text{-Cl})]_2$ have had their molecular structures reported.^{6,7,8} Fortunately two of these cover the extremes of steric bulk as measured by the Tolman cone angle:⁹ methyl ($\text{CH}_3, \theta = 90^\circ$) versus mesityl ($\text{Mes}, 2,4,6\text{-Me}_3\text{C}_6\text{H}_2, \theta \approx 150^\circ$). However, in order to determine if structural trends are real it is desirable to have for comparison the structure of a compound with intermediate steric bulk, i.e., $115^\circ < \theta < 130^\circ$. The steric bulk of the *tert*-butyl group ($\theta = 127^\circ$) make it eminently suitable for such a study.

Results and Discussion

The molecular structure of $[({}^t\text{Bu})_2\text{Al}(\mu\text{-Cl})]_2$ (**6.1**) is shown in Figure 6.1; selected bond length angles are given in Table 6.1. The structure consists of a discrete dimeric

$[({}^t\text{Bu})_2\text{Al}(\mu\text{-Cl})]_2$ unit, with the molecule lying on a center of inversion. As is commonly observed with dimeric aluminum compounds the geometry around each aluminum is distorted from tetrahedral, with the angles associated with the Al_2Cl_2 cycle being the most acute.

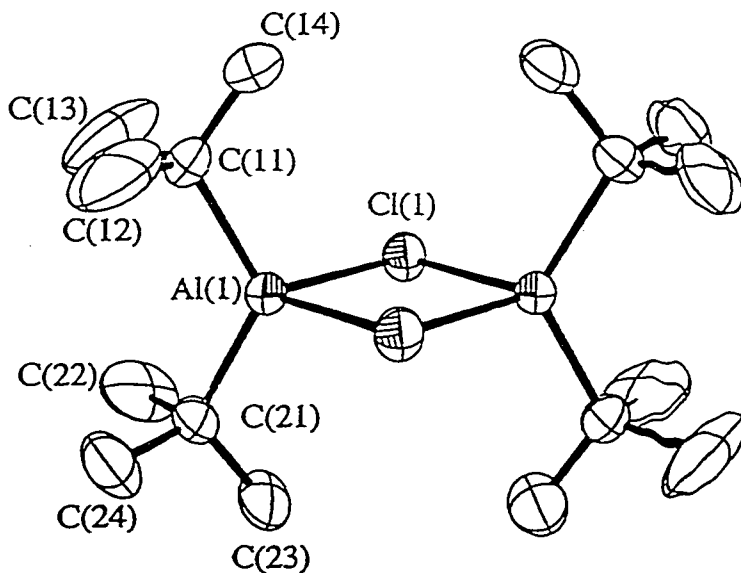


Figure 6.1. Molecular structure of $[({}^t\text{Bu})_2\text{Al}(\mu\text{-Cl})]_2$ (6.1). Thermal ellipsoids are shown at the 30 % level, and all hydrogens are omitted for clarity.

Table 6.1. Selected bond lengths (\AA) and angles ($^\circ$) in $[({}^t\text{Bu})_2\text{Al}(\mu\text{-Cl})]_2$ (6.1).

Al(1)-Cl(1)	2.316(3)	Al(1)-Cl(1a)	2.324(3)
Al(1)-C(11)	1.966(6)	Al(1)-C(21)	1.982(9)
Cl(1)-Al(1)-C(11)	110.9(3)	Cl(1)-Al(1)-C(21)	110.2(3)
Cl(1)-Al(1)-Cl(1a)	87.2(1)	C(11)-Al(1)-C(21)	123.6(3)
C(11)-Al(1)-Cl(1a)	108.6(3)	C(21)-Al(1)-Cl(1a)	110.4(3)
Al(1)-Cl(1)-Al(1a)	92.8(1)		

The Al(1)-Cl(1) bond distances [2.316(3) and 2.324(3) Å] are within the range observed for other di-alkylaluminum chloride compounds [2.303(3) - 2.451(4) Å].¹⁰

One of the *tert*-butyl groups in $[({}^t\text{Bu})_2\text{Al}(\mu\text{-Cl})_2]$ (**6.1**) exhibits rotational disorder about the Al(1)-C(21) bond, see Figure 6.2, resulting in a reversal of the conformation of the *tert*-butyl group with respect to the Al(1)-Cl(1), Al(1)-Cl(1a) and Al(1)-C(11) bonds. In the position with greater site occupancy (57 %) the *tert*-butyl C-C bonds are staggered with respect to the bonds to Al(1), see Figure 6.2a, while in the minor position a near eclipsed conformation is observed (Figure 6.2b).

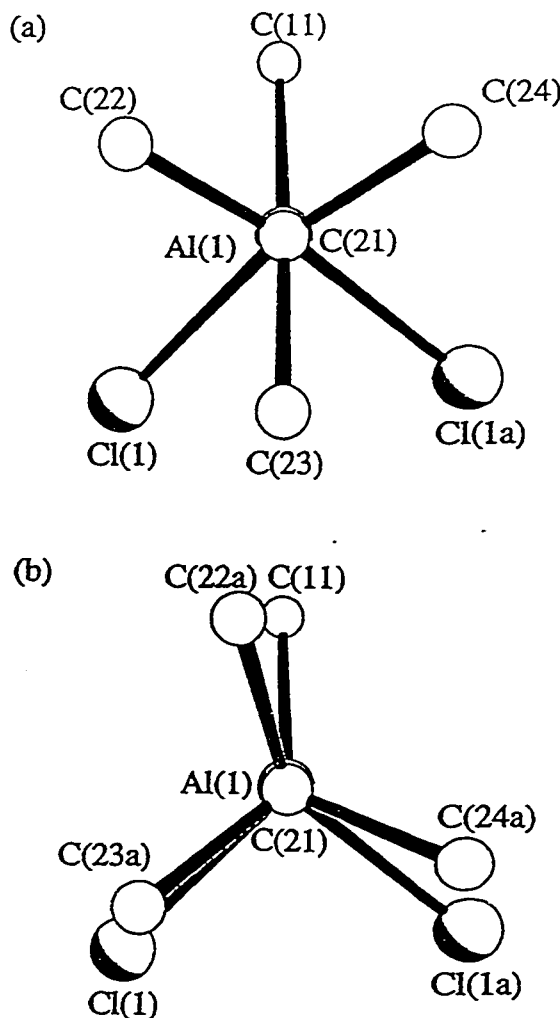


Figure 6.2 Partial coordination sphere of Al(1) in $[({}^t\text{Bu})_2\text{Al}(\mu\text{-Cl})_2]$ (**6.1**) showing the major (a) and minor (b) isomers.

The structure of $[({}^t\text{Bu})_2\text{Al}(\mu\text{-Cl})]_2$ (6.1) can be compared to other aluminum-chloride dimers previously reported.^{6,7,8} As have been shown for other dimeric group 13 compounds^{2,3} the Al-Cl-Al angle is correlated with the Cl-Al-Cl angle, Figure 6.3, consistent with a flat Al_2Cl_2 cycle. It has been shown that for aluminum amido compounds that there exists no apparent correlation between C-Al-C angle and the steric bulk (and hence steric repulsion) of the aluminum alkyl ligands.³ In contrast to these results, comparison of the structural parameters in $[\text{Me}_2\text{Al}(\mu\text{-Cl})]_2$,⁶ $[({}^t\text{Bu})_2\text{Al}(\mu\text{-Cl})]_2$, and $[(\text{Mes})_2\text{Al}(\mu\text{-Cl})]_2$ ($\text{Mes} = 2,4,6\text{-Me}_3\text{C}_6\text{H}_2$),⁷ shows that there exists a definite correlation between the steric bulk of the alkyl ligand, as measured by the Tolman cone angle (θ), and the bond angles defining the molecular core, see Figure 6.4.

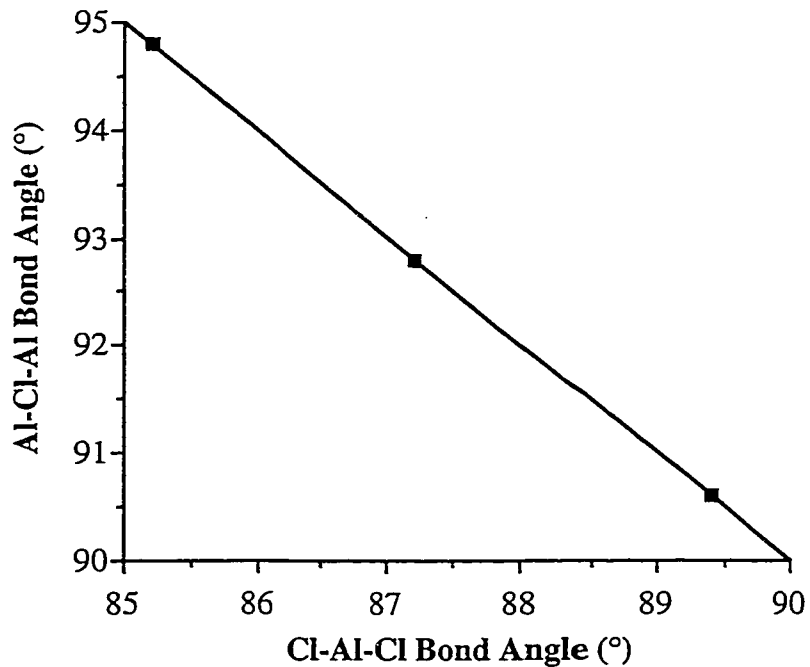


Figure 6.3. Plot of Al-Cl-Al bond angle (°) as a function of Cl-Al-Cl bond angle (°) for dialkylaluminum chloride compounds, $[\text{R}_2\text{Al}(\mu\text{-Cl})]_2$

trend observed for the C-Al-C angle is opposite to that expected based upon steric congestion between ligands on individual aluminum centers (c.f., **Ia**). However, these trends would be expected if the C-Al-C angle was controlled by the steric repulsion between the alkyl groups on adjacent aluminum centers, i.e., **Ib**.

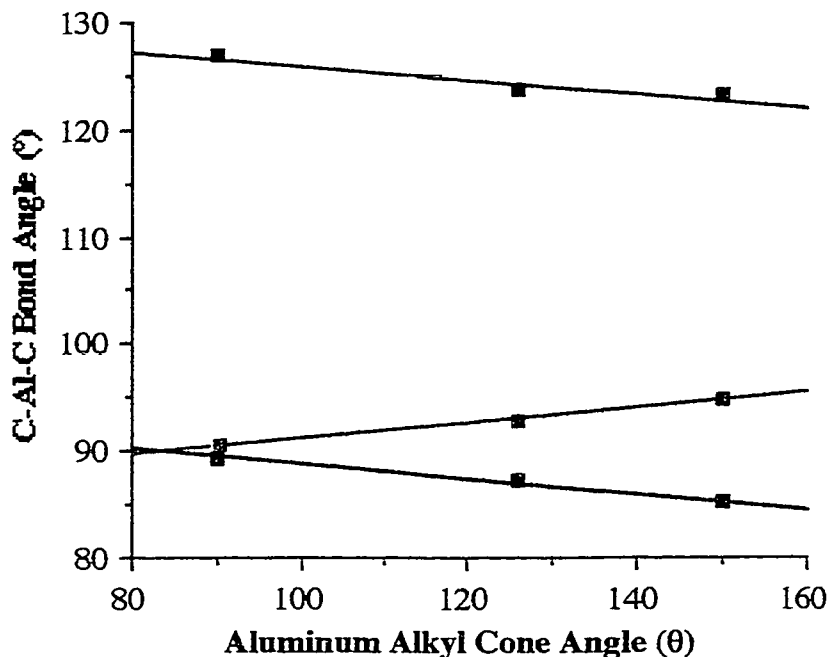
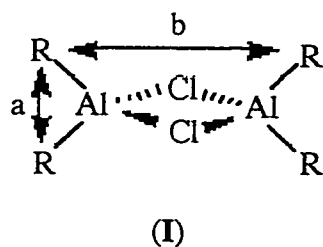


Figure 6.4. Plot of C-Al-C (■), Al-Cl-Al (■), and Cl-Al-Cl (■) bond angles (°) as a function of the Tolman cone angle (θ , °) for the aluminum substituent (R) in $[(R)_2Al(\mu\text{-Cl})]_2$



This effect is also apparent from the increase in both the Al-Cl and Al···Al distances with increased steric bulk of the alkyl groups, Figure 6.5. It should be noted that since the

structure of $[\text{Me}_2\text{Al}(\mu\text{-Cl})]_2$ was determined by gas phase electron diffraction,⁶ packing forces may be discounted as affecting the core structure.

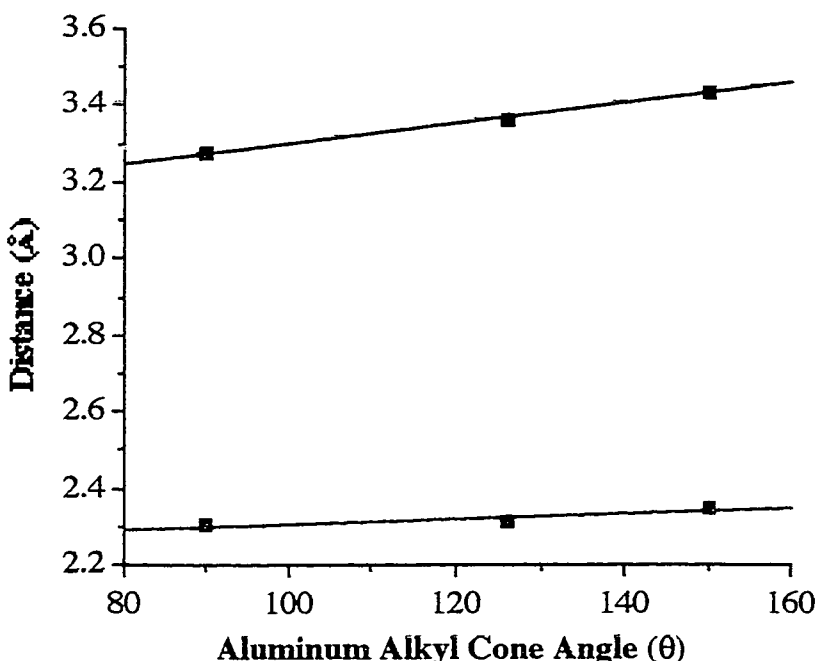


Figure 6.5. Plot of Al-Cl (■) and Al...Al (■) distances (Å) as a function of the Tolman cone angle (θ , °) for the aluminum substituent (R) in $[(\text{R})_2\text{Al}(\mu\text{-Cl})]_2$.

Conclusion

The steric bulk of the substituents at either the Group 13 metal influence the geometry in four-coordinate dimeric dialkylaluminum compounds, $[(\text{R})_2\text{Al}(\mu\text{-X})]_2$. Because the C-Al-C and Cl-Al-Cl angles decrease and the Al-Cl-Al angle increases with increasing steric bulk of the alkyl ligand, we propose that the C-M-C angle of four-coordinate dimeric Group 13 compounds is controlled by the steric repulsion between the alkyl groups on adjacent metal centers, instead of steric congestion between ligands on individual metal centers.

Experimental

$[({}^t\text{Bu})_2\text{Al}(\mu\text{-Cl})]_2$ (**6.1**) was prepared according to the literature¹¹ and recrystallized from hexane. A crystal was sealed in a glass capillary under argon and mounted on the goniometer head of a Rigaku four-circle diffractometer. Data collection unit cell and space group determination were all carried out in a manner previously described in detail.¹² The structures were solved using the direct methods program XS¹³ which readily revealed the positions of the Al, Cl, and most of the C atoms. Subsequent difference Fourier maps revealed the position of all of the non-hydrogen atoms, including two positions for the β -carbon atoms of one of the *tert*-butyl groups. These were initially included in the refinement such that equivalent atoms were treated with linked thermal parameters and the group occupancy was constrained to a total of 1.

The latter values converged at values of 0.574(3) and 0.426(3) and so were fixed at 0.57 [C(22), C(23), and C(24)] and 0.43 [C(22a), C(23a), and C(24a)] for the final refinement, in which all the non-hydrogen atoms were refined anisotropically. All the hydrogen atoms were placed in calculated positions [$U_{\text{iso}} = 0.08$; $d(\text{C-H}) = 0.96 \text{ \AA}$] for refinement. Neutral-atom scattering factors were taken from the usual source.¹⁴ Refinement of positional and anisotropic thermal parameters led to convergence (see Table 6.2).

Table 6.2. Crystal Data and summary of X-ray diffraction data for
[(^tBu)₂Al(μ-Cl)]₂.**(6.1)**

Emp form	C ₁₆ H ₃₆ Al ₂ Cl ₂
Cryst size, mm	0.20 x 0.25 x 0.36
Cryst syst	triclinic
Space group	P-1
<i>a</i> , Å	6.514(1)
<i>b</i> , Å	8.628(2)
<i>c</i> , Å	11.236(2)
α, °	102.05(3)
β, °	105.32(3)
γ, °	103.47(3)
V, Å ³	567.2(3)
Z	1
D _{calc} , g.cm ⁻³	1.034
μ _{calc} , mm ⁻¹	0.356
Temp, K	298
2θ range, °	7.0 - 45.0
no. collected	1593
no. ind	1477
no. obsd	1054 ($ F_0 > 4\sigma F_0 $)
weighting scheme	$w^{-1} = \sigma^2 F_0 $
R	0.0637
R _w	0.0679
largest diff peak, eÅ ⁻³	0.031

References

- 1 See for example, (a) A. R. Barron, *J. Chem. Soc., Dalton Trans.*, 1988, 3047.
(b) J. T. Leman and A. R. Barron, *Organometallics*, 1989, **8**, 1828.
(c) M. D. Healy, J. W. Ziller, and A. R. Barron, *Organometallics*, 1991, **10**, 597.
(d) J. Braddock-Wilking, J. T. Leman, C. T. Farrar; S. C. Larsen, D. J. Singel, and A. R. Barron, *J. Am. Chem. Soc.*, 1995, **117**, 1736.
- 2 W. M. Cleaver, A. R. Barron, A. R. McGuffey, and S. G. Bott, *Polyhedron*, 1994, **13**, 2831.
- 3 S. G. Bott, Y. Koide, and A. R. Barron, *J. Chem. Cryst.*, 1996, in press.
- 4 See for example, (a) W. Uhl, A. Vester, and W. Hiller, *Z. Anorg. Allg. Chem.*, 1990, **589**, 175.
(b) M. D. Healy, J. W. Ziller, and A. R. Barron, *Organometallics*, 1992, **11**, 3042.
(c) G. Allegra, G. Perego, and A. Immirzi, *Makromol. Chem.*, 1963, **61**, 69.
(d) H. -J. Koch, S. Schulz, H. W. Roesky, M. Noltemeyer, H. -G. Schmidt, A. Heine, R. Herbst-Irmer, D. Stalke, and G. M. Sheldrick, *Chem. Ber.*, 1992, **125**, 1107.
- 5 P. R. Schonberg, R. T. Paine, C. F. Campana, and E. N. Duesler, *Organometallics*, 1982, **1**, 799.
- 6 K. Brendhaugen, A. Haaland, and D. P. Novak, *Acta Chem. Scand. A*, 1974, **28**, 45.
- 7 M. S. Lalama, J. Kampf, D. G. Dick, and J. P. Oliver, *Organometallics*, 1995, **14**, 495.
- 8 P. R. Schonberg, R. T. Paine, C. F. Campana, and E. N. Duesler, *Organometallics*, 1982, **1**, 799.
- 9 C. A. Tolman, *Chem. Rev.*, 1977, **77**, 313.
- 10 A. Haaland, in *Coordination Chemistry of Aluminum*, Ed. G. H. Robinson, VCH, New York, 1993, Chapter 1.

- 11 W. Uhl, *Z. Anorg. Allg. Chem.*, 1989, **570**, 37.
- 12 M. D. Healy, D. A. Wierda, and A. R. Barron, *Organometallics*, 1988, **7**, 2543.
- 13 Nicolet Instruments Corporation, Madison, WI, USA, 1988.
- 14 *International Tables for X-Ray Crystallography*, Kynoch Press, Birmingham, 1974, vol. 4.

Conclusions

In order to prepare a model system exhibiting latent Lewis acidity, which is thought responsible for the co-catalytic activity of alumoxanes, a series of dialkylaluminum compounds have been prepared with bi-functional ligands of the general formula $[R_2Al\{\mu-O(CH_2)_nER'_x\}]_2$, where n is 2 or 3, ER'_x is OR' or SR' , and R is tBu , iBu , Et or Me. All these compounds are dimeric species where the interaction of the non-bridged heteroatoms (E) forming a five-coordinate aluminum center is in equilibrium with the four-coordinate species in solution. Equilibrium constants (where $K_{eq} = [4\text{-coord.}]/[5\text{-coord.}]$) have been determined from ^{13}C NMR measurements and are found to be controlled by the various factors. Increasing the ligand back-bone (n), the steric bulk of the alkyl substituents on aluminum (R) and/or on the heteroatom donor (R'), all result in greater dissociation of the neutral Lewis base donor. The extent of coordination of the fifth ligand is also dependent on the identity of the heteroatom donor (E). *Ab initio* calculations on the model system, $[H_2Al(\mu-OCH_2CH_2OH)]_2$, indicates that, in the absence of steric interactions, the strength of the fifth ligand should be comparable to Lewis acid-base complexes in four-coordinate compounds. The fact that the fifth interaction was shown to be only weakly coordinating is due to inter-ligand steric repulsion, and may be used as a thermodynamic measure of steric bulk. Although these compounds are valuable because they allow for the quantification of the intramolecular interaction and the various factors that control it, they are not latent Lewis acids. Latent Lewis acidity is precluded by the formation of dimeric structures.

Therefore, it is of interest to develop an understanding of the geometric as well as the steric or electronic factors that control the extent of oligomerization and coordination number at the aluminum center in compounds with non-delocalized ligands containing both anionic and neutral Lewis base termini; in particular, what controls the relative stability of a monomer versus a dimer. It would appear that the Lewis base termini (Y = ether or thioether) are insufficiently basic to cleave the $Al(\mu-O)_2Al$ core of a dimeric alkoxide to give monomeric chelate compounds. The use of stronger Lewis bases such as pyridyl and

quinolinic compounds was then employed to investigate the extent of oligomerization. It was shown that the formation of monomeric structures for compounds is associated with the rigid conformation of the pyridine and quinoline ligands and not upon the basicity of the chelating ligand. Consequently, the stability of monomeric versus dimeric structures in this system depends upon a combination of factors: the steric bulk at the aluminum, the rigidity of the ligand, and the ring size formed by chelating ligation. Again these compounds were not good examples of latent Lewis acidity, because although a few of them were monomers, the pyridine ligand was too strong of a base for the intramolecular coordination to be cleaved , or the rigidity of the ligand prohibited the 'opening' of the intramolecular coordination.

Monomeric structures are energetically unfavored and can be formed if the dimers are destabilized. This is possible if the steric bulk at the aluminum and the heteroatom is very large, if the potential bridging atom possesses a geometry that is incompatible with the formation of the four membered core of a dimer or if the ligand is rigid. In the quest for a monomeric structure, the substituent on the aluminum was changed to 2,6-di-*tert*-butyl-4-methylphenol (BHT-H from the trivial name butylated hydroxy toluene). Unfortunately, BHT is very easily eliminated and the anionic oxygen of the bidentate ligand formed dimeric structures. The presence of only one BHT on the aluminum does not hinder dimerization.

Throughout these studies we have gleaned an understanding of the formation of intramolecular coordination in dimeric aluminum compounds and various methods of synthesis have been employed, including hydroalumination of allyl ligands. This has led to the study on whether intramolecularly stabilized compounds of aluminum are suitable structural models of the S_N2 transition state. It has been shown that in the absence of steric considerations ,i.e., the model compound [H₂Al(μ-OCH₂CH₂OH)]₂, such compounds faithfully describe the structural changes that occur in the S_N2 cleavage of dimeric aluminum compounds; unfortunately, real compounds are not such good models. Angular

changes during reactivity appear to follow the correct trends, however, the bond distances are controlled by the steric bulk of the aluminum alkyl substituents rather than the coordination of the fifth ligand. This effect was studied carefully using the X-ray crystallographic structure of $[({}^t\text{Bu})_2\text{Al}(\mu\text{-Cl})]_2$. This study emphasized that the C-M-C angle of dimeric Group 13 compounds is controlled by the steric repulsion between the alkyl groups on adjacent metal centers, instead of steric congestion between ligands on individual metal centers.

This research has underlined the factors that influence the formation of an intramolecular coordination site on organoaluminum compounds and has laid the groundwork for the eventual discovery of a latent Lewis acid that accurately mimics the ring opening mechanism of the alumoxanes. Future studies may focus on the formation of a monomeric, cyclic compound that possesses an intramolecular coordination site that cleaves in the presence of a Lewis base. This type of compound is possible if the steric bulk on the aluminum is increased enough to hinder further oligomerization. The choice of ligand is important as it should not be easily eliminated such as BHT, but it should be a bulky organic alcohol which would mimic the inner coordination sphere of the aluminum in alumoxanes.

Appendix A

Quantification of Steric Effects

Steric effects occur as a result of forces (usually nonbonding) between parts of a molecule and is related to the size of the substituents in a molecule. It is very closely linked to electronic effects as it can have important electronic consequences, for example, changing bond angles will change the electronic character of the bond. Similarly, electronic effects such as electronegativities can result in varying bond lengths which in turn affect the sterics. Because these two properties are so closely intertwined, they are difficult to separate and quantify. In general, four procedures may be used to assess and/or quantify steric size. These include (a) the direct physical measurement of steric size from a knowledge of atom sizes, bond lengths and bond angles, (b) inference of relative sizes from some exhibited chemical property, (c) molecular mechanics models, and (d) the use of molecular volumes.¹ The most widely used and accepted steric measure in inorganic chemistry is the cone angle, θ , originally proposed by Tolman in 1970² to explain the reactivity of various phosphine and phosphite ligands.

The cone angle concept is very useful even though it was generated for a specific system because it provides a relative ordering of steric size that can be generalized to any atom or substituent. The steric parameter, θ , for symmetric ligands is the apex angle of a cylindrical cone, centered at 2.28 Å from the central phosphorus atom, which just touches the van der Waals radii of the outermost atoms of the model (see Figure A.1). If there are degrees of freedom in the molecule, then the minimum cone angle is measured by folding back all the substituents. For asymmetric ligands, the total cone angle is defined as the average of the sum of the semivertex angles for each portion of the molecule. This concept is very elegant in its simplicity but there exist several limitations. These include: (a) the cone angles vary with conformational changes, (b) they are only accurate within 2°, (c) minimum conformation is uncertain, (d) the data does not reflect the other ligands present

in the molecule and finally (e) that a constant metal-phosphorus bond length was chosen. Regardless of these limitations, Tolman's cone angle remains the most useful and popular measure of steric bulk and has been applied to most substituents, organic and inorganic.

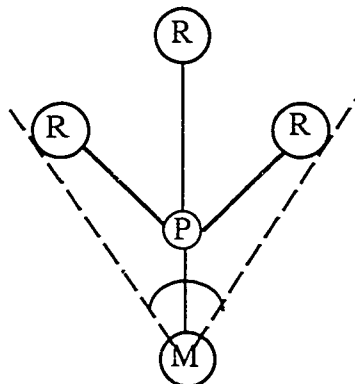


Figure A.1. Measurement of the Tolman cone angle, θ , for a PR_3 ligand.

The use of molecular mechanics have also been employed to quantify steric effects. This method was first reported by Mosbo and co-workers³ to assess and quantify steric size and it involves the use of molecular mechanics to calculate the weighted average of cone angles over several conformers of the ligand based on computer calculations. These calculations accounted for a limited number of conformers, ignoring whether these conformers corresponded to the energy minima or not, and it defined four different cone angles including the maximum cone angle, Tolman's cone angle (maximum cone angle over the minimum configuration), the averaged maximum cone angle and the solid angle. A solid angle refers to the area under a ligand profile. A ligand profile is generated by plotting $\theta/2$ against ϕ (which is the angle of rotation about the M-P bond) for each 1° rotational increment. Ferguson and co-workers⁴ were the first to use ligand profiles to assess the steric effect with regard to the shape of the ligand and it gave information about the spaces between the atoms within a ligand. Many methods for generating ligand profiles have since

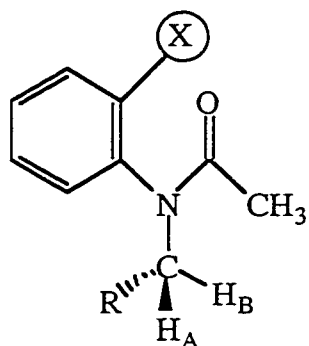
appeared in the literature and they all attempt to quantify the solid angles for various ligands.⁵

Other methods to use molecular attempts to quantify steric effects include the use of the ligand repulsive energy and *ab initio* molecular orbital calculations. In 1992, Brown published a report⁶ stating that steric size can be defined in terms of the repulsive forces that ligands exert on their environment. These forces cause the ligand to distort from their ideal geometries and was defined in terms of the repulsive van der Waals interactions between atoms in a complex. Brown calculated the total energy change for a reaction where the change in repulsive energy was equal to the energy of the product minus the energy of the reactants. Although the change in energy varied with ligand structure, it included electronic as well as steric effects because both the attractive and repulsive van der Waal's interactions were considered. *Ab initio* calculations can also be used to investigate the relationship between sterics and bond angle. From molecular orbital calculations, Baird showed that the bond distance, R_{AX} , in a molecule, X_2A , greatly influenced the X-A-X angle if A is a first row element.⁷ The rate of change slowed considerably if A were a second row element and was independent of electronegativities and the presence of lone electrons. As a consequence, Baird concluded that the optimum X-A-X bond angle was dependent on steric rather than electronic effects. Molecular volumes are also used to evaluate steric size and are calculated from van der Waals radii⁸ and charge densities⁹ to name a couple of methods.

Chemical methods have also been used to quantify steric effects. The most known of these methods is the use of the Taft steric parameter, E_s ,¹⁰ which is defined as the logarithm of the ratio of the rate constant for the acid-catalyzed hydrolysis of a substituted ester, k, to the rate constant of the reference methyl-substituted ester, k_0 , (Eq. A.1).

$$E_s = \log (k/k_0) \quad (\text{A.1})$$

It relates steric effects to the rate at which a chemical reaction progresses in comparison to the rate at which the same reaction progresses where the starting material is substituted. Various modification of this concept have since been published.¹¹ Spectroscopic methods employed to quantify steric effects include using NMR spectroscopy. The chemical shift difference between nonequivalent protons in substituted anilides (see I) was used to infer the van der Waals radius of the substituent and is based on a linear regression analysis.¹²



I

In summary, steric size may be estimated using either chemical means or direct physical measurements. Although these methods include limitations and assumptions, they have been very helpful in explaining the relationship between steric size and reactivities in both organic and inorganic chemistry.

References

- 1 D. White and N. J. Colville, *Adv. Organomet. Chem.*, 1994, **36**, 95.
- 2 C. A. Tolman, *J. Am. Chem. Soc.*, 1970, **92**, 2953.
- 3 J. T. de Santo, J. A. Mosbo, B. N. Storhoff, P. L. Bock, and R. E. Bloss, *Inorg. Chem.*, 1980, **19**, 3086.
- 4 G. Ferguson, P. J. Roberts, E. C. Alyea, and M. Khan, *Inorg. Chem.*, 1978, **17**, 2965.
- 5 (a) E. C Alyea, G. Ferguson, and A. Somogyvani, *Inorg. Chem.*, 1982, **21**, 1369.
(b) J. D. Smith and J. D. Oliver, *Inorg. Chem.*, 1978, **17**, 2585.
(c) D. F. Mullica, S. L. Gipson, E. L. Sappenfield, C. C. Lin, and D. H. Leschnitzer, *Inorg. Chim. Acta.*, 1990, **177**, 89.
(d) D. H. Ferrar and N. C. Payne, *Inorg. Chem.*, 1981, **20**, 821.
- 6 T. L. Brown, *Inorg. Chem.*, 1992, **31**, 1286.
- 7 N. C. Baird, *Inorg. Chem.*, 1989, **28**, 1224.
- 8 J. T. Edward and P. G. Farrell, *Can. J. Chem.*, 1975, **53**, 2965.
- 9 R. F. W. Bader, M. T. Carroll, J. R. Cheeseman, and J. R. Chang, *J. Am. Chem. Soc.*, 1987, **109**, 7968.
- 10 R. W. Taft. in *Steric Effects in Organic Chemistry*, M. S. Newman, Ed., Wiley, New York, 1956, 556.
- 11 (a) C. K. Hancock, E. A. Meyers, and B. J. Yagar, *J. Am. Chem. Soc.*, 1961, **83**, 4211.
(b) M. Charton, *J. Am. Chem. Soc.*, 1969, **91**, 619.
(c) J. A. MacPhee, A. Panaye, and J. E. Dubois, *Tetrahedron*, 1978, **34**, 3553.
- 12 B. J. Staskun, *J. Org. Chem.*, 1981, **46**, 1643.

Appendix B

Lennard-Jones Potential

The Lennard-Jones potential is a mathematical equation (Eq. B.1) that describes the relationship between bond dissociation energy and bond distance (Figure B.1).

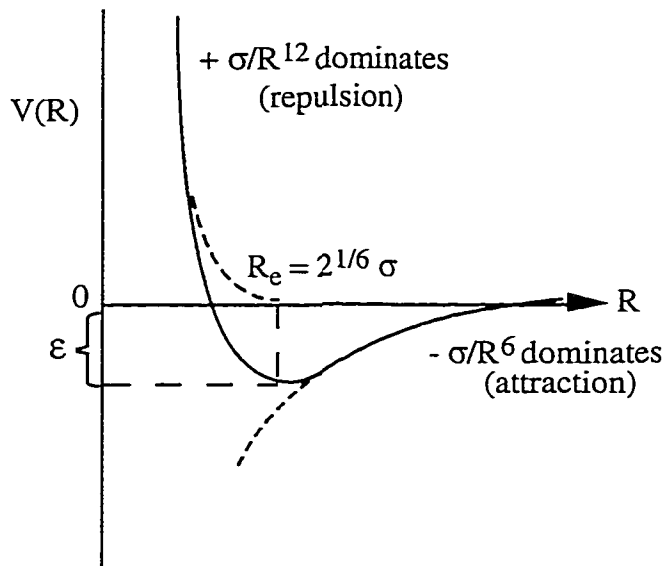


Figure B.1. The Lennard-Jones (12-6)-Potential¹

When atoms approach each other, the nuclear and electronic repulsions start to dominate the attractive forces. At short separations the intermolecular energy rises sharply and although the behavior at short distances is very complicated the Lennard-Jones potential approximates the behavior very well. As the interatomic distance increases, the bond dissociation energy gradually decreases to a minimum. This distance, R_e , is the ideal bond distance and it is described mathematically in Eq. B.2. If the interatomic distance is larger than R_e , then the attractive forces dominate and these gradually approach zero asymptotically as the interatomic distance increases further. At small values of R , R^{12} is much smaller than R^6 so the repulsive term, $(\sigma/R)^{12}$,

dominates the attractive term, $(-\sigma/R)^6$. This is reversed for larger values of R and this results in a good approximation for interatomic forces during bonding.

$$\text{BDE}_R = 4\epsilon \left[\left(\frac{\sigma}{R}\right)^{12} - \left(\frac{\sigma}{R}\right)^6 \right] \quad (\text{Eq. B.1})$$

$$R_e = 2^{1/6}\sigma \quad (\text{Eq. B.2})$$

Reference

- 1 P. W. Atkins, *Physical Chemistry*, Oxford University Press, Oxford, 1978, Chapter 23, p 763.

Appendix C

Publications

1. Molecular structure of $[({}^t\text{Bu})_2\text{Al}(\mu\text{-Cl})_2]_2$. J. A. Francis, C. N. McMahon and A. R. Barron, *J. Chem. Cryst.*, 1997, **27**, 191.
2. 1,3-Diphenylamine and methylaminopyridine complexes of gallium. Y. Koide, J. A. Francis, S. G. Bott and A. R. Barron, *Polyhedron*, 1998, **17**, 983.
3. Steric effects in aluminum compounds containing monoanionic potentially bidentate ligands: towards a quantitative measure of steric bulk. J. A. Francis, C. N. McMahon, S. G. Bott and A. R. Barron, *Organometallics*, submitted for publication.
4. Aluminum - rigid conformation effects of chelate ring size and steric hindrance on the coordination and degree of association. J. A. Francis, S. G. Bott and A. R. Barron, *J. Chem. Soc., Dalton Trans.*, 1998, 3305.
5. Aluminum compounds containing bidentate ligands: ligand base strength and remote geometric control over degree of association. J. A. Francis, C. N. McMahon, S. G. Bott, and A.R. Barron, *J. Chem. Soc., Dalton Trans.*, 1999, **1**, 67.
6. Are intramolecularly stabilized compounds of aluminum suitable structural models of the S_N2 transition state? Molecular structure of $[({}^t\text{Bu})_2\text{Al}(\mu\text{-OC}_6\text{H}_4\text{-2-OMe})_2]$. J. A. Francis, S. G. Bott and A. R. Barron, *Polyhedron*, in press.
7. Hydroalumination of $\text{H}_2\text{C=CHCH}_2\text{SMe}$: synthesis and molecular structure of $({}^t\text{Bu})_2\text{Al}(\text{CH}_2\text{CH}_2\text{CH}_2\text{SMe})$. J. A. Francis, S. G. Bott and A. R. Barron, *Main Group Chemistry*, in press.
8. Sterically crowded aryloxides of aluminum: intramolecular coordination of bidentate ligands. J. A. Francis, S. G. Bott and A. R. Barron, submitted for publication.

VOLUME II

INTRAMOLECULAR COORDINATION IN COMPOUNDS OF ALUMINUM

by

JULIE A. FRANCIS

**Appendix for
Intramolecular Coordination in Compounds of Aluminum
by
Julie A. Francis**

Table of Contents

(1) $[(^t\text{Bu})_2\text{Al}(\mu\text{-OCH}_2\text{CH}_2\text{OMe})]_2$ (1.1)	1
(2) $[(^i\text{Bu})_2\text{Al}(\mu\text{-OCH}_2\text{CH}_2\text{OMe})]_2$ (1.2)	7
(3) $[(^t\text{Bu})_2\text{Al}(\mu\text{-OCH}_2\text{CH}_2\text{CH}_2\text{OMe})]_2$ (1.6)	14
(4) $[\text{Me}_2\text{Al}(\mu\text{-OCH}_2\text{CH}_2\text{CH}_2\text{OMe})]_2$ (1.7)	22
(5) $[(^t\text{Bu})_2\text{Al}(\mu\text{-OCH}_2\text{CH}_2\text{SMe})]_2$ (1.11)	28
(6) $[(^i\text{Bu})_2\text{Al}(\mu\text{-OCH}_2\text{CH}_2\text{SMe})]_2$ (1.12)	36
(7) $[(^t\text{Bu})_2\text{Al}(\mu\text{-OCH}_2\text{CH}_2\text{CH}_2\text{SMe})]_2$ (1.15)	44
(8) $[\text{H}_2\text{Al}(\mu\text{-OCH}_2\text{CH}_2\text{OH})]_2$	52
(9) $[(^t\text{Bu})_2\text{Al}(\mu\text{-O-2-C}_5\text{H}_4\text{N})]_2$ (2.1)	62
(10) $(^t\text{Bu})_2\text{Al(O-8-C}_9\text{H}_6\text{N)}$ (2.3)	69
(11) $[(^i\text{Bu})_2\text{Al}(\mu\text{-O-8-C}_9\text{H}_6\text{N})]_2$ (2.5)	99
(12) $[(^t\text{Bu})_2\text{Al}(\mu\text{-OC}_6\text{H}_4\text{-2-OMe})]_2$ (3.1)	85
(13) $[(\text{BHT})\text{Al(H)}(\mu\text{-OCH}_2\text{CH}_2\text{NMe}_2)]_2$ (4.2)	91
(14) $[(\text{BHT})\text{Al(OCH}_2\text{CH}_2\text{OMe})(\mu\text{-OCH}_2\text{CH}_2\text{OMe})]_2$ (4.6)	97
(15) $(\text{BHT})_2\text{Al}(\mu\text{-OCH}_2\text{CH}_2\text{NMe}_2)_2\text{Li}$ (4.8)	103
(16) $(\text{BHT})_2\text{Al}(\mu\text{-OCH}_2\text{CH}_2\text{SMe})_2\text{Li}(\text{HOCH}_2\text{CH}_2\text{SMe})$ (4.10b)	111
(17) $(^t\text{Bu})_2\text{Al(CH}_2\text{CH}_2\text{CH}_2\text{SMe})$ (5.1)	119
(18) $[(^t\text{Bu})_2\text{Al}(\mu\text{-Cl})]_2$ (6.1)	127

$[(tBu)_2Al(\mu-OCH_2CH_2OMe)]_2$ (**1.1**)

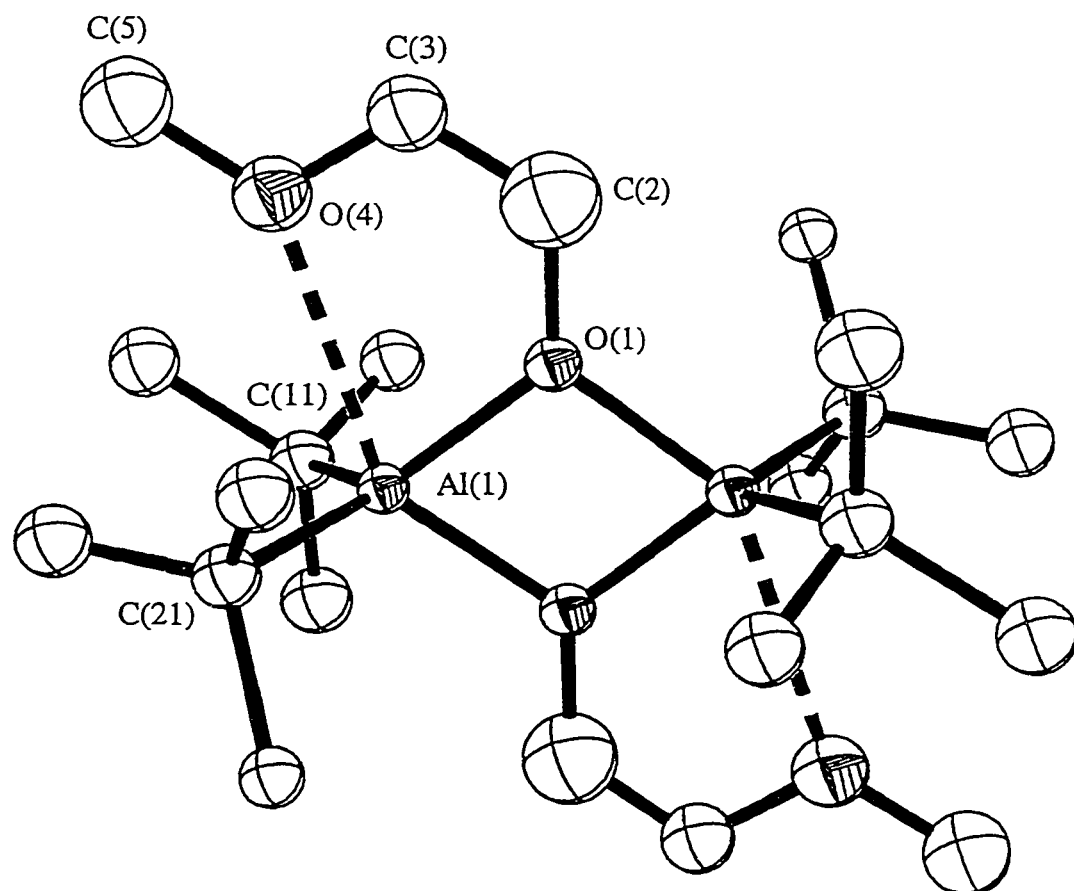


Figure 1. The molecular structure of $[(\text{tBu})_2\text{Al}(\mu\text{-OCH}_2\text{CH}_2\text{OMe})]_2$ (**1.1**).

Hydrogen atoms are omitted, and only one set of the disordered positions of the methyl groups attached to C(11) and C(21) in compound **1.1** is shown, for clarity.

Table of Positional Parameters and their Estimated Standard Deviations.

Atom	x —	y —	z —	B(A2) -----
A1	0.9642(6)	0.0518(7)	0.0740(3)	4.7(1)*
O1	0.914(1)	0.084(1)	-0.0286(6)	5.3(3)*
O4	0.742(2)	0.266(2)	0.0442(9)	9.9(4)*
C2	0.810(4)	0.194(4)	-0.068(2)	16(1)*
C3	0.722(3)	0.282(3)	-0.031(1)	9.9(7)*
C5	0.655(3)	0.365(4)	0.081(2)	14(1)*
C11	0.820(2)	-0.072(3)	0.125(1)	7.6(6)*
C12	0.695(4)	-0.134(4)	0.069(2)	8.3(9)*
C13	0.905(4)	-0.214(5)	0.165(2)	10(1)*
C14	0.710(4)	0.041(5)	0.169(2)	10(1)*
C15	0.823(6)	0.010(7)	0.205(3)	7(2)*
C16	0.640(9)	-0.03(1)	0.109(5)	11(2)*
C17	0.78(1)	-0.23(1)	0.074(5)	14(3)*
C21	1.093(2)	0.200(2)	0.137(1)	7.1(5)*
C22	1.089(9)	0.153(9)	0.239(4)	18(3)*
C23	1.023(5)	0.250(6)	0.202(3)	9(1)*
C24	1.214(8)	0.259(9)	0.105(4)	17(2)*
C25	1.211(5)	0.124(6)	0.200(3)	9(1)*
C27	1.110(5)	0.341(5)	0.089(2)	8(1)*
C28	1.273(4)	0.132(5)	0.159(2)	6(1)*

Starred atoms were refined isotropically.

Table of Positional Parameters and their Estimated Standard Deviations.

Atom	X	Y	Z	B (A2)
H2a	0.7435	0.1408	-0.1059	20*
H2b	0.8702	0.2610	-0.0925	20*
H3a	0.7414	0.3840	-0.0423	12*
H3b	0.6192	0.2592	-0.0507	12*
H5a	0.6747	0.3473	0.1346	17*
H5b	0.6791	0.4654	0.0706	17*
H5c	0.5504	0.3473	0.0624	17*

Table of Bond Distances in Angstroms.

<u>Atom 1</u>	<u>Atom 2</u>	<u>Distance</u>	<u>Atom 1</u>	<u>Atom 2</u>	<u>Distance</u>
A1	O1	1.82(1)	C11	C14	1.69(5)
A1	O1'	1.890(6)	C11	C15	1.58(6)
A1	C11	2.03(2)	C11	C16	1.63(8)
A1	C21	1.98(2)	C11	C17	1.7(1)
O1	C2	1.46(4)	C21	C22	1.86(8)
O4	C3	1.33(3)	C21	C23	1.46(5)
O4	C5	1.41(4)	C21	C24	1.41(8)
C2	C3	1.36(5)	C21	C25	1.56(5)
C11	C12	1.48(4)	C21	C27	1.54(5)
C11	C13	1.58(4)	C21	C28	1.70(4)

Numbers in parentheses are estimated standard deviations in the least significant digits.

Table of Bond Angles in Degrees.

<u>Atom 1</u>	<u>Atom 2</u>	<u>Atom 3</u>	<u>Angle</u>	<u>Atom 1</u>	<u>Atom 2</u>	<u>Atom 3 Angle</u>
O1	Al	C11	117.5(7)	C12	C11	C13 105.(2)
O1	Al	C21	119.2(8)	C12	C11	C14 96.(2)
O1	Al	O1'	74.8(4)	C13	C11	C14 124.(2)
C11	Al	C21	117.8(9)	C15	C11	C16 86.(4)
C11	Al	O1'	107.4(7)	C15	C11	C17 148.(4)
C21	Al	O1'	110.0(7)	C16	C11	C17 89.(4)
Al	O1	C2	128.(2)	Al	C21	C22 107.(3)
Al	O1	Al'	105.2(6)	Al	C21	C23 111.(2)
C2	O1	Al'	127.(2)	Al	C21	C24 116.(3)
C3	O4	C5	114.(2)	Al	C21	C25 112.(2)
O1	C2	C3	123.(3)	Al	C21	C27 109.(2)
O4	C3	C2	115.(2)	Al	C21	C28 109.(2)
Al	C11	C12	112.(2)	C22	C21	C27 138.(3)
Al	C11	C13	110.(2)	C22	C21	C28 83.(3)
Al	C11	C14	110.(2)	C27	C21	C28 104.(2)
Al	C11	C15	103.(2)	C23	C21	C24 131.(4)
Al	C11	C16	119.(3)	C23	C21	C25 84.(3)
Al	C11	C17	107.(4)	C24	C21	C25 89.(4)

Numbers in parenthesis are estimated standard deviations in the least significant digits.

$[(^i\text{Bu})_2\text{Al}(\mu\text{-OCH}_2\text{CH}_2\text{OMe})]_2$ (**1.2**)

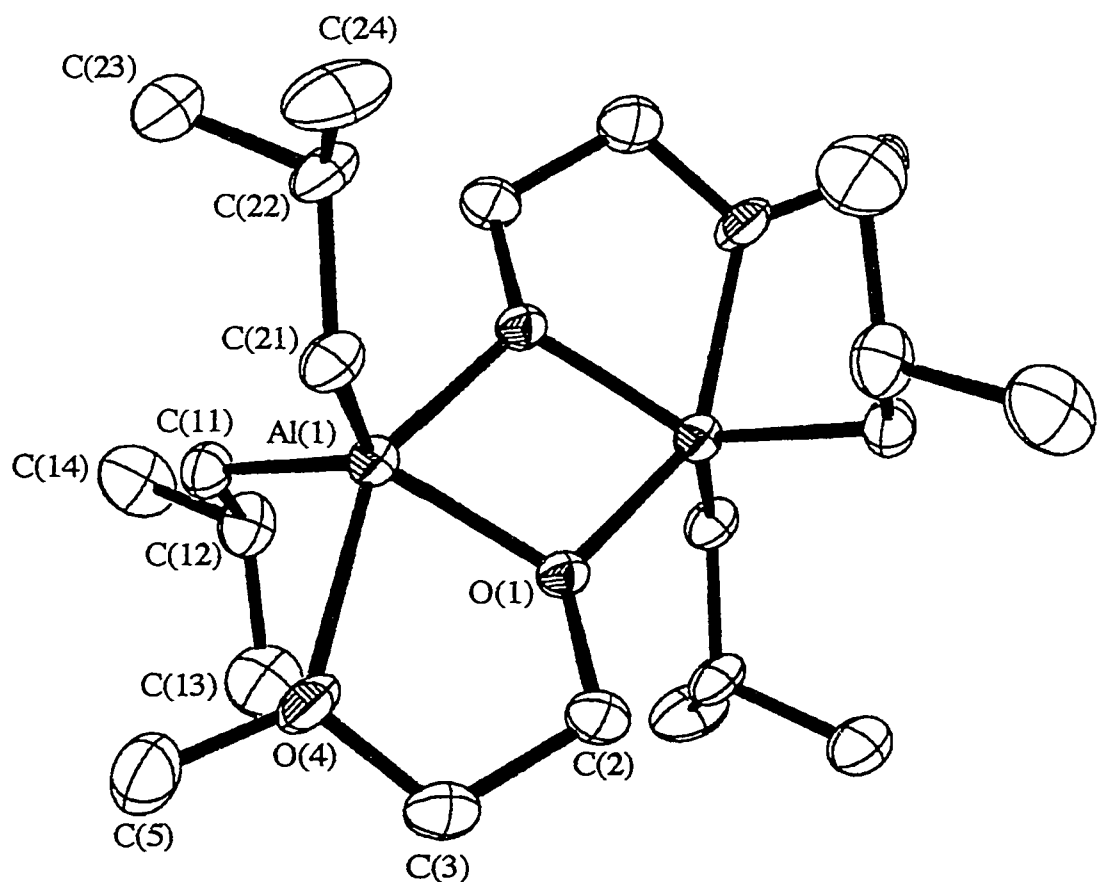


Figure 2. The molecular structure of $[(^{\text{i}}\text{Bu})_2\text{Al}(\mu\text{-OCH}_2\text{CH}_2\text{OMe})]_2$ (**1.2**). Hydrogen atoms are omitted, and only one set of the disordered positions of the methyl groups attached to C(11) and C(21) in compound **1.2** is shown, for clarity.

Table of Positional Parameters and their Estimated Standard Deviations.

Atom	x	y	z	B (Å²)
A1	0.4659(1)	0.86304(9)	-0.00405(9)	3.49(2)
O1	0.4038(2)	1.0158(2)	0.0818(2)	3.44(4)
O4	0.2679(3)	0.8166(2)	0.1363(2)	5.31(6)
C2	0.2552(4)	1.0573(4)	0.1496(3)	5.00(8)
C3	0.2229(4)	0.9132(4)	0.2201(4)	6.5(1)
C5	0.2315(5)	0.6785(4)	0.1802(5)	7.8(1)
C11	0.6499(4)	0.6377(3)	0.0863(3)	4.60(8)
C12	0.7861(4)	0.5983(4)	0.2066(4)	5.7(1)
C13	0.7150(6)	0.5917(5)	0.3453(4)	8.5(1)
C14	0.9444(5)	0.4376(5)	0.2293(5)	8.7(2)
C21	0.3010(4)	0.9212(3)	-0.1694(3)	4.43(7)
C22	0.3552(4)	0.9455(3)	-0.3170(3)	4.86(8)
C23	0.4803(5)	0.7868(4)	-0.3280(4)	6.8(1)
C24	0.2016(5)	1.0307(5)	-0.4348(4)	7.9(1)

Anisotropically refined atoms are given in the form of the isotropic equivalent displacement defined as: $(4/3) * [a_2^2 * B_{(1,1)} + b_2^2 * B_{(2,2)} + c_2^2 * B_{(3,3)} + ab(\cos \gamma) * B_{(1,2)} + ac(\cos \beta) * B_{(1,3)} + bc(\cos \alpha) * B_{(2,3)}]$

Table of Positional Parameters and their Estimated Standard Deviations.

Atom	x -	y -	z -	B (Å ²)
H2a	0.1591	1.1393	0.0799	6*
H2b	0.2712	1.0988	0.2188	6*
H3a	0.2902	0.8515	0.3119	8*
H3b	0.1045	0.9470	0.2300	8*
H5a	0.1209	0.7065	0.2217	10*
H5b	0.3219	0.5881	0.2504	10*
H5c	0.2202	0.6503	0.1002	10*
H11a	0.7100	0.6101	0.0121	5*
H11b	0.5948	0.5677	0.1246	5*
H12	0.8194	0.6859	0.1766	7*
H13a	0.8072	0.5567	0.4280	11*
H13b	0.6665	0.5149	0.3689	11*
H13c	0.6279	0.6977	0.3330	11*
H14a	0.8919	0.3486	0.2507	11*
H14b	1.0240	0.4106	0.3082	11*
H14c	0.9992	0.4443	0.1460	11*
H21a	0.2061	1.0213	-0.1769	5*
H21b	0.2644	0.8360	-0.1470	5*
H22	0.4112	1.0152	-0.3305	6*
H23a	0.5841	0.7264	-0.2400	8*
H23b	0.5245	-0.8085	-0.4163	8*
H23c	0.4244	0.7183	-0.3225	8*
H24a	0.2431	1.0565	-0.5295	10*
H24b	0.1212	1.1294	-0.4258	10*
H24c	0.1479	0.9599	-0.4270	10*

Table of Bond Distances in Angstroms.

<u>Atom 1</u>	<u>Atom 2</u>	<u>Distance</u>	<u>Atom 1</u>	<u>Atom 2</u>	<u>Distance</u>
Al	O1	1.840(2)	C2	C3	1.459(5)
Al	O4	2.283(2)	C11	C12	1.537(5)
Al	C11	1.974(2)	C12	C13	1.505(6)
Al	C21	1.975(3)	C12	C14	1.526(5)
Al	O1'	1.909(1)	C21	C22	1.517(4)
O1	C2	1.414(4)	C22	C23	1.501(5)
O4	C3	1.396(5)	C22	C24	1.526(5)
O4	C5	1.409(5)			

Numbers in parenthesis are estimated standard deviations in the least significant digits.

Table of Bond Angles in Degrees.

<u>Atom 1</u>	<u>Atom 2</u>	<u>Atom 3</u>	<u>Angle</u>	<u>Atom 1</u>	<u>Atom 2</u>	<u>Atom 3</u>	<u>Angle</u>
O1	Al	O4	75.06(9)	Al	O4	C3	110.9(2)
O1	Al	C11	122.8(1)	Al	O4	C5	128.6(2)
O1	Al	C21	114.7(1)	C3	O4	C5	117.1(3)
O1	Al	O1'	76.38(7)	O1	C2	C3	110.6(3)
O4	Al	C11	95.2(1)	O4	C3	C2	108.5(3)
O4	Al	C21	86.9(1)	Al	C11	C12	120.2(2)
O4	Al	O1'	151.41(8)	C11	C12	C13	112.0(3)
C11	Al	C21	121.0(2)	C11	C12	C14	111.8(4)
C11	Al	O1'	101.4(1)	C13	C12	C14	109.8(3)
C21	Al	O1'	103.8(1)	Al	C21	C22	120.4(2)
Al	O1	C2	123.4(2)	C21	C22	C23	112.2(2)
Al	O1	Al'	103.62(9)	C21	C22	C24	112.2(3)
C2	O1	Al'	130.1(2)	C23	C22	C24	109.9(3)

Numbers in parenthesis are estimated standard deviations in the least significant digits.

Table of General Displacement Parameter Expressions - U's

Name	U(1,1)	U(2,2)	U(3,3)	U(1,2)	U(1,3)	U(2,3)
A1	0.0439(3)	0.0439(3)	0.0447(4)	-0.0184(2)	0.0044(3)-0.0167(3)	
O1	0.0413(8)	0.0461(7)	0.0458(9)	-0.0201(6)	0.0121(7)-0.0187(6)	
O4	0.080(1)	0.0724(9)	0.068(1)	-0.0495(7)	0.024(1) -0.0286(8)	
C2	0.058(1)	0.072(1)	0.072(2)	-0.031(1)	0.027(1) -0.038(1)	
C3	0.077(2)	0.093(2)	0.095(2)	-0.047(1)	0.046(2) -0.046(2)	
C5	0.097(2)	0.087(2)	0.132(3)	-0.062(1)	0.031(2) -0.036(2)	
C11	0.061(2)	0.047(1)	0.061(2)	-0.021(1)	0.006(1) -0.017(1)	
C12	0.061(2)	0.054(2)	0.082(2)	-0.019(1)	-0.007(2) -0.007(1)	
C13	0.109(3)	0.108(3)	0.079(2)	-0.022(2)	-0.014(2) -0.032(2)	
C14	0.072(2)	0.091(3)	0.110(3)	-0.002(2)	-0.006(2) -0.012(2)	
C21	0.056(1)	0.061(1)	0.054(1)	-0.029(1)	0.002(1) -0.019(1)	
C22	0.072(2)	0.071(1)	0.051(1)	-0.039(1)	0.007(1) -0.022(1)	
C23	0.105(2)	0.094(2)	0.078(2)	-0.048(2)	0.025(2) -0.048(1)	
C24	0.098(2)	0.138(3)	0.054(2)	-0.046(2)	-0.004(2) -0.028(2)	

The form of the anisotropic displacement parameter is:
 $\exp[-2\pi i \{h^2a^2U(1,1) + k^2b^2U(2,2) + l^2c^2U(3,3) + 2hkabU(1,2) + 2hlacU(1,3) + 2klbcU(2,3)\}]$ where a, b, and c are reciprocal lattice parameters.

$[(t\text{Bu})_2\text{Al}(\mu\text{-OCH}_2\text{CH}_2\text{CH}_2\text{OMe})]_2$ (**1.6**)

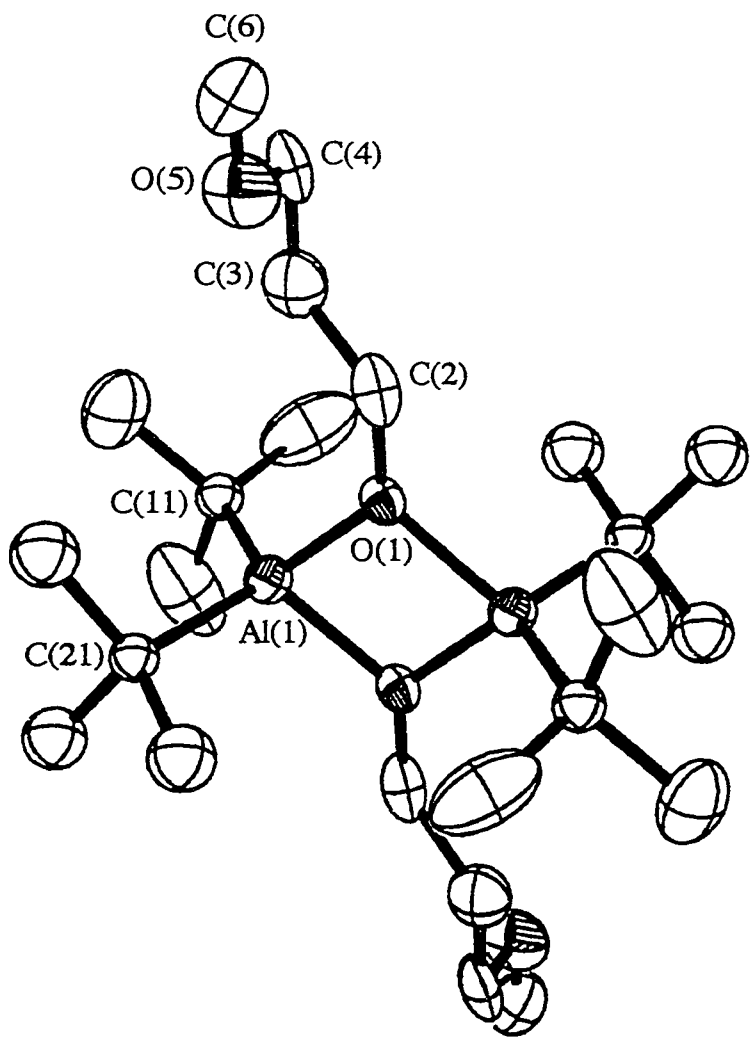


Figure 3. The molecular structure of $[(\text{tBu})_2\text{Al}(\mu\text{-OCH}_2\text{CH}_2\text{CH}_2\text{OMe})]_2$ (**1.6**).

Hydrogen atoms are omitted, and only one set of the disordered positions of the methyl groups attached to C(11) and C(21) in compound **1.6** is shown, for clarity.

Table of Positional Parameters and their Estimated Standard Deviations.

Atom	X	Y	Z	B (Å ²)
A1	0.6172(2)	0.5491(1)	0.0456(3)	3.68(4)
O1	0.4258(4)	0.5360(2)	0.0639(5)	3.6(1)
O5	0.2053(7)	0.7229(3)	0.1952(7)	7.0(2)
C2	0.3212(9)	0.5825(5)	0.119(1)	6.1(2)
C3	0.376(1)	0.6233(5)	0.262(1)	6.8(3)
C4	0.261(1)	0.6713(5)	0.309(1)	7.3(3)
C6	0.119(1)	0.7612(6)	0.227(1)	7.9(3)
C11	0.7654(8)	0.5371(4)	0.2466(9)	5.0(2)*
C12	0.800(1)	0.6068(6)	0.338(1)	8.9(3)
C13	0.906(1)	0.5111(8)	0.204(1)	12.1(4)
C14	0.722(1)	0.4850(7)	0.364(1)	11.7(4)
C21	0.6496(8)	0.6302(4)	-0.0973(9)	4.5(2)*
C22a	0.812(2)	0.629(1)	-0.124(2)	7.8(5)*
C22b	0.691(2)	0.603(1)	-0.244(3)	7.6(6)*
C23a	0.624(2)	0.702(1)	-0.027(2)	8.2(5)*
C23b	0.762(3)	0.685(1)	-0.025(3)	8.8(7)*
C24a	0.556(2)	0.625(1)	-0.265(2)	8.3(5)*
C24b	0.513(2)	0.675(1)	-0.138(3)	7.6(6)*

Starred atoms were refined isotropically.

Anisotropically refined atoms are given in the form of the isotropic equivalent displacement parameter defined as:

$$(4/3) * [a^2 * B(1,1) + b^2 * B(2,2) + c^2 * B(3,3) + ab(\cos \gamma) * B(1,2) + ac(\cos \beta) * B(1,3) + bc(\cos \alpha) * B(2,3)]$$

Table of Positional Parameters and their Estimated Standard Deviations.

<u>Atom</u>	<u>x</u>	<u>y</u>	<u>z</u>	<u>B (A2)</u>
H2a	0.2431	0.5539	0.1399	7*
H2b	0.2863	0.6151	0.0346	7*
H3a	0.4549	0.6517	0.2425	8*
H3b	0.4087	0.5912	0.3477	8*
H4a	0.1831	0.6421	0.3278	9*
H4b	0.3025	0.6952	0.4052	9*
H6a	0.0894	0.7935	0.1407	10*
H6b	0.0369	0.7345	0.2456	10*
H6c	0.1578	0.7872	0.3214	10*
H12a	0.8699	0.5984	0.4319	11*
H12b	0.8363	0.6404	0.2715	11*
H12c	0.7135	0.6251	0.3677	11*
H13a	0.9763	0.5054	0.2988	15*
H13b	0.8905	0.4666	0.1494	15*
H13c	0.9400	0.5449	0.1354	15*
H14a	0.7962	0.4818	0.4558	15*
H14b	0.6345	0.5007	0.3953	15*
H14c	0.7063	0.4394	0.3147	15*

Table of Positional Parameters and their Estimated Standard Deviations.

<u>Atom</u>	<u>x</u>	<u>y</u>	<u>z</u>	<u>B(A2)</u>
H22aa	0.8277	0.6674	-0.1917	10*
H22ab	0.8753	0.6335	-0.0232	10*
H22ac	0.8308	0.5851	-0.1726	10*
H22ba	0.7063	0.6417	-0.3115	9*
H22bb	0.7781	0.5760	-0.2176	9*
H22bc	0.6161	0.5732	-0.2991	9*
H23aa	0.6411	0.7387	-0.0999	10*
H23ab	0.5270	0.7052	-0.0102	10*
H23ac	0.6888	0.7083	0.0720	10*
H23ba	0.7685	0.7212	-0.1025	11*
H23bb	0.7330	0.7062	0.0665	11*
H23bc	0.8531	0.6627	0.0055	11*
H24aa	0.5753	0.6651	-0.3275	10*
H24ab	0.5772	0.5825	-0.3156	10*
H24ac	0.4560	0.6257	-0.2558	10*
H24ba	0.5297	0.7136	-0.2060	9*
H24bb	0.4355	0.6467	-0.1918	9*
H24bc	0.4883	0.6939	-0.0420	9*

Table of Bond Distances in Angstroms.

<u>Atom 1</u>	<u>Atom 2</u>	<u>Distance</u>	<u>Atom 1</u>	<u>Atom 2</u>	<u>Distance</u>
A1	O1	1.844(5)	C11	C12	1.52(1)
A1	O1'	1.852(2)	C11	C13	1.51(1)
A1	C11	2.005(7)	C11	C14	1.50(2)
A1	C21	1.999(8)	C21	C22a	1.58(2)
O1	C2	1.45(1)	C21	C22b	1.46(3)
O5	C4	1.40(1)	C21	C23a	1.51(2)
O5	C6	1.15(1)	C21	C23b	1.52(2)
C2	C3	1.45(1)	C21	C24a	1.53(2)
C3	C4	1.51(1)	C21	C24b	1.52(2)

Numbers in parentheses are estimated standard deviations in the least significant digits.

Table of Bond Angles in Degrees.

<u>Atom 1</u>	<u>Atom 2</u>	<u>Atom 3</u>	<u>Angle</u>	<u>Atom 1</u>	<u>Atom 2</u>	<u>Atom 3</u>	<u>Angle</u>
O1	Al	C11	116.7(3)	C12	C11	C13	106.6(8)
O1	Al	C21	114.1(3)	C12	C11	C14	106.3(8)
O1	Al	O1'	78.4(2)	C13	C11	C14	107.7(9)
C11	Al	C21	116.2(3)	Al	C21	C22a	109.3(8)
C11	Al	O1'	112.5(3)	Al	C21	C22b	110.(1)
C21	Al	O1'	113.3(2)	Al	C21	C23a	113.1(9)
Al	O1	C2	132.1(4)	Al	C21	C23b	116(1)
Al	O1	Al'	101.6(2)	Al	C21	C24a	113.0(9)
C2	O1	Al'	125.4(4)	Al	C21	C24b	110(1)
C4	O5	C6	117.6(8)	C22a	C21	C23a	107.(1)
O1	C2	C3	115.3(7)	C22a	C21	C24a	106.(1)
C2	C3	C4	111.9(7)	C22b	C21	C23b	108.(1)
O5	C4	C3	115.4(8)	C22b	C21	C24b	110.(1)
Al	C11	C12	112.6(6)	C23a	C21	C24a	108.(1)
Al	C11	C13	109.5(6)	C23b	C21	C24b	102.(1)
Al	C11	C14	113.8(6)				

Numbers in parentheses are estimated standard deviations in the least significant digits.

Table of General Displacement Parameter Expressions - U's

Name	U(1,1)	U(2,2)	U(3,3)	U(1,2)	U(1,3)	U(2,3)
A1	0.047(1)	0.045(1)	0.047(1)	-0.000(1)	0.0070(9)	-0.000(1)
O1	0.042(3)	0.041(3)	0.054(3)	0.007(2)	0.013(2)	-0.000(2)
O5	0.117(4)	0.075(4)	0.077(4)	0.035(4)	0.021(3)	0.013(3)
C2	0.064(5)	0.068(5)	0.096(6)	0.018(5)	0.010(5)	-0.020(5)
C3	0.096(7)	0.093(7)	0.066(5)	0.014(6)	0.010(5)	-0.012(5)
C4	0.091(6)	0.077(6)	0.120(7)	0.004(5)	0.048(5)	-0.043(5)
C6	0.109(7)	0.081(7)	0.110(7)	-0.018(6)	0.018(6)	-0.014(6)
C12	0.123(8)	0.110(8)	0.090(7)	-0.002(8)	-0.022(7)	-0.021(7)
C13	0.093(7)	0.25(1)	0.102(8)	0.080(8)	-0.024(7)	-0.048(9)
C14	0.17(1)	0.17(1)	0.088(7)	-0.037(9)	-0.044(8)	0.044(8)

The form of the anisotropic displacement parameter is:
 $\exp[-2\pi i 2\{h^2a^2U(1,1) + k^2b^2U(2,2) + l^2c^2U(3,3) + 2hkabU(1,2) + 2hlacU(1,3) + 2klbcU(2,3)\}]$ where a, b, and c are reciprocal lattice parameters.

[Me₂Al(μ-OCH₂CH₂CH₂OMe)]₂ (**1.7**)

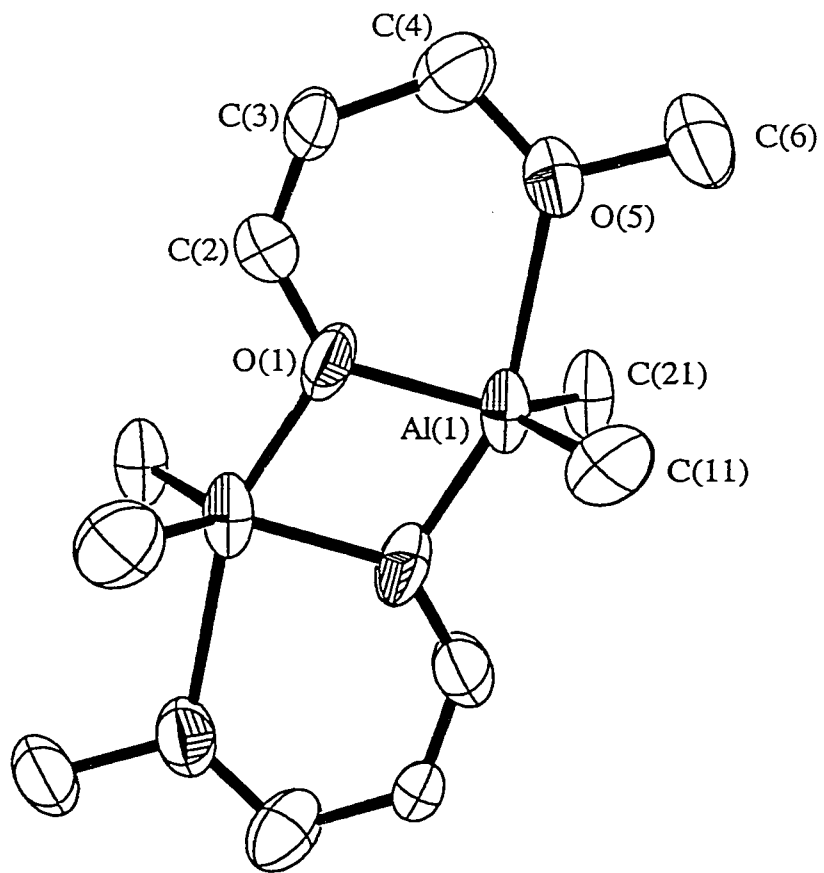


Figure 4. The molecular structure of $[\text{Me}_2\text{Al}(\mu\text{-OCH}_2\text{CH}_2\text{CH}_2\text{OMe})]_2$ (**1.7**).

Hydrogen atoms are omitted, and only one set of the disordered positions of the methyl groups attached to C(11) and C(21) in compound **1.7** is shown, for clarity.

Atomic coordinates [$\times 10^4$] and equivalent isotropic displacement parameters [$\text{\AA}^2 \times 10^3$]. U(eq) is defined as one third of the trace of the orthogonalized tensor.

	x	y	z	U(eq)
Al(1)	227(1)	-562(1)	3972(1)	37(1)
O(1)	1023(3)	331(1)	5800(2)	38(1)
O(2)	2313(3)	1466(2)	4955(3)	60(1)
C(1)	2260(4)	704(2)	6731(4)	41(1)
C(2)	2993(4)	1307(2)	6291(4)	48(1)
C(2A)	2993(7)	2103(3)	4436(6)	97(2)
C(3)	4274(5)	1687(3)	7174(5)	64(1)
C(4)	4819(5)	1464(3)	8489(6)	70(1)
C(5)	4095(5)	880(3)	8934(4)	63(1)
C(6)	2811(5)	497(2)	8057(4)	52(1)
C(11)	1483(4)	143(2)	2836(4)	48(1)
C(12)	1036(6)	-702(3)	2365(5)	75(1)
C(13)	1226(7)	628(3)	1566(5)	87(2)
C(14)	3257(5)	133(3)	3589(5)	79(2)
C(21)	-1360(5)	1455(2)	3492(4)	51(1)
C(22)	-2987(6)	1213(3)	3510(7)	97(2)
C(23)	-1575(7)	1790(3)	2125(5)	98(2)
C(24)	-847(7)	2124(3)	4472(6)	99(2)

Hydrogen coordinates [x 10⁴] and equivalent isotropic displacement parameters [Å² x 10³].

	x	y	z	U(eq)
H(2AA)	2430 (7)	2163 (3)	3500 (6)	145
H(2AB)	4083 (7)	1993 (3)	4571 (6)	145
H(2AC)	2916 (7)	2574 (3)	4894 (6)	145
H(3A)	4763 (5)	2090 (3)	6879 (5)	77
H(4A)	5691 (5)	1713 (3)	9082 (6)	84
H(5A)	4466 (5)	739 (3)	9829 (4)	76
H(6A)	2320 (5)	100 (2)	8364 (4)	63
H(12A)	-76 (6)	-731 (3)	1882 (5)	112
H(12B)	1293 (6)	-1040 (3)	3126 (5)	112
H(12C)	1615 (6)	-860 (3)	1795 (5)	112
H(13A)	119 (7)	649 (3)	1063 (5)	131
H(13B)	1782 (7)	393 (3)	1035 (5)	131
H(13C)	1617 (7)	1146 (3)	1809 (5)	131
H(14A)	3468 (5)	-165 (3)	4392 (5)	119
H(14B)	3625 (5)	656 (3)	3811 (5)	119
H(14C)	3793 (5)	-96 (3)	3037 (5)	119
H(22A)	-2889 (6)	996 (3)	4366 (7)	145
H(22B)	-3429 (6)	831 (3)	2829 (7)	145
H(22C)	-3667 (6)	1659 (3)	3347 (7)	145
H(23A)	-1900 (7)	1386 (3)	1468 (5)	147
H(23B)	-595 (7)	2009 (3)	2118 (5)	147
H(23C)	-2368 (7)	2189 (3)	1923 (5)	147
H(24A)	-697 (7)	1940 (3)	5358 (6)	148
H(24B)	-1647 (7)	2520 (3)	4242 (6)	148
H(24C)	126 (7)	2337 (3)	4437 (6)	148

Bond lengths [Å] and angles [°].

Al(1)-O(1)	1.876(2)	Al(1)-O(1)*	1.966(2)
Al(1)-C(11)	2.040(4)	Al(1)-C(21)	2.042(4)
Al(1)-O(2)	2.390(3)	O(1)-C(1)	1.376(4)
O(2)-C(2)	1.374(5)	O(2)-C(2A)	1.451(5)
C(1)-C(6)	1.376(5)	C(1)-C(2)	1.391(5)
C(2)-C(3)	1.382(6)	C(3)-C(4)	1.373(7)
C(4)-C(5)	1.365(7)	C(5)-C(6)	1.384(6)
C(11)-C(14)	1.525(6)	C(11)-C(13)	1.539(6)
C(11)-C(12)	1.546(6)	C(21)-C(23)	1.516(6)
C(21)-C(24)	1.518(6)	C(21)-C(22)	1.526(6)
O(1)-Al(1)-O(1)*	75.03(11)	O(1)-Al(1)-C(11)	116.38(14)
O(1)*-Al(1)-C(11)	104.40(13)	O(1)-Al(1)-C(21)	114.22(14)
O(1)*-Al(1)-C(21)	103.83(14)	C(11)-Al(1)-C(21)	126.6(2)
O(1)-Al(1)-O(2)	73.31(10)	O(1)*-Al(1)-O(2)	148.33(11)
C(11)-Al(1)-O(2)	88.94(13)	C(21)-Al(1)-O(2)	89.97(14)
C(1)-O(1)-Al(1)	125.7(2)	C(1)-O(1)-Al(1)*	129.2(2)
Al(1)-O(1)-Al(1)*	104.97(11)	C(2)-O(2)-C(2A)	116.5(4)
C(2)-O(2)-Al(1)	109.6(2)	C(2A)-O(2)-Al(1)	133.9(3)
O(1)-C(1)-C(6)	123.0(3)	O(1)-C(1)-C(2)	117.7(3)
C(6)-C(1)-C(2)	119.3(3)	O(2)-C(2)-C(3)	126.2(4)
O(2)-C(2)-C(1)	113.5(3)	C(3)-C(2)-C(1)	120.3(4)
C(4)-C(3)-C(2)	119.5(4)	C(5)-C(4)-C(3)	120.7(4)
C(4)-C(5)-C(6)	120.2(4)	C(1)-C(6)-C(5)	120.0(4)
C(14)-C(11)-C(13)	106.9(4)	C(14)-C(11)-C(12)	105.8(4)
C(13)-C(11)-C(12)	106.2(4)	C(14)-C(11)-Al(1)	112.4(3)
C(13)-C(11)-Al(1)	112.2(3)	C(12)-C(11)-Al(1)	112.9(3)
C(23)-C(21)-C(24)	106.4(4)	C(23)-C(21)-C(22)	107.5(4)
C(24)-C(21)-C(22)	105.7(4)	C(23)-C(21)-Al(1)	112.4(3)
C(24)-C(21)-Al(1)	111.9(3)	C(22)-C(21)-Al(1)	112.5(3)

Symmetry transformations used to generate equivalent atoms:

* -x, -y, 1-z

Table of General Displacement Parameter Expressions - U's

	U11	U22	U33	U23	U13	U12
A(1)	47(1)	26(1)	41(1)	2(1)	18(1)	-1(1)
O(1)	40(1)	28(1)	44(1)	1(1)	11(1)	-6(1)
O(2)	76(2)	46(2)	65(2)	5(1)	32(2)	-21(1)
C(1)	37(2)	32(2)	53(2)	-7(2)	12(2)	-1(2)
C(2)	48(2)	36(2)	62(3)	-8(2)	22(2)	-6(2)
C(2A)	126(5)	69(3)	111(4)	16(3)	60(4)	-40(3)
C(3)	61(3)	43(2)	91(4)	-18(2)	29(3)	-17(2)
C(4)	51(3)	55(3)	92(4)	-31(3)	8(3)	-4(2)
C(5)	60(3)	56(3)	57(3)	-12(2)	-2(2)	7(2)
C(6)	58(2)	44(2)	50(2)	-2(2)	10(2)	-1(2)
C(11)	54(2)	47(2)	50(2)	2(2)	24(2)	1(2)
C(12)	85(3)	62(3)	91(4)	-26(3)	48(3)	3(3)
C(13)	122(4)	94(4)	66(3)	16(3)	59(3)	17(3)
C(14)	58(3)	100(4)	85(3)	-14(3)	30(2)	4(3)
C(21)	64(2)	32(2)	60(2)	5(2)	26(2)	7(2)
C(22)	69(3)	57(3)	174(6)	21(3)	53(4)	24(3)
C(23)	136(5)	77(4)	89(4)	48(3)	49(4)	50(3)
C(24)	112(4)	54(3)	124(5)	-23(3)	30(4)	24(3)

$[(tBu)_2Al(\mu-OCH_2CH_2SMe)]_2$ (**1.11**)

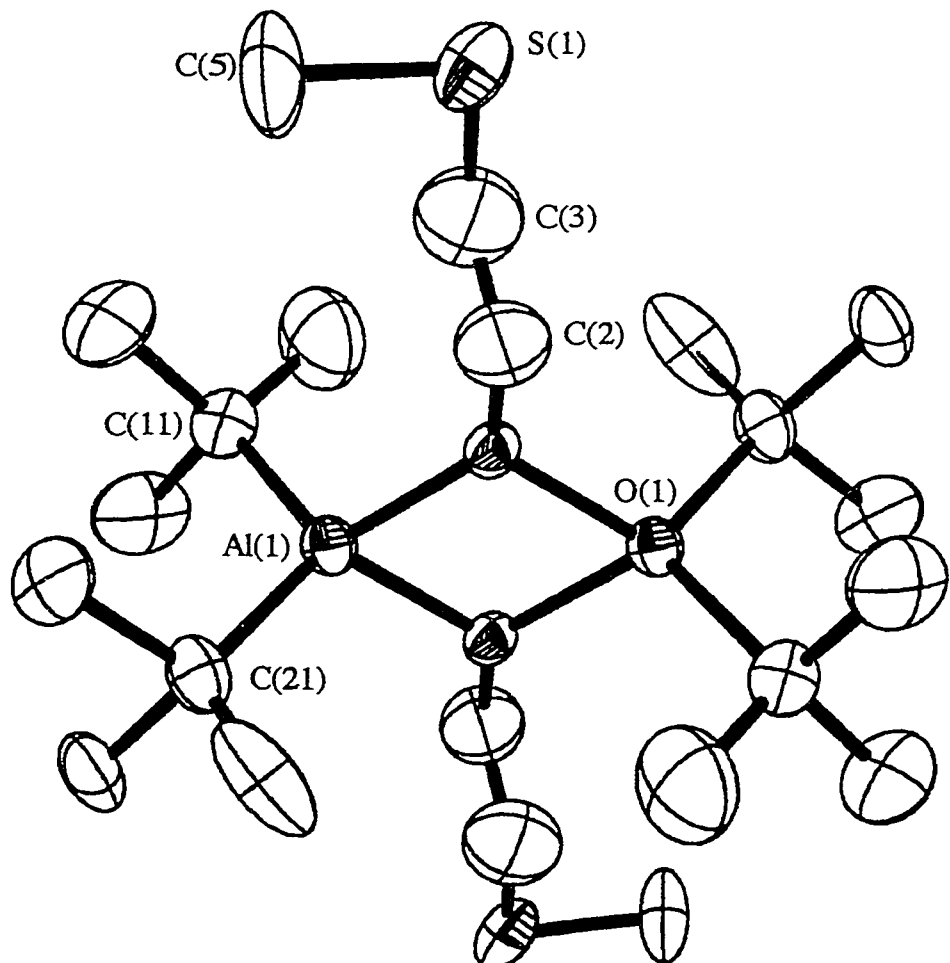


Figure 5. The molecular structure of $[(\text{tBu})_2\text{Al}(\mu\text{-OCH}_2\text{CH}_2\text{SMe})]_2$ (**1.11**).

Hydrogen atoms are omitted, and only one set of the disordered positions of the methyl groups attached to C(11) and C(21) in compound **1.11** is shown, for clarity.

Table of Positional Parameters and their Estimated Standard Deviations.

Atom	x	y	z	B (A2)
S	-0.0093(3)	0.8462(3)	0.6865(3)	11.40(8)
Al	0.5070(2)	0.3747(2)	0.6324(2)	4.92(4)
O	0.3870(4)	0.5835(4)	0.5393(3)	4.9(1)
C2	0.268(1)	0.710(1)	0.590(1)	12.4(4)
C3	0.136(2)	0.686(2)	0.614(1)	15.5(5)
C5	0.010(2)	0.746(2)	0.848(1)	17.0(5)
C11	0.3834(9)	0.2019(8)	0.6841(7)	7.1(2)
C12	0.270(1)	0.195(1)	0.810(1)	11.5(3)
C13	0.500(1)	0.034(1)	0.717(1)	12.9(4)
C14	0.281(1)	0.224(1)	0.576(1)	13.4(3)
C21	0.6395(9)	0.3637(9)	0.7730(7)	7.3(2)
C22	0.537(2)	0.339(2)	0.912(1)	11.6(5)
C23	0.763(2)	0.191(2)	0.821(1)	8.4(5)
C24	0.730(2)	0.478(2)	0.747(2)	13.3(5)
C22a	0.820(3)	0.348(3)	0.724(2)	12.3(6)*
C23a	0.591(3)	0.523(3)	0.803(2)	12.0(6)*
C24a	0.641(5)	0.259(5)	0.873(4)	23(1)*

Anisotropically refined atoms are given in the form of the isotropic equivalent displacement defined as: $(4/3) * [a^2 * B(1,1) + b^2 * B(2,2) + c^2 * B(3,3) + ab(\cos \gamma) * B(1,2) + ac(\cos \beta) * B(1,3) + bc(\cos \alpha) * B(2,3)]$

Table of Positional Parameters and their Estimated Standard Deviations.

<u>Atom</u>	<u>x</u>	<u>y</u>	<u>z</u>	<u>B (A2)</u>
H2a	0.2638	0.8156	0.5225	16*
H2b	0.3063	0.7049	0.6707	16*
H3a	0.0957	0.6960	0.5333	20*
H3b	0.1407	0.5792	0.6797	20*
H5a	-0.0556	0.8105	0.8977	22*
H5b	-0.0233	0.6466	0.8742	22*
H5c	0.1219	0.7212	0.8668	22*
H12a	0.2138	0.1109	0.8299	14*
H12b	0.3315	0.1716	0.8838	14*
H12c	0.1923	0.2971	0.7937	14*
H13a	0.4394	-0.0469	0.7410	16*
H13b	0.5720	0.0304	0.6390	16*
H13c	0.5623	0.0128	0.7902	16*
H14a	0.2255	0.1385	0.6059	17*
H14b	0.2036	0.3267	0.5556	17*
H14c	0.3494	0.2210	0.4963	17*
H22a	0.6022	0.3338	0.9779	15*

Table of Positional Parameters and their Estimated Standard Deviations.

Atom	x -	y -	z -	B(A2)
H22b	0.4433	0.4279	0.9016	15*
H22c	0.5030	0.2394	0.9408	15*
H23a	0.8274	0.1841	0.8883	10*
H23b	0.7042	0.1075	0.8580	10*
H23c	0.8332	0.1755	0.7454	10*
H24a	0.7848	0.4534	0.8255	17*
H24b	0.8076	0.4745	0.6729	17*
H24c	0.6582	0.5842	0.7251	17*
H22a1	0.8802	0.3435	0.7937	16*
H22b1	0.8618	0.2514	0.7037	16*
H22c1	0.8316	0.4408	0.6449	16*
H23a1	0.6569	0.5125	0.8709	15*
H23b1	0.6069	0.6117	0.7227	15*
H23c1	0.4788	0.5419	0.8354	15*
H24a1	0.7081	0.2673	0.9316	29*
H24b1	0.5325	0.2638	0.9139	29*
H24c1	0.6834	0.1583	0.8591	29*

Table of Bond Distances in Angstroms.

<u>Atom 1</u>	<u>Atom 2</u>	<u>Distance</u>	<u>Atom 1</u>	<u>Atom 2</u>	<u>Distance</u>
S	C3	1.94(1)	C11	C13	1.52(1)
S	C5	1.62(1)	C11	C14	1.48(2)
Al	O	1.852(3)	C21	C22	1.56(2)
Al	C11	1.994(9)	C21	C23	1.57(2)
Al	C21	1.984(9)	C21	C24	1.38(2)
Al	O'	1.851(2)	C21	C22a	1.53(2)
O	C2	1.51(1)	C21	C23a	1.54(3)
C2	C3	1.17(2)	C21	C24a	1.12(3)
C11	C12	1.51(1)			

Numbers in parentheses are estimated standard deviations in the least significant digits.

Table of Bond Angles in Degrees.

Atom 1	Atom 2	Atom 3	Angle	Atom 1	Atom 2	Atom 3	Angle
C3	S	C5	99.9(6)	C12	C11	C13	106.1(7)
O	Al	C11	113.8(2)	C12	C11	C14	106.5(8)
O	Al	C21	114.1(3)	C13	C11	C14	107.5(9)
O	Al	O'	78.8(1)	Al	C21	C22	110.6(9)
C11	Al	C21	116.8(3)	Al	C21	C23	108.9(9)
C11	Al	O'	113.5(3)	Al	C21	C24	121.2(8)
C21	Al	O'	114.2(2)	Al	C21	C22a	112.(1)
Al	O	C2	131.1(4)	Al	C21	C23a	112.0(9)
Al	O	Al'	101.2(2)	Al	C21	C24a	117.(3)
C2	O	Al'	125.7(4)	C22	C21	C23	95.7(8)
O	C2	C3	111.(1)	C22	C21	C24	111.(1)
S	C3	C2	110.(1)	C23	C21	C24	106.(1)
Al	C11	C12	112.6(7)	C22a	C21	C23a	104.(1)
Al	C11	C13	110.5(6)	C22a	C21	C24a	104.(2)
Al	C11	C14	113.2(5)	C23a	C21	C24a	107.(3)

Table of General Displacement Parameter Expressions - U's

35

Name	U(1,1)	U(2,2)	U(3,3)	U(1,2)	U(1,3)	U(2,3)
S	0.127(2)	0.143(2)	0.140(2)	0.018(1)	0.014(1)	-0.071(1)
Al	0.0704(9)	0.0614(8)	0.0557(8)	-0.0224(7)	-0.0082(7)	-0.0154(6)
O	0.064(2)	0.060(2)	0.063(2)	-0.017(2)	0.000(2)	-0.025(1)
C2	0.131(7)	0.165(8)	0.141(8)	-0.062(6)	0.015(6)	-0.010(7)
C3	0.180(9)	0.24(1)	0.196(9)	-0.072(7)	-0.037(7)	-0.086(7)
C5	0.24(1)	0.209(9)	0.139(7)	0.094(8)	-0.051(8)	-0.084(6)
C11	0.105(4)	0.077(4)	0.086(4)	-0.039(3)	0.004(4)	-0.019(3)
C12	0.156(7)	0.140(6)	0.135(7)	-0.083(5)	0.041(6)	-0.030(5)
C13	0.155(8)	0.075(4)	0.25(1)	-0.045(5)	0.000(8)	-0.043(5)
C14	0.244(7)	0.174(5)	0.129(7)	-0.162(4)	-0.036(5)	-0.005(5)
C21	0.113(5)	0.100(4)	0.062(3)	-0.027(4)	-0.023(3)	-0.017(3)
C22	0.15(1)	0.27(1)	0.061(6)	-0.07(1)	-0.007(6)	-0.095(5)
C23	0.13(1)	0.096(8)	0.095(8)	-0.003(8)	-0.060(7)	-0.035(6)
C24	0.23(1)	0.15(1)	0.15(1)	-0.102(8)	-0.137(7)	0.016(8)

The form of the anisotropic displacement parameter is:

$\exp[-2\pi i 2\{h^2a^2U(1,1) + k^2b^2U(2,2) + l^2c^2U(3,3) + 2hkabU(1,2) + 2hlacU(1,3) + 2klbcU(2,3)\}]$ where a, b, and c are reciprocal lattice parameters.

$[(iBu)_2Al(\mu-OCH_2CH_2SMe)]_2$ (**1.12**)

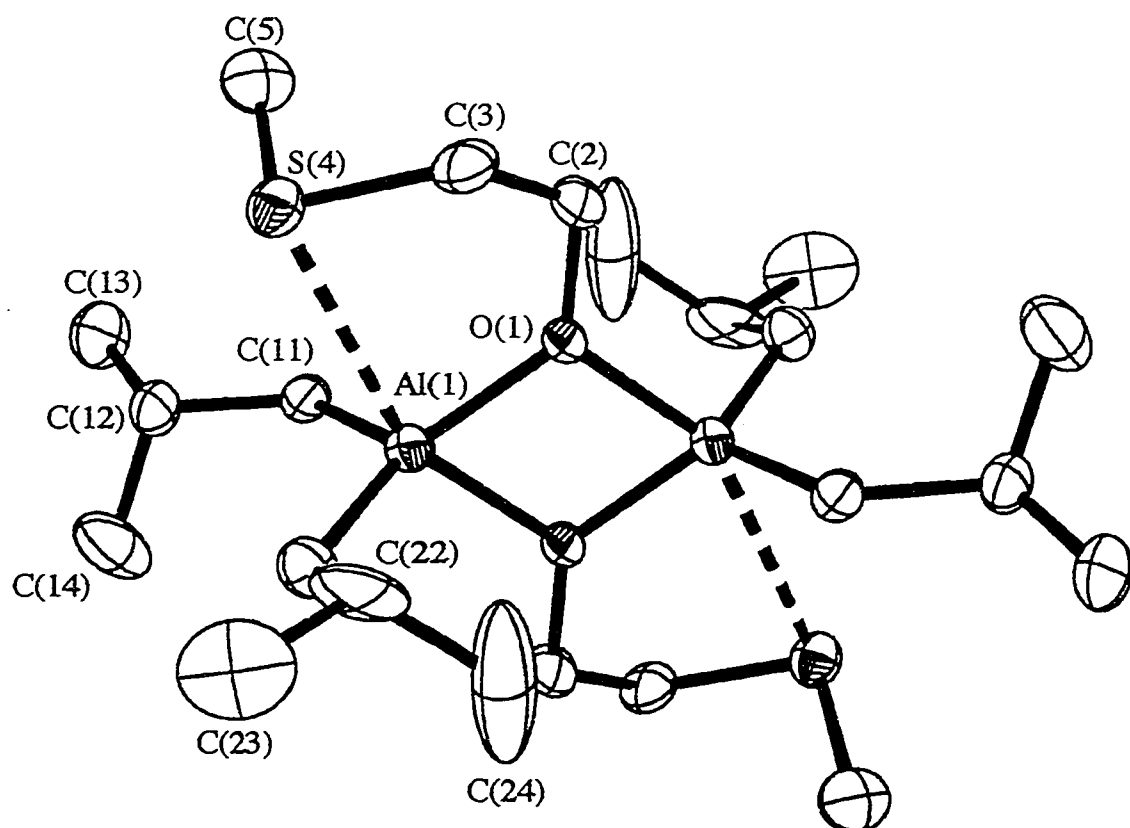


Figure 6. The molecular structure of $[(^{\text{i}}\text{Bu})_2\text{Al}(\mu\text{-OCH}_2\text{CH}_2\text{SMe})]_2$ (**1.12**).

Hydrogen atoms are omitted, and only one set of the disordered positions of the methyl groups attached to C(11) and C(21) in compound **1.12** is shown, for clarity.

Table of Positional Parameters and their Estimated Standard Deviations.

Atom	x	y	z	B(A2)
S4	-0.0204(1)	0.92337(6)	0.3533(1)	5.62(2)
A1	0.1077(1)	0.95622(6)	0.1020(1)	4.08(2)
O1	-0.0934(3)	0.9993(1)	0.0729(2)	4.33(5)
C2	-0.2246(5)	0.9948(3)	0.1444(4)	6.1(1)
C3	-0.1663(5)	0.9945(3)	0.2963(4)	6.4(1)
C5	-0.1401(6)	0.8404(3)	0.3241(5)	7.9(1)
C11	0.1186(5)	0.8479(2)	0.0689(4)	4.79(9)
C12	0.2380(5)	0.8004(2)	0.1679(5)	6.2(1)
C13	0.1995(7)	0.7177(3)	0.1568(6)	8.7(2)
C14	0.4061(6)	0.8127(3)	0.1448(9)	12.1(2)
C21	0.2892(5)	1.0045(2)	0.2245(4)	5.7(1)
C22	0.2807(6)	1.0802(3)	0.2892(7)	10.1(2)
C23	0.4184(9)	1.0973(4)	0.4044(7)	12.8(2)
C24	0.273(1)	1.1387(4)	0.1864(9)	23.6(3)

Anisotropically refined atoms are given in the form of the isotropic equivalent displacement parameter defined as:

$$(4/3) * [a2*B(1,1) + b2*B(2,2) + c2*B(3,3) + ab(\cos \gamma)*B(1,2) + ac(\cos \beta)*B(1,3) + bc(\cos \alpha)*B(2,3)]$$

Table of Positional Parameters and their Estimated Standard Deviations.

Atom	x	y	z	B (A2)
H2a	-0.2829	0.9501	0.1184	7*
H2b	-0.2933	1.0365	0.1203	7*
H3a	-0.1190	1.0416	0.3227	8*
H3b	-0.2560	0.9868	0.3399	8*
H5a	-0.2011	0.8362	0.2135	10*
H5b	-0.2195	0.8415	0.3804	10*
H5c	-0.0727	0.7981	0.3472	10*
H11a	0.1441	0.8417	-0.0199	6*
H11b	0.0143	0.8281	0.0693	6*
H12	0.2289	0.8160	0.2578	8*
H13a	0.2771	0.6841	0.2226	11*
H13b	0.2017	0.7022	0.0653	11*
H13c	0.0942	0.7106	0.1754	11*

Table of Positional Parameters and their Estimated Standard Deviations.

40

<u>Atom</u>	<u>x</u>	<u>y</u>	<u>z</u>	<u>B (A2)</u>
H14a	0.4399	0.8572	0.1880	15*
H14b	0.4072	0.8160	0.0491	15*
H14c	0.4740	0.7729	0.1837	15*
H21a	0.3729	1.0079	0.1727	7*
H21b	0.3202	0.9708	0.2989	7*
H22	0.1854	1.0787	0.3271	13*
H23a	0.4965	1.1001	0.3673	16*
H23b	0.4321	1.0584	0.4709	16*
H23c	0.4009	1.1432	0.4473	16*
H24a	0.2681	1.1860	0.2287	30*
H24b	0.3670	1.1365	0.1462	30*
H24c	0.1804	1.1318	0.1170	30*

Starred atoms were refined isotropically.

Table of Bond Distances in Angstroms.

<u>Atom 1</u>	<u>Atom 2</u>	<u>Distance</u>	<u>Atom 1</u>	<u>Atom 2</u>	<u>Distance</u>
S4	C3	1.789(4)	C2	C3	1.492(6)
S4	C5	1.790(5)	C11	C12	1.527(5)
A1	O1	1.841(2)	C12	C13	1.517(6)
A1	C11	1.973(4)	C12	C14	1.497(8)
A1	C21	1.969(4)	C21	C22	1.507(7)
A1	O1'	1.888(1)	C22	C23	1.502(8)
O1	C2	1.424(5)	C22	C24	1.45(1)

Numbers in parentheses are estimated standard deviations in the least significant digits.

Table of Bond Angles in Degrees.

<u>Atom 1</u>	<u>Atom 2</u>	<u>Atom 3</u>	<u>Angle</u>	<u>Atom 1</u>	<u>Atom 2</u>	<u>Atom 3</u>	<u>Angle</u>
C3	S4	C5	101.8(2)	O1	C2	C3	111.1(3)
O1	Al	C11	117.2(1)	S4	C3	C2	113.5(3)
O1	Al	C21	120.2(2)	Al	C11	C12	119.1(3)
O1	Al	O1'	77.31(8)	C11	C12	C13	113.0(4)
C11	Al	C21	118.6(2)	C11	C12	C14	110.6(4)
C11	Al	O1'	105.0(1)	C13	C12	C14	109.3(4)
C21	Al	O1'	106.8(1)	Al	C21	C22	124.3(3)
Al	O1	C2	132.8(2)	C21	C22	C23	114.5(4)
Al	O1	Al'	102.7(1)	C21	C22	C24	110.5(6)
C2	O1	Al'	123.8(2)	C23	C22	C24	108.0(5)

Numbers in parenthesis are estimated standard deviations in the least significant digits.

Table of General Displacement Parameter Expressions - U's

Name	U(1,1)	U(2,2)	U(3,3)	U(1,2)	U(1,3)	U(2,3)
S4	0.0829(6)	0.0700(6)	0.0614(5)	0.0016(6)	0.0152(5)	0.0047(6)
A1	0.0478(5)	0.0493(5)	0.0571(6)	0.0043(5)	0.0080(4)	0.0066(6)
O1	0.046(1)	0.061(1)	0.060(1)	0.009(1)	0.017(1)	0.011(1)
C2	0.061(2)	0.098(3)	0.080(2)	0.015(2)	0.030(2)	0.024(2)
C3	0.089(2)	0.086(3)	0.079(2)	0.017(2)	0.043(2)	0.010(2)
C5	0.106(3)	0.085(3)	0.117(3)	-0.015(3)	0.040(3)	0.006(3)
C11	0.064(2)	0.059(2)	0.060(2)	0.007(2)	0.014(2)	0.002(2)
C12	0.077(3)	0.057(2)	0.096(3)	0.017(2)	0.004(2)	0.001(2)
C13	0.116(4)	0.067(3)	0.147(4)	0.019(3)	0.021(4)	0.022(3)
C14	0.072(3)	0.084(4)	0.294(8)	0.017(3)	0.013(5)	0.007(5)
C21	0.069(2)	0.067(2)	0.077(3)	-0.006(2)	0.009(2)	0.005(2)
C22	0.068(3)	0.116(4)	0.198(6)	-0.025(3)	0.015(3)	-0.059(4)
C23	0.216(6)	0.157(5)	0.121(4)	-0.089(4)	0.046(4)	-0.045(4)
C24	0.350(8)	0.067(4)	0.357(8)	0.003(5)	-0.252(5)	0.004(5)

The form of the anisotropic displacement parameter is:
 $\exp[-2\pi i \{h^2a^2U(1,1) + k^2b^2U(2,2) + l^2c^2U(3,3) + 2hkabU(1,2) + 2hlacU(1,3) + 2klbcU(2,3)\}]$ where a, b, and c are reciprocal lattice parameters.

$[(t\text{Bu})_2\text{Al}(\mu\text{-OCH}_2\text{CH}_2\text{CH}_2\text{SMe})]_2$ (**1.15**)

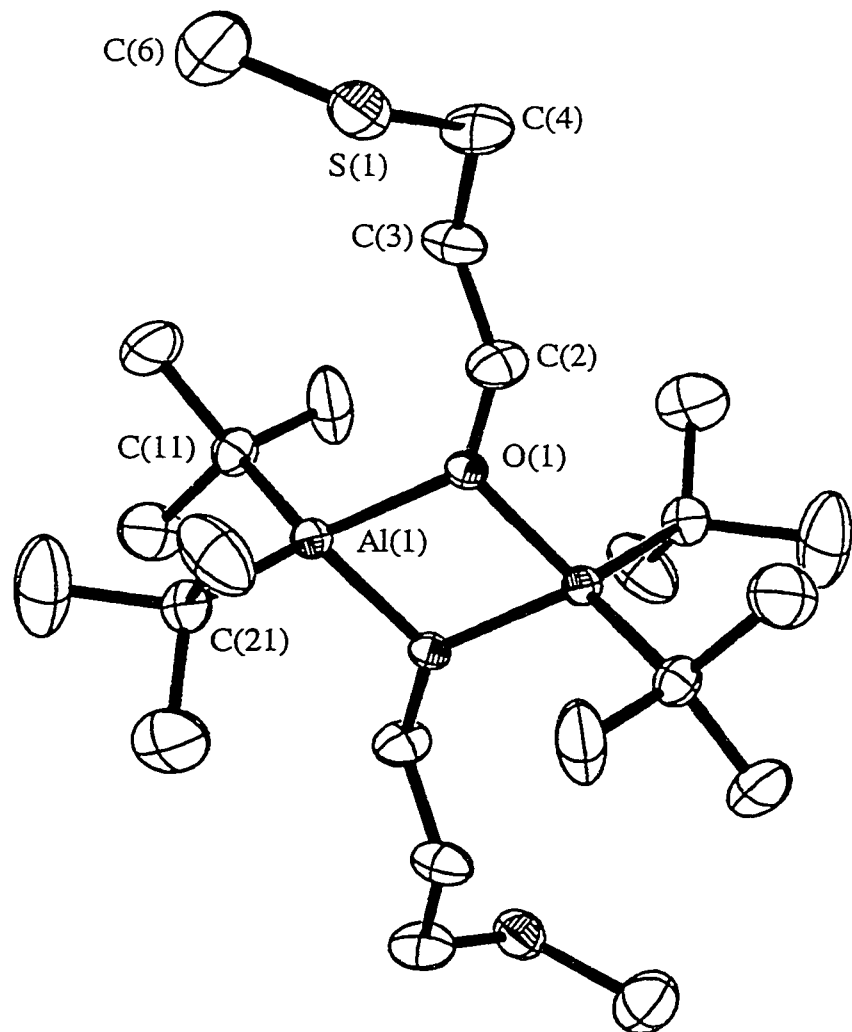


Figure 7. The molecular structure of $[(\text{tBu})_2\text{Al}(\mu-\text{OCH}_2\text{CH}_2\text{CH}_2\text{SMe})]_2$ (1.15). Thermal ellipsoids are drawn at the 30% probability level, and hydrogen atoms are omitted for clarity.

Table of Positional Parameters and their Estimated Standard Deviations.

Atom	X	Y	Z	B (Å²)
S5	0.3495(1)	-0.18970(7)	0.37317(9)	6.92(2)
A1	0.02695(8)	0.05364(5)	0.10455(7)	3.38(1)
O1	0.0846(2)	-0.0497(1)	0.0467(2)	3.40(3)
C2	0.1672(3)	-0.1198(2)	0.1065(3)	5.69(8)
C3	0.3243(4)	-0.1017(2)	0.1484(3)	6.66(9)
C4	0.3975(4)	-0.1752(2)	0.2221(3)	6.82(8)
C6	0.4537(6)	-0.1106(3)	0.4497(5)	10.3(1)
C11	0.1886(3)	0.1418(2)	0.1105(3)	5.06(7)
C12	0.2949(5)	0.1365(3)	0.2291(4)	9.0(1)
C13	0.1200(5)	0.2288(3)	0.1095(5)	9.3(1)
C14	0.2866(5)	0.1365(3)	0.0055(5)	11.0(1)
C21	-0.1035(3)	0.0470(2)	0.2452(3)	4.79(7)
C22	-0.2724(5)	0.0584(3)	0.2016(4)	9.2(1)
C23	-0.0952(6)	-0.0372(3)	0.3079(4)	10.7(1)
C24	-0.0716(6)	0.1149(4)	0.3372(5)	14.1(2)

Anisotropically refined atoms are given in the form of the isotropic equivalent displacement parameter defined as:

$$(4/3) * [a2*B(1,1) + b2*B(2,2) + c2*B(3,3) + ab(\cos \gamma)*B(1,2) + ac(\cos \beta)*B(1,3) + bc(\cos \alpha)*B(2,3)]$$

Table of Positional Parameters and their Estimated Standard Deviations.

47

Atom	X	Y	Z	B (Å ²)
-----	-----	-----	-----	-----
H2a	0.1661	-0.1648	0.0498	7*
H2b	0.1156	-0.1361	0.1752	7*
H3a	0.3276	-0.0533	0.1988	8*
H3b	0.3800	-0.0916	0.0794	8*
H4a	0.3699	-0.2248	0.1779	8*
H4b	0.5051	-0.1677	0.2259	8*
H6a	0.3963	-0.0596	0.4384	13*
H6b	0.5496	-0.1046	0.4169	13*
H6c	0.4696	-0.1235	0.5344	13*
H12a	0.3815	0.1877	0.2269	11*
H12b	0.3446	0.0837	0.2342	11*
H12c	0.2375	0.1435	0.2978	11*
H13a	0.2030	0.2719	0.1295	12*
H13b	0.0476	0.2316	0.1687	12*

Table of Positional Parameters and their Estimated Standard Deviations.

Atom	X	Y	Z	B (Å²)
H13c	0.0703	0.2400	0.0305	12*
H14a	0.2147	0.1457	-0.0835	14*
H14b	0.3338	0.0830	0.0056	14*
H14c	0.3629	0.1786	0.0143	14*
H22a	-0.3022	0.0170	0.1419	12*
H22b	-0.3320	0.0527	0.2692	12*
H22c	-0.2878	0.1123	0.1664	12*
H23a	-0.1635	-0.0444	0.3642	13*
H23b	0.0045	-0.0436	0.3478	13*
H23c	-0.1129	-0.0791	0.2469	13*
H24a	-0.0045	0.1712	0.3053	18*
H24b	-0.0145	0.0913	0.4065	18*
H24c	-0.1667	0.1347	0.3603	18*

Table of Bond Distances in Angstroms.

<u>Atom 1</u>	<u>Atom 2</u>	<u>Distance</u>	<u>Atom 1</u>	<u>Atom 2</u>	<u>Distance</u>
S5	C4	1.761(4)	C3	C4	1.534(5)
S5	C6	1.733(5)	C11	C12	1.534(5)
A1	O1	1.857(2)	C11	C13	1.516(5)
A1	C11	1.998(3)	C11	C14	1.500(6)
A1	C21	2.006(3)	C21	C22	1.528(5)
A1	O1'	1.850(2)	C21	C23	1.510(6)
O1	C2	1.459(3)	C21	C24	1.491(6)
C2	C3	1.444(4)			

Numbers in parentheses are estimated standard deviations in the least significant digits.

Table of Bond Angles in Degrees.

<u>Atom 1</u>	<u>Atom 2</u>	<u>Atom 3</u>	<u>Angle</u>	<u>Atom 1</u>	<u>Atom 2</u>	<u>Atom 3</u>	<u>Angle</u>
C4	S5	C6	101.4(2)	Al	C11	C12	111.5(2)
O1	Al	C11	115.1(1)	Al	C11	C13	111.5(2)
O1	Al	C21	114.1(1)	Al	C11	C14	113.0(2)
O1	Al	O1'	78.6(1)	C12	C11	C13	105.5(3)
C11	Al	C21	117.8(1)	C12	C11	C14	107.4(3)
C11	Al	O1'	111.8(1)	C13	C11	C14	107.6(3)
C21	Al	O1'	113.2(1)	Al	C21	C22	111.1(2)
Al	O1	C2	132.1(2)	Al	C21	C23	112.9(3)
Al	O1	Al'	101.40(8)	Al	C21	C24	113.3(3)
C2	O1	Al'	125.3(2)	C22	C21	C23	104.7(3)
O1	C2	C3	114.3(3)	C22	C21	C24	104.1(3)
C2	C3	C4	110.9(3)	C23	C21	C24	110.0(3)
S5	C4	C3	118.2(3)				

Numbers in parentheses are estimated standard deviations in the least significant digits.

Table of General Displacement Parameter Expressions - U's

Name	U(1,1)	U(2,2)	U(3,3)	U(1,2)	U(1,3)	U(2,3)
S5	0.0874(6)	0.0903(7)	0.0855(6)	-0.0025(5)	0.0095(5)	0.0198(5)
A1	0.0442(3)	0.0393(4)	0.0449(4)	0.0007(4)	0.0037(3)	-0.0007(4)
O1	0.0428(8)	0.0400(9)	0.0459(9)	0.0058(7)	0.0020(7)	0.0055(8)
C2	0.074(2)	0.058(2)	0.081(2)	0.021(1)	-0.012(2)	0.004(2)
C3	0.064(2)	0.097(2)	0.092(2)	0.019(2)	0.005(2)	0.026(2)
C4	0.081(2)	0.100(2)	0.077(2)	0.044(2)	-0.003(2)	0.015(2)
C6	0.130(3)	0.147(4)	0.112(3)	-0.010(3)	-0.005(3)	-0.011(3)
C11	0.063(2)	0.051(2)	0.078(2)	-0.012(1)	0.004(2)	-0.014(2)
C12	0.089(2)	0.109(3)	0.136(3)	-0.030(2)	-0.030(2)	-0.013(3)
C13	0.102(3)	0.064(2)	0.186(5)	-0.016(2)	-0.001(3)	-0.006(3)
C14	0.132(2)	0.137(3)	0.160(4)	-0.091(2)	0.079(2)	-0.055(3)
C21	0.073(2)	0.065(2)	0.046(1)	0.007(1)	0.013(1)	-0.002(1)
C22	0.089(2)	0.176(4)	0.091(3)	0.019(3)	0.035(2)	-0.008(3)
C23	0.164(3)	0.145(4)	0.111(3)	0.023(3)	0.078(2)	0.049(3)
C24	0.203(4)	0.211(5)	0.136(3)	-0.088(4)	0.096(3)	-0.098(3)

The form of the anisotropic displacement parameter is:

$\exp[-2\pi i \{h^2a^2U(1,1) + k^2b^2U(2,2) + l^2c^2U(3,3) + 2hkabU(1,2) + 2hlacU(1,3) + 2klbcU(2,3)\}]$ where a, b, and c are reciprocal lattice parameters.

Optimized structural parameters and energies for *ab initio* calculations
for $[H_2Al(\mu-OCH_2CH_2OH)]_2$

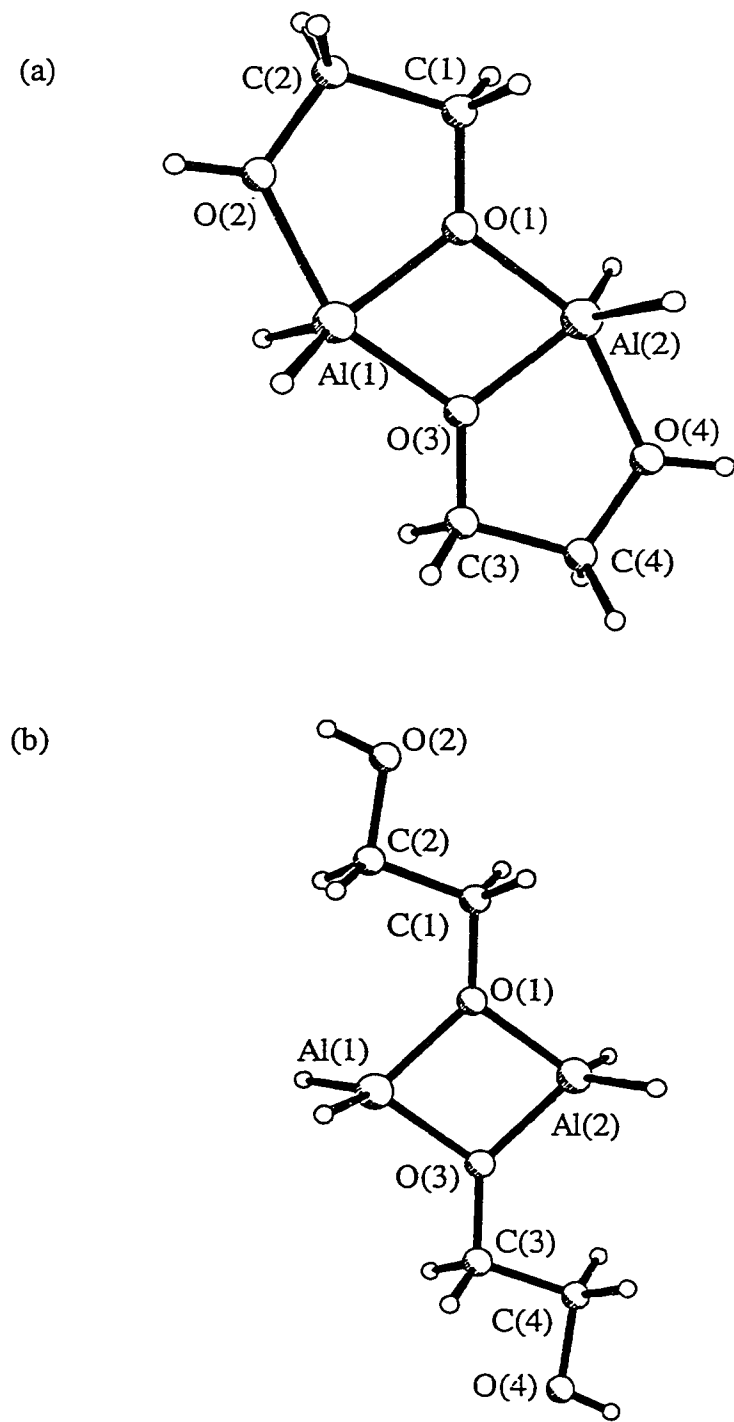


Figure 8. Ab initio HF/3-21G(*) calculated structures of (a) five-coordinate and (b) four-coordinate isomers of $[H_2Al(\mu-OCH_2CH_2OH)]_2$.

Optimized atomic coordinates (3-21G* level) and energy (MP2) of $[H_2Al(\mu-OCH_2CH_2OH)]_2$ (5-coordinate dimer).

Center Number	Atomic Number	X	Coordinates (\AA)	
			Y	Z
1	13	-1.467735	.000000	.000000
2	13	1.467735	.000000	.000000
3	8	-.035021	1.150105	.000000
4	8	.035021	-1.150105	.000000
5	8	-2.347184	1.814840	.000000
6	8	2.347184	-1.814840	.000000
7	6	-.070578	2.569135	.000000
8	6	.070578	-2.569135	.000000
9	6	-1.556017	3.034098	.000000
10	6	1.556017	-3.034098	.000000
11	1	-2.177924	-.447266	1.385874
12	1	-2.177924	-.447266	-1.385874
13	1	2.177924	.447266	1.385874
14	1	2.177924	.447266	-1.385874
15	1	-3.302641	1.938845	.000000
16	1	3.302641	-1.938845	.000000
17	1	.432805	2.947234	-.877857
18	1	.432805	2.947234	.877857
19	1	-.432805	-2.947234	-.877857
20	1	-.432805	-2.947234	.877857
21	1	-1.789204	3.608874	.883647
22	1	-1.789204	3.608874	-.883647
23	1	1.789204	-3.608874	.883647
24	1	1.789204	-3.608874	-.883647

EUMP2 energy = -938.99004324233 Hartrees

Optimized atomic coordinates (3-21G* level) and energy (MP2) of [H₂Al(μ-OCH₂CH₂OH)]₂ (4-coordinate dimer).

Center Number	Atomic Number	Coordinates (Å)		
		X	Y	Z
1	13	-1.384872	.000000	.000000
2	13	1.384872	.000000	.000000
3	8	.000933	1.198651	.000000
4	8	-.000933	-1.198651	.000000
5	8	-.992924	4.697072	.000000
6	8	.992924	-4.697072	.000000
7	6	.107611	2.648745	.000000
8	6	-.107611	-2.648745	.000000
9	6	-1.273303	3.286710	.000000
10.	6	1.273303	-3.286710	.000000
11	1	-2.197743	.000000	1.372365
12	1	-2.197743	.000000	-1.372365
13	1	2.197743	.000000	1.372365
14	1	2.197743	.000000	-1.372365
15	1	-1.804122	5.220124	.000000
16	1	1.804122	-5.220124	.000000
17	1	.643468	2.964861	-.880864
18	1	.643468	2.964861	.880864
19	1	-.643468	-2.964861	-.880864
20	1	-.643468	-2.964861	.880864
21	1	-1.822526	2.982892	.883465
22	1	-1.822526	2.982892	-.883465
23	1	1.822526	-2.982892	.883465
24	1	1.822526	-2.982892	-.883465

EUMP2 energy = -938.94057382592 Hartrees

Optimized atomic coordinates (3-21G* level) and energy (MP2) of $[H_2Al(\mu-OCH_2CH_2OH)]_2$ with Al-O(ether) fixed at 2.164 Å.

Center Number	Atomic Number	Coordinates (Å)		
		X	Y	Z
1	13	-1.461980	.000000	.000000
2	13	1.461980	.000000	.000000
3	8	-.013577	1.151722	.000000
4	8	.013577	-1.151722	.000000
5	8	-2.282566	2.000000	.000000
6	8	2.282566	-2.000000	.000000
7	6	.040061	2.573446	.000000
8	6	-.040061	-2.573446	.000000
9	6	-1.402476	3.147902	.000000
10	6	1.402476	-3.147902	.000000
11	1	-2.199831	-.377456	1.384238
12	1	-2.199831	-.377456	-1.384238
13	1	2.199831	.377456	1.384238
14	1	2.199831	.377456	-1.384238
15	1	-3.223033	2.209481	.000000
16	1	3.223033	-2.209481	.000000
17	1	.571617	2.912660	-.877342
18	1	.571617	2.912660	.877342
19	1	-.571617	-2.912660	-.877342
20	1	-.571617	-2.912660	.877342
21	1	-1.583956	3.744120	.882462
22	1	-1.583956	3.744120	-.882462
23	1	1.583956	-3.744120	.882462
24	1	1.583956	-3.744120	-.882462

EUMP2 energy = -938.98625261743 Hartrees

Optimized atomic coordinates (3-21G* level) and energy (MP2) of $[H_2Al(\mu-OCH_2CH_2OH)]_2$ with Al-O(ether) fixed at 2.249 Å.

Center Number	Atomic Number	X	Coordinates (Å)	
			Y	Z
1	13	-1.454679	.000000	.000000
2	13	1.454679	.000000	.000000
3	8	-.009271	1.156155	.000000
4	8	.009271	-1.156155	.000000
5	8	-2.260231	2.100000	.000000
6	8	2.260231	-2.100000	.000000
7	6	.084564	2.578142	.000000
8	6	-.084564	-2.578142	.000000
9	6	-1.334150	3.206945	.000000
10	6	1.334150	-3.206945	.000000
11	1	-2.202315	-.341749	1.384426
12	1	-2.202315	-.341749	-1.384426
13	1	2.202315	.341749	1.384426
14	1	2.202315	.341749	-1.384426
15	1	-3.189566	2.354340	.000000
16	1	3.189566	-2.354340	.000000
17	1	.628382	2.898094	-.877073
18	1	.628382	2.898094	.877073
19	1	-.628382	-2.898094	-.877073
20	1	-.628382	-2.898094	.877073
21	1	-1.486926	3.812884	.881769
22	1	-1.486926	3.812884	-.881769
23	1	1.486926	-3.812884	.881769
24	1	1.486926	-3.812884	-.881769

EUMP2 energy = -938.98182453730 Hartrees

Optimized atomic coordinates (3-21G* level) and energy (MP2) of [H₂Al(μ-OCH₂CH₂OH)]₂ with Al-O(ether) fixed at 2.338890 Å.

Center Number	Atomic Number	X	Coordinates (Å)	
			Y	Z
1	13	-1.447024	.000000	.000000
2	13	1.447024	.000000	.000000
3	8	-.007262	1.161201	.000000
4	8	.007262	-1.161201	.000000
5	8	-2.241005	2.200000	.000000
6	8	2.241005	-2.200000	.000000
7	6	.123981	2.582650	.000000
8	6	-.123981	-2.582650	.000000
9	6	-1.269745	3.263946	.000000
10	6	1.269745	-3.263946	.000000
11	1	-2.202526	-.310222	1.384310
12	1	-2.202526	-.310222	-1.384310
13	1	2.202526	.310222	1.384310
14	1	2.202526	.310222	-1.384310
15	1	-3.156843	2.499368	.000000
16	1	3.156843	-2.499368	.000000
17	1	.678956	2.883673	-.876808
18	1	.678956	2.883673	.876808
19	1	-.678956	-2.883673	-.876808
20	1	-.678956	-2.883673	.876808
21	1	-1.393621	3.878106	.881082
22	1	-1.393621	3.878106	-.881082
23	1	1.393621	-3.878106	.881082
24	1	1.393621	-3.878106	-.881082

EUMP2 energy = -938.97666988322 Hartrees

Optimized atomic coordinates (3-21G* level) and energy (MP2) of $[H_2Al(\mu-OCH_2CH_2OH)]_2$ with Al-O(ether) fixed at 2.520568 Å.

Center Number	Atomic Number	Coordinates (Å)		
		X	Y	Z
1	13	-1.431477	.000000	.000000
2	13	1.431477	.000000	.000000
3	8	-.005876	1.172355	.000000
4	8	.005876	-1.172355	.000000
5	8	-2.201712	2.400000	.000000
6	8	2.201712	-2.400000	.000000
7	6	.195962	2.590331	.000000
8	6	-.195962	-2.590331	.000000
9	6	-1.143840	3.372037	.000000
10	6	1.143840	-3.372037	.000000
11	1	-2.198705	-.255135	1.384072
12	1	-2.198705	-.255135	-1.384072
13	1	2.198705	.255135	1.384072
14	1	2.198705	.255135	-1.384072
15	1	-3.083697	2.788086	.000000
16	1	3.083697	-2.788086	.000000
17	1	.770425	2.854195	-.876273
18	1	.770425	2.854195	.876273
19	1	-.770425	-2.854195	-.876273
20	1	-.770425	-2.854195	.876273
21	1	-1.209643	3.998093	.879796
22	1	-1.209643	3.998093	-.879796
23	1	1.209643	-3.998093	.879796
24	1	1.209643	-3.998093	-.879796

EUMP2 energy = -938.96569315605 Hartrees

Optimized atomic coordinates (3-21G* level) and energy (MP2) of $[H_2Al(\mu-OCH_2CH_2OH)]_2$ with Al-O(ether) fixed at 2.702150 Å.

Center Number	Atomic Number	Coordinates (Å)		
		X	Y	Z
1	13	-1.417965	.000000	.000000
2	13	1.417965	.000000	.000000
3	8	-.005305	1.183556	.000000
4	8	.005305	-1.183556	.000000
5	8	-2.153908	2.600000	.000000
6	8	2.153908	-2.600000	.000000
7	6	.263912	2.595167	.000000
8	6	-.263912	-2.595167	.000000
9	6	-1.016186	3.472361	.000000
10	6	1.016186	-3.472361	.000000
11	1	-2.194184	-.210456	1.383145
12	1	-2.194184	-.210456	-1.383145
13	1	2.194184	.210456	1.383145
14	1	2.194184	.210456	-1.383145
15	1	-2.993619	3.073164	.000000
16	1	2.993619	-3.073164	.000000
17	1	.854568	2.822670	-.875738
18	1	.854568	2.822670	.875738
19	1	-.854568	-2.822670	-.875738
20	1	-.854568	-2.822670	.875738
21	1	-1.023973	4.104410	.878645
22	1	-1.023973	4.104410	-.878645
23	1	1.023973	-4.104410	.878645
24	1	1.023973	-4.104410	-.878645

EUMP2 energy = -938.95480459677 Hartrees

Optimized atomic coordinates (3-21G* level) and energy (MP2) of $[H_2Al(\mu-OCH_2CH_2OH)]_2$ with Al-O(ether) fixed at 2.792922 Å.

Center Number	Atomic Number	X	Coordinates (Å)
			Y Z
1	13	-1.412247	.000000 .000000
2	13	1.412247	.000000 .000000
3	8	-.005229	1.188980 .000000
4	8	.005229	-1.188980 .000000
5	8	-2.126678	2.700000 .000000
6	8	2.126678	-2.700000 .000000
7	6	.296492	2.596332 .000000
8	6	-.296492	-2.596332 .000000
9	6	-.951763	3.519394 .000000
10	6	.951763	-3.519394 .000000
11	1	-2.191426	-.192591 1.382800
12	1	-2.191426	-.192591 -1.382800
13	1	2.191426	.192591 1.382800
14	1	2.191426	.192591 -1.382800
15	1	-2.941897	3.214355 .000000
16	1	2.941897	-3.214355 .000000
17	1	.894219	2.805798 -.875467
18	1	.894219	2.805798 .875467
19	1	-.894219	-2.805798 -.875467
20	1	-.894219	-2.805798 .875467
21	1	-.930572	4.152439 .878046
22	1	-.930572	4.152439 -.878046
23	1	.930572	-4.152439 .878046
24	1	.930572	-4.152439 -.878046

EUMP2 energy = -938.94943388872 Hartrees

4_{4z}

[(tBu)₂Al(μ-O-2-C₅H₄N)]₂ (**2.1**).

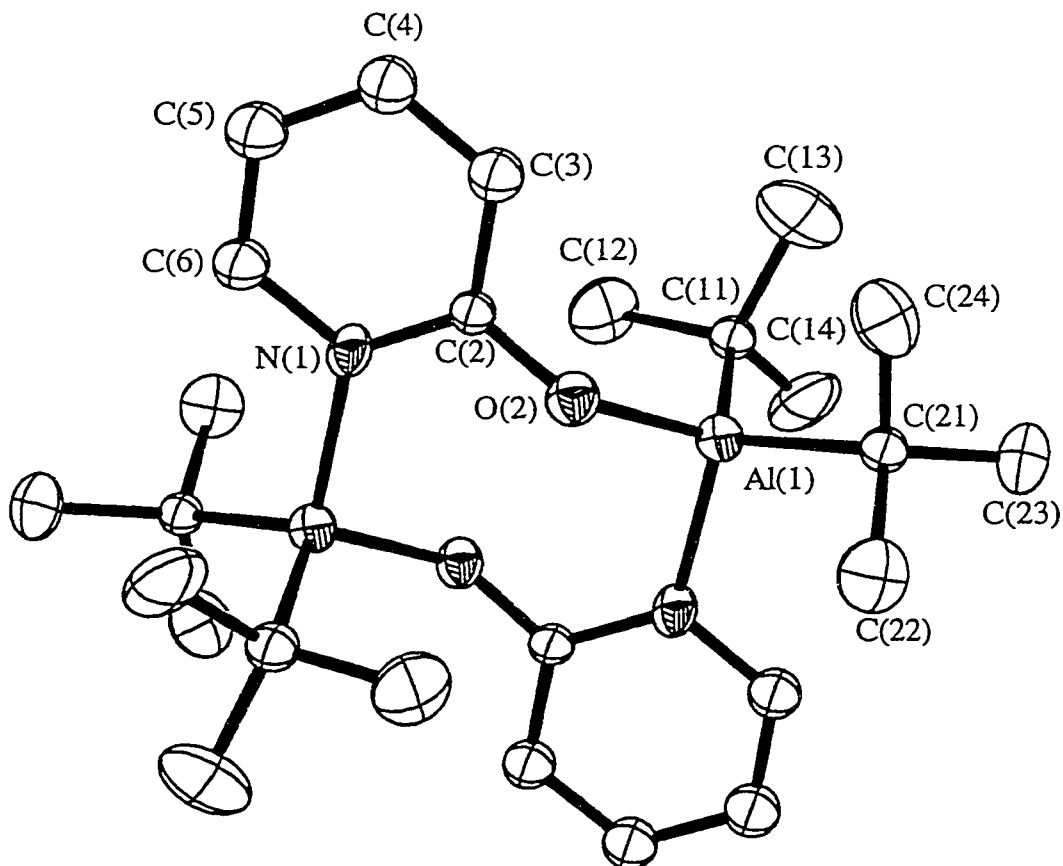


Figure 9. The molecular structure of $[(^t\text{Bu})_2\text{Al}(\mu-\text{O}-2-\text{C}_5\text{H}_4\text{N})]_2$ (2.1).

Thermal ellipsoids are drawn at the 30% probability level, and hydrogen atoms are omitted for clarity.

Table of Positional Parameters and their Estimated Standard Deviations.

Atom	x	y	z	B(A2)
A1	0.4110(3)	0.3622(2)	0.3028(2)	3.08(5)
O2	0.3167(5)	0.4384(5)	0.4338(4)	3.6(1)
N1	0.3371(6)	0.4658(6)	0.6367(4)	3.3(1)
C2	0.2441(8)	0.3913(7)	0.5149(6)	3.3(1)*
C3	0.066(1)	0.2676(8)	0.4775(7)	4.8(2)*
C4	-0.007(1)	0.2265(9)	0.5670(7)	5.4(2)*
C5	0.088(1)	0.3051(9)	0.6912(7)	5.5(2)*
C6	0.260(1)	0.4237(8)	0.7242(6)	4.7(2)*
C11	0.4353(9)	0.1460(8)	0.2747(6)	4.0(2)*
C12	0.486(1)	0.1321(9)	0.4000(8)	7.3(3)
C13	0.260(1)	-0.0037(9)	0.1971(9)	7.5(3)
C14	0.580(1)	0.121(1)	0.2053(9)	7.6(3)
C21	0.2753(9)	0.3860(7)	0.1613(6)	3.7(1)*
C22	0.317(1)	0.5735(9)	0.1903(7)	5.7(2)
C23	0.304(1)	0.300(1)	0.0281(7)	6.3(3)
C24	0.073(1)	0.3088(9)	0.1544(7)	5.9(2)

Starred atoms were refined isotropically.

Anisotropically refined atoms are given in the form of the isotropic equivalent displacement parameter defined as:

$$(4/3) * [a_2 * B(1,1) + b_2 * B(2,2) + c_2 * B(3,3) + ab(\cos \gamma) * B(1,2) + ac(\cos \beta) * B(1,3) + bc(\cos \alpha) * B(2,3)]$$

Table of Positional Parameters and their Estimated Standard Deviations.

Atom	x -	y -	z -	B (A2)
H3	-0.0009	0.2136	0.3906	6*
H4	-0.1251	0.1423	0.5421	7*
H5	0.0366	0.2785	0.7542	7*
H6	0.3272	0.4782	0.8111	6*
H12a	0.5013	0.0245	0.3834	9*
H12b	0.3917	0.1379	0.4431	9*
H12c	0.5960	0.2231	0.4523	9*
H13a	0.2710	-0.1199	0.1913	9*
H13b	0.2328	-0.0112	0.1129	9*
H13c	0.1650	0.0126	0.2365	9*
H14a	0.5907	-0.0011	0.1903	10*
H14b	0.6935	0.2092	0.2548	9*
H14c	0.5503	0.1222	0.1246	9*
H22a	0.4659	0.6441	0.2111	7*
H22b	0.2742	0.6235	0.2624	7*
H22c	0.2570	0.5796	0.1181	7*
H23a	0.2177	0.3033	-0.0498	8*
H23b	0.2805	0.1850	0.0099	8*
H23c	0.4268	0.3547	0.0302	8*
H24a	0.0536	0.3881	0.2549	7*
H24b	0.0390	0.1933	0.1390	7*
H24c	0.0010	0.3170	0.0881	7*

Table of Bond Distances in Angstroms.

66

<u>Atom 1</u>	<u>Atom 2</u>	<u>Distance</u>	<u>Atom 1</u>	<u>Atom 2</u>	<u>Distance</u>
A1	O2	1.774(5)	C4	C5	1.35(1)
A1	C11	1.963(8)	C5	C6	1.372(9)
A1	C21	1.990(8)	C11	C12	1.53(1)
A1	N1'	1.991(2)	C11	C13	1.514(9)
O2	C2	1.296(9)	C11	C14	1.51(1)
N1	C2	1.329(7)	C21	C22	1.54(1)
N1	C6	1.36(1)	C21	C23	1.53(1)
C2	C3	1.417(8)	C21	C24	1.53(1)
C3	C4	1.36(1)			

Numbers in parentheses are estimated standard deviations in the least significant digits.

Table of Bond Angles in Degrees.

<u>Atom 1</u>	<u>Atom 2</u>	<u>Atom 3</u>	<u>Angle</u>	<u>Atom 1</u>	<u>Atom 2</u>	<u>Atom 3 Angle</u>
O2	Al	C11	113.3(3)	C4	C5	C6 118.8(8)
O2	Al	C21	104.8(3)	N1	C6	C5 122.1(6)
O2	Al	N1'	102.4(1)	Al	C11	C12 112.6(4)
C11	Al	C21	120.3(3)	Al	C11	C13 112.2(6)
C11	Al	N1'	106.1(2)	Al	C11	C14 111.8(6)
C21	Al	N1'	108.5(2)	C12	C11	C13 105.6(7)
Al	O2	C2	140.0(4)	C12	C11	C14 106.7(7)
C2	N1	C6	119.6(5)	C13	C11	C14 107.5(6)
C2	N1	Al'	122.4(4)	Al	C21	C22 111.7(4)
C6	N1	Al'	118.0(3)	Al	C21	C23 116.3(6)
O2	C2	N1	118.7(5)	Al	C21	C24 106.8(6)
O2	C2	C3	121.5(5)	C22	C21	C23 107.3(7)
N1	C2	C3	119.7(6)	C22	C21	C24 106.3(7)
C2	C3	C4	119.5(6)	C23	C21	C24 107.9(5)
C3	C4	C5	120.3(6)			

Numbers in parentheses are estimated standard deviations in
the least significant digits.

Table of General Displacement Parameter Expressions - U's

68

Name	U(1,1)	U(2,2)	U(3,3)	U(1,2)	U(1,3)	U(2,3)
A1	0.0394(9)	0.0408(8)	0.0384(8)	0.0159(7)	0.0099(8)	0.0178(6)
O2	0.043(2)	0.052(2)	0.042(2)	0.018(2)	0.014(2)	0.021(2)
N1	0.041(3)	0.055(3)	0.036(2)	0.017(2)	0.020(2)	0.024(2)
C12	0.133(7)	0.073(4)	0.095(5)	0.060(4)	0.024(5)	0.044(3)
C13	0.094(6)	0.050(4)	0.121(7)	0.019(4)	-0.004(6)	0.028(4)
C14	0.130(6)	0.080(4)	0.109(6)	0.068(4)	0.057(5)	0.042(4)
C22	0.076(5)	0.081(4)	0.076(4)	0.039(3)	0.018(4)	0.043(3)
C23	0.099(6)	0.093(5)	0.046(4)	0.035(4)	0.013(4)	0.029(3)
C24	0.066(5)	0.088(4)	0.069(4)	0.029(3)	-0.004(4)	0.037(3)

The form of the anisotropic displacement parameter is:
 $\exp[-2\pi i \{h^2a^2U(1,1) + k^2b^2U(2,2) + l^2c^2U(3,3) + 2hkabU(1,2) + 2hlacU(1,3) + 2klacU(2,3)\}]$ where a, b, and c are reciprocal lattice parameters.

(^tBu)₂Al(O-8-C₉H₆N) (2.3)

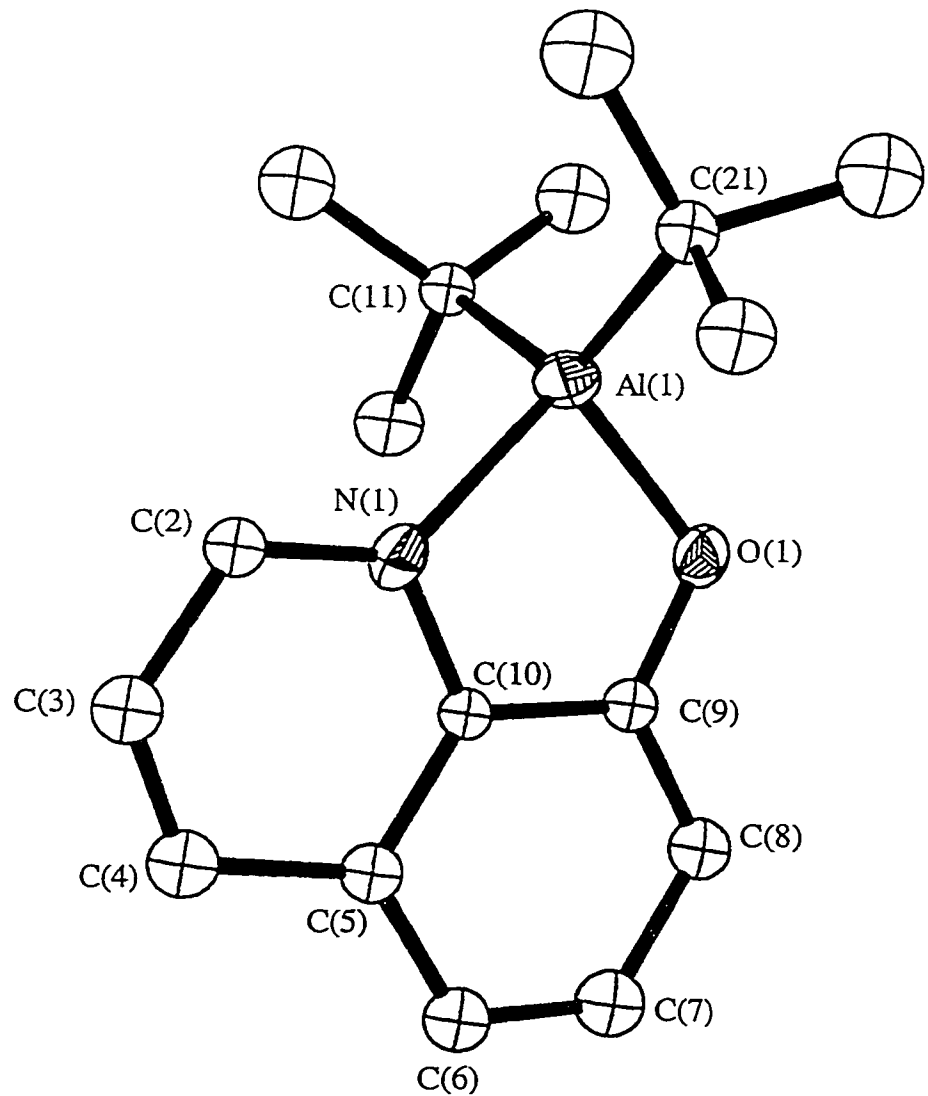


Figure 10. The molecular structure of $(^t\text{Bu})_2\text{Al}(\mu\text{-O-8-C}_9\text{H}_6\text{N})$ (2.3).

Thermal ellipsoids are drawn at the 30% probability level, and hydrogen atoms are omitted for clarity.

Table of Positional Parameters and their Estimated Standard Deviations.

Atom	x	y	z	B(A2)
A1	0.8132(1)	0.1195(2)	0.1848(1)	4.28(4)
O	0.9260(3)	0.0793(3)	0.1133(2)	4.8(1)
N	0.9678(3)	0.1604(3)	0.2943(3)	3.9(1)
C2	0.9821(5)	0.2067(5)	0.3848(4)	4.7(1)*
C3	1.1086(6)	0.2186(5)	0.4520(5)	6.2(2)*
C4	1.2118(5)	0.1857(5)	0.4230(4)	6.1(2)*
C5	1.2009(4)	0.1409(5)	0.3287(4)	4.9(1)*
C6	1.3003(5)	0.1048(5)	0.2886(4)	6.0(1)*
C7	1.2751(5)	0.0620(5)	0.1962(4)	6.7(2)*
C8	1.1494(5)	0.0484(5)	0.1306(4)	5.8(1)*
C9	1.0486(4)	0.0835(4)	0.1664(4)	4.3(1)*
C10	1.0749(4)	0.1283(5)	0.2654(3)	3.9(1)*
C11	0.7367(5)	-0.0034(5)	0.2385(4)	4.6(1)*
C12	0.6772(6)	0.0252(6)	0.3229(5)	8.5(2)*
C13	0.8392(6)	-0.0874(5)	0.2783(5)	7.4(2)*
C14	0.6372(6)	-0.0547(6)	-0.1496(5)	8.2(2)*
C21	0.7144(5)	0.2420(5)	0.1219(4)	5.1(1)*
C22	0.7995(5)	0.3377(5)	0.1166(5)	6.9(2)*
C23	0.6113(7)	0.2812(6)	0.1705(6)	9.8(2)*
C24	0.6459(7)	0.2159(7)	0.0075(6)	9.5(2)*

Starred atoms were refined isotropically.

Anisotropically refined atoms are given in the form of the isotropic equivalent displacement parameter defined as:

$$(4/3) * [a_2 * B(1,1) + b_2 * B(2,2) + c_2 * B(3,3) + ab(\cos \gamma) * B(1,2) + ac(\cos \beta) * B(1,3) + bc(\cos \alpha) * B(2,3)]$$

Table of Positional Parameters and their Estimated Standard Deviations.

72

<u>Atom</u>	<u>x</u>	<u>y</u>	<u>z</u>	<u>B (A2)</u>
H2	0.9091	0.2318	0.4051	6*
H3	1.1192	0.2503	0.5178	8*
H4	1.2947	0.1935	0.4691	7*
H6	1.3870	0.1110	0.3282	7*
H7	1.3457	0.0387	0.1717	8*
H8	1.1357	0.0163	0.0646	7*
H12a	0.7522	0.0641	0.3797	11*
H12b	0.6489	-0.0367	0.3509	11*
H12c	0.6064	0.0718	0.2984	11*
H13a	0.8781	-0.0674	0.3421	9*
H13b	0.8987	-0.0894	0.2370	9*
H13c	0.8009	-0.1555	0.2781	9*

Table of Positional Parameters and their Estimated Standard Deviations.

Atom	x	y	z	B (Å ²)
H14a	0.6804	-0.0905	0.0977	10*
H14b	0.5791	-0.0016	0.1147	10*
H14c	0.5911	-0.1070	0.1764	10*
H22a	0.8349	0.3662	0.1898	9*
H22b	0.7502	0.3912	0.0740	9*
H22c	0.8685	0.3166	0.0890	9*
H23a	0.6436	0.3108	0.2451	12*
H23b	0.5548	0.2235	0.1720	12*
H23c	0.5652	0.3363	0.1282	12*
H24a	0.6782	0.1592	-0.0171	12*
H24b	0.6537	0.2758	-0.0334	12*
H24c	0.5575	0.2029	0.0023	12*

Table of Bond Distances in Angstroms.

<u>Atom 1</u>	<u>Atom 2</u>	<u>Distance</u>	<u>Atom 1</u>	<u>Atom 2</u>	<u>Distance</u>
Al	O	1.806(4)	C5	C10	1.410(6)
Al	N	1.979(3)	C6	C7	1.314(8)
Al	C11	1.974(6)	C7	C8	1.419(7)
Al	C21	1.937(6)	C8	C9	1.369(8)
O	C9	1.327(5)	C9	C10	1.405(7)
N	C2	1.322(7)	C11	C12	1.486(9)
N	C10	1.370(6)	C11	C13	1.521(8)
C2	C3	1.432(7)	C11	C14	1.524(8)
C3	C4	1.336(9)	C21	C22	1.525(9)
C4	C5	1.363(8)	C21	C23	1.51(1)
C5	C6	1.395(8)	C21	C24	1.557(9)

Numbers in parentheses are estimated standard deviations in the least significant digits.

Table of Bond Angles in Degrees.

<u>Atom 1</u>	<u>Atom 2</u>	<u>Atom 3</u>	<u>Angle</u>	<u>Atom 1</u>	<u>Atom 2</u>	<u>Atom 3 Angle</u>
O	Al	N	85.3(2)	O	C9	C8 124.5(5)
O	Al	C11	112.2(2)	O	C9	C10 116.8(4)
O	Al	C21	111.1(2)	C8	C9	C10 118.7(4)
N	Al	C11	106.4(2)	N	C10	C5 123.0(4)
N	Al	C21	112.1(2)	N	C10	C9 114.3(4)
C11	Al	C21	123.2(2)	C5	C10	C9 122.7(5)
Al	O	C9	114.5(3)	Al	C11	C12 113.2(4)
Al	N	C2	132.2(3)	Al	C11	C13 109.8(4)
Al	N	C10	108.6(3)	Al	C11	C14 108.7(4)
C2	N	C10	119.1(4)	C12	C11	C13 108.5(5)
N	C2	C3	119.3(5)	C12	C11	C14 110.3(5)
C2	C3	C4	120.6(6)	C13	C11	C14 106.1(5)
C3	C4	C5	121.6(5)	Al	C21	C22 112.3(4)
C4	C5	C6	127.3(4)	Al	C21	C23 116.9(5)
C4	C5	C10	116.3(5)	Al	C21	C24 109.1(4)
C6	C5	C10	116.4(5)	C22	C21	C23 106.3(5)
C5	C6	C7	120.6(5)	C22	C21	C24 104.8(5)
C6	C7	C8	124.3(6)	C23	C21	C24 106.6(5)
C7	C8	C9	117.2(5)			

Numbers in parentheses are estimated standard deviations in the least significant digits.

Table of General Displacement Parameter Expressions - U's

Name	U(1,1)	U(2,2)	U(3,3)	U(1,2)	U(1,3)	U(2,3)
A1	0.0444(7)	0.058(1)	0.0605(9)	0.003(1)	0.0141(7)	-0.018(1)
O	0.061(2)	0.075(3)	0.048(2)	0.003(2)	0.017(2)	-0.020(2)
N	0.064(2)	0.046(3)	0.045(2)	-0.009(2)	0.024(2)	-0.016(2)

The form of the anisotropic displacement parameter is:

$\exp[-2\pi i^2 \{h^2 a^2 U(1,1) + k^2 b^2 U(2,2) + l^2 c^2 U(3,3) + 2hkabU(1,2) + 2hlacU(1,3) + 2klbcU(2,3)\}]$ where a, b, and c are reciprocal lattice parameters.

$[(iBu)_2Al(\mu-O-8-C_9H_6N)]_2$ (2.5).

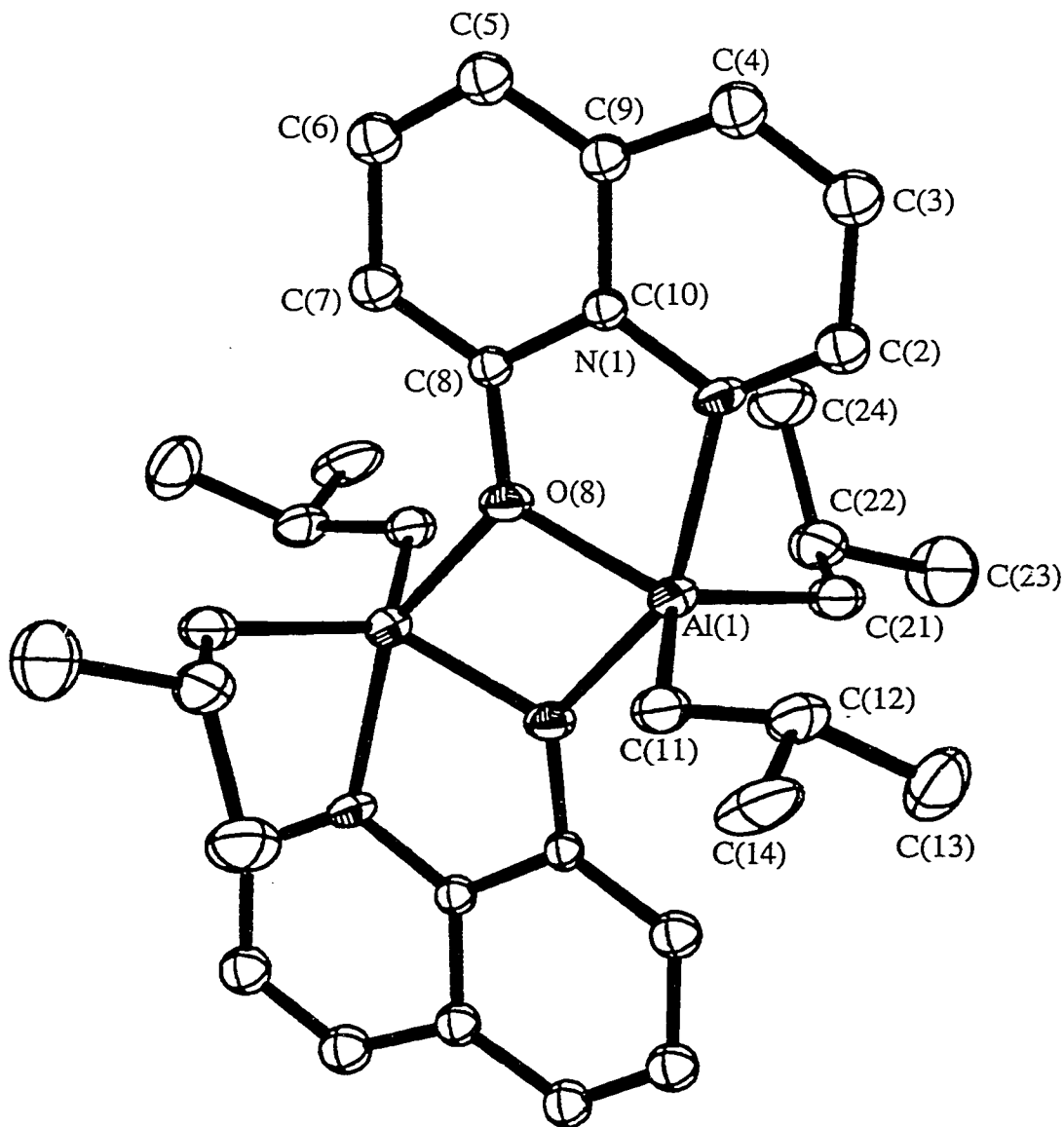


Figure 11. The molecular structure of $[(i\text{Bu})_2\text{Al}(\mu-\text{O}-8-\text{C}_9\text{H}_6\text{N})]_2$ (2.5).

Thermal ellipsoids are drawn at the 30% probability level, and hydrogen atoms are omitted for clarity.

Table of Positional Parameters and their Estimated Standard Deviations.

Atom	X	Y	Z	B(A2)
A1	0.4658(2)	0.5189(2)	0.6449(2)	3.68(5)
O8	0.5552(5)	0.5996(4)	0.4718(4)	4.0(1)
N1	0.5439(6)	0.6908(5)	0.6764(5)	3.9(1)
C2	0.5352(8)	0.7290(8)	0.7882(8)	5.3(2)*
C3	0.5956(9)	0.8494(8)	0.7866(8)	6.0(2)*
C4	0.6613(9)	0.9214(8)	0.6741(8)	5.9(2)*
C5	0.7472(9)	0.9521(8)	0.4306(8)	5.6(2)*
C6	0.7561(9)	0.9062(8)	0.3236(8)	5.4(2)*
C7	0.6921(8)	0.7830(8)	0.3296(8)	5.1(2)*
C8	0.6197(7)	0.7174(6)	0.4495(6)	3.6(1)*
C9	0.6771(8)	0.8883(7)	0.5533(7)	4.6(2)*
C10	0.6124(7)	0.7656(6)	0.5619(6)	3.7(1)*
C11	0.2520(8)	0.6070(7)	0.6522(7)	4.4(2)
C12	0.1844(8)	0.6404(8)	0.7785(8)	5.2(2)
C13	0.199(1)	0.504(1)	0.9063(9)	7.6(3)
C14	0.0233(9)	0.725(1)	0.754(1)	7.6(3)
C21	0.5804(8)	0.3523(7)	0.7997(7)	4.8(2)
C22	0.7312(9)	0.2696(8)	0.7754(8)	6.2(2)
C23	0.791(1)	0.131(1)	0.904(1)	9.6(4)
C24	0.843(1)	0.366(1)	0.725(1)	7.6(3)

Starred atoms were refined isotropically.

Anisotropically refined atoms are given in the form of the isotropic equivalent displacement parameter defined as:

$$(4/3) * [a2*B(1,1) + b2*B(2,2) + c2*B(3,3) + ab(\cos \gamma)*B(1,2) + ac(\cos \beta)*B(1,3) + bc(\cos \alpha)*B(2,3)]$$

Tables of Positional Parameters and their Estimated Standard Deviations

Atom	x	y	z	B (Å²)
---	-	-	-	-----
H2	0.4880	0.6753	0.8699	6*
H3	0.5883	0.8772	0.8663	7*
H4	0.7007	1.0017	0.6750	7*
H5	0.7913	1.0327	0.4221	7*
H6	0.8055	0.9549	0.2412	7*
H7	0.6999	0.7492	0.2534	6*
H11a	0.2005	0.5400	0.6391	5*
H11b	0.2324	0.6991	0.5752	5*
H12	0.2394	0.7038	0.7929	6*
H13a	0.3231	0.4492	0.9354	9*
H13b	0.1538	0.4342	0.8901	9*
H13c	0.1511	0.5298	0.9815	9*

Table of Positional Parameters and their Estimated Standard Deviations.

Atom	x	y	z	B (A2)
---	-	-	-	-----
H14a	-0.0251	0.6726	0.7211	9*
H14b	0.0173	0.8232	0.6877	9*
H14c	-0.0195	0.7307	0.8396	9*
H21a	0.5212	0.2800	0.8360	6*
H21b	0.5925	0.3918	0.8685	6*
H22	0.7172	0.2372	0.7018	8*
H23a	0.7162	0.0852	0.9380	12*
H23b	0.8245	0.1606	0.9723	12*
H23c	0.8698	0.0662	0.8779	12*
H24a	0.8250	0.4333	0.6253	9*
H24b	0.9390	0.3040	0.7337	9*
H24c	0.8364	0.4258	0.7806	9*

Table of Bond Distances in Angstroms.

<u>Atom 1</u>	<u>Atom 2</u>	<u>Distance</u>	<u>Atom 1</u>	<u>Atom 2</u>	<u>Distance</u>
A1	O8	1.879(4)	C5	C9	1.38(1)
A1	N1	2.124(7)	C6	C7	1.45(1)
A1	C11	1.983(7)	C7	C8	1.370(9)
A1	C21	1.975(6)	C8	C10	1.39(1)
A1	O8'	2.003(3)	C9	C10	1.44(1)
O8	C8	1.364(8)	C11	C12	1.51(1)
N1	C2	1.33(1)	C12	C13	1.48(1)
N1	C10	1.341(8)	C12	C14	1.53(1)
C2	C3	1.42(1)	C21	C22	1.50(1)
C3	C4	1.30(1)	C22	C23	1.53(1)
C4	C9	1.39(1)	C22	C24	1.50(1)
C5	C6	1.33(1)			

Numbers in parentheses are estimated standard deviations in the least significant digits.

Table of Bond Angles in Degrees.

<u>Atom 1</u>	<u>Atom 2</u>	<u>Atom 3</u>	<u>Angle</u>	<u>Atom 1</u>	<u>Atom 2</u>	<u>Atom 3</u>	<u>Angle</u>
O8	Al	N1	79.3(2)	C5	C6	C7	121.4(7)
O8	Al	C11	114.7(2)	C6	C7	C8	117.4(8)
O8	Al	C21	120.5(3)	O8	C8	C7	124.4(7)
O8	Al	O8'	72.2(2)	O8	C8	C10	114.9(5)
N1	Al	C11	96.4(3)	C7	C8	C10	120.7(7)
N1	Al	C21	96.0(3)	C4	C9	C5	129.8(8)
N1	Al	O8'	151.5(2)	C4	C9	C10	113.6(6)
C11	Al	C21	124.7(3)	C5	C9	C10	116.6(7)
C11	Al	O8'	96.6(3)	N1	C10	C8	116.2(6)
C21	Al	O8'	97.2(3)	N1	C10	C9	122.9(7)
Al	O8	C8	118.9(4)	C8	C10	C9	120.8(6)
Al	O8	Al'	107.8(2)	Al	C11	C12	121.7(5)
C8	O8	Al'	133.3(4)	C11	C12	C13	112.3(7)
Al	N1	C2	129.9(5)	C11	C12	C14	112.6(7)
Al	N1	C10	110.7(5)	C13	C12	C14	110.5(6)
C2	N1	C10	119.5(6)	Al	C21	C22	120.9(5)
N1	C2	C3	120.5(6)	C21	C22	C23	112.2(7)
C2	C3	C4	119.2(9)	C21	C22	C24	113.8(7)
C3	C4	C9	124.3(9)	C23	C22	C24	110.6(8)
C6	C5	C9	123.1(8)				

Numbers in parentheses are estimated standard deviations in the least significant digits.

Table of General Displacement Parameter Expressions - U's

Name	U(1,1)	U(2,2)	U(3,3)	U(1,2)	U(1,3)	U(2,3)
A1	0.047(1)	0.0466(9)	0.046(1)	-0.0112(8)	0.0025(9)	-0.0172(7)
O8	0.054(3)	0.047(2)	0.059(2)	-0.022(2)	0.006(2)	-0.025(2)
N1	0.045(3)	0.057(3)	0.053(3)	-0.008(2)	0.006(3)	-0.030(2)
C11	0.052(4)	0.054(3)	0.061(4)	-0.016(3)	-0.000(4)	-0.019(3)
C12	0.051(4)	0.077(4)	0.071(5)	-0.019(3)	0.009(4)	-0.028(3)
C13	0.078(6)	0.128(7)	0.067(5)	-0.007(5)	0.016(5)	-0.029(5)
C14	0.062(5)	0.097(6)	0.125(7)	-0.011(5)	0.021(5)	-0.042(5)
C21	0.058(4)	0.056(4)	0.071(4)	-0.014(3)	-0.008(4)	-0.023(3)
C22	0.087(6)	0.066(4)	0.080(5)	0.001(4)	-0.024(4)	-0.031(3)
C23	0.126(8)	0.089(6)	0.114(7)	0.015(6)	-0.047(7)	-0.011(6)
C24	0.068(6)	0.109(6)	0.111(6)	-0.013(5)	-0.007(5)	-0.040(5)

The form of the anisotropic displacement parameter is:

$$\exp[-2\pi i \{h^2a^2U(1,1) + k^2b^2U(2,2) + l^2c^2U(3,3) + 2hkabU(1,2) + 2hlacU(1,3) + 2klbcU(2,3)\}]$$
 where a, b, and c are reciprocal lattice parameters.

$[(^t\text{Bu})_2\text{Al}(\mu-\text{OC}_6\text{H}_4-2\text{-OMe})]_2$ (**3.1**).

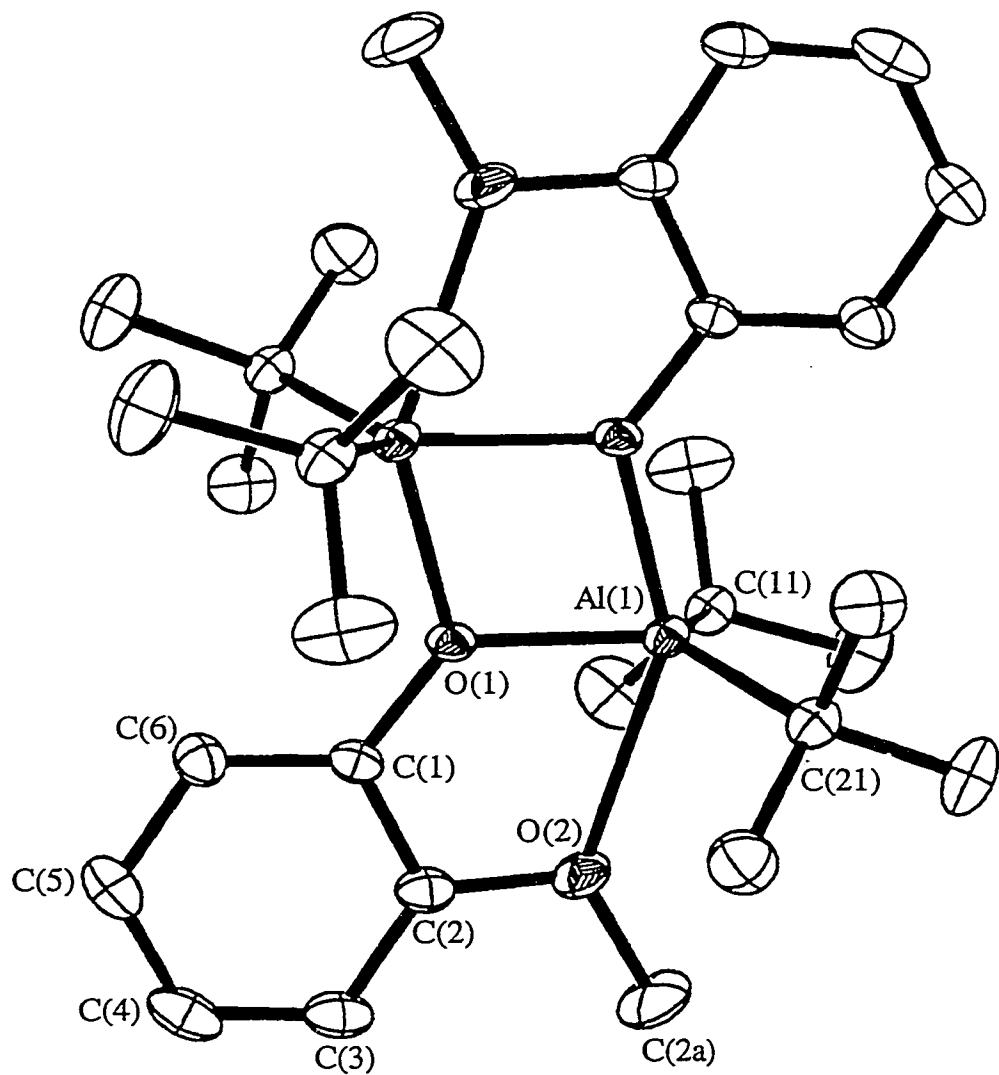


Figure 12. The molecular structure of $[(\text{tBu})_2\text{Al}(\mu-\text{OC}_6\text{H}_4-2\text{-OMe})]_2$ (3.1).

Thermal ellipsoids are drawn at the 30% probability level, and hydrogen atoms are omitted for clarity.

Tables of Positional Parameters and their Estimated Standard Deviations

	x	y	z	U(eq)
Al(1)	227(1)	562(1)	3972(1)	37(1)
O(1)	1023(3)	331(1)	5800(2)	38(1)
O(2)	2313(3)	1466(2)	4955(3)	60(1)
C(1)	2260(4)	704(2)	6731(4)	41(1)
C(2)	2993(4)	1307(2)	6291(4)	48(1)
C(2A)	2993(7)	2103(3)	4436(6)	97(2)
C(3)	4274(5)	1687(3)	7174(5)	64(1)
C(4)	4819(5)	1464(3)	8489(6)	70(1)
C(5)	4095(5)	880(3)	8934(4)	63(1)
C(6)	2811(5)	497(2)	8057(4)	52(1)
C(11)	1483(4)	143(2)	2836(4)	48(1)
C(12)	1036(6)	-702(3)	2365(5)	75(1)
C(13)	1226(7)	628(3)	1566(5)	87(2)
C(14)	3257(5)	133(3)	3589(5)	79(2)
C(21)	-1360(5)	1455(2)	3492(4)	51(1)
C(22)	-2987(6)	1213(3)	3510(7)	97(2)
C(23)	-1575(7)	1790(3)	2125(5)	98(2)
C(24)	-847(7)	2124(3)	4472(6)	99(2)

Tables of Positional Parameters and their Estimated Standard Deviations

	x	y	z	U(eq)
H(2AA)	2430 (7)	2163 (3)	3500 (6)	145
H(2AB)	4083 (7)	1993 (3)	4571 (6)	145
H(2AC)	2916 (7)	2574 (3)	4894 (6)	145
H(3A)	4763 (5)	2090 (3)	6879 (5)	77
H(4A)	5691 (5)	1713 (3)	9082 (6)	84
H(5A)	4466 (5)	739 (3)	9829 (4)	76
H(6A)	2320 (5)	100 (2)	8364 (4)	63
H(12A)	-76 (6)	-731 (3)	1882 (5)	112
H(12B)	1293 (6)	-1040 (3)	3126 (5)	112
H(12C)	1615 (6)	-860 (3)	1795 (5)	112
H(13A)	119 (7)	649 (3)	1063 (5)	131
H(13B)	1782 (7)	393 (3)	1035 (5)	131
H(13C)	1617 (7)	1146 (3)	1809 (5)	131
H(14A)	3468 (5)	-165 (3)	4392 (5)	119
H(14B)	3625 (5)	656 (3)	3811 (5)	119
H(14C)	3793 (5)	-96 (3)	3037 (5)	119
H(22A)	-2889 (6)	996 (3)	4366 (7)	145
H(22B)	-3429 (6)	831 (3)	2829 (7)	145
H(22C)	-3667 (6)	1659 (3)	3347 (7)	145
H(23A)	-1900 (7)	1386 (3)	1468 (5)	147
H(23B)	-595 (7)	2009 (3)	2118 (5)	147
H(23C)	-2368 (7)	2189 (3)	1923 (5)	147
H(24A)	-697 (7)	1940 (3)	5358 (6)	148
H(24B)	-1647 (7)	2520 (3)	4242 (6)	148
H(24C)	126 (7)	2337 (3)	4437 (6)	148

Al(1)-O(1)	1.876(2)	Al(1)-O(1)*	1.966(2)
Al(1)-C(11)	2.040(4)	Al(1)-C(21)	2.042(4)
Al(1)-O(2)	2.390(3)	O(1)-C(1)	1.376(4)
O(2)-C(2)	1.374(5)	O(2)-C(2A)	1.451(5)
C(1)-C(6)	1.376(5)	C(1)-C(2)	1.391(5)
C(2)-C(3)	1.382(6)	C(3)-C(4)	1.373(7)
C(4)-C(5)	1.365(7)	C(5)-C(6)	1.384(6)
C(11)-C(14)	1.525(6)	C(11)-C(13)	1.539(6)
C(11)-C(12)	1.546(6)	C(21)-C(23)	1.516(6)
C(21)-C(24)	1.518(6)	C(21)-C(22)	1.526(6)
O(1)-Al(1)-O(1)*	75.03(11)	O(1)-Al(1)-C(11)	116.38(14)
O(1)*-Al(1)-C(11)	104.40(13)	O(1)-Al(1)-C(21)	114.22(14)
O(1)*-Al(1)-C(21)	103.83(14)	C(11)-Al(1)-C(21)	126.6(2)
O(1)-Al(1)-O(2)	73.31(10)	O(1)*-Al(1)-O(2)	148.33(11)
C(11)-Al(1)-O(2)	88.94(13)	C(21)-Al(1)-O(2)	89.97(14)
C(1)-O(1)-Al(1)	125.7(2)	C(1)-O(1)-Al(1)*	129.2(2)
Al(1)-O(1)-Al(1)*	104.97(11)	C(2)-O(2)-C(2A)	116.5(4)
C(2)-O(2)-Al(1)	109.6(2)	C(2A)-O(2)-Al(1)	133.9(3)
O(1)-C(1)-C(6)	123.0(3)	O(1)-C(1)-C(2)	117.7(3)
C(6)-C(1)-C(2)	119.3(3)	O(2)-C(2)-C(3)	126.2(4)
O(2)-C(2)-C(1)	113.5(3)	C(3)-C(2)-C(1)	120.3(4)
C(4)-C(3)-C(2)	119.5(4)	C(5)-C(4)-C(3)	120.7(4)
C(4)-C(5)-C(6)	120.2(4)	C(1)-C(6)-C(5)	120.0(4)
C(14)-C(11)-C(13)	106.9(4)	C(14)-C(11)-C(12)	105.8(4)
C(13)-C(11)-C(12)	106.2(4)	C(14)-C(11)-Al(1)	112.4(3)
C(13)-C(11)-Al(1)	112.2(3)	C(12)-C(11)-Al(1)	112.9(3)
C(23)-C(21)-C(24)	106.4(4)	C(23)-C(21)-C(22)	107.5(4)
C(24)-C(21)-C(22)	105.7(4)	C(23)-C(21)-Al(1)	112.4(3)
C(24)-C(21)-Al(1)	111.9(3)	C(22)-C(21)-Al(1)	112.5(3)

Symmetry transformations used to generate equivalent atoms:

* -x,-y,1-z

Table of General Displacement Parameter Expressions - U's

90

	U11	U22	U33	U23	U13	U12
A1(1)	47(1)	26(1)	41(1)	2(1) 18(1)		-1(1)
O(1)	40(1)	28(1)	44(1)	1(1) 11(1)		-6(1)
O(2)	76(2)	46(2)	65(2)	5(1) 32(2)		-21(1)
C(1)	37(2)	32(2)	53(2)	-7(2) 12(2)		-1(2)
C(2)	48(2)	36(2)	62(3)	-8(2) 22(2)		-6(2)
C(2A)	126(5)	69(3) 111(4)		16(3) 60(4)		-40(3)
C(3)	61(3)	43(2)	91(4)	-18(2) 29(3)		-17(2)
C(4)	51(3)	55(3)	92(4)	-31(3) 8(3)		-4(2)
C(5)	60(3)	56(3)	57(3)	-12(2) -2(2)		7(2)
C(6)	58(2)	44(2)	50(2)	-2(2) 10(2)		-1(2)
C(11)	54(2)	47(2)	50(2)	2(2) 24(2)		1(2)
C(12)	85(3)	62(3)	91(4)	-26(3) 48(3)		3(3)
C(13)	122(4)	94(4)	66(3)	16(3) 59(3)		17(3)
C(14)	58(3)	100(4)	85(3)	-14(3) 30(2)		4(3)
C(21)	64(2)	32(2)	60(2)	5(2) 26(2)		7(2)
C(22)	69(3)	57(3) 174(6)		21(3) 53(4)		24(3)
C(23)	136(5)	77(4)	89(4)	48(3) 49(4)		50(3)
C(24)	112(4)	54(3)	124(5)	-23(3) 30(4)		24(3)

$[(\text{BHT})\text{Al}(\text{H})(\mu\text{-OCH}_2\text{CH}_2\text{NMe}_2)]_2$ (**4.2**)

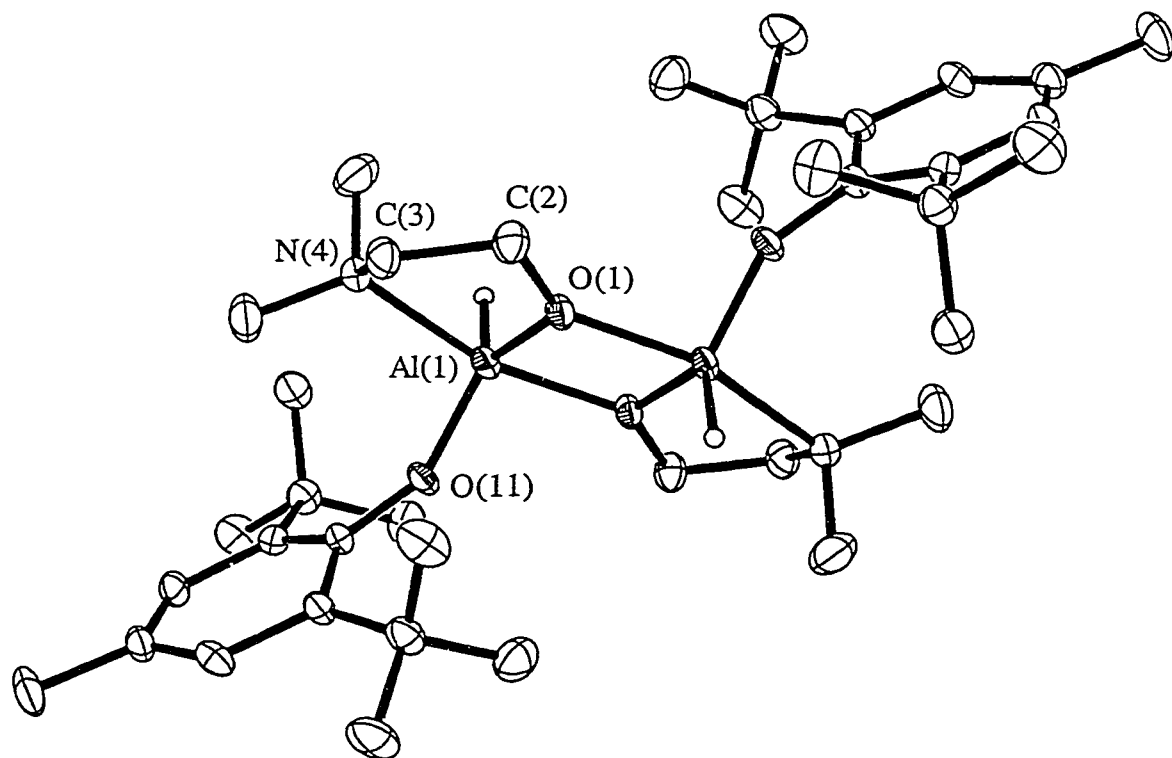


Figure 13. The molecular structure of $[(\text{BHT})\text{Al}(\text{H})(\mu\text{-OCH}_2\text{CH}_2\text{NMe}_2)]_2$ (4.2). Thermal ellipsoids are drawn at the 30% probability level, and hydrogen atoms are omitted for clarity.

Tables of Positional Parameters and their Estimated Standard Deviations

	x	y	z	U(eq)
Al	6280(1)	91(1)	5296(1)	28(1)
O(1)	4861(2)	692(2)	4755(2)	31(1)
O(11)	6843(2)	776(2)	6363(2)	33(1)
N(4)	2658(3)	1032(2)	4127(3)	35(1)
C(2)	4643(4)	1555(3)	4486(4)	39(1)
C(3)	3426(4)	1622(3)	3750(4)	43(1)
C(11)	7639(3)	1000(3)	7277(3)	30(1)
C(12)	8718(4)	1348(3)	7247(4)	33(1)
C(13)	9581(4)	1391(3)	8225(4)	37(1)
C(14)	9395(4)	1177(3)	9203(4)	38(1)
C(15)	8276(4)	983(3)	9218(4)	37(1)
C(16)	7369(4)	909(3)	8275(3)	32(1)
C(41)	2345(5)	1414(4)	5058(5)	61(2)
C(42)	1584(4)	919(3)	3252(5)	61(2)
C(121)	8973(4)	1702(3)	6213(4)	39(1)
C(122)	10050(4)	2279(3)	6490(4)	55(2)
C(123)	9226(4)	991(3)	5489(4)	46(1)
C(124)	7958(4)	2242(3)	5591(4)	52(1)
C(141)	10369(4)	1191(4)	10229(4)	58(2)
C(161)	6120(4)	756(3)	8371(4)	39(1)
C(162)	6031(5)	901(4)	9528(4)	59(2)
C(163)	5723(5)	-150(3)	8067(4)	56(2)
C(164)	5287(4)	1388(3)	7658(4)	55(1)
C(1S)	12477(5)	-1024(4)	7535(5)	71(2)
Cl(1)	11696(2)	-1923(1)	7601(2)	105(1)
Cl(2)	11779(2)	-109(2)	7773(2)	115(1)

	x	y	z	U(eq)
H(2A)	5199(4)	1766(3)	4125(4)	47
H(2B)	4708(4)	1887(3)	5129(4)	47
H(3A)	3144(4)	2197(3)	3755(4)	52
H(3B)	3430(4)	1480(3)	3022(4)	52
H(13A)	10314(4)	1573(3)	8213(4)	44
H(15A)	8117(4)	898(3)	9876(4)	44
H(41A)	3031(5)	1493(4)	5634(5)	92
H(41B)	1822(5)	1046(4)	5289(5)	92
H(41C)	1980(5)	1952(4)	4854(5)	92
H(42A)	1076(4)	538(3)	3483(5)	91
H(42B)	1773(4)	690(3)	2633(5)	91
H(42C)	1209(4)	1456(3)	3075(5)	91
H(12A)	10708(4)	1961(3)	6882(4)	82
H(12B)	9920(4)	2746(3)	6919(4)	82
H(12C)	10191(4)	2490(3)	5840(4)	82
H(12D)	9865(4)	657(3)	5887(4)	69
H(12E)	9416(4)	1237(3)	4879(4)	69
H(12F)	8556(4)	639(3)	5252(4)	69
H(12G)	7808(4)	2681(3)	6048(4)	79
H(12H)	7284(4)	1893(3)	5353(4)	79
H(12I)	8145(4)	2490(3)	4981(4)	79
H(14A)	10076(4)	1024(4)	10820(4)	87
H(14B)	10682(4)	1752(4)	10350(4)	87
H(14C)	10964(4)	805(4)	10164(4)	87
H(16A)	6275(5)	1467(4)	9750(4)	89
H(16B)	6518(5)	503(4)	10002(4)	89
H(16C)	5245(5)	824(4)	9552(4)	89
H(16D)	6249(5)	-539(3)	8518(4)	83
H(16E)	5707(5)	-250(3)	7331(4)	83
H(16F)	4962(5)	-230(3)	8160(4)	83
H(16G)	5545(4)	1955(3)	7857(4)	82
H(16H)	4525(4)	1312(3)	7750(4)	82
H(16I)	5270(4)	1293(3)	6921(4)	82
H(1SA)	12614(5)	-988(4)	6831(5)	85
H(1SB)	13222(5)	-1063(4)	8060(5)	85
H(1)	6785(34)	176(26)	4264(33)	39(12)

Al-O(11)	1.744(3)	Al-O(1)'	1.832(3)
Al-O(1)	1.913(3)	Al-N(4)'	2.196(4)
O(1)-C(2)	1.415(5)	O(11)-C(11)	1.354(5)
N(4)-C(42)	1.482(6)	N(4)-C(3)	1.482(6)
N(4)-C(41)	1.482(6)	C(2)-C(3)	1.520(6)
C(11)-C(16)	1.420(6)	C(11)-C(12)	1.417(6)
C(12)-C(13)	1.408(6)	C(12)-C(121)	1.554(6)
C(13)-C(14)	1.384(6)	C(14)-C(15)	1.382(6)
C(14)-C(141)	1.518(6)	C(15)-C(16)	1.408(6)
C(16)-C(161)	1.555(6)	C(121)-C(124)	1.529(6)
C(121)-C(123)	1.543(7)	C(121)-C(122)	1.544(7)
C(161)-C(163)	1.527(7)	C(161)-C(164)	1.536(7)
C(161)-C(162)	1.546(6)	C(1S)-Cl(1)	1.717(7)
C(1S)-Cl(2)	1.739(7)		
O(11)-Al-O(1)'	125.2(2)	O(11)-Al-O(1)	95.82(14)
O(1)'-Al-O(1)	74.83(14)	O(11)-Al-N(4)'	99.48(14)
O(1)'-Al-N(4)'	80.10(13)	O(1)-Al-N(4)'	154.91(14)
C(2)-O(1)-Al'	123.6(3)	C(2)-O(1)-Al	131.1(3)
Al'-O(1)-Al	105.17(14)	C(11)-O(11)-Al	152.7(3)
C(42)-N(4)-C(3)	108.4(4)	C(42)-N(4)-C(41)	108.3(4)
C(3)-N(4)-C(41)	108.9(4)	C(42)-N(4)-Al'	118.1(3)
C(3)-N(4)-Al'	105.3(3)	C(41)-N(4)-Al'	107.6(3)
O(1)-C(2)-C(3)	107.8(4)	N(4)-C(3)-C(2)	109.2(4)
O(11)-C(11)-C(16)	119.3(4)	O(11)-C(11)-C(12)	121.0(4)
C(16)-C(11)-C(12)	119.7(4)	C(13)-C(12)-C(11)	117.0(4)
C(13)-C(12)-C(121)	119.3(4)	C(11)-C(12)-C(121)	123.6(4)
C(14)-C(13)-C(12)	123.4(4)	C(13)-C(14)-C(15)	117.5(4)
C(13)-C(14)-C(141)	121.4(4)	C(15)-C(14)-C(141)	121.1(5)
C(14)-C(15)-C(16)	122.4(4)	C(15)-C(16)-C(11)	118.0(4)
C(15)-C(16)-C(161)	118.9(4)	C(11)-C(16)-C(161)	123.1(4)
C(124)-C(121)-C(123)	110.2(4)	C(124)-C(121)-C(122)	107.0(4)
C(123)-C(121)-C(122)	106.5(4)	C(124)-C(121)-C(12)	110.0(4)
C(123)-C(121)-C(12)	112.1(4)	C(122)-C(121)-C(12)	111.0(4)
C(163)-C(161)-C(164)	110.2(4)	C(163)-C(161)-C(162)	107.0(4)
C(164)-C(161)-C(162)	106.5(4)	C(163)-C(161)-C(16)	111.5(4)
C(164)-C(161)-C(16)	109.7(4)	C(162)-C(161)-C(16)	111.7(4)
Cl(1)-C(1S)-Cl(2)	112.7(4)		
Al - H1	1.61(2)		
O(1)-Al-H1	99(1)	O(11)-Al-H1	117(1)
O(1)'-Al-H1	118(1)	N(4)'-Al-H1	92(1)

Symmetry transformations used to generate equivalent atoms:
` -x+1,-y,-z+1

Table of General Displacement Parameter Expressions - U's

	U11	U22	U33	U23	U13	U12
A1	25(1)	36(1)	20(1)	0(1)	0(1)	-2(1)
O(1)	25(2)	31(2)	30(2)	3(1)	-3(1)	0(1)
O(11)	27(2)	45(2)	23(2)	-8(1)	0(1)	-6(1)
N(4)	29(2)	38(2)	33(2)	-1(2)	1(2)	2(2)
C(2)	34(3)	36(3)	43(3)	10(2)	3(2)	1(2)
C(3)	42(3)	39(3)	42(3)	7(2)	0(2)	5(2)
C(11)	24(2)	33(3)	28(3)	-4(2)	0(2)	-2(2)
C(12)	28(2)	32(3)	36(3)	-4(2)	4(2)	2(2)
C(13)	23(2)	36(3)	45(3)	-7(2)	-2(2)	-5(2)
C(14)	37(3)	35(3)	32(3)	0(2)	-7(2)	4(2)
C(15)	44(3)	41(3)	22(3)	-1(2)	2(2)	-5(2)
C(16)	30(2)	37(3)	25(2)	-3(2)	2(2)	-3(2)
C(41)	61(4)	59(4)	67(4)	-3(3)	22(3)	21(3)
C(42)	44(3)	51(4)	68(4)	3(3)	-18(3)	5(3)
C(121)	33(3)	43(3)	40(3)	0(2)	12(2)	-5(2)
C(122)	54(3)	56(3)	56(4)	2(3)	18(3)	-17(3)
C(123)	39(3)	64(3)	38(3)	-3(3)	13(2)	-5(3)
C(124)	50(3)	58(4)	51(3)	21(3)	16(3)	4(3)
C(141)	47(3)	64(4)	44(3)	4(3)	-20(3)	-3(3)
C(161)	37(3)	52(3)	29(3)	-3(2)	10(2)	-7(2)
C(162)	64(4)	85(4)	35(3)	-15(3)	22(3)	-13(3)
C(163)	57(3)	68(4)	47(3)	-5(3)	22(3)	-24(3)
C(164)	42(3)	65(4)	61(4)	0(3)	20(3)	7(3)
C(1S)	54(3)	107(5)	48(4)	8(3)	6(3)	-5(3)
C1(1)	89(1)	118(2)	103(2)	26(1)	18(1)	-27(1)
C1(2)	137(2)	117(2)	83(1)	24(1)	18(1)	40(1)

[(BHT)Al(OCH₂CH₂OMe)(μ-OCH₂CH₂OMe)]₂ (**4.6**).

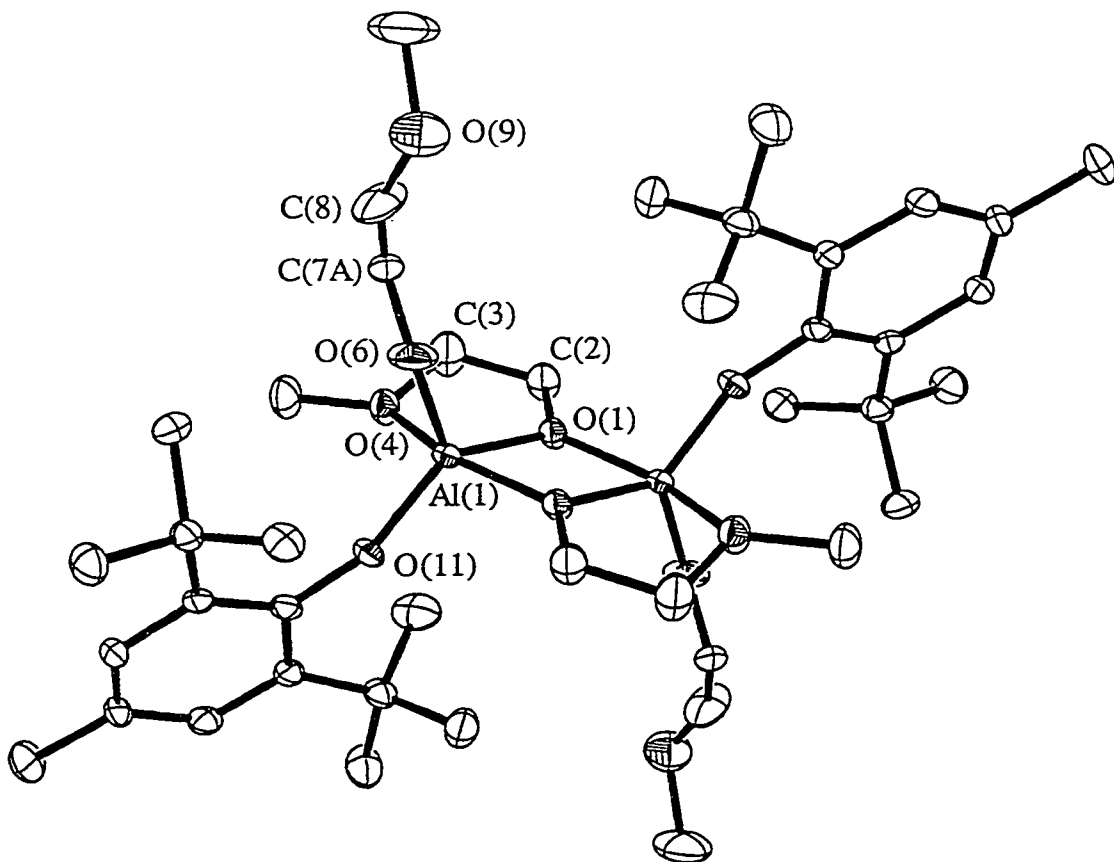


Figure 14. The molecular structure of $[(\text{BHT})\text{Al}(\text{OCH}_2\text{CH}_2\text{OMe})(\mu-\text{OCH}_2\text{CH}_2\text{OMe})]_2$ (4.6). Thermal ellipsoids are drawn at the 30% probability level, and hydrogen atoms are omitted for clarity.

	x	y	z	U(eq)
Al	412(1)	4933(1)	9006(1)	27(1)
O(1)	1098(3)	4452(3)	10295(2)	33(1)
O(4)	967(3)	4042(3)	12082(2)	41(1)
O(6)	-68(4)	3527(3)	8878(3)	58(1)
O(9A)	-1367(10)	428(7)	9363(7)	75(2)
O(9B)	-1902(16)	997(10)	8389(8)	132(5)
O(11)	2124(3)	5595(2)	8397(2)	31(1)
C(2)	2496(5)	3902(5)	10723(3)	45(1)
C(3)	2496(6)	3892(7)	11740(4)	70(2)
C(5)	729(6)	3849(5)	13116(3)	56(2)
C(7A)	-1070(10)	2928(9)	8567(7)	41(2)
C(7B)	-44(11)	2312(9)	9164(7)	39(2)
C(8)	-1052(9)	1618(6)	8794(5)	86(2)
C(10)	-2733(8)	-80(7)	9080(6)	101(3)
C(11)	3153(4)	6169(4)	7635(3)	29(1)
C(12)	3428(5)	7493(4)	7405(3)	31(1)
C(13)	4387(5)	8083(4)	6572(3)	36(1)
C(14)	5106(5)	7446(4)	5992(3)	36(1)
C(15)	4915(5)	6140(4)	6274(3)	35(1)
C(16)	3979(5)	5466(4)	7105(3)	28(1)
C(121)	2791(5)	8270(4)	8054(3)	38(1)
C(122)	1009(6)	8376(5)	8085(5)	63(2)
C(123)	3381(7)	9653(5)	7678(4)	64(2)
C(124)	3365(6)	7666(5)	9105(3)	51(1)
C(141)	6115(6)	8121(5)	5073(3)	56(2)
C(161)	3916(5)	4005(4)	7366(3)	33(1)
C(162)	5281(6)	3484(5)	6853(4)	49(1)
C(163)	4012(5)	3316(4)	8466(3)	42(1)
C(164)	2407(5)	3661(5)	6997(4)	44(1)
C(1S)	1834(12)	7909(12)	4543(10)	172(5)
Cl(1A)	564(14)	6929(14)	4375(9)	198(7)
Cl(2A)	2099(8)	9450(6)	3860(5)	149(2)
Cl(1B)	831(11)	6691(8)	4491(6)	92(2)
Cl(2B)	851(7)	9138(5)	4573(5)	151(2)

Tables of Positional Parameters and their Estimated Standard Deviations

	x	y	z	U(eq)
H(2A)	3370(5)	4385(5)	10346(3)	55
H(2B)	2609(5)	3039(5)	10708(3)	55
H(3A)	2939(6)	3094(7)	12152(4)	84
H(3B)	3126(6)	4578(7)	11775(4)	84
H(5A)	-352(6)	3975(5)	13266(3)	84
H(5B)	1333(6)	4444(5)	13289(3)	84
H(5C)	1047(6)	2998(5)	13486(3)	84
H(7AA)	-1017(10)	3285(9)	7852(7)	50
H(7AB)	-2087(10)	3161(9)	8788(7)	50
H(7BA)	-220(11)	2024(9)	9876(7)	47
H(7BB)	1008(11)	2049(9)	9032(7)	47
H(13A)	4544(5)	8951(4)	6403(3)	43
H(15A)	5427(5)	5693(4)	5899(3)	42
H(12A)	665(6)	8869(5)	8499(5)	95
H(12B)	581(6)	7541(5)	8347(5)	95
H(12C)	666(6)	8785(5)	7429(5)	95
H(12D)	2956(7)	10104(5)	8104(4)	96
H(12E)	3058(7)	10069(5)	7019(4)	96
H(12F)	4495(7)	9641(5)	7680(4)	96
H(12G)	2968(6)	8151(5)	9512(3)	77
H(12H)	4481(6)	7660(5)	9081(3)	77
H(12I)	3006(6)	6809(5)	9376(3)	77
H(14A)	6512(6)	7514(5)	4770(3)	84
H(14B)	6965(6)	8516(5)	5256(3)	84
H(14C)	5502(6)	8759(5)	4614(3)	84
H(16A)	5267(6)	3895(5)	6151(4)	73
H(16B)	5177(6)	2584(5)	7003(4)	73
H(16C)	6246(6)	3649(5)	7085(4)	73
H(16D)	4955(5)	3536(4)	8690(3)	63
H(16E)	4003(5)	2415(4)	8592(3)	63
H(16F)	3137(5)	3562(4)	8813(3)	63
H(16G)	2357(5)	4100(5)	6301(4)	66
H(16H)	1529(5)	3907(5)	7341(4)	66
H(16I)	2396(5)	2760(5)	7120(4)	66

Al-O(6)	1.704 (3)	Al-O(11)	1.730 (3)
Al-O(1)'	1.844 (3)	Al-O(1)	1.874 (3)
Al-O(4)'	2.025 (3)	O(1)-C(2)	1.410 (5)
O(4)-C(3)	1.403 (5)	O(4)-C(5)	1.430 (5)
O(6)-C(7B)	1.278 (9)	O(6)-C(7A)	1.293 (9)
O(9A)-C(8)	1.337 (9)	O(9A)-C(10)	1.459 (10)
O(9B)-C(8)	1.306 (11)	O(9B)-C(10)	1.462 (12)
O(11)-C(11)	1.364 (5)	C(2)-C(3)	1.455 (7)
C(7A)-C(8)	1.386 (11)	C(7B)-C(8)	1.417 (11)
C(11)-C(16)	1.409 (6)	C(11)-C(12)	1.427 (6)
C(12)-C(13)	1.397 (6)	C(12)-C(121)	1.534 (6)
C(13)-C(14)	1.369 (6)	C(14)-C(15)	1.389 (6)
C(14)-C(141)	1.525 (6)	C(15)-C(16)	1.408 (6)
C(16)-C(161)	1.547 (6)	C(121)-C(122)	1.536 (7)
C(121)-C(124)	1.539 (7)	C(121)-C(123)	1.550 (6)
C(161)-C(163)	1.517 (6)	C(161)-C(164)	1.539 (6)
C(161)-C(162)	1.547 (6)	C(1S)-Cl(2B)	1.594 (13)
C(1S)-Cl(1A)	1.66 (2)	C(1S)-Cl(1B)	1.66 (2)
C(1S)-Cl(2A)	1.690 (13)		
O(6)-Al-O(11)	116.0 (2)	O(6)-Al-O(1)'	112.8 (2)
O(11)-Al-O(1)'	131.0 (2)	O(6)-Al-O(1)	103.4 (2)
O(11)-Al-O(1)	97.49 (14)	O(1)'-Al-O(1)	75.01 (14)
O(6)-Al-O(4)'	92.8 (2)	O(11)-Al-O(4)'	94.88 (13)
O(1)'-Al-O(4)'	78.40 (13)	O(1)-Al-O(4)'	152.58 (14)
C(2)-O(1)-Al'	121.3 (3)	C(2)-O(1)-Al	133.2 (3)
Al'-O(1)-Al	104.99 (14)	C(3)-O(4)-C(5)	116.7 (4)
C(3)-O(4)-Al'	113.0 (3)	C(5)-O(4)-Al'	126.8 (3)
C(7B)-O(6)-Al	151.5 (5)	C(7A)-O(6)-Al	146.4 (5)
C(8)-O(9A)-C(10)	113.5 (8)	C(8)-O(9B)-C(10)	115.3 (9)
C(11)-O(11)-Al	159.3 (3)	O(1)-C(2)-C(3)	110.2 (4)
O(4)-C(3)-C(2)	109.5 (4)	O(6)-C(7A)-C(8)	123.4 (8)
O(6)-C(7B)-C(8)	122.1 (8)	O(11)-C(11)-C(16)	121.0 (4)
O(11)-C(11)-C(12)	118.8 (4)	C(16)-C(11)-C(12)	120.1 (4)
C(13)-C(12)-C(11)	117.8 (4)	C(13)-C(12)-C(121)	119.1 (4)
C(11)-C(12)-C(121)	123.1 (4)	C(14)-C(13)-C(12)	123.3 (4)
C(13)-C(14)-C(15)	117.9 (4)	C(13)-C(14)-C(141)	122.1 (4)
C(15)-C(14)-C(141)	120.0 (4)	C(14)-C(15)-C(16)	122.7 (4)
C(15)-C(16)-C(11)	117.8 (4)	C(15)-C(16)-C(161)	117.7 (4)
C(11)-C(16)-C(161)	124.5 (3)	C(12)-C(121)-C(122)	112.5 (4)
C(12)-C(121)-C(124)	109.3 (4)	C(122)-C(121)-C(124)	110.2 (4)
C(12)-C(121)-C(123)	112.2 (4)	C(122)-C(121)-C(123)	106.1 (4)
C(124)-C(121)-C(123)	106.3 (4)	C(163)-C(161)-C(164)	110.0 (4)
C(163)-C(161)-C(162)	106.5 (4)	C(164)-C(161)-C(162)	106.9 (4)
C(163)-C(161)-C(16)	112.3 (4)	C(164)-C(161)-C(16)	109.2 (3)
C(162)-C(161)-C(16)	111.7 (3)	Cl(2B)-C(1S)-Cl(1B)	116.4 (7)
Cl(1A)-C(1S)-Cl(2A)	127.2 (10)		

Symmetry transformations used to generate equivalent atoms:

$$(x, y, z) \rightarrow (-x, -y+1, -z+2)$$

	U11	U22	U33	U23	U13	U12
Al	23(1)	32(1)	27(1)	-8(1)	1(1)	-8(1)
O(1)	21(2)	49(2)	27(2)	-10(1)	-2(1)	1(1)
O(4)	34(2)	57(2)	28(2)	-11(2)	-2(1)	3(2)
O(6)	49(2)	48(2)	88(3)	-37(2)	10(2)	-24(2)
O(9A)	79(6)	56(5)	88(6)	-18(5)	-4(5)	-11(4)
O(9B)	195(12)	92(7)	119(9)	-33(7)	-75(9)	-53(8)
O(11)	25(2)	32(2)	33(2)	-8(1)	7(1)	-7(1)
C(2)	33(3)	63(3)	38(3)	-14(2)	-4(2)	9(2)
C(3)	29(3)	139(6)	47(3)	-36(3)	-9(2)	13(3)
C(5)	49(3)	86(4)	28(3)	-13(3)	-3(2)	2(3)
C(7A)	28(5)	61(7)	40(6)	-24(5)	-2(4)	-13(5)
C(7B)	35(5)	38(6)	40(6)	-5(5)	-2(5)	-9(4)
C(8)	155(7)	42(4)	66(4)	-18(3)	-13(4)	-46(4)
C(10)	79(5)	89(5)	144(7)	-48(5)	5(5)	-51(4)
C(11)	21(2)	35(3)	29(2)	-7(2)	-3(2)	-5(2)
C(12)	33(2)	32(3)	26(2)	-6(2)	-1(2)	-8(2)
C(13)	42(3)	29(3)	33(3)	-5(2)	-2(2)	-12(2)
C(14)	35(3)	44(3)	23(2)	-5(2)	2(2)	-10(2)
C(15)	28(2)	49(3)	29(2)	-14(2)	2(2)	-9(2)
C(16)	22(2)	36(3)	27(2)	-10(2)	-4(2)	-5(2)
C(121)	41(3)	30(3)	44(3)	-12(2)	7(2)	-11(2)
C(122)	57(4)	48(3)	93(5)	-35(3)	-1(3)	1(3)
C(123)	93(4)	42(3)	59(4)	-21(3)	24(3)	-23(3)
C(124)	62(3)	57(3)	38(3)	-19(3)	1(2)	-5(3)
C(141)	69(4)	56(3)	33(3)	-2(2)	16(3)	-21(3)
C(161)	30(2)	34(3)	38(3)	-15(2)	2(2)	-3(2)
C(162)	48(3)	46(3)	53(3)	-20(3)	8(2)	0(2)
C(163)	43(3)	34(3)	45(3)	-8(2)	0(2)	0(2)
C(164)	44(3)	45(3)	50(3)	-25(2)	-2(2)	-10(2)
C(1S)	94(7)	158(10)	255(14)	-54(10)	2(8)	-21(7)
Cl(1A)	109(6)	399(19)	125(7)	-128(10)	10(5)	-131(9)
Cl(2A)	159(5)	141(5)	141(5)	-33(4)	-22(4)	-24(4)
Cl(1B)	102(5)	125(4)	55(3)	-42(3)	25(3)	-28(4)
Cl(2B)	149(5)	120(4)	179(6)	-48(4)	12(4)	19(4)

(BHT)₂Al(μ -OCH₂CH₂NMe₂)₂Li (**4.8**)

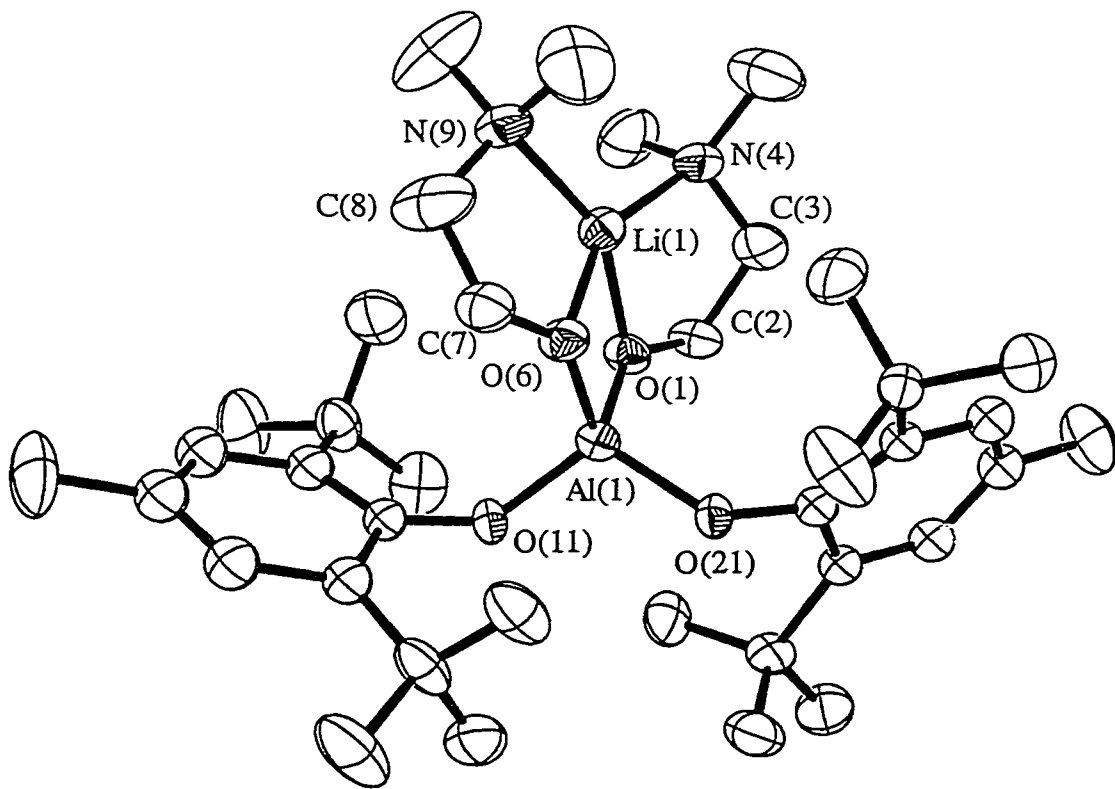


Figure 15. The molecular structure of $(\text{BHT})_2\text{Al}(\mu\text{-OCH}_2\text{CH}_2\text{NMe}_2)_2\text{Li}$ (**4.8**).

Thermal ellipsoids are drawn at the 30% probability level, and hydrogen atoms are omitted for clarity.

	x	y	z	U(eq)
Al	2262(1)	727(1)	3956(1)	47(1)
O(1)	1693(2)	233(2)	4381(2)	53(1)
O(6)	3057(3)	396(2)	4271(2)	57(1)
O(11)	2258(2)	619(2)	3171(2)	50(1)
O(21)	2079(2)	1525(2)	4123(2)	47(1)
N(4)	1680(4)	-398(3)	5481(3)	69(2)
N(9)	3536(4)	-681(3)	4878(3)	69(2)
C(2)	1019(4)	234(4)	4702(3)	65(2)
C(3)	1166(4)	125(4)	5379(4)	74(3)
C(5A)	1351(6)	-1005(4)	5288(5)	114(4)
C(5B)	1886(6)	-433(5)	6129(4)	130(4)
C(7)	3784(4)	189(4)	4132(4)	75(3)
C(8)	3873(5)	-485(6)	4322(5)	148(5)
C(10A)	3926(6)	-459(6)	5399(5)	160(6)
C(10B)	3507(7)	-1374(5)	4895(7)	173(6)
C(11)	2704(4)	296(3)	2781(3)	49(2)
C(12)	3284(4)	642(3)	2495(3)	57(2)
C(13)	3825(4)	283(4)	2185(3)	72(2)
C(14)	3779(4)	-366(4)	2118(4)	72(2)
C(15)	3146(4)	-677(4)	2325(3)	72(2)
C(16)	2579(4)	-350(4)	2635(3)	58(2)
C(21)	1610(4)	1779(3)	4542(3)	46(2)
C(22)	880(4)	1962(3)	4358(3)	49(2)
C(23)	367(4)	2107(3)	4819(3)	59(2)
C(24)	549(4)	2102(3)	5432(4)	61(2)
C(25)	1294(4)	2022(3)	5582(3)	60(2)
C(26)	1841(4)	1895(3)	5148(3)	45(2)
C(121)	3355(5)	1372(4)	2515(4)	71(2)
C(122)	2617(5)	1690(4)	2341(4)	93(3)
C(123)	3602(5)	1613(4)	3141(4)	90(3)
C(124)	3921(5)	1637(5)	2054(4)	117(4)
C(141)	4391(5)	-746(5)	1784(4)	125(4)
C(161)	1883(5)	-725(4)	2817(4)	72(2)
C(162)	1173(5)	-317(4)	2840(4)	100(3)
C(163)	1711(6)	-1259(4)	2346(4)	122(4)
C(164)	1987(5)	-1054(4)	3439(4)	104(3)
C(221)	655(4)	2028(4)	3684(3)	59(2)
C(222)	1213(5)	2467(4)	3353(3)	85(3)
C(223)	605(4)	1379(4)	3363(3)	82(3)
C(224)	-113(4)	2351(4)	3609(4)	94(3)
C(241)	-28(4)	2224(5)	5921(4)	109(3)
C(261)	2657(4)	1883(3)	5363(3)	51(2)
C(262)	2760(4)	2309(4)	5926(3)	69(2)
C(263)	3179(4)	2136(5)	4859(4)	97(3)
C(264)	2897(4)	1207(4)	5558(4)	88(3)
Li	2513(7)	-175(6)	4825(5)	61(4)

	x	y	z	U(eq)
H(2A)	699(4)	-100(4)	4547(3)	77
H(2B)	771(4)	641(4)	4646(3)	77
H(3A)	1366(4)	513(4)	5557(4)	89
H(3B)	701(4)	30(4)	5583(4)	89
H(5AA)	1698(6)	-1345(4)	5358(5)	171
H(5AB)	1233(6)	-985(4)	4861(5)	171
H(5AC)	907(6)	-1083(4)	5518(5)	171
H(5BA)	2227(6)	-780(5)	6189(4)	194
H(5BB)	1450(6)	-503(5)	6370(4)	194
H(5BC)	2117(6)	-39(5)	6250(4)	194
H(7A)	4142(4)	454(4)	4345(4)	90
H(7B)	3873(4)	228(4)	3698(4)	90
H(8A)	3678(5)	-753(6)	3998(5)	177
H(8B)	4400(5)	-573(6)	4351(5)	177
H(10A)	3679(6)	-603(6)	5762(5)	240
H(10B)	3939(6)	0(6)	5395(5)	240
H(10C)	4423(6)	-623(6)	5392(5)	240
H(10D)	3243(7)	-1529(5)	4544(7)	259
H(10E)	3257(7)	-1510(5)	5259(7)	259
H(10F)	4002(7)	-1543(5)	4893(7)	259
H(13A)	4231(4)	495(4)	2019(3)	87
H(15A)	3096(4)	-1114(4)	2256(3)	86
H(23A)	-115(4)	2211(3)	4708(3)	71
H(25A)	1432(4)	2054(3)	5990(3)	72
H(12A)	2462(5)	1539(4)	1948(4)	140
H(12B)	2681(5)	2145(4)	2328(4)	140
H(12C)	2247(5)	1584(4)	2640(4)	140
H(12D)	3639(5)	2071(4)	3133(4)	135
H(12E)	4076(5)	1434(4)	3241(4)	135
H(12F)	3245(5)	1487(4)	3443(4)	135
H(12G)	3790(5)	1500(5)	1650(4)	175
H(12H)	4407(5)	1481(5)	2154(4)	175
H(12I)	3920(5)	2096(5)	2071(4)	175
H(14A)	4264(5)	-1192(5)	1780(4)	187
H(14B)	4855(5)	-688(5)	1991(4)	187
H(14C)	4433(5)	-594(5)	1372(4)	187
H(16A)	761(5)	-581(4)	2956(4)	150
H(16B)	1081(5)	-135(4)	2445(4)	150
H(16C)	1234(5)	19(4)	3134(4)	150
H(16D)	1274(6)	-1486(4)	2470(4)	183
H(16E)	2122(6)	-1550(4)	2325(4)	183
H(16F)	1631(6)	-1071(4)	1952(4)	183
H(16G)	1545(5)	-1285(4)	3542(4)	157
H(16H)	2082(5)	-736(4)	3746(4)	157
H(16I)	2398(5)	-1344(4)	3418(4)	157

	x	y	z	U(eq)
H(22A)	1237(5)	2871(4)	3559(3)	127
H(22B)	1054(5)	2531(4)	2940(3)	127
H(22C)	1694(5)	2270(4)	3355(3)	127
H(22D)	463(4)	1441(4)	2945(3)	122
H(22E)	242(4)	1118(4)	3564(3)	122
H(22F)	1079(4)	1171(4)	3379(3)	122
H(22G)	-108(4)	2762(4)	3805(4)	140
H(22H)	-487(4)	2087(4)	3793(4)	140
H(22I)	-221(4)	2404(4)	3183(4)	140
H(24A)	201(4)	2201(5)	6316(4)	163
H(24B)	-412(4)	1908(5)	5892(4)	163
H(24C)	-238(4)	2642(5)	5864(4)	163
H(26A)	2617(4)	2739(4)	5829(3)	104
H(26B)	3271(4)	2302(4)	6048(3)	104
H(26C)	2457(4)	2151(4)	6253(3)	104
H(26D)	3126(4)	1878(5)	4499(4)	146
H(26E)	3683(4)	2117(5)	4999(4)	146
H(26F)	3053(4)	2571(5)	4765(4)	146
H(26G)	2844(4)	919(4)	5220(4)	132
H(26H)	2592(4)	1065(4)	5890(4)	132
H(26I)	3406(4)	1215(4)	5686(4)	132

Al-O(1)	1.730(5)	Al-O(6)	1.736(5)
Al-O(11)	1.735(5)	Al-O(21)	1.741(5)
O(1)-C(2)	1.405(8)	O(1)-Li	1.965(14)
O(6)-C(7)	1.414(8)	O(6)-Li	1.967(13)
O(11)-C(11)	1.354(7)	O(21)-C(21)	1.357(7)
N(4)-C(3)	1.451(9)	N(4)-C(5A)	1.465(10)
N(4)-C(5B)	1.469(10)	N(4)-Li	2.130(14)
N(9)-C(10A)	1.418(11)	N(9)-C(8)	1.423(10)
N(9)-C(10B)	1.451(11)	N(9)-Li	2.131(14)
C(2)-C(3)	1.524(9)	C(7)-C(8)	1.479(12)
C(11)-C(16)	1.406(9)	C(11)-C(12)	1.420(9)
C(12)-C(13)	1.406(9)	C(12)-C(121)	1.531(10)
C(13)-C(14)	1.367(9)	C(14)-C(15)	1.390(10)
C(14)-C(141)	1.546(10)	C(15)-C(16)	1.406(9)
C(16)-C(161)	1.532(10)	C(21)-C(26)	1.415(9)
C(21)-C(22)	1.430(9)	C(22)-C(23)	1.403(9)
C(22)-C(221)	1.538(9)	C(23)-C(24)	1.382(9)
C(24)-C(25)	1.393(9)	C(24)-C(241)	1.516(9)
C(25)-C(26)	1.397(9)	C(26)-C(261)	1.545(9)
C(121)-C(123)	1.530(10)	C(121)-C(122)	1.536(10)
C(121)-C(124)	1.540(10)	C(161)-C(164)	1.539(11)
C(161)-C(162)	1.540(11)	C(161)-C(163)	1.552(10)
C(221)-C(223)	1.532(10)	C(221)-C(222)	1.542(10)
C(221)-C(224)	1.550(9)	C(261)-C(262)	1.533(9)
C(261)-C(264)	1.539(10)	C(261)-C(263)	1.545(10)

O(1)-Al-O(6)	92.1(2)	O(1)-Al-O(11)	117.0(2)
O(6)-Al-O(11)	110.3(2)	O(1)-Al-O(21)	110.3(2)
O(6)-Al-O(21)	117.1(2)	O(11)-Al-O(21)	109.4(2)
C(2)-O(1)-Al	141.5(5)	C(2)-O(1)-Li	113.8(5)
Al-O(1)-Li	94.6(4)	C(7)-O(6)-Al	143.4(5)
C(7)-O(6)-Li	114.1(6)	Al-O(6)-Li	94.3(4)
C(11)-O(11)-Al	133.4(4)	C(21)-O(21)-Al	129.5(4)
C(3)-N(4)-C(5A)	110.4(7)	C(3)-N(4)-C(5B)	110.4(7)
C(5A)-N(4)-C(5B)	109.7(7)	C(3)-N(4)-Li	100.6(6)
C(5A)-N(4)-Li	106.3(6)	C(5B)-N(4)-Li	119.0(7)
C(10A)-N(9)-C(8)	112.6(9)	C(10A)-N(9)-C(10B)	109.0(9)
C(8)-N(9)-C(10B)	109.0(9)	C(10A)-N(9)-Li	108.1(7)
C(8)-N(9)-Li	100.4(6)	C(10B)-N(9)-Li	117.8(7)
O(1)-C(2)-C(3)	109.7(6)	N(4)-C(3)-C(2)	111.9(7)
O(6)-C(7)-C(8)	109.5(7)	N(9)-C(8)-C(7)	118.0(9)
O(11)-C(11)-C(16)	121.9(7)	O(11)-C(11)-C(12)	117.5(6)
C(16)-C(11)-C(12)	120.5(7)	C(13)-C(12)-C(11)	116.8(7)
C(13)-C(12)-C(121)	119.2(7)	C(11)-C(12)-C(121)	123.9(7)
C(14)-C(13)-C(12)	122.7(8)	C(13)-C(14)-C(15)	118.8(8)
C(13)-C(14)-C(141)	121.1(8)	C(15)-C(14)-C(141)	120.0(8)
C(14)-C(15)-C(16)	121.8(8)	C(11)-C(16)-C(15)	117.4(7)
C(11)-C(16)-C(161)	124.3(7)	C(15)-C(16)-C(161)	118.2(7)
O(21)-C(21)-C(26)	121.2(6)	O(21)-C(21)-C(22)	119.3(6)
C(26)-C(21)-C(22)	119.4(6)	C(23)-C(22)-C(21)	117.5(6)
C(23)-C(22)-C(221)	119.9(6)	C(21)-C(22)-C(221)	122.5(6)
C(24)-C(23)-C(22)	122.8(7)	C(23)-C(24)-C(25)	117.4(7)
C(23)-C(24)-C(241)	121.5(7)	C(25)-C(24)-C(241)	121.0(7)
C(26)-C(25)-C(24)	122.9(7)	C(25)-C(26)-C(21)	117.6(6)
C(25)-C(26)-C(261)	118.0(6)	C(21)-C(26)-C(261)	124.3(6)
C(123)-C(121)-C(12)	112.3(7)	C(123)-C(121)-C(122)	109.3(7)
C(12)-C(121)-C(122)	110.6(7)	C(123)-C(121)-C(124)	106.0(6)
C(12)-C(121)-C(124)	113.3(7)	C(122)-C(121)-C(124)	104.9(7)
C(16)-C(161)-C(164)	111.1(7)	C(16)-C(161)-C(162)	114.0(7)
C(164)-C(161)-C(162)	108.6(7)	C(16)-C(161)-C(163)	111.1(7)
C(164)-C(161)-C(163)	107.0(7)	C(162)-C(161)-C(163)	104.7(7)
C(223)-C(221)-C(22)	112.1(6)	C(223)-C(221)-C(222)	110.4(7)
C(22)-C(221)-C(222)	109.5(6)	C(223)-C(221)-C(224)	106.6(6)
C(22)-C(221)-C(224)	112.1(6)	C(222)-C(221)-C(224)	106.0(6)
C(262)-C(261)-C(264)	106.0(6)	C(262)-C(261)-C(263)	107.6(6)
C(264)-C(261)-C(263)	110.0(7)	C(262)-C(261)-C(26)	110.5(6)
C(264)-C(261)-C(26)	111.6(6)	C(263)-C(261)-C(26)	110.9(6)
O(1)-Li-O(6)	78.8(5)	O(1)-Li-N(4)	84.1(5)
O(6)-Li-N(4)	154.3(7)	O(1)-Li-N(9)	153.4(7)
O(6)-Li-N(9)	84.5(5)	N(4)-Li-N(9)	117.7(6)

Table of General Displacement Parameter Expressions - U's

110

	U11	U22	U33	U23	U13	U12
A1	47(1)	49(1)	43(1)	3(1)	-1(1)	-1(1)
O(1)	47(3)	63(3)	50(3)	9(3)	11(3)	-3(3)
O(6)	45(3)	63(3)	61(3)	10(3)	2(3)	10(3)
O(11)	53(3)	56(3)	42(3)	-11(3)	5(2)	4(3)
O(21)	49(3)	48(3)	44(3)	-11(2)	-1(2)	2(2)
N(4)	85(5)	59(5)	63(5)	17(4)	3(4)	6(5)
N(9)	67(5)	57(5)	83(5)	23(4)	2(4)	4(4)
C(2)	57(5)	78(6)	59(6)	21(5)	-1(5)	-2(5)
C(3)	68(6)	79(7)	74(7)	15(5)	18(5)	-8(5)
C(5A)	132(10)	66(7)	144(10)	5(7)	21(8)	-9(7)
C(5B)	121(9)	180(12)	88(8)	46(8)	4(7)	18(8)
C(7)	56(6)	93(7)	76(6)	19(5)	3(5)	14(5)
C(8)	89(8)	179(13)	175(12)	98(10)	69(8)	75(8)
C(10A)	105(9)	245(16)	129(10)	-36(10)	-51(8)	58(10)
C(10B)	136(11)	71(8)	312(19)	22(10)	7(11)	26(8)
C(121)	79(6)	89(7)	46(5)	-2(5)	15(5)	-36(5)
C(122)	115(8)	72(6)	93(7)	15(5)	1(6)	-7(6)
C(123)	117(8)	92(7)	61(6)	0(5)	9(5)	-56(6)
C(124)	143(9)	142(9)	65(6)	-2(6)	30(6)	-62(8)
C(141)	76(6)	187(11)	111(8)	-58(8)	8(6)	45(7)
C(161)	89(6)	66(6)	62(6)	-15(5)	13(5)	-21(6)
C(162)	79(7)	100(7)	122(8)	-15(7)	8(6)	-25(6)
C(163)	151(10)	99(7)	117(9)	-52(7)	32(8)	-51(7)
C(164)	133(9)	82(7)	98(8)	12(6)	17(7)	-22(6)
C(221)	43(5)	79(6)	54(5)	7(5)	-14(4)	21(5)
C(222)	96(7)	96(7)	62(6)	19(5)	1(5)	7(6)
C(223)	84(6)	94(7)	67(6)	-23(5)	-29(5)	16(6)
C(224)	92(7)	99(7)	90(7)	4(6)	-20(6)	34(6)
C(241)	67(6)	174(9)	85(7)	-24(7)	31(6)	5(7)
C(261)	45(5)	56(5)	52(5)	-11(4)	-12(4)	8(4)
C(262)	61(5)	72(6)	75(6)	-8(5)	-6(5)	-14(5)
C(263)	44(5)	179(10)	69(6)	-22(6)	7(5)	-43(6)
C(264)	88(7)	82(6)	95(7)	-14(6)	-35(6)	26(6)
Li	75(9)	48(8)	60(8)	-1(7)	4(7)	-1(7)

(BHT)₂Al(μ-OCH₂CH₂SMe)₂Li(HOCH₂CH₂SMe) (**4.10b**)

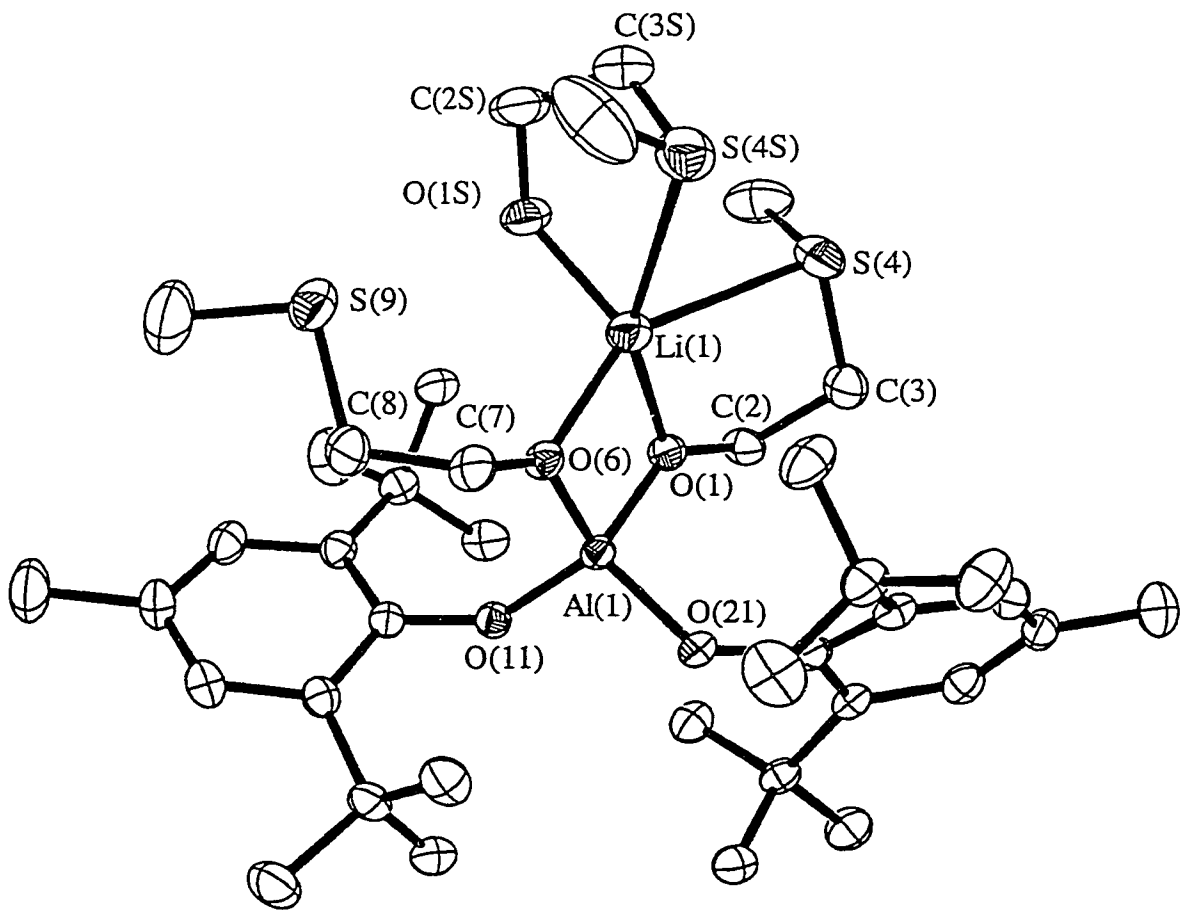


Figure 16. The molecular structure of $(\text{BHT})_2\text{Al}(\mu-\text{OCH}_2\text{CH}_2\text{SMe})_2\text{Li}(\text{HOCH}_2\text{CH}_2\text{SMe})$ (**4.10b**). Thermal ellipsoids are drawn at the 30% probability level, and hydrogen atoms are omitted for clarity.

Tables of Positional Parameters and their Estimated Standard Deviations

	x	y	z	U(eq)
Al	7527(1)	7454(1)	3835(1)	44(1)
S(4)	6912(1)	10394(1)	2520(1)	83(1)
S(9)	6304(1)	5868(1)	-441(1)	90(1)
O(1)	7744(2)	8667(2)	3474(2)	54(1)
O(6)	6657(2)	7020(2)	2411(2)	53(1)
O(11)	8364(2)	6756(2)	4001(2)	50(1)
O(21)	7231(2)	7517(2)	5207(2)	49(1)
C(2)	8238(3)	9639(3)	4114(4)	64(1)
C(3)	7596(3)	10354(3)	4054(4)	76(1)
C(5)	7782(4)	10863(5)	1838(5)	125(2)
C(7)	6027(3)	6084(3)	1850(4)	70(1)
C(8)	6371(4)	5445(3)	1005(4)	79(1)
C(10)	6900(6)	5089(5)	-1113(6)	149(3)
C(11)	8602(3)	6027(3)	3332(3)	48(1)
C(12)	9118(3)	6284(3)	2511(3)	53(1)
C(13)	9202(3)	5490(3)	1715(4)	70(1)
C(14)	8852(4)	4485(3)	1737(4)	77(1)
C(15)	8470(3)	4268(3)	2662(4)	69(1)
C(16)	8359(3)	5008(3)	3497(4)	54(1)
C(21)	7147(3)	8307(3)	5970(3)	49(1)
C(22)	6287(3)	8577(3)	5778(3)	53(1)
C(23)	6287(3)	9503(3)	6426(4)	61(1)
C(24)	7071(3)	10131(3)	7264(4)	63(1)
C(25)	7857(3)	9758(3)	7570(4)	61(1)
C(26)	7922(3)	8836(3)	6987(3)	51(1)
C(121)	9581(3)	7367(3)	2447(4)	60(1)
C(122)	10006(3)	8030(3)	3733(4)	75(1)
C(123)	8871(4)	7844(3)	1617(4)	77(1)
C(124)	10372(4)	7394(4)	1875(6)	108(2)
C(141)	8940(5)	3646(4)	812(5)	121(2)
C(161)	8052(3)	4707(3)	4611(4)	62(1)
C(162)	7961(4)	3569(3)	4651(5)	94(2)
C(163)	8799(4)	5270(4)	5793(4)	86(2)
C(164)	7118(4)	4927(3)	4595(5)	85(2)
C(221)	5350(3)	7885(3)	4951(4)	64(1)
C(222)	5310(4)	6783(4)	5091(6)	103(2)
C(223)	4523(3)	8158(4)	5297(4)	88(2)
C(224)	5214(3)	8013(4)	3597(4)	90(2)
C(241)	7057(4)	11157(3)	7906(5)	90(2)
C(261)	8755(3)	8391(3)	7525(3)	55(1)
C(262)	8376(3)	7335(3)	7777(4)	72(1)
C(263)	9389(3)	9012(3)	8779(4)	80(1)
C(264)	9370(3)	8340(3)	6683(4)	68(1)
O(1S)	6825(2)	8260(2)	227(3)	77(1)
C(2S)	6199(4)	8391(5)	-888(5)	103(2)
C(3S)	5553(5)	8944(5)	-696(5)	110(2)
S(4S)	4885(1)	8470(1)	282(2)	107(1)
C(5S)	4095(6)	7449(5)	-677(9)	201(4)
Li	6729(6)	8376(5)	1887(6)	69(2)

Table of Positional Parameters and their Estimated Standard Deviations.

	x	y	z	U(eq)
H(2A)	8718(3)	9895(3)	3753(4)	77
H(2B)	8535(3)	9604(3)	4972(4)	77
H(3A)	7966(3)	11028(3)	4435(4)	91
H(3B)	7184(3)	10153(3)	4536(4)	91
H(5A)	7494(4)	10919(5)	994(5)	188
H(5B)	8183(4)	10407(5)	1860(5)	188
H(5C)	8138(4)	11515(5)	2292(5)	188
H(7A)	5443(3)	6207(3)	1378(4)	84
H(7B)	5910(3)	5714(3)	2492(4)	84
H(8A)	6009(4)	4755(3)	847(4)	95
H(8B)	7011(4)	5447(3)	1422(4)	95
H(10A)	6905(6)	5255(5)	-1908(6)	224
H(10B)	6590(6)	4393(5)	-1208(6)	224
H(10C)	7526(6)	5200(5)	-583(6)	224
H(13A)	9509(3)	5643(3)	1138(4)	83
H(15A)	8278(3)	3595(3)	2730(4)	83
H(23A)	5731(3)	9703(3)	6285(4)	73
H(25A)	8373(3)	10141(3)	8199(4)	74
H(12A)	9534(3)	8037(3)	4129(4)	113
H(12B)	10263(3)	8706(3)	3647(4)	113
H(12C)	10487(3)	7762(3)	4226(4)	113
H(12D)	8361(4)	7842(3)	1943(4)	116
H(12E)	8648(4)	7461(3)	794(4)	116
H(12F)	9161(4)	8525(3)	1596(4)	116
H(12G)	10645(4)	8081(4)	1849(6)	162
H(12H)	10133(4)	7015(4)	1050(6)	162
H(12I)	10834(4)	7103(4)	2368(6)	162
H(14A)	9219(5)	3940(4)	238(5)	181
H(14B)	8335(5)	3230(4)	369(5)	181
H(14C)	9319(5)	3242(4)	1248(5)	181
H(16A)	7495(4)	3184(3)	3917(5)	141
H(16B)	7787(4)	3412(3)	5366(5)	141
H(16C)	8544(4)	3406(3)	4694(5)	141
H(16D)	9383(4)	5126(4)	5793(4)	129
H(16E)	8639(4)	5056(4)	6497(4)	129
H(16F)	8847(4)	5982(4)	5836(4)	129
H(16G)	6652(4)	4569(3)	3846(5)	127
H(16H)	7162(4)	5639(3)	4635(5)	127
H(16I)	6953(4)	4713(3)	5295(5)	127
H(22A)	5396(4)	6717(4)	5943(6)	154
H(22B)	5791(4)	6568(4)	4828(6)	154
H(22C)	4717(4)	6372(4)	4590(6)	154
H(22D)	4522(3)	8848(4)	5221(4)	132
H(22E)	4574(3)	8069(4)	6135(4)	132
H(22F)	3956(3)	7726(4)	4751(4)	132
H(22G)	5241(3)	8709(4)	3527(4)	135
H(22H)	4621(3)	7607(4)	3091(4)	135
H(22I)	5694(3)	7803(4)	3327(4)	135

	x	y	z	U(eq)
H(24A)	7665 (4)	11480 (3)	8452 (5)	135
H(24B)	6627 (4)	11068 (3)	8375 (5)	135
H(24C)	6869 (4)	11568 (3)	7297 (5)	135
H(26A)	8882 (3)	7036 (3)	8115 (4)	109
H(26B)	7974 (3)	6918 (3)	7017 (4)	109
H(26C)	8034 (3)	7392 (3)	8357 (4)	109
H(26D)	9901 (3)	8712 (3)	9085 (4)	121
H(26E)	9043 (3)	9021 (3)	9360 (4)	121
H(26F)	9618 (3)	9690 (3)	8675 (4)	121
H(26G)	9877 (3)	8057 (3)	7068 (4)	103
H(26H)	9608 (3)	9007 (3)	6552 (4)	103
H(26I)	9012 (3)	7924 (3)	5902 (4)	103
H(2SA)	6552 (4)	8737 (5)	-1368 (5)	124
H(2SB)	5864 (4)	7732 (5)	-1370 (5)	124
H(3SA)	5127 (5)	8957 (5)	-1495 (5)	132
H(3SB)	5886 (5)	9635 (5)	-334 (5)	132
H(5SA)	3697 (6)	7134 (5)	-242 (9)	302
H(5SB)	4413 (6)	6976 (5)	-942 (9)	302
H(5SC)	3730 (6)	7665 (5)	-1385 (9)	302

Table of Bond Distances in Angstroms.

Al-O(11)	1.736(3)	Al-O(21)	1.746(2)
Al-O(1)	1.747(3)	Al-O(6)	1.753(3)
S(4)-C(5)	1.782(6)	S(4)-C(3)	1.789(4)
S(9)-C(10)	1.783(6)	S(9)-C(8)	1.789(5)
O(1)-C(2)	1.406(4)	O(1)-Li	1.982(8)
O(6)-C(7)	1.413(4)	O(6)-Li	2.004(7)
O(11)-C(11)	1.363(4)	O(21)-C(21)	1.368(4)
C(2)-C(3)	1.518(6)	C(7)-C(8)	1.507(6)
C(11)-C(12)	1.418(5)	C(11)-C(16)	1.420(5)
C(12)-C(13)	1.392(5)	C(12)-C(121)	1.536(5)
C(13)-C(14)	1.383(6)	C(14)-C(15)	1.375(6)
C(14)-C(141)	1.530(6)	C(15)-C(16)	1.387(5)
C(16)-C(161)	1.542(6)	C(21)-C(22)	1.412(5)
C(21)-C(26)	1.421(5)	C(22)-C(23)	1.401(5)
C(22)-C(221)	1.550(6)	C(23)-C(24)	1.378(6)
C(24)-C(25)	1.379(6)	C(24)-C(241)	1.523(6)
C(25)-C(26)	1.401(5)	C(26)-C(261)	1.533(6)
C(121)-C(124)	1.533(6)	C(121)-C(123)	1.537(6)
C(121)-C(122)	1.537(6)	C(161)-C(163)	1.522(6)
C(161)-C(164)	1.527(6)	C(161)-C(162)	1.545(6)
C(221)-C(222)	1.526(6)	C(221)-C(224)	1.534(6)
C(221)-C(223)	1.538(6)	C(261)-C(264)	1.534(6)
C(261)-C(263)	1.541(5)	C(261)-C(262)	1.540(5)
O(1S)-C(2S)	1.421(5)	O(1S)-Li	1.932(8)
C(2S)-C(3S)	1.416(7)	C(3S)-S(4S)	1.805(6)
S(4S)-C(5S)	1.706(8)		

O(11)-Al-O(21)	106.60(12)	O(11)-Al-O(1)	120.52(14)
O(21)-Al-O(1)	108.71(13)	O(11)-Al-O(6)	110.69(13)
O(21)-Al-O(6)	119.83(13)	O(1)-Al-O(6)	90.71(12)
C(5)-S(4)-C(3)	101.6(3)	C(10)-S(9)-C(8)	102.4(3)
C(2)-O(1)-Al	136.6(2)	C(2)-O(1)-Li	125.0(3)
Al-O(1)-Li	96.3(2)	C(7)-O(6)-Al	134.1(2)
C(7)-O(6)-Li	130.1(3)	Al-O(6)-Li	95.3(2)
C(11)-O(11)-Al	139.9(2)	C(21)-O(21)-Al	131.9(2)
O(1)-C(2)-C(3)	110.9(3)	C(2)-C(3)-S(4)	114.3(3)
O(6)-C(7)-C(8)	113.0(4)	C(7)-C(8)-S(9)	113.5(3)
O(11)-C(11)-C(12)	120.5(3)	O(11)-C(11)-C(16)	119.4(3)
C(12)-C(11)-C(16)	120.0(3)	C(13)-C(12)-C(11)	116.9(4)
C(13)-C(12)-C(121)	118.7(4)	C(11)-C(12)-C(121)	124.4(3)
C(14)-C(13)-C(12)	123.4(4)	C(15)-C(14)-C(13)	117.6(4)
C(15)-C(14)-C(141)	121.3(4)	C(13)-C(14)-C(141)	121.0(5)
C(14)-C(15)-C(16)	122.9(4)	C(15)-C(16)-C(11)	117.8(4)
C(15)-C(16)-C(161)	119.2(4)	C(11)-C(16)-C(161)	122.8(3)
O(21)-C(21)-C(22)	120.4(3)	O(21)-C(21)-C(26)	119.5(4)
C(22)-C(21)-C(26)	120.0(3)	C(23)-C(22)-C(21)	117.4(4)
C(23)-C(22)-C(221)	118.7(4)	C(21)-C(22)-C(221)	123.7(4)
C(24)-C(23)-C(22)	123.1(4)	C(23)-C(24)-C(25)	117.0(4)
C(23)-C(24)-C(241)	121.8(4)	C(25)-C(24)-C(241)	121.1(4)
C(24)-C(25)-C(26)	123.7(4)	C(25)-C(26)-C(21)	116.6(4)
C(25)-C(26)-C(261)	120.3(3)	C(21)-C(26)-C(261)	122.8(3)
C(124)-C(121)-C(12)	111.7(4)	C(124)-C(121)-C(123)	106.7(4)
C(12)-C(121)-C(123)	109.8(4)	C(124)-C(121)-C(122)	106.4(4)
C(12)-C(121)-C(122)	112.3(3)	C(123)-C(121)-C(122)	109.7(4)
C(163)-C(161)-C(164)	110.2(4)	C(163)-C(161)-C(16)	108.3(4)
C(164)-C(161)-C(16)	112.8(3)	C(163)-C(161)-C(162)	106.7(4)
C(164)-C(161)-C(162)	107.0(4)	C(16)-C(161)-C(162)	111.7(4)
C(222)-C(221)-C(224)	110.6(4)	C(222)-C(221)-C(223)	106.8(4)
C(224)-C(221)-C(223)	106.9(4)	C(222)-C(221)-C(22)	111.0(4)
C(224)-C(221)-C(22)	109.5(4)	C(223)-C(221)-C(22)	112.0(4)
C(26)-C(261)-C(264)	113.4(3)	C(26)-C(261)-C(263)	111.9(3)
C(264)-C(261)-C(263)	106.4(4)	C(26)-C(261)-C(262)	107.5(3)
C(264)-C(261)-C(262)	111.0(3)	C(263)-C(261)-C(262)	106.5(3)
C(2S)-O(1S)-Li	129.9(4)	C(3S)-C(2S)-O(1S)	113.6(5)
C(2S)-C(3S)-S(4S)	115.6(4)	C(5S)-S(4S)-C(3S)	102.5(4)
O(1S)-Li-O(1)	128.1(5)	O(1S)-Li-O(6)	108.7(4)
O(1)-Li-O(6)	77.3(3)		

Table of General Displacement Parameter Expressions - U's

	U11	U22	U33	U23	U13	U12
A1	48(1)	43(1)	40(1)	5(1)	14(1)	8(1)
S(4)	80(1)	67(1)	89(1)	13(1)	2(1)	23(1)
S(9)	106(1)	87(1)	67(1)	-5(1)	19(1)	15(1)
O(1)	65(2)	42(1)	50(1)	5(1)	15(1)	7(1)
O(6)	55(2)	50(2)	44(1)	1(1)	9(1)	4(1)
O(11)	54(2)	48(1)	51(1)	8(1)	21(1)	13(1)
O(21)	51(2)	56(2)	39(1)	6(1)	15(1)	11(1)
C(2)	72(3)	46(2)	62(3)	10(2)	8(2)	4(2)
C(3)	88(4)	51(2)	74(3)	-3(2)	11(3)	11(2)
C(5)	136(6)	115(5)	108(4)	55(4)	20(4)	-1(4)
C(7)	72(3)	59(3)	60(3)	0(2)	7(2)	-3(2)
C(8)	89(4)	59(3)	69(3)	-9(2)	4(3)	10(2)
C(10)	200(9)	126(5)	139(6)	-14(4)	93(6)	39(5)
C(11)	43(2)	50(2)	47(2)	4(2)	11(2)	13(2)
C(12)	49(3)	58(2)	54(2)	6(2)	17(2)	16(2)
C(13)	75(3)	79(3)	65(3)	3(2)	35(2)	26(3)
C(14)	89(4)	63(3)	83(3)	-5(2)	35(3)	26(3)
C(15)	72(3)	52(2)	83(3)	3(2)	25(3)	17(2)
C(16)	47(2)	51(2)	61(2)	6(2)	14(2)	13(2)
C(21)	58(3)	52(2)	40(2)	10(2)	19(2)	10(2)
C(22)	52(3)	64(2)	42(2)	13(2)	17(2)	11(2)
C(23)	64(3)	70(3)	59(2)	14(2)	28(2)	24(2)
C(24)	73(3)	62(3)	60(3)	8(2)	31(2)	18(2)
C(25)	67(3)	60(3)	51(2)	1(2)	19(2)	5(2)
C(26)	56(3)	57(2)	40(2)	7(2)	18(2)	10(2)
C(121)	56(3)	66(3)	66(3)	16(2)	30(2)	10(2)
C(122)	62(3)	70(3)	78(3)	14(2)	13(2)	-8(2)
C(123)	94(4)	82(3)	61(3)	25(2)	28(3)	21(3)
C(124)	95(5)	97(4)	158(5)	21(4)	86(4)	14(3)
C(141)	163(7)	88(4)	126(5)	-15(3)	76(5)	37(4)
C(161)	66(3)	51(2)	72(3)	20(2)	24(2)	13(2)
C(162)	114(5)	67(3)	115(4)	36(3)	47(4)	25(3)
C(163)	115(5)	83(3)	68(3)	28(3)	35(3)	26(3)
C(164)	80(4)	75(3)	118(4)	37(3)	57(3)	15(3)
C(221)	49(3)	81(3)	64(3)	9(2)	23(2)	13(2)
C(222)	61(4)	84(4)	148(5)	12(3)	26(3)	-3(3)
C(223)	52(3)	125(4)	84(3)	0(3)	32(3)	9(3)
C(224)	64(3)	145(5)	59(3)	3(3)	15(2)	33(3)
C(241)	96(4)	72(3)	99(4)	-10(3)	32(3)	23(3)
C(261)	55(3)	63(2)	38(2)	3(2)	7(2)	6(2)
C(262)	83(4)	76(3)	59(3)	18(2)	18(2)	22(2)
C(263)	85(4)	85(3)	52(3)	-3(2)	0(2)	16(3)
C(264)	55(3)	88(3)	59(3)	8(2)	13(2)	17(2)
O(1S)	76(2)	101(2)	55(2)	22(2)	12(2)	28(2)
C(2S)	116(5)	140(5)	70(3)	48(3)	30(3)	50(4)
C(3S)	143(6)	119(5)	80(4)	42(3)	31(4)	51(4)
S(4S)	105(1)	128(1)	112(1)	43(1)	50(1)	51(1)
C(5S)	177(9)	84(5)	335(13)	63(6)	55(9)	33(5)
Li	84(6)	63(4)	63(4)	14(3)	23(4)	16(4)

(^tBu)₂Al(CH₂CH₂CH₂SMe) (**5.1**).

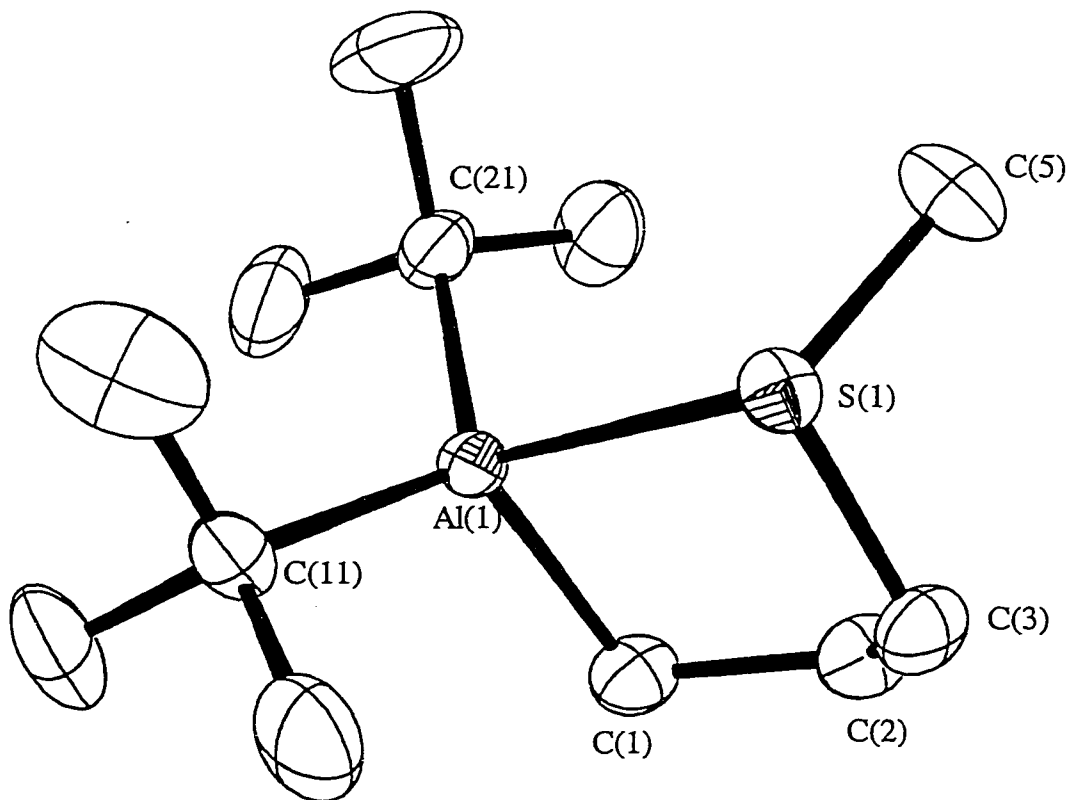


Figure 17. The molecular structure of (*t*Bu)₂Al(CH₂CH₂CH₂SMe) (**5.1**).

Thermal ellipsoids are drawn at the 30% probability level, and hydrogen atoms are omitted for clarity.

Table of Positional Parameters and Their Estimated Standard Deviations

Atom	X	Y	Z	B (Å²)
S	0.0216(2)	0.40573(9)	0.40812(7)	3.38(2)
A1	0.2271(2)	0.2518(1)	0.42991(7)	2.94(2)
C1	0.4741(7)	0.3322(4)	0.4202(3)	4.5(1)
C2	0.4240(7)	0.4301(4)	0.3792(3)	4.4(1)
C3	0.2500(7)	0.4814(3)	0.4150(3)	4.4(1)
C5	-0.0689(8)	0.4204(4)	0.3049(3)	5.2(1)
C11	0.1711(7)	0.2192(3)	0.5401(3)	3.9(1)
C12	0.201(1)	0.3089(5)	0.5936(3)	7.3(2)
C13	0.314(1)	0.1398(5)	0.5737(4)	7.9(2)
C14	-0.045(1)	0.1830(6)	0.5452(4)	9.0(2)
C21	0.1610(8)	0.1567(4)	0.3417(3)	4.5(1)
C22	0.280(1)	0.0636(5)	0.3639(4)	8.4(2)
C23	0.230(1)	0.1937(5)	0.2646(3)	7.6(2)
C24	-0.064(1)	0.1309(5)	0.3273(4)	8.3(2)

Anisotropically refined atoms are given in the form of the isotropic equivalent displacement parameter defined as:

$$(4/3) * [a2*B(1,1) + b2*B(2,2) + c2*B(3,3) + ab(\cos \gamma)*B(1,2) + ac(\cos \beta)*B(1,3) + bc(\cos \alpha)*B(2,3)]$$

Table of Positional Parameters and Their Estimated Standard Deviations

122

Atom	x	y	z	B (Å²)
	-	-	-	-----
H1a	0.5634	0.2965	0.3902	5*
H1b	0.5382	0.3445	0.4717	5*
H2a	0.3868	0.4186	0.3245	5*
H2b	0.5402	0.4711	0.3851	5*
H3a	0.2895	0.4950	0.4691	5*
H3b	0.2208	0.5411	0.3873	5*
H5a	0.0254	0.4027	0.2734	6*
H5b	-0.1035	0.4871	0.2952	6*
H5c	-0.1853	0.3805	0.2933	6*
H12a	0.1765	0.2939	0.6473	9*
H12b	0.1105	0.3589	0.5740	9*
H12c	0.3367	0.3313	0.5930	9*
H13a	0.2945	0.0845	0.5345	10*
H13b	0.2805	0.1196	0.6244	10*

Table of Positional Parameters and Their Estimated Standard Deviations

123

Atom	x	y	z	B(A2)
	-	-	-	-----
H13c	0.4504	0.1623	0.5776	10*
H14a	-0.0758	0.1658	0.5951	11*
H14b	-0.0657	0.1269	0.5120	11*
H14c	-0.1351	0.2336	0.5262	11*
H22a	0.2220	0.0353	0.4099	10*
H22b	0.4189	0.0789	0.3771	10*
H22c	0.2679	0.0185	0.3210	10*
H23a	0.1567	0.2532	0.2394	9*
H23b	0.2143	0.1414	0.2274	9*
H23c	0.3692	0.2101	0.2740	9*
H24a	-0.1289	0.1039	0.3735	10*
H24b	-0.0791	0.0834	0.2861	10*
H24c	-0.1352	0.1889	0.3105	10*

Table of Bond Distances in Angstroms.

124

Atom 1	Atom 2	Distance	Atom 1	Atom 2	Distance
=====	=====	=====	=====	=====	=====
S	A1	2.511(2)	C2	C3	1.524(7)
S	C3	1.828(5)	C11	C12	1.525(8)
S	C5	1.807(5)	C11	C13	1.515(8)
A1	C1	1.991(5)	C11	C14	1.528(9)
A1	C11	1.989(5)	C21	C22	1.523(8)
A1	C21	1.996(5)	C21	C23	1.513(8)
C1	C2	1.527(7)	C21	C24	1.533(8)

Numbers in parentheses are estimated standard deviations in the least significant digits.

Atom 1	Atom 2	Atom 3	Angle	Atom 1	Atom 2	Atom 3	Angle
=====	=====	=====	=====	=====	=====	=====	=====
A1	S	C3	91.5(2) A1	C11	C12	C13	110.8(3)
A1	S	C5	111.2(?) A1	C11	C13	C14	110.3(4)
C3	S	C5	101.3(2) A1	C11	C14	C12	112.7(3)
S	A1	C1	88.1(1) C12	C11	C13	C14	107.8(4)
S	A1	C11	100.2(1) C12	C11	C14	C13	107.3(5)
S	A1	C21	110.8(2) C13	C11	C14	C12	107.9(5)
C1	A1	C11	115.4(2) A1	C21	C22	C23	106.4(4)
C1	A1	C21	114.8(2) A1	C21	C23	C24	111.6(4)
C11	A1	C21	120.8(2) A1	C21	C24	C22	114.2(4)
A1	C1	C2	111.9(3) C22	C21	C23	C24	107.4(5)
C1	C2	C3	111.1(4) C22	C21	C24	C23	108.9(5)
S	C3	C2	111.8(3) C23	C21	C24	C22	108.0(5)

Numbers in parentheses are estimated standard deviations in the least significant digits.

Table of General Displacement Parameter Expressions - U's

126

Name	U(1,1)	U(2,2)	U(3,3)	U(1,2)	U(1,3)	U(2,3)
S	0.0418(5)	0.0452(6)	0.0421(5)	0.0042(6)	0.0074(5)	0.0054(6)
A1	0.0390(6)	0.0343(6)	0.0380(6)	-0.0007(6)	0.0009(5)	0.0006(7)
C1	0.038(3)	0.056(3)	0.076(3)	-0.005(2)	0.004(2)	0.004(3)
C2	0.043(3)	0.053(3)	0.073(3)	-0.013(2)	0.011(2)	0.007(3)
C3	0.058(3)	0.039(3)	0.069(3)	-0.010(2)	0.005(3)	0.002(3)
C5	0.059(3)	0.093(4)	0.046(3)	0.013(3)	0.000(2)	0.019(3)
C11	0.062(3)	0.047(3)	0.040(2)	0.000(2)	-0.001(2)	0.011(2)
C12	0.141(6)	0.091(4)	0.047(3)	0.009(4)	0.007(4)	-0.003(3)
C13	0.133(5)	0.098(4)	0.067(4)	0.034(4)	-0.009(4)	0.024(4)
C14	0.107(5)	0.165(6)	0.072(4)	-0.037(5)	0.025(3)	0.034(4)
C21	0.072(3)	0.050(3)	0.051(3)	-0.001(3)	0.007(2)	-0.018(2)
C22	0.144(6)	0.062(4)	0.111(5)	0.020(4)	0.016(5)	-0.026(4)
C23	0.139(5)	0.097(5)	0.057(3)	0.001(4)	0.024(4)	-0.024(3)
C24	0.095(4)	0.119(5)	0.099(4)	-0.030(4)	-0.006(4)	-0.053(4)

$[(tBu)_2Al(\mu-Cl)]_2$ (**6.1**).

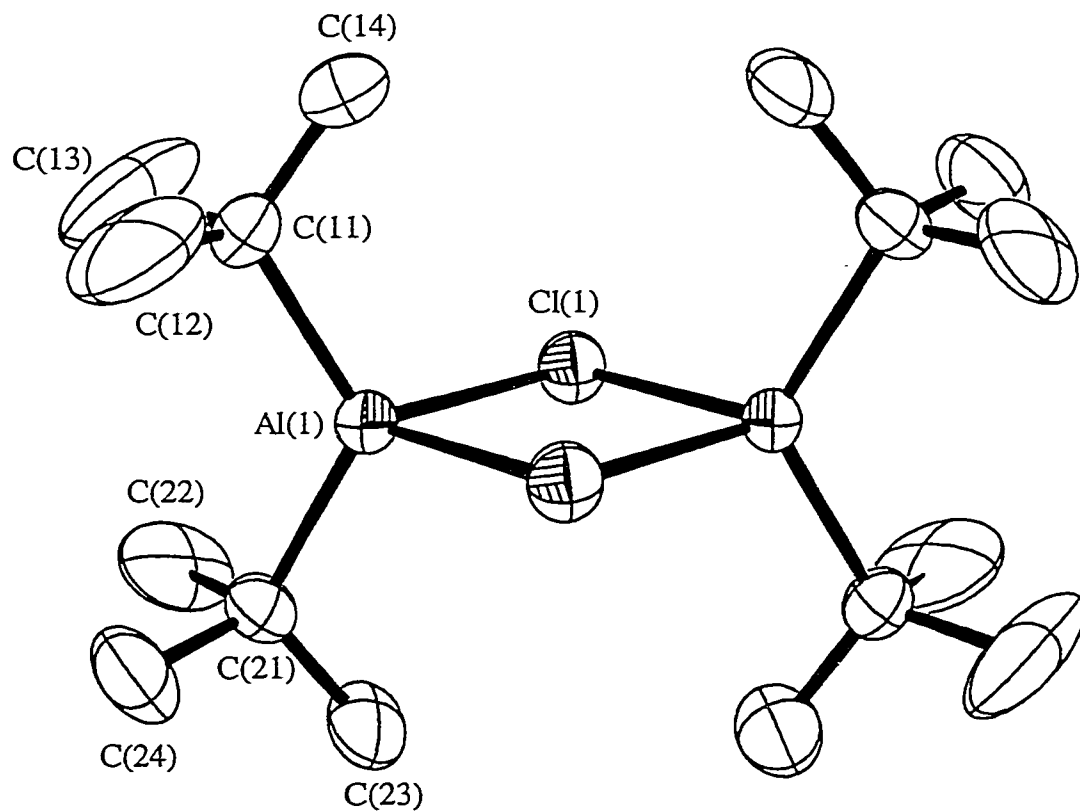


Figure 18. The molecular structure of $[(\text{t-Bu})_2\text{Al}(\mu\text{-Cl})]_2$ (6.1). Thermal ellipsoids are drawn at the 30% probability level, and hydrogen atoms are omitted for clarity.

Table of Positional Parameters and Their Estimated Standard Deviations

	x	y	z	U(eq)
Al(1)	4364(3)	4998(3)	3450(2)	57(1)
Cl(1)	2984(3)	5718(2)	5117(2)	67(1)
C(11)	2289(14)	2955(9)	2135(7)	79(4)
C(12)	3543(21)	2162(14)	1394(12)	195(9)
C(13)	576(19)	3259(14)	1166(11)	211(8)
C(14)	1215(22)	1685(13)	2596(10)	231(9)
C(21)	5801(14)	7018(10)	3040(7)	78(4)
C(22)	4073(52)	7576(42)	2302(33)	183(24)
C(23)	7236(47)	8423(25)	4147(17)	130(14)
C(24)	7166(46)	6541(26)	2177(24)	127(13)
C(22A)	4812(86)	7071(61)	1702(36)	233(38)
C(23A)	5437(72)	8552(45)	3800(44)	179(32)
C(24A)	8312(41)	7362(37)	3438(41)	137(19)

Table of Positional Parameters and Their Estimated Standard Deviations

	x	y	z	U
H(12A)	2583	1158	739	80
H(12B)	4220	2935	1003	80
H(12C)	4687	1909	1988	80
H(13A)	-404	2240	535	80
H(13B)	-270	3793	1602	80
H(13C)	1272	3983	746	80
H(14A)	247	738	1887	80
H(14B)	2306	1349	3157	80
H(14C)	348	2133	3066	80
H(22A)	4744	8555	2096	80
H(22B)	3147	6720	1521	80
H(22C)	3178	7834	2825	80
H(23A)	7861	9347	3868	80
H(23B)	6428	8756	4705	80
H(23C)	8418	8063	4606	80
H(24A)	7899	7475	1943	80
H(24B)	8252	6060	2576	80
H(24C)	6080	5725	1418	80
H(22D)	5470	8036	1475	80
H(22E)	4780	6087	1102	80
H(22F)	3314	7030	1676	80
H(23D)	6137	9528	3599	80
H(23E)	3871	8422	3618	80
H(23F)	6112	8667	4696	80
H(24D)	8963	8347	3232	80
H(24E)	9048	7470	4326	80
H(24F)	8485	6413	2900	80

Table of Bond Distances in Angstroms.

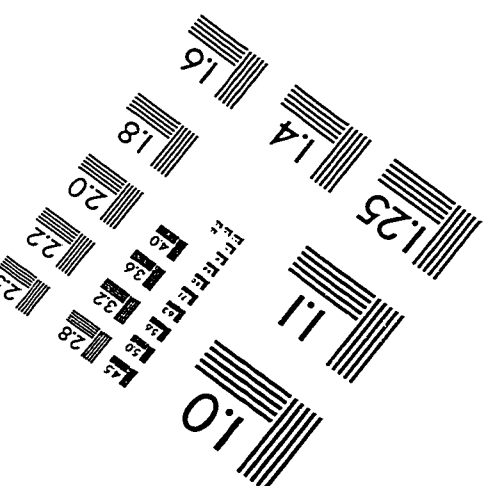
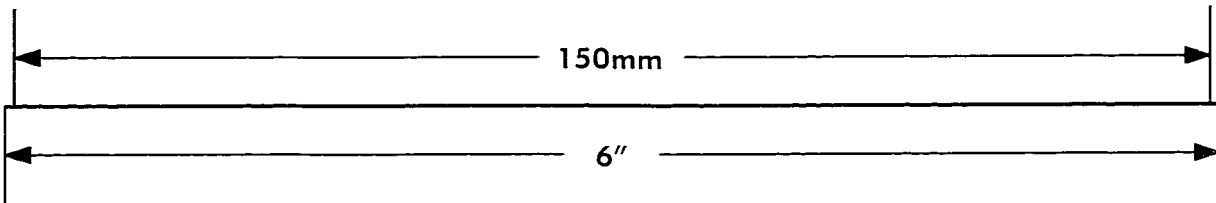
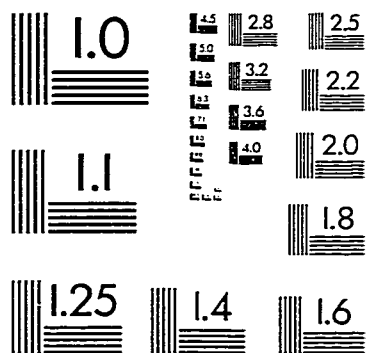
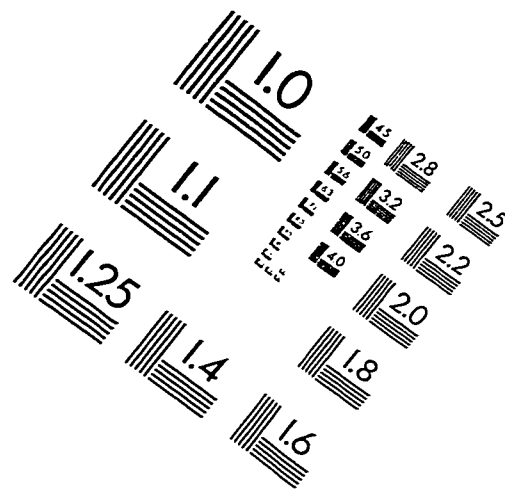
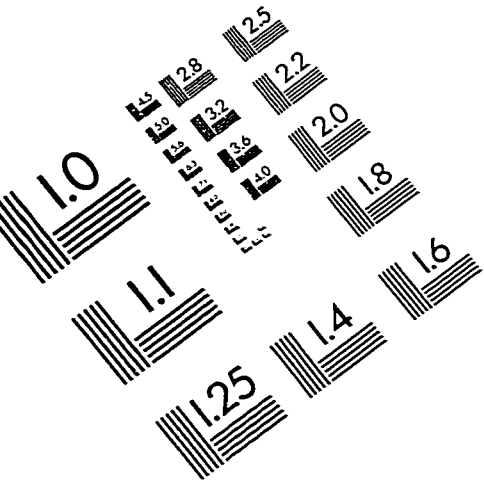
131

Al(1)-Cl(1)	2.316(3)	Al(1)-C(11)	1.966(6)
Al(1)-C(21)	1.982(9)	Al(1)-Cl(1a)	2.324(3)
Cl(1)-Al(1a)	2.324(3)	C(11)-C(12)	1.48(1)
C(11)-C(13)	1.45(1)	C(11)-C(14)	1.42(1)
C(21)-C(22)	1.45(3)	C(21)-C(23)	1.45(1)
C(21)-C(24)	1.53(3)	C(21)-C(22a)	1.48(4)
C(21)-C(23a)	1.52(4)	C(21)-C(24a)	1.51(2)
C(22)-C(22a)	1.01(6)	C(22)-C(23a)	1.61(5)
C(23)-C(23a)	1.17(5)	C(23)-C(24a)	1.50(4)
C(24)-C(22a)	1.68(6)	C(24)-C(24a)	1.35(4)

Cl(1)-Al(1)-C(11)	110.9(3)	Cl(1)-Al(1)-C(21)	110.2(3)
C(11)-Al(1)-C(21)	123.6(3)	Cl(1)-Al(1)-Cl(1a)	87.2(1)
C(11)-Al(1)-Cl(1a)	108.6(3)	C(21)-Al(1)-Cl(1a)	110.4(3)
Al(1)-Cl(1)-Al(1a)	92.8(1)	Al(1)-C(11)-C(12)	109.1(6)
Al(1)-C(11)-C(13)	113.4(6)	C(12)-C(11)-C(13)	104.3(8)
Al(1)-C(11)-C(14)	116.4(6)	C(12)-C(11)-C(14)	104.7(9)
C(13)-C(11)-C(14)	108.0(8)	Al(1)-C(21)-C(22)	109.0(14)
Al(1)-C(21)-C(23)	115.5(10)	C(22)-C(21)-C(23)	107.3(17)
Al(1)-C(21)-C(24)	108.2(10)	C(22)-C(21)-C(24)	107.4(19)
C(23)-C(21)-C(24)	109.2(15)	Al(1)-C(21)-C(22a)	115.4(19)
C(22)-C(21)-C(22a)	40.2(28)	C(23)-C(21)-C(22a)	126.7(21)
C(24)-C(21)-C(22a)	67.8(25)	Al(1)-C(21)-C(23a)	110.9(20)
C(22)-C(21)-C(23a)	65.6(21)	C(23)-C(21)-C(23a)	46.4(19)
C(24)-C(21)-C(23a)	140.3(21)	C(22a)-C(21)-C(23a)	100.4(29)
Al(1)-C(21)-C(24a)	110.8(16)	C(22)-C(21)-C(24a)	139.6(22)
C(23)-C(21)-C(24a)	60.6(19)	C(24)-C(21)-C(24a)	52.8(18)
C(22a)-C(21)-C(24a)	112.7(29)	C(23a)-C(21)-C(24a)	105.6(20)
C(21)-C(22)-C(22a)	71.7(35)	C(21)-C(22)-C(23a)	59.3(21)
C(22a)-C(22)-C(23a)	121.9(39)	C(21)-C(23)-C(23a)	69.8(21)
C(21)-C(23)-C(24a)	61.7(13)	C(23a)-C(23)-C(24a)	129.1(27)
C(21)-C(24)-C(22a)	54.7(19)	C(21)-C(24)-C(24a)	62.8(19)
C(22a)-C(24)-C(24a)	109.9(26)	C(21)-C(22a)-C(22)	68.2(30)
C(21)-C(22a)-C(24)	57.5(21)	C(22)-C(22a)-C(24)	124.9(38)
C(21)-C(23a)-C(22)	55.2(20)	C(21)-C(23a)-C(23)	63.8(24)
C(22)-C(23a)-C(23)	113.5(38)	C(21)-C(24a)-C(23)	57.7(15)
C(21)-C(24a)-C(24)	64.4(17)	C(23)-C(24a)-C(24)	117.1(25)

	U ₁₁	U ₂₂	U ₃₃	U ₁₂	U ₁₃	U ₂₃
Al(1)	60(1)	58(1)	45(1)	9(1)	13(1)	17(1)
Cl(1)	59(1)	87(1)	61(1)	29(1)	22(1)	25(1)
C(11)	93(6)	68(5)	50(4)	2(4)	12(4)	5(4)
C(12)	199(14)	122(10)	159(12)	-23(9)	32(10)	-58(9)
C(13)	203(13)	117(10)	169(12)	9(9)	-111(10)	9(8)
C(14)	316(18)	143(10)	76(7)	-137(11)	13(9)	3(7)
C(21)	97(6)	63(5)	69(5)	5(4)	30(5)	28(4)
C(22)	142(20)	200(37)	202(40)	8(20)	-2(24)	172(37)
C(23)	211(28)	63(13)	81(13)	-25(15)	49(15)	20(10)
C(24)	160(21)	127(17)	109(16)	17(16)	78(16)	51(14)
C(22a)	326(82)	155(35)	82(24)	-120(46)	9(31)	46(22)
C(23a)	217(46)	139(30)	267(51)	96(34)	111(43)	148(35)
C(24a)	121(23)	91(20)	221(35)	10(16)	76(24)	87(23)

IMAGE EVALUATION TEST TARGET (QA-3)



APPLIED IMAGE, Inc.
1653 East Main Street
Rochester, NY 14609 USA
Phone: 716/482-0300
Fax: 716/288-5989

© 1993, Applied Image, Inc., All Rights Reserved

